UNIVERSITAT POLITÈCNICA
DE CATALUNYA

Ph.D. Dissertation

# Antenna Arrays for Multipath and Interference Mitigation in GNSS Receivers

Author: Gonzalo Seco Granados
Advisor: Prof. Juan A. Fernández Rubio

Department of Signal Theory and Communications
Universitat Politècnica de Catalunya

Barcelona, July 2000

# Abstract

This thesis deals with the synchronization of one or several replicas of a known signal received in a scenario with multipath propagation and directional interference. A connecting theme along this work is the systematic application of the maximum likelihood (ML) principle together with a signal model in which the spatial signatures are unstructured and the noise term is Gaussian-distributed with an unknown correlation matrix. This last assumption is key in obtaining estimators that are capable of mitigating the disturbing signals that exhibit a certain structure, and this is achieved without resorting to the estimation of the parameters of those signals. On the other hand, the assumption of unstructured spatial signatures is interesting from a practical standpoint and facilitates the estimation problem since the estimates of these signatures can be obtained in closed form. This constitutes a first step towards the elimination of the multidimensional searches required by many estimators, which is one of the objectives pursued in this work.

In the first part of the thesis, the maximum likelihood solution to the general time delay estimation problem for the case of noise with unknown spatial correlation is derived. The resulting criterion for the delays is shown to be consistent and asymptotically efficient; but it is highly non-linear due to the presence of a matrix determinant operator, and does not lead to simple optimization procedures. It is proven using systematic and heuristic methods that the optimal ML criterion can be approximated by a simpler and asymptotically equivalent cost function. Unlike many other estimation problems, the asymptotic efficiency is not maintained if the optimal criterion is approximated by its first term in the Taylor series expansion. The interesting feature of the new cost function is the fact that it depends linearly on the projection matrix onto the subspace spanned by the signals, and hence it can be minimized using the computationally efficient IQML algorithm. Furthermore, the existence of simple yet robust against the interference initialization schemes based on identity weightings and possibly ESPRIT makes the approach viable for practical implementation. The proposed cost function can be applied identically to the estimation of the "frame delay" in a FIR channel. In this case, the IQML algorithm is modified in such a way that each iteration comes down to rooting a polynomial whose order is equal to the length of the FIR channel.

The goal of the estimators presented in the second part of the thesis is to take advantage of one particularity of the GNSS (Global Navigation Satellite Systems) systems consisting in that the direction-of-arrival of the line-of-sight signal may be known a priori. Resting on this additional information and assuming that the antenna is calibrated, a simplified and approximate model for the received signal is proposed. It consists in gathering all the signals except for the direct one into a equivalent term with unknown spatial correlation. The ML estimators of the time delay and carrier phase of the line-of-sight signal derived under the simplified model are analyzed. They largely reduce the bias produced by multipath components and, as a matter of fact, their RMSE is in many situations very close to or even better than the best possible performance attainable with more detailed models of the multipath channel. Two polynomial-rooting algorithms for computing the time delay estimate are presented. It is also shown that the ML estimates can be obtained from the output signal of a hybrid beamformer. Since the beamformer itself depends on the time delay and amplitude estimates of the direct signal, an iterative algorithm arises naturally. The hybrid beamformer provides insights into the ML estimators and may be appropriate for a practical design. It is shown both analytically and numerically that the proposed ML time delay estimator is robust against errors in the a priori steering vector of the direct signal, and an approach to extend the range of tolerable pointing errors is presented.

In the last part of the thesis, the synchronization of a desired user transmitting a known training sequence in a DS-CDMA communication system is addressed. A model in which the multiple-access interference, the external interference and the noise are included into an equivalent disturbance term with unknown and arbitrary space-time correlation is considered. Starting from this model, a large-sample ML code-timing estimator that operates in frequency-nonselective, slowly fading channels is derived. It is a single-user and near-far resistant method. The significance of the proposed estimator is that it takes advantage of the structure of the signals in both the space and time domains, so it contrasts with other methods put forward up to date that, while also employing antenna arrays, only exploit the structure of the signals in one of the domains. In a CDMA communication system, the desired user is interfered by the signals of a generally large number of users and by possible external interferers. In accordance with this fact, numerical results show that the joint use of all the spatial and temporal degrees of freedom is indispensable for the correct acquisition and tracking of the synchronization parameters in heavily loaded systems and/or in the presence of external interference.

# Resumen

Esta tesis aborda la sincronización de una o varias réplicas de una señal conocida recibidas en un entorno con propagación multicamino e interferencias direccionales. Uno de los hilos conductores de este trabajo es la aplicación sistemática del principio de máxima verosimilitud (ML) junto con un modelo de señal en el cual las firmas espaciales no tienen estructura, y en cual el ruido es Gaussiano y presenta una matriz de correlación desconocida. Esta última suposición es fundamental a la hora de obtener estimadores capaces de atenuar las señales interferentes que presentan algún tipo de estructura, y esto se consigue sin necesidad de recurrir a la estimación de ciertos parámetros de dichas señales. Por otra parte, la suposición de que las firmas espaciales carecen de estructura tiene ventajas desde un punto de vista práctico, al mismo tiempo que simplifica la estimación del resto de parámetros ya que las estimaciones de estas firmas se pueden calcular de forma cerrada. Esto constituye un primer paso hacia la eliminación de las búsquedas en múltiples dimensiones, que es otro de los objetivos perseguidos en este trabajo.

En la primera parte de la tesis se deduce la solución de máxima verosimilitud para el problema general de estimación de retardos cuando el ruido tiene correlación espacial desconocida. Se demuestra que el criterio resultante para los retardos es consistente y asintóticamente eficiente, pero también es altamente no-lineal debido a la presencia del determinante de una matriz y no permite, por tanto, el uso de procedimientos sencillos de optimización. Asimismo, se demuestra y se argumenta intuitivamente que el criterio óptimo ML se puede aproximar por una función de coste más sencilla que es asintóticamente equivalente. A diferencia de otros problemas de estimación, en el caso tratado aquí, el primer término del desarrollo de Taylor del estimador ML no conserva la eficiencia asintótica. La característica esencial de la nueva función de coste es que depende linealmente de la matriz de proyección sobre el subespacio de las señales y, por lo tanto, admite ser minimizada mediante el algoritmo IQML, que es eficiente desde el punto de vista computacional. Además, la existencia de métodos de inicialización sencillos y robustos a las interferencias, los cuales se basan en el uso de una matriz de pesos igual a la identidad y posiblemente también en el algoritmo ESPRIT, hace que el esquema de estimación propuesto pueda ser viable para un diseño práctico. La nueva función de coste se puede aplicar de la misma manera a la estimación del retardo en un canal FIR. En este caso, el algoritmo IQML se puede modificar de forma que, en cada iteración, la estimación del retardo se obtiene a partir de las

raíces de un polinomio cuyo orden es igual a la longitud del canal.

El objetivo perseguido por los estimadores presentados en la segunda parte de la tesis es aprovechar una particularidad de los sistemas GNSS (Global Navigation Satellite Systems), que consiste en que la dirección de llegada de la señal directa puede ser conocida a priori. Basándose en esta información adicional y suponiendo que el *array* está calibrado, se propone un modelo simplificado, aunque al mismo tiempo aproximado, para la señal recibida. En este modelo todas las señales excepto la señal directa se engloban en un término con correlación espacial desconocida. Se analizan los estimadores ML del retardo y de la fase de portadora de la señal directa. El sesgo producido por las componentes multicamino al utilizar estos estimadores se reduce de forma muy importante con respecto al sesgo que sufren otros métodos. De hecho, el error cuadrático medio de los estimadores propuestos es en muchas ocasiones muy próximo o incluso inferior al mínimo error que se puede alcanzar con modelos más detallados del canal multicamino. Asimismo, se presentan dos algoritmos de estimación del retardo basados en el cálculo de las raíces de un polinomio. Se demuestra también que las estimaciones ML se pueden obtener a partir de la señal de salida de un conformador de haz híbrido. Debido a que el propio conformador depende de las estimaciones del retardo y de la amplitud de la señal directa, el uso de un algoritmo iterativo surge de forma natural. La formulación mediante el conformador híbrido proporciona una interpretación alternativa interesante de la estimación ML, y podría ser apropiada para una realización práctica. Finalmente, se demuestra analíticamente y numéricamente que el estimador propuesto para el retardo es robusto frente a errores en el valor nominal del vector de enfoque de la señal directa, y se presenta una manera de extender el margen tolerable de errores de apuntamiento.

En la última parte de la tesis se trata la sincronización de un usuario deseado que transmite una secuencia de entrenamiento conocida en un sistema de comunicaciones DS-CDMA. El modelo de señal utilizado agrupa el ruido, y la interferencia externa y de acceso múltiple en un término de ruido equivalente que presenta una matriz de correlación espacio-temporal desconocida. Partiendo de este modelo, se deduce un estimador del retardo que es una aproximación para un número grande de muestras del estimador ML exacto y que es apropiado para canales con desvanecimientos lentos y no selectivos en frecuencia. El estimador propuesto es una técnica de un solo usuario y es resistente al efecto *near-far*. Su importancia radica en el hecho de que aprovecha la estructura de las señales en el dominio temporal y espacial, lo que contrasta con otros métodos existentes que, a pesar de utilizar un *array* de antenas, sólo utilizan la estructura de las señales en uno de los dos dominios. En un sistema de comunicaciones móviles, el usuario deseado está interferido por un número generalmente elevado de señales de otros usuarios y por posibles interferencias externas. En concordancia con este hecho, los resultados numéricos han mostrado que el uso conjunto de todos los grados de libertad espacio-temporales es indispensable para la correcta adquisición y seguimiento del retardo en sistemas con una carga elevada de usuarios y/o en presencia de interferencias externas.

*A mis padres,*

# Agradecimientos

Aparte del propio autor, otras personas han contribuido a este trabajo, y me satisface poder nombrarlas aquí. Agradezco en primer lugar a mi director de tesis, Juan A. Fernández Rubio, su apoyo y sus consejos. Creo que él siempre ha tenido mucha más confianza en mí que yo mismo. Lee Swindlehurst, who has coauthored some of the work, also deserves my deepest appreciation. He made my stay at BYU a pleasant and rewarding experience that was the beginning of a fruitful collaboration. La puerta de Gregori Vázquez nunca ha estado cerrada. Entrar en su despacho ha sido mucho más fácil que salir de él, ya que las discusiones sobre sincronización han estado seguidas en muchas ocasiones por otras igualmente apasionantes. Lo mismo puedo decir de Jaume Riba, quien siempre aporta una visión nueva y valiosa de las cosas. Finalmente, quiero dar las gracias a Gustavo Hernández Ábrego por la ayuda recibida, y también dejar constancia de mi gratitud a Roger Gaspa, Xavi Mestre, Daniel Pérez-Palomar, Christian Pomar y Francesc Rey por ofrecerse a revisar esta tesis.

Este trabajo ha sido parcialmente financiado por el Comissionat per a Universitats i Recerca del Departament de la Presidència de la Generalitat de Catalunya mediante la beca 1997FI 00755 APDT.

# Contents

# Chapter 1

# Introduction

The focus of this thesis is on the use of antenna arrays for the synchronization of a known signal in the presence of multipath propagation and directional interference. The primary framework of this work has been the positioning systems. Notwithstanding, synchronization is a rather general problem, common to communication, radar and sonar systems. Therefore, the general design criteria, initially tailored to positioning systems, have been extended in order to derive synchronization methods also for communications systems. In the sequel, the problems associated with both types of systems are introduced, and subsequently the objectives and the organization of this thesis are described.

## 1.1 Positioning Systems

There is hardly any doubt that Global Navigation Satellite Systems (GNSS) will complement or even replace in a near future all other positioning, navigation and synchronization systems. At the present time there are two such operative systems: the American GPS (Global Positioning System) and the Russian GLONASS (GLObal'naya NAvigasionnay Sputnikovaya Sistema). Their deployment was started in the 70s and both of them consist basically of a constellation of satellites and a set of terrestrial control stations. Under all weather conditions and everywhere on and around the Earth, a user equipped with an adequate receiver can obtain round-the-clock its position and the time [Kap96]. Originally developed as military systems, GPS and to a lesser extent GLONASS have also attracted the attention of the civilian community. Indeed, in the last decades there has been a surprising increase of their applications, to mention only a few: surveying, atmospheric study, synchronization/time transfer, communications, fleet control, en route/precise navigation, etc. Such a fast evolution has led to stringent requirements for GNSS systems, particularly in regard to their accuracy. GPS and GLONASS have been augmented in order to satisfy the requirements of some precise applications. The augmentation programs are

the Wide/Local Area Augmentation System (WAAS, LAAS) in the USA, the MSAS in Japan, and the GNSS1(EGNOS) in Europe. However, these improvements do not even allow the use of present GNSS in the most demanding applications, such as airplane approaches of category III, where the requirements are 60cm and 4m of vertical and lateral accuracy (2 sigma values), respectively. This is one of the main reasons, together with the lack of civil control over the systems, why Europe is contributing under the program GNSS2/GALILEO to build a new and civil system [ESA96, FR97]. These facts show clearly the great interest that global navigation satellite systems have arisen among the international community. Future systems will overcome many of the limitations of present ones, but, besides the systems themselves, the receivers need also to be improved. This is one of the general issues that is going to be studied in this thesis; the reasons for that necessity, the existing approaches and our proposed methods will be explained.

The existing global navigation satellite systems (GPS and GLONASS) and the future GNSS2, according to recent studies, share the same operating principle and the same guidelines in the signal structure [Sch98a, Sch98b]. The fundamental signal(s) that each satellite transmits is one (or several) direct sequence – spread spectrum signal(s) (DS–SS) [Hol90]. Modulated on that signal or on another one, the satellite also sends precise information, named navigation message, about its position and the time when a temporal mark in the DS-SS signal is transmitted. The receiver obtains from the propagation delay of the direct signal (line-of-sight signal, LOSS) the distance to each satellite. This is the essential task of a GNSS receiver, since the additional information is provided by the system and its accuracy or availability cannot be improved in the receiver. But, given a system configuration, the quality of the final data presented to the user depends largely on the accuracy in the measurement of the propagation delay. Using the navigation message and the propagation delay from as many satellites as unknowns (usually four: three for the position coordinates and one for the receiver clock error), the antenna location can be computed by means of a simple triangulation procedure. It is important to remark that only the signal that propagates through the direct path carries information about the distance between the satellite and the receiver.

The propagation delay is embedded in two parameters of the received signal: the delay of the complex envelope and the carrier phase. The essential duty of the signal processing unit of a GNSS receiver is to measure these two parameters (usually named *observables* in the GNSS nomenclature), which reduces to the synchronization of the receiver clock and carrier phase. Next, these measured parameters are fed to the navigation processor in order to compute the position, time or any other final parameter. In formulae, if the complex transmitted signal is $a\left(t\right)\, e^{j2\pi f_c t}$, the received signal under ideal propagation conditions is proportional to $a\left(t-\tau_0\right)\, e^{-j2\pi f_c \tau_0}\, e^{j2\pi f_c t}$. The value of $\tau_0$ (scaled by the light speed) obtained by comparing the received complex envelope $a\left(t-\tau_0\right)$ with a local replica of $a\left(t\right)$ is called *pseudorange, code phase/range* or *time delay* [Zhu95b, HW97]. It is virtually an absolute measure of the distance since its possible ambiguity is easily solved, and its typical accuracy in GPS is about 3 meters

(considering only thermal noise errors). Note that all the pseudoranges measured by a receiver differ in a fixed quantity from the true distances because of the receiver clock offset, as the name itself suggests. In the same way, the value of $\tau_0$ measured from the phase of the term $e^{-j2\pi f_c \tau_0}$ is referred to as *carrier phase* [Zhu96, HW97]. This observable is much more precise than the pseudorange (the thermal noise produces an error on the order of 5 millimeters in GPS). On the other hand it is an ambiguous measure, whose absolute determination (i.e., the computation of the integer number of wavelengths) needs costly procedures [Teu97, Has98]. High-end receivers use both pseudorange and carrier-phase ranging [Kap96].

Several errors degrade the accuracy of the global navigation satellite systems [ESA96, Par96a]. A simple classification of the error sources can be presented according to their origin: *i)* satellite induced errors (e.g., ephemerides, clock errors and the recently turned off Selective Availability), *ii)* propagation induced errors (variation of the propagation speed in the ionosphere and the troposphere), and *iii)* receiver local errors (thermal noise, multipath propagation and interferences). Whereas the first two types of errors can be almost completely eliminated or, at least, reduced to centimeter level using certain augmentations such as differential operation (i.e., correction of the observables based on the measurements done by reference stations at known positions) or observations at several frequencies, the receiver local errors can only be reduced with an appropriate receiver design. Furthermore, if the differential corrections generated by a reference station are based on multipath or interference corrupted observables, the position accuracies of all the users connected to that station are deteriorated. These are the reasons why multipath and interference remain as the dominant error sources in most high precision applications and are the limiting factors in achieving the ultimate GNSS accuracy [Wei97a, Nee95].

Specifically, multipath refers to the reception of replicas of the GNSS signal arriving at the antenna by means of one or more reflected paths. Multipath signals are received with a delay relative to the direct signal because they travel an extra path length, so they do not help in determining the geometric distance between the receiver and the satellite, but quite the opposite. Coherent multipath denotes those reflections that are correlated with the direct signal, and this is the type of reflections considered in this thesis. These replicas satisfy two conditions: their time delay and Doppler frequency differences with respect to the LOSS are on the order of or smaller than the inverse of the signal bandwidth (approximately the chip period in a DS-SS signal) and the inverse of the observation time (usually on the order of the symbol period), respectively. Coherent multipath bias the pseudorange and carrier phase measurements because synchronization methods in a conventional receiver lock to a combination of the direct signal with the coherent reflections [Gau99, Nee93b, Zhu95a, Nee95, Mac99]. In other words, coherent multipath introduces systematic errors in the measurements. It is worth remarking that, in order to study the multipath problem in GNSS receivers, it is not appropriate to employ the model usually adopted in communication systems, whereby the time delay differences between

coherent reflections and the direct signal are neglected so the coherent multipath is modeled as multiplicative distortion (i.e., frequency-nonselective fading). On the other hand, non-coherent multipath provides a source of diversity often used in communications systems to improve their performance (basically the symbol error rate). However, this type of multipath components is not so relevant in GNSS because they hardly influence the estimation of the LOSS parameters, and moreover the bit error rate is not an essential performance measure of a GNSS receiver. To make evident the importance of multipath errors it suffices to present their magnitude in the particular case of GPS. The pseudorange error may be on the order of tens or even a hundred meters, and the error in the carrier phase may reach some centimeters [Par96a, chapter 14], [Wei94, Wei97a, Bra96, Bro97]. Moreover, these large multipath errors in the pseudorange hamper the ambiguity resolution process needed for carrier phase ranging. Unlike kinematic applications, in static ones the evolution of the multipath errors is so slow that they are not averaged out [Nee95]. Those values contrast with the level of accuracy achieved in a multipath-free scenario (on the order of a few meters) and with the sub-meter accuracy required by category III airplane approaches [ESA96]. Furthermore, like any other system, the GNSS may also be exposed to external interference. Indeed, specially designed interferers are already available on the market. The interferences can increase the errors in the observables up to several magnitude orders and can even turn the system useless, so receivers should be endowed with interference cancelling techniques in order to make possible the use of GNSS in safety-critical applications, such as automatic guidance and landing systems. GPS and GLONASS are very vulnerable to intentional and also unintentional jamming sources, such as radar transmitters. Although the spread-spectrum modulation provides some level of antijam capability, the received power is so low (about -160dBW for GPS) that 1W of radiated power suffices to completely block the GPS or GLONASS signals within a range of 30km.

## 1.2 Communication Systems

Precise synchronization is not only the key to obtaining location estimates with accuracies of a few meters or better in GNSS receivers, but also a critical aspect of virtually all communication systems. Accurate frame and symbol synchronization is especially important in time-division multiple access (TDMA) and packet-based systems, or code-division multiple access systems (CDMA). Timing information is also needed for any other application where range measurements are made, as in active radar and sonar systems. In these fields the problem is usually referred to as propagation delay or time delay estimation, but in mathematical terms there is little difference between this and synchronization. We will use all these terms, along with code timing, interchangeably.

The last part of this thesis addresses the problem of synchronization of DS-CDMA wireless

communication systems, which use the same modulation format as the present positioning systems. Multiple-access interference (MAI) is inherent to asynchronous DS-CDMA systems, since orthogonality among the users' codes cannot in general be achieved. The MAI can make the conventional detector (i.e., a bank of filters, each matched to a specific user's code) become useless when the powers of the signals received from different users are unequal [Pro95]. This is the so-called near-far problem. One alternative to overcome this problem is the use of power-control schemes. However, these schemes have some limitations because they increase the overall complexity of the system, do not guarantee an optimal performance (e.g., they limit the performance of users with good channels, and some cross-talk still occurs even though power control is used), and there are certain system configurations in which a proper power control cannot be employed (e.g., when several receivers are used) [Par96b]. The use of multi-user detectors is, therefore, necessary in most communication systems in order to combat the near-far problem. The optimum receiver proposed in [Ver86] has been followed by a number of sub-optimum ones (see [Ver98] for a review). All these receivers require the knowledge of one or several parameters, such as the users' code timings, powers and carrier phases. Moreover, the code timings generally need to be estimated with high accuracy, since errors thereof have large impact on the performance of many detectors [Par96c]. The employ of near-far resistant and accurate code synchronization techniques for acquisition and tracking is therefore essential to achieve a correct performance in a DS-CDMA system. This statement is corroborated by the suggestion in [Mad91], stating that the capacity of a DS-CDMA system is limited by the ability to achieve code acquisition. Besides, the MAI is not the only type of interference that may be received. The receiver can be disturbed by any other intentional or fortuitous signal, which we will denote in general as external interference. Consequently, the design of synchronization techniques that are also robust against external interference is of fundamental importance in many situations. There is a vast literature on time delay estimation, the majority of which focuses on the case where the data is measured from a single receiver. However, the performance of single channel timing recovery methods is limited when multipath or co-channel interference (CCI) is present, such as in many wireless communications applications. For this reason, attention has recently shifted to the use of antenna arrays for addressing these problems. The spatial selectivity offered by an antenna array can dramatically improve the performance in environments with severe CCI.

## 1.3 Objectives

Due to the limitations of the multipath and interference mitigating techniques proposed to date for GNSS receivers, we find interesting to further investigate new methods to combat those error sources. We will argue the shortcomings of the single-antenna methods, and the use of an antenna array in the receiver will be proven as a highly effective alternative because arrays can exploit the virtually sole diversity source, that is spatial diversity, present in GNSS

scenarios subject to multipath propagation. Therefore, the overall objective of this thesis is to study and propose estimators of the unknown parameters (time delay, and carrier phase or spatial signature) of the incoming signals when an antenna array is used in the receiver, and multipath components and interferences are present. Given the increase of the receiver complexity introduced by an antenna array, it is worth investigating techniques that efficiently exploit the use of the array and thus are able to combat those two main disturbing effects, and not only one of them like many previous works. Note that we focus on signal processing techniques and not on data/observables processing methods. The common thread of all the proposed estimators is that they are derived using the Maximum Likelihood (ML) principle and assuming an arbitrary unknown correlation of the noise. The ML principle is one of the chief systematic approaches to many estimation problems. While ML estimators are often readily derived, they usually lead to excessively complex problems. Therefore, interest is placed in obtaining, either systematically or ad hoc, simpler techniques that may be viable for practical implementation. However, a thorough analysis of the computational complexity of the different techniques, as compared to present implementations limits, will not be carried out.

In order to overcome the limitations of many existing methods, an initial premise was to impose no restrictions on the array geometry, along with reducing as much as possible the number of variables of the resulting cost functions. The parameters that are not of interest in our application have to be modeled in such a way that their contribution can be eliminated in closed form. This refers especially to the directions-of-arrival (DOA) of the signals. Hence, the estimators do not have to rely on DOA estimation procedures. The effort invested in estimating the DOAs, which would be important because spatial searches are generally needed, could hardly be justified since the parameters of interest in a GNSS application are not the DOAs themselves.

Another objective is the exploitation of a particularity of GNSS systems consisting in that the positions of the transmitter and the receiver are approximately known. This will make possible the derivation of a technique able to combat specular and diffuse multipath. The former refers to a few reflections produced by smooth surfaces such as the wings of a plane, the sea or the earth surface, and certain buildings. The diffuse reflections are produced by rough surfaces, and are often modeled as a discrete summation of a large number of weak reflections.

The methodology of derivation of ML estimators can be also applied to DS-CDMA communication systems. However, there are some important differences between the communication and navigation systems. In the latter, the focus is on combating the reflections of the direct signal, in addition to the external interferences. Since the number of external interferences is assumed small or comparable with the number of antennas, it is possible to largely mitigate those interferences using only the spatial degrees of freedom, which is related to considering the noise is correlated only in the spatial domain. Whereas, in CDMA communications systems, the signal of a desired user is interfered by the signals of a large number of users. Since the number

of disturbing signals usually exceeds the number of spatial or temporal degrees of freedom separately, it is necessary (at least in heavily loaded systems) to employ jointly all these degrees to combat the MAI. Hence, the signal model has to be modified in order to take into account the space-time correlation of the interference.

## 1.4 Organization of the Thesis

After the descriptive **Chapter 2**, the contributions of this thesis are included in **Chapters 3-5**. These chapters are written so that they are essentially self-containing, avoiding continuous references to previous definitions. This is done to help the reader interested in only one part of the material, and to abstract the basic techniques from the surrounding details regarding the application. As a result of this approach, some definitions or background material may occur more than once.

**Chapter 2** outlines the synchronization techniques used by conventional GNSS receivers and the multipath-induced errors they experience. This chapter also reviews existing approaches to the mitigation of multipath and interference errors in GNSS receivers, and techniques that exploit antenna arrays for synchronization in a general framework. Next, some relevant parameters of certain GNSS signals are presented. The general array signal model used in the following two chapters and the main assumptions involved are introduced. The signal model employed in chapter 5 is somewhat different, so its description is deferred to the corresponding chapter. The relationships between the general model and the signals (before and after the despreading) in a GNSS receiver are explored. A frequency-domain representation of the signal model is also sketched. The use of a general model is useful because it makes the derivation of the techniques in the following chapters independent of the particular type of employed signals, and it bears out that the proposed estimators have a rather wide scope. **Chapter 3** delves into the problem of estimating the time delays of multiple replicas of a known signal received by an antenna array in spatially colored noise. The highly non-linear ML criterion is approximated by an asymptotically equivalent criterion. The new estimator allows the use of the computationally attractive iterative quadratic maximum likelihood (IQML) algorithm. A modification of this algorithm when the channel is modeled as a FIR filter is proposed. Based on the knowledge of the steering vector of the direct signal, an estimator of the time delay and carrier phase of the LOSS is proposed in **Chapter 4**. The estimator rests on a simplified and approximate model which gathers all disturbing signals in a single term. It is argued that the knowledge of that steering vector is essential for the suitability of the model, but at the same time the degree of accuracy of this vector is not critical. Closed form and iterative variants of the estimator are presented. The latter provides an interesting connection between the ML estimator and a hybrid beamformer. **Chapter 5** is devoted to the synchronization of a desired user transmitting a known training

sequence in a DS-CDMA wireless communication system. It is assumed that the receiver consists of an arbitrary antenna array and works in a near-far, frequency-nonselective, slowly fading channel. The obtained estimator makes efficient use of the structure of the disturbing signals in both the space and time domains in order to mitigate their effects. Finally, a brief summary of the contributions, along with overall conclusions and possible topics for future research are included in **Chapter 6**. A glossary and a list of usual notations can be found at the end of this document.

# Chapter 2

# A Short Technical Background

This chapter provides some background material. Section 2.1 contains a description of the synchronization techniques used in conventional GNSS receivers. It is followed by a review of multipath and interference mitigation single-sensor methods in Section 2.2 and a survey of the use of antenna arrays for synchronization in Section 2.3. Next, the parameters of some GNSS signals are described in Section 2.4, and the array signal model employed in the following two chapters is introduced in Section 2.5.

## 2.1 Conventional Code Timing and Carrier Phase Estimation

A direct-sequence spread-spectrum (DS-SS) signal $q(t)$ can be expressed as

$$q\left(t\right) = \sum_{l=-\infty}^{\infty} d\left(l\right) p\left(t - lT\right) \ . \tag{2.1}$$

The sequence of symbols $\{d(l)\}$ is transmitted at rate $1/T$. Expression (2.1) actually represents any linearly modulated signal. A distinctive characteristic of DS-SS signals is that $p(t)$ is not a simple shaping pulse, but a spreading waveform which can be written as

$$p\left(t\right) = \sum_{n=0}^{P-1} c\left(n\right) g\left(t - nT_c\right) \ , \tag{2.2}$$

where $g(t)$ is the chip-shaping pulse, $T_c$ is the chip period, and $\{c(n)\}$ is the sequence of chips of the pseudo-noise (PN) code, whose length is $P = T/T_c$. If $d$ delayed replicas of the signal $q(t)$ arrive at a single sensor, the complex baseband received signal is

$$x\left(t\right) = \alpha_0 \, q\left(t - \tau_0\right) + \sum_{k=1}^{d-1} \alpha_k \, q\left(t - \tau_k\right) + w\left(t\right) \ , \tag{2.3}$$

where $\alpha_k$ and $\tau_k$ are the complex amplitude and propagation delay of the $k$th replica, respectively. The term $w(t)$ represents the additive noise and all other disturbing components. The subscript 0 stands for the line-of-sight signal (LOSS); the rest of replicas correspond to reflections, and hence $\tau_0 < \tau_k$, $\forall k \geq 1$ due to clear physical reasons. The desired carried phase information $\varphi_0$ is embedded into the phase of $\alpha_0$ (i.e., $\varphi_0 = \angle\alpha_0$).

The conventional synchronization methods used by most GNSS receivers can be derived by applying the maximum likelihood (ML) principle to the signal model in (2.3) with the assumptions that $d = 1$ and that $w(t)$ is white Gaussian noise [Men97, Mey98]. With regard to the estimation of the time delay, different cost functions to be maximized are obtained depending on different assumptions about the other parameters. For instance,

$$L_c(\tau_0) = \mathrm{Re}\left\{ \sum_l \hat{d}^*(l)\, e^{-j\,\hat{\varphi}_0}\, y(lT + \tau_0) \right\} \tag{2.4}$$

is used in a decision-directed, phase-directed case, and

$$L_{nc}(\tau_0) = \sum_l \left| y(lT + \tau_0) \right|^2 \tag{2.5}$$

corresponds to a non-data-aided, phase-independent criterion. In both cases, $y(lT + \tau_0)$ are samples of the output of the code matched filter $p^*(-t)$ taken at instants $lT+\tau_0$. The summations in these two cost functions cover a certain observation window. Estimates of the carrier phase, $\hat{\varphi}_0$, and of the symbols, $\hat{d}(l)$, are needed in (2.4). In the terminology of DS-SS systems, the matched filter is often named *correlator* and the processing it performs is called *despreading*. Both cost functions are generally driven to the maximum using feedback loops that employ the derivative of the $l$th term in the right-hand side of (2.4) or (2.5) as timing error detector. Since it is convenient to dispense with the calculation of the derivative in order to simplify the receiver, the derivative is approximated with a finite difference. Thus, the following two timing error detectors or discriminators result from (2.4) and (2.5), respectively:

$$e_c(l, \tau_0) = \mathrm{Re}\left\{ \hat{d}^*(l)\, e^{-j\,\hat{\varphi}_0} \left( y(lT + \tau_0 + \delta\, T_c) - y(lT + \tau_0 - \delta\, T_c) \right) \right\} \tag{2.6}$$

$$e_{eml}(l, \tau_0) = \left| y(lT + \tau_0 + \delta\, T_c) \right|^2 - \left| y(lT + \tau_0 - \delta\, T_c) \right|^2 , \tag{2.7}$$

which form the widespread coherent DLL (delay lock loop) and non-coherent early-minus-late (EML) power DLL, respectively ([Die92, Zhu95b, Kap96, Fel97]). A variation of (2.7) is the detector used by the dot-product DLL:

$$e_{dot}(l, \tau_0) = \mathrm{Re}\Big\{ y^*(lT + \tau_0) \left( y(lT + \tau_0 + \delta\, T_c) - y(lT + \tau_0 - \delta\, T_c) \right) \Big\} . \tag{2.8}$$

The value $2\delta$ is usually named early-late spacing of the DLL, and $0 < \delta < 1$.

The expected value of the discriminator output, that is $\mathrm{E}\{e(m)\}$, as a function of the trial value $\tau_0$ is called discrimination curve or S-curve, and the position of its zero-crossing is the

mean of the time-delay estimate [Sim85, Vol.3], [Zhu95b, Gau99]. In the absence of multipath components, the DLL (any of them) provides unbiased estimates. However, the effect of the reflections is to distort the S-curve in such a way that the zero-crossing is shifted away from the true time-delay of the LOSS and the estimates obtained with the DLL become biased [She94, Nee93b, Zhu95a, Nee95, Sec96]. It is straightforward that the S-curves of the coherent, EML and dot product DLLs are [Gau99]

$$S_c(\tau_0) = \sigma_d^2 \sum_{k=0}^{d-1} |\alpha_k| \cos(\varphi_k - \hat{\varphi}_0) \operatorname{Re}\{c_{pp}(\tau_0 - \check{\tau}_k + \delta T_c) - c_{pp}(\tau_0 - \check{\tau}_k - \delta T_c)\} \tag{2.9}$$

$$\begin{aligned} S_{eml}(\tau_0) = {} & \sigma_d^2 \sum_l \sum_{k=0}^{d-1} \sum_{r=0}^{d-1} \alpha_k^* \alpha_r c_{pp}^*(lT + \tau_0 - \check{\tau}_k + \delta T_c) c_{pp}(lT + \tau_0 - \check{\tau}_r + \delta T_c) \\ & - \sigma_d^2 \sum_l \sum_{k=0}^{d-1} \sum_{r=0}^{d-1} \alpha_k^* \alpha_r c_{pp}^*(lT + \tau_0 - \check{\tau}_k - \delta T_c) c_{pp}(lT + \tau_0 - \check{\tau}_r - \delta T_c) \end{aligned} \tag{2.10}$$

$$\begin{aligned} S_{dot}(\tau_0) = {} & \sigma_d^2 \sum_l \sum_{k=0}^{d-1} \sum_{r=0}^{d-1} \operatorname{Re}\Big\{ \alpha_k^* \alpha_r c_{pp}^*(lT + \tau_0 - \check{\tau}_k) \\ & \cdot \big(c_{pp}(lT + \tau_0 - \check{\tau}_r + \delta T_c) - c_{pp}(lT + \tau_0 - \check{\tau}_r - \delta T_c)\big) \Big\} \end{aligned} \tag{2.11}$$

where $\check{(\cdot)}$ is used to denote the true values of the parameters, and $c_{pp}(t)$ is the code autocorrelation, i.e.,

$$c_{pp}(t) = p(t) * p^*(-t) \ . \tag{2.12}$$

In computing (2.9)-(2.11) we have assumed that $\{d(l)\}$ is a *iid* sequence with variance $\sigma_d^2$, and expression (2.9) is conditioned on $\hat{\varphi}_0$. In (2.9) we have also considered that $\hat{d}(l) = d(l)$. In general, any of these S-curves satisfies $S(\check{\tau}_0) = 0$ only when $d = 1$.

In order to measure the carrier phase of the LOSS, conventional receivers employ different types of phase lock loops (PLL), such as the well-known Costas loop [Hol90]. Despite the fact that a complete analysis of such loops is involved, some insight can be gained by simply considering that the carrier phase is estimated as the argument of the samples of the despread signal taken at certain instants [Zhu96]:

$$\hat{\varphi}_0(l) = \angle y(lT + \hat{\tau}_0) \tag{2.13}$$

Again it is not difficult to show that the mean value of $\hat{\varphi}_0$ only coincides in general with $\check{\varphi}_0$ when no reflections are received, otherwise the carrier phase estimate is biased [Nee93b, Zhu95a, Nee95]. The examples in Figure 2.1 are plotted to make clear how deleterious multipath errors can be. These figures represent the maximum biases produced by a single reflection as a function of its delay separation with respect to the LOSS. The large magnitude of these errors is remarkable, since a chip period $T_c$ of the GPS C/A code amounts to 300 meters approximately, and a wavelength of the GPS L1 carrier is about 20 centimeters (see Section 2.4). The reduction

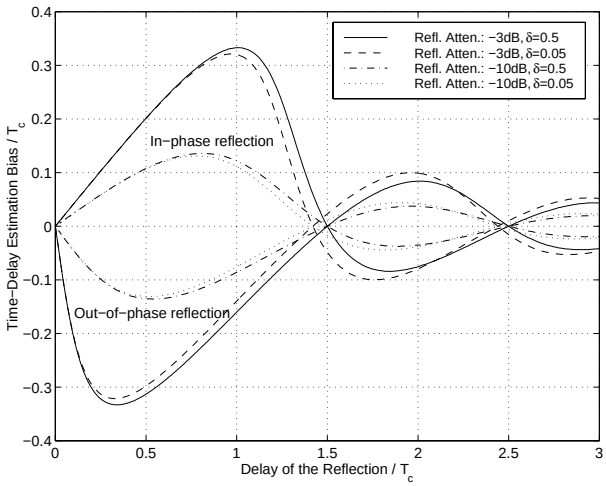


The time-delay estimate is obtained with a DLL. The absolute maximum biases are the same for the three types of DLL presented above, and they occur when the phase of the reflection with respect to the LOSS is 0 or $\pi$. Different early-late spacings are considered.

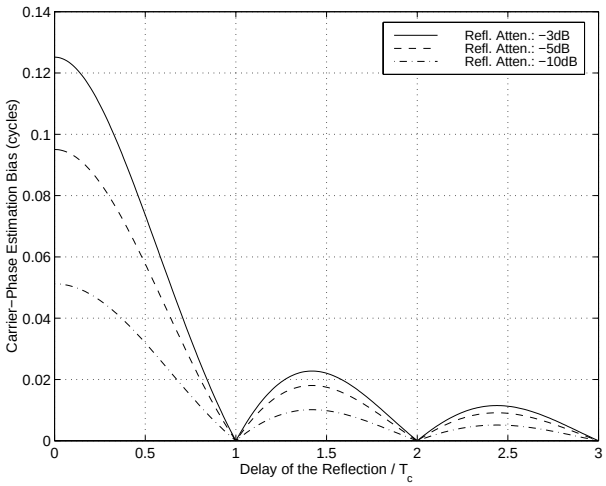


The carrier phase bias is computed in absence of errors in the time-delay estimate of the LOSS. The expression of the phase of the reflection that produces the maximum errors can be easily derived, see e.g., [Nee93b].

Figure 2.1: Absolute maximum biases of the time-delay and carrier phase estimates produced by a single reflection for different attenuations of the reflection. The chip shaping pulse is a Nyquist square-root raised cosine pulse with 0.2 roll-off.

of the biases in the time-delay and carrier phase estimates produced by the multipath components is one major objective of this thesis.

In addition to the bias, the other performance measure of the estimators is the variance, which is produced by thermal noise, interferences and self-noise. The latter is negligible given the long codes normally used in GNSS systems. The DLL and PLL used in most receivers are designed under the assumption that white noise is the only disturbing received signal, so they do not offer any protection against interferences, apart from the own protection of the DS-SS signal. Then, the variances of the time-delay and carrier phase estimates are roughly inversely proportional to the SINR (signal to interference plus noise ratio) and the performance of the DLL and PLL may be seriously degraded in the presence of strong interferences [LA98a, LA98b]. The design of estimators with an intrinsic capability of cancelling interferences is another major objective of this thesis.

## 2.2 Review of the Single-Antenna Techniques

Although some studies about the effects of multipath and interferences on the observables were already carried out in the 80s [Cou81], and even earlier, it is in the last decade when there has been an increasing interest of the manufactures and the research community in reception schemes capable of mitigating those effects. For certain, one of the reasons for this interest arises from the present technological development that makes feasible the implementation of more complex receivers. The methods proposed up till now differ in many aspects, such as the application, the signal scenario or the type of receiver they are tailored to. Grouping some of their common threads, these methods may be classified according to two criteria:

- use of one versus several antennas
- data processing versus signal processing techniques

Data or observables processing techniques are usually associated with post-processing methods. The idea behind this approach is to first measure the observables from the received signal using a conventional receiver (i.e., a receiver without special capabilities to combat the multipath and interferences). Then, a set of raw observables is processed (usually not in real-time) in order to obtain some new observables or final parameters (position, speed...) in which the disturbing effects of those error sources have been mitigated. On the other hand, it is customary to associate signal processing techniques with real-time techniques. They are the ones that lead to the design of alternative reception schemes. These methods seek to obtain observables free of the effects of the multipath and interferences starting from the GNSS signals corrupted by those phenomena. Our work will center on signal processing techniques that employ antenna arrays because this seems to be the choice with greatest potential and these techniques are also more flexible than the post-processing ones. Below we review the state-of-the-art according to the previous classification.

### 2.2.1 Post-Processing Techniques

The common basis of many of these techniques is that the changing geometry of the satellites causes a slow change of the relative delays of the reflections, which in its turn produces low-frequency variations in the carrier phase and in the signal-to-noise ratio of the composite signal [Axe96, Bre97, Sle97, Com98]. The contribution of the dominant reflected path can be identified from the variations of the signal-to-noise ratio and subtracted from the multipath corrupted observables. The high-frequency error signals, that arise because of the receiver movement can be filtered out by a low-pass filter in many applications [Zha96]. Since these procedures need data recording for several minutes or hours, they are restricted to a small number of applications.

Moreover, they can only cope with specular multipath and cannot combat the interferences. Lately, a tool employing neural networks for detecting and mitigating in real-time the code multipath in LEO (Low Earth Orbiter) has been proposed in [HP00].

### 2.2.2 Signal Processing Techniques

These techniques are often referred to as correlation methods or correlation technology because most of them are modifications of the conventional delay lock loops presented in the previous section. They emerge from an insightful inspection of the cross-correlation curve between the received signal and the spreading code, in an attempt to find out which samples of this curve are less distorted by the reflections or how the contribution of the multipath can be estimated and eliminated [Dor95]. Major receiver manufacturers have devoted a great development and research effort to these techniques, but often only limited simulated results and vague descriptions are revealed.

The first and the undoubtedly most extended multipath mitigation technique is the Narrow Correlator DLL [Die92, Nee92a]. It consists in using a precorrelation bandwidth as wide as possible and a small value of the early-late spacing $\delta$ (introduced in Section 2.1), on the order of 0.05 or 0.1, which contrasts with the usual value: 0.5, employed by first receivers. A wider precorrelation bandwidth leads to a sharper cross-correlation curve, thus facilitating obviously the time-delay measurement. With the small values of $\delta$, the finite difference formed with the early and late samples of the cross-correlation function becomes a better approximation of the derivative of the correlator output. This reduces the variance of the DLL because the correlation of the noise between the early and late samples increases, and also improves the performance against multipath (only for non-bandlimited or rectangular chip-shaping pulses, but not for square-root raised cosine pulses, see Figure 2.1 and [Sch98a]) since those samples are closer to the correlation peak, where the distortion due to multipath signals is less severe. The narrow spacing DLL can reduce the magnitude of the multipath errors (only for certain pulses), but not the range of multipath delays that cause them. The Multipath Elimination Technology (MET) is a slight improvement of the narrow spacing DLL, especially for large multipath delays [Tow94]. One alternative to reduce that range of delays causing biases is the Strobe correlator$^{TM}$ (patented by Ashtech Inc.) [Gar96, Die97], which despreads the received signal using a special waveform, as done also in [Wei97b]. Actually, the Strobe correlator rests on the same principle as the high resolution correlator or compensated correlators [Dor97]. The compensated correlators employ more complex finite differences obtained using several advanced and delayed samples of $y(t)$ that yield a S-curve narrower than that of the conventional DLL. Combining several samples of $y(t)$ is equivalent to using a special despreading waveform. The robustness gained by the Strobe correlator against long-delay reflections is at the price of a certain (up to 10dB) noise amplification [Die97]. The Strobe correlator also recalls the

second-derivative correlator [Wei97a], and some enhanced versions thereof have been proposed [Gar97, Zhd99]. Other approaches that exploit the fact that the reflections are always delayed with respect to the direct signal are the Edge Correlator™ (patented by Ashtech Inc.) and the e1/e2 tracker [Gar96, Die97]. These last methods try to determine the location of the leading edge of the cross-correlation, instead of attempting to estimate the location of its peak. Again multipath mitigation is traded off against noise amplification.

An important limitation of all the correlation techniques presented up to this point is that they only combat the multipath errors in the time-delay measurements, but not in the carrier phase. This problem can be partially solved with the Multipath Estimating DLL (MEDLL™), which has been included in commercial receivers by Novatel Inc (although details are not available). From our point of view, the MEDLL was the first attempt of addressing the multipath problem rigorously and was proposed by R. van Nee [Nee93a, Nee94, Nee95]. It is derived as the maximum likelihood estimator of the delays and amplitudes of all the signals present in model (2.3) when the noise $w(t)$ is white and Gaussian. This means that, unlike the DLL, the MEDLL is matched to a multipath scenario. Notwithstanding, its performance is excellent with moderately or largely spaced (in delay) reflections [She98]; but in the presence of short-delay multipath it suffers from convergence problems, its performance is comparable to that of the narrow spacing DLL or the Strobe correlator, and its implementation needs some simplifying assumptions [Lax97]. The estimation of the time delays of a superposition of closely spaced signals with known shapes has also been considered in [Wu99a, Wu99b]. In these works, using a relaxation-based optimization approach, a multidimensional problem is reduced into a set of 1-D (one-dimensional) problems that need to be solved iteratively. In [Wu99b], a method to initialize the iterations is provided as well. The main difference between the estimators in [Wu99a] and [Wu99b] is that the former can cope with noise correlated in the temporal domain, so it is able to combat narrow-band interferences. The work of [Sou98] presents a Maximum A Posteriori (MAP) estimator, obtained by introducing a priori distributions of the delay and amplitude parameters into the MEDLL. To our knowledge, the employ of the Bayesian theory for the estimation of the multipath parameters has hardly received attention in the literature and remains an open topic of research.

Finally, several methods can be used to cancel narrow-band interferences in single antenna receivers. The traditional approach is the linear interpolator-subtracter [Ilt84, Mou98, Lan97], and recently extensions of multiuser detectors have appeared, e.g., [Poo97a, Poo97b]. The linear interpolator-subtracter is simply an adaptive transversal notch filter applied before the despreader. It minimizes the output total power, and thus places nulls at the frequencies where the interferences are received.

## 2.3 Review of Synchronization using Antenna Arrays

Spatial filtering is probably the most effective approach to overcome the limitations of the single-antenna multipath mitigation techniques and to cancel wide-band interferences. Indeed, using antennas with special reception patterns (choke rings) and locating them wisely have been, among the GPS community, the traditional ways of filtering out spatially the undesired signals [Cou98]. A much more powerful alternative is to employ adaptive arrays of antennas, as it was proven in an initial work of the author [Sec96]. The spatial diversity introduced by the antenna array can be used to discriminate the direct signal from the interferences and the reflections, so the multiple antennas can be thought as forming a directional beam pattern responsive to the LOSS but not to other disturbing signals.

However, the use of adaptive antenna arrays in GNSS receivers has not been deeply studied, and most of the few approaches appeared in the literature have centered on interference mitigation. For instance, in [Zol95, Moe96b, Moe96a, Mou98, Fan98, Myr00] and [Hat98] the weight vector of a beamformer is computed either as the one that maximizes a certain average SINR or as the one that minimizes the output power subject to some constraints to avoid the null solution. This yields in most cases the well-known minimum variance distortionless response (MVDR) beamformer and the power inversion (or linear prediction) beamformer [Pil89]. When these two beamformers are applied directly to the received signals, they cancel the interferences but not the reflections of the GNSS signal, which are well below the noise floor. In [Mou98] and [Fan98], the broad-band combiner structure is employed in order to cancel the narrow-band interferences in the temporal domain and the wide-band ones in the spatial domain. Ramos *et al.* presented in [Ram96] a prototype that performs the array processing after the despreading using a pseudo-PRO-ESPRIT algorithm [Ram95]. This prototype can separate the GNSS signal from other uncorrelated signals, but it combines the reflections with the direct signal, instead of canceling them. Although this behavior is adequate with respect to the bit error rate, it is inappropriate for the propagation delay estimation.

As stated above, an early paper of the author [Sec96] showed the significant benefits of using an antenna array to combat both the interferences and the multipath in a GNSS application. In order to cancel both types of disturbing components, the array processor has to operate with the received signals after the despreading, what makes the array sensitive to the direct and reflected GNSS signals thanks to the processing gain of the DS-SS system. Furthermore, processing the despread signals, instead of directly the received ones, has the advantage that the array processor handles a low-rate data stream. In that paper, a linearly constrained beamformer that sets nulls in the directions of arrival (DOA) of the undesired signals and gain one for the LOSS appears to be an effective choice. Thus, the design of an appropriate beamformer comes down to a DOA estimation problem, which is a challenging task in coherent scenarios. The high degree of

coherence between the LOSS and the reflections makes conventional DOA estimation algorithms (e.g., MUSIC, minimum variance method) and conventional beamformers (e.g., MVDR beamformer) completely fail [Pil89, Joh93]. All these methods only work properly if the signals are decorrelated using, for instance, the spatial smoothing technique, which has two serious drawbacks: it reduces the array aperture (the resolution worsens) and is restricted to arrays formed by several identical translated subarrays. To overcome the limitations imposed by the spatial smoothing it is possible to apply other DOA estimation algorithms that work with correlated signals, such as the generalized MUSIC [Zol86] and the maximum likelihood DOA estimator by alternating projection [Zis88]. The former requires multidimensional optimizations over the DOAs of sets of coherent sources, whereas the latter brings forward an iterative algorithm that transforms a multivariate nonlinear optimization problem into a sequence of much simpler one or two-dimensional problems. Despite the good results reported in [Sec96], these algorithms have several drawbacks that prevent them from being a definitive solution: the computational load may be too high because spectral searches need to be performed, they can only cope with specular multipath, and the number of received signals has to be bounded by the number of antennas. Moreover, the performance of the methods based on DOA estimation is suboptimal since they do not exploit the temporal structure of the signals. The methods developed in this thesis aim at overcoming all these drawbacks and also the limitations of the spatial smoothing technique.

To our knowledge, very few papers about the cancellation of multipath in GNSS using antenna arrays have been published. Some of these papers, apart from the author's work, are: [Moe97, Ray98, Ray99a, Ray99b]. In [Moe97] two techniques are proposed. The first simply averages the code and carrier measures obtained at different antennas, while the second one uses a nulling beamformer computed from the estimated DOAs of the multipath signals. The conventional MUSIC algorithm is applied to estimate the DOAs. The basic idea behind this second technique is very similar to that employed in [Sec96], but it is much less developed because many problems, such as the coherence of the signal scenario and the presence of external interferences, are not addressed. A different method is proposed in [Ray98, Ray99a] to estimate the parameters (amplitude, phase and DOA) of a single reflection which tries to model all the actually received reflections. To this end, the actual phase evolution along the aperture is compared with the theoretical phase evolution when only the LOSS and one reflection are received, assuming that the direction of arrival of the direct signal and the array attitude are known. In [Ray99b], the previous method is extended in order to take also into account the evolution of the pseudorange and signal-to-noise ratio. Since these algorithms deal with the phases, and possibly pseudoranges and SNR measurements, instead of the received signals, the estimation process is highly non-linear; and they are not signal processing techniques but data processing ones, though they can work in real-time. Moreover, none of these methods mitigates the interferences.

Unlike navigation systems, the employ of antenna arrays in wireless communication systems has arisen lately great interest since the multiple benefits they provide (e.g., interference suppression, fading diversity, transmit diversity) ultimately result in an improvement of the system capacity, coverage and quality. A number of techniques that exploit antenna arrays for synchronization have been developed, each differing from the others on its assumptions regarding multipath, CCI (co-channel interference), signal parameterization, and computational load. One of the first such techniques was presented in [Bre82] for DS-CDMA systems, in which a least-squares beamformer is calculated for each possible location of the desired user's codeword over one symbol period, assuming no transition has occurred between consecutive symbols. A similar approach was presented in [Lea96] for TDMA communication systems, using a minimum mean-squared error (MMSE) beamformer calculated for each possible position of a training sequence in a given frame of data. The beamformer that results in an output that is the most strongly correlated with the training sequence is used to cancel CCI and any uncorrelated multipath. The guard intervals present in such systems are also included in order to remove CCI not present during the training interval. More recently, this approach has been revised and extended to better deal with CCI [Kee98], and to handle very short bursts of training data [Kuz99]. In this last paper, the ill-definition of the problem is avoided by regularizing the MMSE criterion with a constant modulus condition.

Other researchers have taken a parameter estimation point of view, attempting to determine the direction of arrival and time delay of each arrival of a given signal at the array. These techniques exploit the full space-time structure of the multipath, but many of them do not take CCI into account. The methods of [Vee98, CT99] do not operate directly on the data; instead, they assume that the channel matrix has been estimated in a previous step. The DOAs and time delays are then determined by fitting the model to the estimated channel. While suboptimal, the advantage of this approach is that in certain cases, the channel estimate may be obtained blindly, without the need for training data. In case a training sequence is available, it can be used to obtain a least-square estimate of the channel. The algorithm of [CT99] requires either a multidimensional (MD) search, or a series of suboptimal 1-D searches, while that of [Vee98] assumes an array composed of shift-invariant subarrays (e.g., a uniform linear array (ULA)) and achieves closed-form estimates using a 2-D version of the ESPRIT technique [Roy86]. Since in the 2-D ESPRIT the time delay and DOA estimations are decoupled, the time delays can be computed even without knowledge of the array manifold [Van98]. However, the estimates obtained with the method of [Vee98] are slightly biased and in general do not achieve the Cramér-Rao Bound. The exploitation of the shift-invariances present in the data is carried one step further in [Haa98], where a uniform rectangular array is used to estimate both azimuth and elevation DOAs along with the time delays using a 3-D ESPRIT implementation. It should be noted that [Haa98] works directly on the received data to estimate the parameters in a single step.

A maximum likelihood (ML) approach is taken in [Ced96, Wax97, Ber99, Fle99], in which both the interference and noise are modeled together as a temporally white Gaussian process. The methods of [Wax97, Ber99, Fle99] also assume spatial whiteness, so only [Ced96] is able to combat the CCI. Actually, the work of [Ber99] is the extension of the well-known ML DOA estimator in [Zis88] to a space-time manifold parameterized by the DOA and the time-delay. The same concept of space-time manifold was already employed in [Ral98, Van98], and is further extended to include polarization information in [Des99] using a well-known linear decomposition of the array steering vector [Fer83]. The conceptual resemblance between the space-time manifold and the space-only manifold employed in DOA estimation problems makes straightforward the extension of some DOA estimators, such as the subspace fitting family [Ott93], to the delay-DOA estimation problem. In [Pel99], the joint angle and delay estimation problem is solved via weighted least squares (WLS), where the weighting matrices are designed to account for spatial color, array calibration errors, etc. While offering some claim to optimality, the primary drawback of the ML and WLS approaches is that complicated search procedures are required to estimate the desired parameters.

To obtain DOA estimates of each arrival, the parametric approaches described above must assume the availability of a calibrated antenna array, and a single arrival at each time delay. Errors in the array calibration or deviations of the array from uniformity are inevitable, and can lead to significant performance degradation. Furthermore, in multipath-rich propagation environments, there may be numerous arrivals at each delay due to local scattering near the array. To overcome these difficulties, an unstructured parameterization of the spatial response can be used, as in [Swi98a]. While this leads to an increase in the number of parameters to be estimated, the model is linear in the additional parameters, and they can be estimated in closed form. Once the spatial parameters are eliminated from the ML criterion in [Swi98a], the time delays are solved for iteratively using either IQML [Bre86] or MODE [Sto90c, Sto90b]. A suboptimal delay estimator based on ESPRIT is also presented in [Swi98a]. These techniques have recently been extended in [Swi99] to the blind case where no training data is available, although without exploiting additional knowledge about the signal (e.g., known pulse shaping), an absolute time base cannot be established in this case. Note that [Swi98a, Swi99] both assume spatially and temporally white noise, and thus are not suited for situations involving strong CCI. If the desired signal is digitally modulated with a known pulse shape, the iterative method of [Pel98b] can be used to account for spatially colored interference via prewhitening. The algorithm presented in [Ast99b] also allows for interference with arbitrary unknown spatial color as well as an unstructured array response for the desired signal, although it assumes a slightly different temporal model. Instead of modeling the multipath arrivals using arbitrary delays, the arrivals are assumed to occur on a uniformly spaced time-domain grid with an unknown starting location. This model leads to an ML solution requiring only a 1-D search for the starting position of the training sequence.

Other work has focused on the special nature of the synchronization problem in various applications. The use of antenna arrays in code timing recovery for CDMA applications has been addressed in [Bre82] as mentioned above, and more recently in [Dlu89, Liu98a, Jak98a, Che99]. Each of these approaches estimates the code timing for one user at a time while treating the multiple access CCI as Gaussian interference with unknown spatial color. In [Dlu89, Liu98a] the interference is restricted to be temporally white, while the other methods allow for CCI with unknown temporal color. The methods described in [Dlu89, Jak98a] assume flat fading and an unstructured spatial response model for the desired user, and use a maximum likelihood approach that leads to a simple 1-D search for the location of the user's codeword. The algorithm in [Dlu89] is general enough for either case, but it operates using only one symbol's worth of data, and the time delay is restricted to be an integer multiple of the chip period. The estimator in [Jak98a] is blind, but is also derived using only one symbol's worth of data; however, an *ad hoc* extension to several symbols is proposed. The approach described in [Liu98a] also assumes flat fading and an unstructured array response, but it resorts to an unnecessary asymptotic approximation of the ML criterion to achieve a 1-D parameter search. However, [Liu98a] does present a method for transforming the 1-D search for the time delay into rooting a second order polynomial if the chip-shaping pulse is rectangular. As an alternative to the above approaches, [Che99] assumes a uniform linear array and processes the data in the frequency domain to estimate the DOAs and time delays of all of the desired user's multipath arrivals via 2-D ESPRIT, while a pseudo-Procrustes-ESPRIT algorithm [Ram95] is used in [Ram00] to estimate the time delays. The review of the synchronization in DS-CDMA communication systems continues in the introduction of Chapter 5.

Finally, we also mention the work of [Bel96, Jak98b, Dog99], which focus on exploiting antenna arrays not only for estimation of multipath time delays, but also Doppler shifts as well. In [Bel96] the Expectation-Maximization (EM) algorithm is employed, while in [Jak98b] ML and signal/noise subspace fitting estimators are proposed. A rather general study about the ML estimation of signal parameters in unknown spatially correlated noise can be found in [Dog00]. The ML estimator presented therein can be particularized for specific scenarios resulting in estimators already proposed in the literature. However, efficient optimization methods are not addressed and the computation of the estimates involves a search in a large-dimensional space.

## 2.4 Examples of GNSS Signals

This section offers a brief survey of the parameters, especially concerning the transmitted signals, of the GPS, GLONASS and GALILEO systems. Although the methods presented in the following chapters are rather general, this description is appropriate to contextualize this thesis. To start with GPS, its nominal constellation consists of 24 satellites, placed in 6 nearly circular

orbital planes with 60° separation in right ascension of the ascending node. Each plane contains 4 satellites which are not uniformly spaced. The orbits are inclined 55° and their altitude is about 20200km (26600km radius), which results in a period of half sidereal day. Each GPS satellite transmits navigation signals at two frequencies: L1=154×10.23 MHz and L2=120×10.23 MHz. The L1 carrier is modulated in quadrature by the C/A (coarse/acquisition) and P (precision) codes. Both are binary codes (i.e., they take the values $+1, -1$), and are the pseudo-noise codes employed to spread the spectrum. Therefore, the resulting signals are DS-SS signals. All the GPS satellites transmit continuously and employ the same frequency bands, but utilize different codes, which means that the multiplexing technique is CDMA. The L2 carrier is modulated by either the P code or the C/A code. Normal operation would provide P-modulation on the L2 signal.

The C/A code is a Gold sequence with period $P_0 = 1023$ chips (i.e., it is generated with two feedback shift-registers of 10 cells each), and chip rate equal to 1.023 Mchips/s. Thus, a period of the C/A code last 1 millisecond. The P code is faster and much longer than the C/A code. The chip rate of the P code is 10.23 Mchips/s, and its length is $2.3547 \cdot 10^{14}$ chips, which corresponds to a time span of approximately 266.4 days. The total length code is partitioned into 37 one-week segments, and each segment is assigned to a satellite during one week. Direct synchronization to the P code is impossible due to its length, so the receivers have to synchronize first to the C/A code and next to the P code. However, the P code is usually encrypted, and in this case it receives the name of P(Y) code. The encryption, which is named Anti-Spoofing (AS), consists in the module-2 addition of the P code with a W code known only by authorized users. Therefore, civil users have only access to the C/A code. There are, however, on the market *codeless* receivers capable of making certain measures at L2 without knowledge of the P(Y) code [HW97], though with an important deterioration. The L1 carrier is also modulated by a very low data-rate binary sequence named navigation message. The L2 signal may or may not be modulated by this sequence. Since the navigation message is transmitted at 50 bits/s, the spreading factor of the data spread with the C/A code is $P = 1.023 \cdot 10^6/50 = 20 \times 1023$, while the spreading factor is 10 times higher if the P code is used. The navigation message provides the user with the data needed to perform the navigation computation: clock and position of the satellite, atmospheric corrections, etc. The clock and the position information are received every 30 seconds (the duration of one frame). The message also includes information that makes possible the synchronization of the P code by indicating portion of this code that is transmitted by the satellite. About 3% of bits of the navigation message are known (training bits). Indeed, the redundancy is greater, since many bits, yet initially unknown, are repeated between frames or subframes (see [Par96a, ch. 4, vol I] for a detailed description of the navigation message).

The minimum specified received power of the L1 C/A signal for a user employing a 0dBic antenna for a satellite at elevation angles above 5° is -160dBW. If, as a simple example, the equivalent noise temperature of the reception chain is 290K, the noise spectral density is $N_0 =$

$-204$dBW/Hz, and thus the carrier-to-noise spectral density ratio is $CN_0 = 44$dB-Hz. The actual received $CN_0$ may vary with respect to this value due to many factors (e.g., variation of the satellite transmitted power, antenna gain, polarization losses, foliage attenuation, reduced path loss at high elevation angles, etc.), and the usual range of $CN_0$ is approximately 40–55dB-Hz. With $CN_0 = 44$dB-Hz, the signal-to-noise ratio (SNR) in a bandwidth of 1.023MHz is -16dB; similarly, if the bandwidth is taken as 20.46MHz, then the SNR is -29dB. This last value of the bandwidth is meaningful because it is exactly the transmit bandwidth of the GPS satellites at both the L1 and L2 bands. In any case, it is apparent that the received GPS signals are completely buried, even at their spectral peaks, by the additive noise. The spreading gain of the GPS, also of the other navigation systems, is very large. In particular, it is $10\log(P) \approx 43$dB for the C/A code, and is 10dB higher for the P code. Consequently, if the received SNR is -16dB, after despreading it becomes 27dB (as a first approximation).

The effect of multiple access interference (MAI) does not need special consideration in GPS because the signals from different satellites are received with similar powers (absence of near-far effect) and because the PN codes are very long. That is to say, the inherent spreading gain of the DS-SS signals suffices to attenuate the MAI to negligible levels. As a matter of fact, it is shown in [Par96a, ch. 3, vol. I] that MAI introduces in the C/A signal only 0.8dB degradation relative to the thermal noise when $CN_0$=45.2dB, 11 satellites are in view and the power received from all of them is the same.

GPS is almost a quarter century old, so the U.S. is moving ahead to modernize the system. Part of that planned effort is the inclusion of the C/A code on the L2 frequency and the addition of a new civil frequency (L5) centered at 1176.45MHz. C/A on L2 will constitute a second non-safety-critical civil signal. It will support direct acquisition of the L2 signal during situations where the L1 signal may not be available, such as in cases of interference, and will improve the ionospheric delay correction for civilian users. The new signal on L5 meets the needs of critical safety-of-life applications such as civil aviation. This signal will have increased power (+6dB) relative to L1, two different channels in quadrature, a 24MHz bandwidth allocation, and the potential for more accurate pseudorange resolution than can be obtained with the current C/A and P codes. The proposed codes on L5 have a rate equal to 10.23Mchips/s and code length between 4000 and 10.230 bits. To take full advantage of L5, it is planned to transmit two signals in phase quadrature, only one of which would carry data modulation. All of this ensures a signal that is very robust and very resilient against pulsed interference sources. And, most importantly, the L5 frequency will allow dual widelaning. This will provide a major improvement to reliable, single-epoch, carrier-phase positioning.

The nominal GLONASS constellation consists of 24 satellites, uniformly located in three orbital planes $120^o$ apart in right ascension. Unlike GPS, the actual GLONASS constellation may have less than 24 satellites due to budget cuts. The orbits are circular with $64.8^o$ inclination

and 19100km altitude. Each satellite transmits at two bands: L1 between 1602.5625MHz and 1615.5MHz, and L2 between 1246.4375 and 1256.5MHz. Instead of using CDMA as GPS, GLONASS is based on Frequency Division Multiple Access (FDMA), and hence all the satellites can employ the same codes. The C/A code has a chip rate of 511Kchips/s and modulates the L1 and L2 carriers, whereas the restricted-access P code, with chip rate 5.11MHz, modulates only the L2 carrier. The navigation message is a 50bits/s data stream, as in GPS.

The study in [Sch98a] provides guidelines for the design of the signal and constellation of the future GALILEO system. One of the targets in the design is to achieve a User Equivalent Range Error (UERE) on the order of 1-2 meter with single carrier ranging and 1-2 cm with three-carrier differential phase positioning techniques. There are basically two options for the constellation. The first is a regional constellation formed by inclined geosynchronous and geostationary satellites, whereas the second is a global constellation of medium orbit satellites. The multiple access technique will be CDMA, which is preferred in front of a hybrid CDMA/FDMA solution; and three carrier frequencies will be used. The possible candidates are: 1589.742, 1561.098, 1256.244, 1598.949, 1250.106 and 5014.746MHz. The data broadcasting capabilities will be increased to 1.5, 3 and 24 Kbits/s. Since each satellite will transmit several signals, different data rates could be used by different signals. In general complex spreading codes will be considered, with rates 3.069, 15.345 and 24.552 Mchips/s. A significant characteristic is the use of the Nyquist square-root raised-cosine pulse with roll-off factor equal to 0.2 as chip shaping waveform. This fact contrasts with the lack of chip shaping in GPS, which amounts to using "nearly" rectangular pulses. The study of [Sch98a] has proven that DS-SS signals with square-root raised-cosine chip-shaping provide a timing jitter reduction compared with the conventional rectangular shaping for a given $CN_0$ and available bandwidth. Finally, coding and interleaving of the data are also proposed in order to counteract certain effects, such as fading, of the channel.

## 2.5 Array Signal Model

In this section, a general signal model for the signals received by an antenna array is presented along with some assumptions made throughout this thesis. This is intended to avoid the repetition of some descriptions in the following chapters. The general model presented herein corresponds basically to the ones used in Chapters 3-4. Nonetheless, the explanation or justification of some concrete hypothesis are deferred to the corresponding chapters. Finally, the relationship between the model and the actual received signals is analyzed.

### 2.5.1 General Signal Model

We assume that an arbitrary $m$ element array receives $d$ scaled and delayed replicas of a known signal $s(t)$. The baseband array output is modeled as the $m \times 1$ complex vector

$$\mathbf{y}[n] = \sum_{k=0}^{d-1} \boldsymbol{\alpha}_k s(nT_s - \tau_k) + \mathbf{e}[n] \ , \tag{2.14}$$

where $T_s$ is the sampling period, $\boldsymbol{\alpha}_k \in \mathcal{C}^m$ and $\tau_k$ are the spatial signature and time delay of the $k$th arrival, and $\mathbf{e}[n] \in \mathcal{C}^m$ represents additive noise and all other disturbing terms. We may write (2.14) in matrix form as follows:

$$\mathbf{y}\,[n] = \mathbf{A}\,\mathbf{s}\,[n, \boldsymbol{\tau}] + \mathbf{e}\,[n] \ , \tag{2.15}$$

where

$$\boldsymbol{\tau} = [\tau_0 \ \cdots \ \tau_{d-1}]^T \qquad d \times 1 \tag{2.16}$$

$$\mathbf{A} = [\boldsymbol{\alpha}_0 \ \cdots \ \boldsymbol{\alpha}_{d-1}] \qquad m \times d \tag{2.17}$$

$$\mathbf{s}[n, \boldsymbol{\tau}] = \left[ \ s\,(nT_s - \tau_0) \quad s\,(nT_s - \tau_1) \quad \cdots \quad s\,(nT_s - \tau_{d-1}) \ \right]^T \qquad d \times 1 \ . \tag{2.18}$$

If $N$ samples are collected from the array, they all may be grouped together into the following $m \times N$ matrix equation:

$$\mathbf{Y} = \big[\mathbf{y}[1] \ \ \mathbf{y}[2] \ \ \cdots \ \ \mathbf{y}[N]\big] = \mathbf{A}\,\mathbf{S}\,(\boldsymbol{\tau}) + \mathbf{E} \ , \tag{2.19}$$

where $\mathbf{S}\,(\boldsymbol{\tau}) \in \mathcal{C}^{d \times N}$ and $\mathbf{E} \in \mathcal{C}^{m \times N}$ are formed identically to $\mathbf{Y}$.

It is clear from the above model that we are invoking the standard "narrowband assumption" common to many array signal processing problems; i.e., we assume that the time required for the signal to propagate across the array is much smaller than its inverse bandwidth. As such, a phase shift can be used to describe the effect of the propagation from one antenna to the next. This assumption is natural for the parameters of the navigation systems, since the bandwidth of the GNSS signals is on the order of some MHz, while the size of the array (e.g., less than ten wavelengths) is smaller than a few (e.g., two) meters given a carrier frequency on the order one or two GHz. The $l$th element of $\boldsymbol{\alpha}_k$, denoted by $[\boldsymbol{\alpha}_k]_l$, represents the amplitude of the $k$th replica at the $l$th antenna, and gathers all the effects of the attenuation and phase shift during propagation, the transmitted power, the reception pattern of the antenna, etc. Hence, the argument of $[\boldsymbol{\alpha}_k]_l$ is the value of the carrier phase of the $k$th signal at the corresponding antenna. The narrowband model does not introduce necessarily an error in the value of the carrier phases. Since each baseband signal is represented with the same delay $\tau_k$ in all the antennas, this introduces an uncertainty in the value of the time delay equal to the propagation time across the array. However, this uncertainty is always neglected because its value is smaller than the standard deviation of the time delay estimates caused by other disturbing effects.

An additional technical assumption is needed for the asymptotic results presented in next chapters.

**Assumption A1**: $s(t)$ is a band-limited finite-average-power signal, and is sampled above the Nyquist rate. Therefore, its analog autocorrelation function

$$c_{ss}(\tau) = \lim_{T_{obs}\to\infty} \frac{1}{T_{obs}} \int_{T_{obs}} s(t+\tau)\, s^*(t)\, dt \tag{2.20}$$

is assumed to be continuous with continuous derivatives. Since the sampling period $T_s$ satisfies the Nyquist criterion, then

$$\lim_{N\to\infty} \frac{1}{N} \sum_{N} s(nT_s - \tau_l)\, s^*(nT_s - \tau_k) = c_{ss}(\tau_k - \tau_l) \ . \tag{2.21}$$

The next assumption involves the statistical characterization of the signal, which is necessary for the formulation of maximum likelihood methods.

**Assumption A2**: Since the "noise" $\mathbf{e}[n]$ may include in general the contribution of several phenomena, we model it as a complex, circularly symmetric Gaussian vector process. It is moreover assumed to be zero-mean, temporally white, and with spatial correlation matrix $\mathbf{Q}$; that is,

$$\mathrm{E}\{\mathbf{e}[n]\} = \mathbf{0}, \qquad \mathrm{E}\{\mathbf{e}[n]\ \mathbf{e}^T[l]\} = \mathbf{0}, \qquad \mathbf{R}_{ee}[n-l] = \mathrm{E}\{\mathbf{e}[n]\ \mathbf{e}^*[l]\} = \mathbf{Q}\,\delta_{n,l}\ . \tag{2.22}$$

The estimators derived with the assumption of temporally white noise undergo certain degradation if the noise is actually colored, but they retain the capacity of spatially mitigating the undesired signals. Moreover, the hypothesis of temporal whiteness is not as restrictive as it could seem at first glance, because some other cases can be transformed into this one. In this section and in the next one, we briefly comment on other temporal models of the noise, but it should be kept in mind that, unless otherwise stated, in the following chapters the noise model that we consider to be valid is that in assumption (**A2**). For example, let us now consider that $\mathbf{e}[n]$ is a wide-sense stationary process with a correlation that can be split into a spatial correlation matrix $\mathbf{Q}$ and into a temporal correlation sequence $t[n]$, i.e.,

$$\mathbf{R}_{ee}[n-l] = \mathbf{Q}\, t[n-l] \ . \tag{2.23}$$

Then, the signals are made temporally white by multiplying with a decorrelating matrix, that is to say, $\mathbf{Y}$ and $\mathbf{S}(\boldsymbol{\tau})$ are replaced by $\mathbf{Y}\,\mathbf{T}^{-\frac{1}{2}}$ and $\mathbf{S}(\boldsymbol{\tau})\,\mathbf{T}^{-\frac{1}{2}}$, respectively, where

$$\mathbf{T} = \begin{bmatrix} t[0] & t[1] & \cdots & t[N-1] \\ t[-1] & t[0] & \cdots & t[N-2] \\ \vdots & & \ddots & \vdots \\ t[1-N] & t[2-N] & \cdots & t[0] \end{bmatrix} . \tag{2.24}$$

The decomposition of the correlation in (2.23) means that the space-time correlation of vector vec $(\mathbf{E})$ is not completely arbitrary, but it can be expressed as the Kronecker product of two matrices: $\mathbf{T}^T \otimes \mathbf{Q}$. It is clear that in this prewhitening approach the sequence $t[n]$ has to be known or estimated. In [Jak98a], an approximate method for estimating $t[n]$ in the frequency domain is provided. A computationally attractive alternative to carry out the prewhitening is presented in [Swi98b]. It assumes a vector autoregressive (VAR) model for the temporal variation of the noise. This method can be used even when (2.23) is not satisfied, which means that the space-time correlation of the noise is completely arbitrary. In this situation, the computational advantage stems from the fact that a small number of VAR parameters need to be estimated, rather than a large number of temporal covariance lags. Once the VAR parameters are obtained, the signal is whitened by simply applying the inverse VAR filter. In [Swi98b], an algorithm for estimating the VAR parameters using data without the contribution of the desired signals is outlined. However, the extension of this algorithm to other situations is not clear.

Finally, note that the signals are only parameterized by the time delay, and not by the Doppler frequencies. This fact implicitly means that the signals are assumed to be approximately Doppler compensated (i.e., the Doppler frequency has been roughly estimated and corrected), which is an usual assumption in most works. The residual Doppler frequency has to be small compared with the reciprocal of the observation interval. Hence, the amplitudes of the signals, that is, the elements of $\mathbf{A}$ vary so slowly that can be taken as constant during one observation interval, although they can vary between different intervals. As a matter of fact, only the direct signal is necessarily required to satisfy the previous condition of the Doppler frequency. If the difference between the Doppler of one reflection and that of the direct signal is on the order of or greater than the reciprocal of the observation interval, then this reflection cannot be modeled by the signal component $\mathbf{A}\,\mathbf{S}(\boldsymbol{\tau})$ and is included in the noise term $\mathbf{E}$. This is the reason why the performance of the estimator presented in Chapter 4 improves when the residual Doppler frequencies of the reflections are large. The difference between the Doppler frequencies of the reflections and that of the direct signal depends on the geometry (satellite - receiver - reflectors) and on the velocity of the reflectors and the receiver [Nee92b].

### 2.5.2 Frequency-Domain Representation

Some methods presented in the next chapters take advantage of the special dependence of the signals upon the time delays when a frequency-domain representation is employed. The time-domain samples are transformed into the frequency domain using the Discrete Fourier Transform (DFT); that is to say, the DFT is applied to each row of $\mathbf{Y}$. Let $\mathbf{F}$ be the $N \times N$ unitary Fourier

matrix[1]; then, recalling (2.19), the frequency samples of the signal are

$$\mathbf{Y}_F \triangleq \mathbf{Y}\,\mathbf{F}^T = \big(\mathbf{A}\,\mathbf{S}\,(\boldsymbol{\tau}) + \mathbf{E}\big)\,\mathbf{F}^T = \mathbf{A}\,\mathbf{S}_F\,(\boldsymbol{\tau}) + \mathbf{E}_F\ , \tag{2.25}$$

where we have defined $\mathbf{S}_F(\boldsymbol{\tau})$ and $\mathbf{E}_F$ in an evident way. If the frequency bins are ordered so that their frequencies appear in increasing order, the signals satisfy the following relationship:

$$\mathbf{S}_F^*(\boldsymbol{\tau}) = \mathbf{S}_\omega^*\,\mathbf{V}(\boldsymbol{\tau})\ , \tag{2.26}$$

where $\mathbf{S}_\omega$ is a diagonal matrix whose entries are the DFT of the vector samples $[s\,(T_s)\,,\cdots,s\,(N\,T_s)]$, and

$$\mathbf{V}(\boldsymbol{\tau}) = \left[\ \mathbf{v}\,(\tau_0)\quad\cdots\quad\mathbf{v}\,(\tau_{d-1})\ \right] \tag{2.27}$$

$$\mathbf{v}\,(\tau_k) = \left[\ \exp\,(j\omega_1\tau_k)\quad\cdots\quad\exp\,(j\omega_N\tau_k)\ \right]^T \tag{2.28}$$

$$\omega_i = \frac{2\pi}{N\,T_s}\left(i-1-\left\lfloor\frac{N}{2}\right\rfloor\right)\ . \tag{2.29}$$

Actually, the transformation of the delays into linear phase shifts in (2.26) is only approximate. It is asymptotically (large N) exact whenever the sampling rate is above the Nyquist frequency. For a finite number of samples, it is exact only for certain special cases involving, for example, a periodic signal (if $(N-1)T_s$ is a multiple of the period) or a signal with finite time support, since a linear phase shift equals a circular shift of the time-domain samples. However, provided that $NT_s \gg \max_k \tau_k$ and that the Nyquist criterion is satisfied, the error induced by the finite length DFT is negligible (as illustrated by the simulation results), and the relation (2.26) will be taken as exact.

Since $\mathbf{F}$ is a unitary transform, if the noise is white in the time-domain, it is also white in the frequency-domain, and the spatial correlation matrix $\mathbf{Q}$ is exactly the same in both domains. In other words, if the columns of $\mathbf{E}$ satisfy the assumption (**A2**), then the columns of $\mathbf{E}_F$ satisfy the same assumption as well. Therefore, from the statistical point of view there is no difference between $\mathbf{E}$ and $\mathbf{E}_F$, and the maximum likelihood estimators can be indifferently applied to the time- or frequency-domain data. This is the reason why the same notation ($\mathbf{Y}$ and $\mathbf{S}(\boldsymbol{\tau})$) will be used in the following chapters for both domains. It should be clear from the context the cases in which only one domain is referred to because a specific dependence on the delays is to be exploited.

Let us now assume that the noise satisfies (2.23), instead of being white. The signals transformed into the frequency domain, after temporal prewhitening, would be: $\mathbf{Y}_F = \mathbf{Y}\,\mathbf{T}^{-\frac{1}{2}}\,\mathbf{F}^T$. It is well known that [Bri81]

$$\mathbf{F}\,\mathbf{T}^T\,\mathbf{F}^* \to \mathbf{D} \qquad \text{as} \quad N \to \infty\ , \tag{2.30}$$

[1] The $r,s$ th element of $\mathbf{F}$ is $1/\sqrt{N}e^{-j\frac{2\pi}{N}(r-1-\lfloor N/2\rfloor)\,(s-1)}$, for $r,s=1,\ldots,N$.

where $\mathbf{D}$ is a diagonal matrix whose entries are the Fourier Transform of $t[n]$ (that is, the power spectral density of a process with autocorrelation function $t[n]$) evaluated at the DFT frequencies. Expression (2.30) implies that asymptotically the columns of $\mathbf{E}\,\mathbf{F}^T$ are uncorrelated, and the spatial autocorrelation of any column is proportional to $\mathbf{Q}$. If we consider (2.30) to be also valid in the finite-sample case, which is a good approximation when the data record length $N$ is much greater than the effective duration of $t[n]$, it follows that the matrix that prewhitens and transforms the signals to the frequency domain is

$$\mathbf{T}^{-\frac{1}{2}}\,\mathbf{F}^T = \mathbf{F}^T\,\mathbf{D}^{-\frac{1}{2}}\ . \tag{2.31}$$

This last equation implies that the temporal prewhitening can be easily done after computing DFT, since it simple amounts to an appropriate scaling of the frequency bins.

### 2.5.3 Relationship with the Received Signals

In this section, we show how the general model sketched in Section 2.5.1 unifies the representation of the signals before and after the despreading operation. The expression of the signal received by a single antenna before the despreading, presented in (2.3), can be readily extended for an antenna array, as follows:

$$\mathbf{x}\,[n] = \mathbf{A}\,\mathbf{q}\,[n, \boldsymbol{\tau}] + \mathbf{w}\,[n]\ , \tag{2.32}$$

where $\mathbf{A}$ was defined in (2.17), $\mathbf{q}\,[n, \boldsymbol{\tau}]$ is constructed similarly to $\mathbf{s}\,[n, \boldsymbol{\tau}]$, and $\mathbf{w}[n]$ represents the disturbing components received at each antenna. The parallelism between (2.32) and the model in (2.15) is complete.

In order to formulate the signals after the despreading process, it is necessary to recall the expression of the DS-SS signal $q(t)$ given by (2.1) and (2.2). For clarity in the discussion, let assume the received signals are sampled twice per chip, i.e., $T_s = T_c/2$. Nevertheless, the development below can be easily extended to any sampling frequency equal to a rational fraction of the chip rate. We consider that the duration of the chip-shaping waveform, $g(t-\tau)$, is at most $(L-1)\,T_c/2$, with $L$ odd. Therefore, the whole contribution of the $l$th symbol, $d(l)$, in $q(t-\tau)$ is confined to the following set of $2P+L-2$ samples[2]:

$$\mathbf{q}_l\,(\tau) = \begin{bmatrix} q\big(lT - (L-1)\,T_c/4 - \tau\big) \\ q\big(lT - (L-3)\,T_c/4 - \tau\big) \\ \vdots \\ q\big(lT + (P-1)\,T_c + (L-1)\,T_c/4 - \tau\big) \end{bmatrix}\ . \tag{2.33}$$

[2] As it was explained in Section 2.1, $P$ is the spreading factor, i.e., the number of chips in one symbol.

This vector can be expressed as

$$\mathbf{q}_l^T(\tau) = d(l)\,\mathbf{g}^T(\tau)\,\mathbf{C} + d(l-1)\ldots + d(l+1)\ldots\,, \tag{2.34}$$

where the $L\times 1$ vector $\mathbf{g}(\tau)$ contains shifted samples of the shaping pulse and the $L\times(2P+L-2)$ Toeplitz matrix $\mathbf{C}$ is formed by the chips of the PN code as follows

$$\mathbf{g}(\tau) = \left[\begin{array}{cccc} g(-(L-1)T_c/4-\tau) & g(-(L-3)T_c/4-\tau) & \ldots & g((L-1)T_c/4-\tau) \end{array}\right]^T \tag{2.35}$$

$$\mathbf{C} = \left[\begin{array}{ccccccccccc} c(0) & 0 & c(1) & 0 & c(2) & \ddots & \ddots & 0 & 0 & 0 \\ 0 & c(0) & 0 & c(1) & 0 & \ddots & c(P-1) & \ddots & \ddots & \vdots \\ 0 & 0 & c(0) & 0 & c(1) & \ddots & 0 & c(P-1) & 0 & 0 \\ \vdots & \ddots & \ddots & \ddots & 0 & \ddots & c(P-2) & 0 & c(P-1) & 0 \\ 0 & 0 & 0 & 0 & \ddots & \ddots & 0 & c(P-2) & 0 & c(P-1) \end{array}\right]. \tag{2.36}$$

The value of $L$ has to be chosen large enough to assure that $\mathbf{q}_l(\tau)$ contains the totality (or the most) of the contribution of the $l$th symbol, what is equivalent to assuring that $\mathbf{g}(\tau)$ includes all the non-zero (or the significant) samples of the chip-shaping pulse. In order to prevent $L$ from being too large (i.e., much larger than the value determined by the actual duration of $g(t)$), the range of possible values of $\tau$ has to be limited to a few chip periods, which amounts to considering that a rough previous synchronization has been achieved. When processing the despread signals, we will assume that this previous synchronization has been already carried out. Since it is a very coarse synchronization (the time-delay error can be larger than $T_c$), it does not involves in general any difficulty.

In (2.34) only the contribution of the "central" symbol has been written explicitly; the terms corresponding to the adjacent symbols are negligible with respect to the central one given the large spreading factors employed by GNSS systems. The samples of $\mathbf{x}[n]$ in (2.32) received during the $l$th symbol interval (i.e., at the sampling points $lT-(L-1)T_c/4$, $lT-(L-3)T_c/4$, ..., $lT+(P-1)T_c+(L-1)T_c/4$) can be arranged in the following $m\times(2P+L-2)$ matrix

$$\mathbf{X}_l = \mathbf{A}\,\mathbf{Q}_l(\boldsymbol{\tau}) + \mathbf{W}_l\,, \tag{2.37}$$

where the columns of $\mathbf{W}_l$ are the vectors $\mathbf{w}[n]$ at the corresponding sampling instants, and

$$\mathbf{Q}_l(\boldsymbol{\tau}) = \left[\begin{array}{cccc} \mathbf{q}_l(\tau_0) & \mathbf{q}_l(\tau_1) & \ldots & \mathbf{q}_l(\tau_{d-1}) \end{array}\right]^T \qquad d\times(2P+L-2)\,. \tag{2.38}$$

Using (2.34), the matrix $\mathbf{X}_l$ can be written as

$$\mathbf{X}_l = d(l)\,\mathbf{A}\,\mathbf{G}(\boldsymbol{\tau})\,\mathbf{C} + \mathbf{V}_l\,, \tag{2.39}$$

where

$$\mathbf{G}(\boldsymbol{\tau}) = \left[ \begin{array}{cccc} \mathbf{g}(\tau_0) & \mathbf{g}(\tau_1) & \ldots & \mathbf{g}(\tau_{d-1}) \end{array} \right]^T \qquad d \times L \; . \tag{2.40}$$

To be exact, the matrix $\mathbf{V}_l$ is equal to $\mathbf{W}_l$ plus the negligible contribution of the "interfering" symbols $d(l-1)$ and $d(l+1)$. This description of the signals allows to formulate the despreading operation simply as the product by the matrix $\mathbf{C}^*/P$. Therefore, the signals despread during the $l$th symbol interval are

$$\mathbf{Y}_l = \frac{1}{P} \mathbf{X}_l \, \mathbf{C}^* = d(l) \; \mathbf{A} \, \mathbf{G}(\boldsymbol{\tau}) + \mathbf{E}_l \; , \tag{2.41}$$

where the "equivalent" noise term is $\mathbf{E}_l = \mathbf{V}_l \, \mathbf{C}^*/P$, and we have used that

$$\mathbf{C} \, \mathbf{C}^* \approx P \, \mathbf{I} \; , \tag{2.42}$$

which is a very good approximation for the long PN codes used in GNSS. If the columns of $\mathbf{V}_l$ satisfy the assumption (**A2**) (see Section 2.5.1) with a spatial correlation matrix denoted as $\mathbf{Q}_V$, it is easy to show that, thanks to (2.42), the columns of $\mathbf{E}_l$ also satisfy the assumption (**A2**) with a spatial correlation matrix $\mathbf{Q} = \mathbf{Q}_V/P$. Next, considering that the observation interval spans $M$ symbol intervals, the matrices $\mathbf{Y}_l$, ..., $\mathbf{Y}_{l+M-1}$ given by (2.41) can be concatenated as follows

$$\begin{aligned} \mathbf{Y} = \left[ \begin{array}{ccc} \mathbf{Y}_l & \ldots & \mathbf{Y}_{l+M-1} \end{array} \right] = \mathbf{A} \underbrace{\left[ \begin{array}{ccc} d(l) \; \mathbf{G}(\boldsymbol{\tau}) & \ldots & d(l+M-1) \; \mathbf{G}(\boldsymbol{\tau}) \end{array} \right]}_{\mathbf{S}(\boldsymbol{\tau})} \\ + \underbrace{\left[ \begin{array}{ccc} \mathbf{E}_l & \ldots & \mathbf{E}_{l+M-1} \end{array} \right]}_{\mathbf{E}} \; . \end{aligned} \tag{2.43}$$

As a consequence of this, comparing the equations (2.43) and (2.19), along with the fact that $\mathbf{E}_l$ also satisfies assumption (**A2**), it becomes clear that the general model of Section 2.5.1 can also represent the signals after the despreading operation. The number of columns of $\mathbf{Y}$ is $N = L \cdot M$. The underlying signal whose samples form $\mathbf{S}(\boldsymbol{\tau})$ in (2.43) is a finite-average-power signal, as required by assumption (**A1**), when $M \to \infty$ (but not when $L \to \infty$). Hence, the limit $N \to \infty$ involved by some the asymptotic results actually is $M \to \infty$. A final remark is that $\mathbf{S}(\boldsymbol{\tau})$ represents the contribution of only one of the DS-SS signals transmitted by a given satellite. The contributions of the signals transmitted by this satellite using other codes and/or other frequency bands, and those of the signals from other satellites are negligible thanks to the despreading operation (see the example concerning the effect of the MAI in Section 2.4); and in any case they can be included into the term $\mathbf{E}$ since they are uncorrelated with $\mathbf{S}(\boldsymbol{\tau})$.

Note that the despreading process, which consists in multiplying the received sampled signals by $\mathbf{C}^*/P$ (see equation (2.41)), can also be interpreted as filtering the analog received signals at

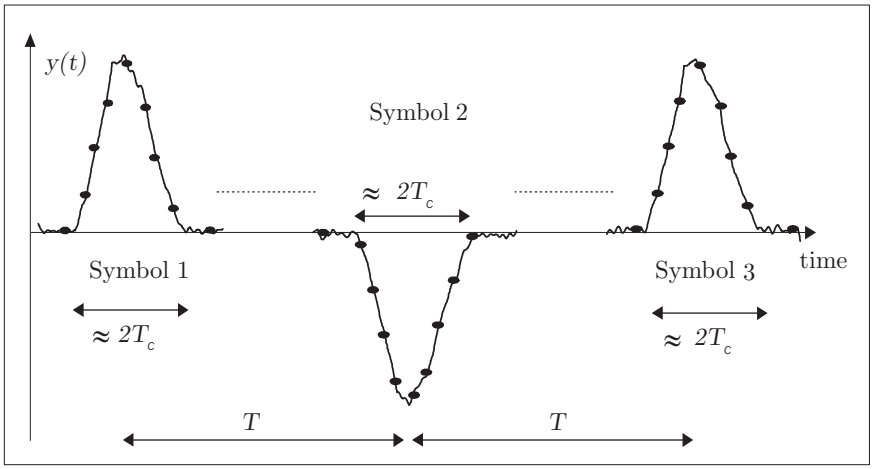


Figure 2.2: Qualitative example of the despread signals.

each antenna with the filter

$$h\left(t\right) = \sum_{n=0}^{P-1} c^{*}\left(n\right) \, \delta\left(t + nT_c\right) \ , \tag{2.44}$$

followed by sampling the output of this filter. This approach allows to consider any sampling frequency, since the output of $h(t)$ need not be sampled at a rational fraction of the chip rate. The output of this filter consists of train of pulses spaced $T$ apart (see Figure 2.2). Each pulse is usually named *finger*, and appears at the instant when the code of the incoming signal and the code of $h(t)$ are aligned. The coarse synchronization commented on above, which is needed to process the despread signals, is as simple as locating the fingers at the output of $h(t)$.

In general, processing the despread signals may have some advantages, apart from reducing the rate of the samples delivered to the array processor since $L \ll P$. Those advantages stem from the improvement of the SNR provided by the despreading process, and are specially manifest when the system is under-modeled (i.e., the assumed value of $d$ is smaller than the true one), as happens in Chapter 4.

The estimators proposed in the two following chapters require the knowledge of $\mathbf{S}(\boldsymbol{\tau})$ as a function of $\boldsymbol{\tau}$. Given the expression of $\mathbf{S}(\boldsymbol{\tau})$ in (2.43), this implies that the chip-shaping waveform $g(t)$ and the corresponding symbols have to be known. Actually, only the changes between symbols are needed, since it will be possible to include any unknown multiplicative constant of $\mathbf{S}(\boldsymbol{\tau})$ into the spatial signatures. During the transmission of training sequences, the receiver has an exact knowledge of the symbols. However, when data symbols are being transmitted, symbols' decisions (possibly differential) have to be used. This situation should not represent a serious limitation in real scenarios since the symbol error probability usually is very low [Par96a, Sch98a]. On the other hand, when the observation interval spans only one symbol (i.e., $M = 1$), the value of this symbol need not be known. As an exception to the

need for the knowledge of the symbols when $M > 1$, an estimator that does not require this information is outlined in Chapter 3.

# Chapter 3

# Time Delay Estimation of Multiple Replicas of a Signal

The goal pursued in this chapter is to present an asymptotically efficient approximation to the maximum likelihood estimator of the time delays of multiple replicas of a known signal received in a noise field with unknown spatial correlation. Several ways of deriving the new estimator are presented, and its performance is analyzed theoretically and using simulation results. The form of this estimator makes possible the use of computationally appealing optimization algorithms.

## 3.1 Introduction

The estimation of the parameters of multipath channels has arisen an important interest. These parameters can be used for a number of purposes: localization, adjusting a space-time RAKE receiver in the uplink, selective transmission in the downlink, etc. A rather exhaustive review of the techniques that exploit antenna arrays for estimating the channel parameters can be found in Section 2.3. Some work has focused on determining the direction-of-arrival (DOA) and time delay of each arrival of a given signal at the array; some examples are [Vee98, CT99, Ced96, Wax97, Ber99, Fle99]. Except for some cases that resort to a particular configuration of the antenna array [Vee98], the primary drawback of these approaches is that they lead to the optimization of multidimensional criteria. This is caused in part by the fact that the DOAs are estimated, which, on the other hand, is advantageous because it allows to fully exploit the spatial structure of the signals. Moreover, to obtain the DOA estimates it is necessary to have a calibrated antenna array, and a relatively small number of rays with a perfect pairing between time delays and DOAs. Errors in the array calibration are inevitable, and the latter assumption is unlikely to be valid in a multipath-rich propagation environment. The failure of these two assumptions can lead to significant performance degradation in practical

scenarios. Apart from gradient-search algorithms, other methods have been used to solve the multidimensional optimizations needed by the approaches above. The common thread of some methods is to split the initial problem into several problems of smaller dimensionality that are solved iteratively. For instance, the EM (Expectation Maximization) algorithm is employed in [Bel96], and a modification thereof, named SAGE (Space-Alternating Generalized Expectation-Maximization), is used in [Fle99]. The work of [Wax97] is based on the technique of alternating projections. Other optimization methods that have been proposed for the single-antenna estimators could be also applied to the multi-channel case. An example is the relaxation technique utilized in [Wu99a, Wu99b]. A different alternative to solve multidimensional problems is proposed in [Fuc98, Fuc99]. The search over the parameter space is replaced by an overdetermined deconvolution approach which is regularized by a criterion that introduces parsimony in the representation of the data. The result is a linear or quadratic programing problem.

To alleviate the difficulties associated with the estimation of the directions of arrival and to avoid the optimization multidimensional functions, two key modeling features are introduced in [Swi98a], namely: *i)* the spatial signatures are taken as unstructured vectors, *ii)* the noise is considered to be spatially white. With these two assumptions, and interchanging the roles of space and time, the time delay estimation problem becomes formally identical to the more familiar framework of DOA estimation. Thus, using a frequency-domain representation of the signals, the computationally efficient algorithms IQML and ESPRIT can also be applied for time delay estimation. Since IQML and ESPRIT estimate all parameters jointly, these algorithms are believed to be less exposed to convergence difficulties than the EM and the alternating-projection methods. However, due to the assumption of spatial whiteness, the techniques in [Swi98a] are not suited for scenarios with strong CCI (co-channel interference). This is a clear limitation of these techniques, since it is always desirable that an antenna array should provide the receiver with certain interference mitigation capability. Therefore, in this chapter the approach of [Swi98a] is extended to the case of noise with arbitrary spatial correlation, in such a way that the resulting estimators are robust against the CCI. However, it is no longer possible to establish a parallelism between the usual ML DOA estimator and the ML time delay estimator in spatially correlated noise. The latter does not allow the use of simple minimization procedures. The main contribution of this chapter is a new estimator that is asymptotically efficient (and asymptotically equivalent to the ML solution), and whose form lends itself to minimization with the computationally attractive IQML and ESPRIT algorithms. Simulation results show that the new estimator and the ML one perform nearly identically, and both of them are very close to the Cramér-Rao bound even for small sample sizes.

The chapter is organized as follows. In the next section, the data model is briefly described. In Section 3.3, the maximum likelihood estimator for the previous data model is presented along with its statistical characterization. The new time delay estimator is introduced in Section 3.4, and systematic and heuristic derivations thereof can be found in Sections 3.5 and 3.6. The

application of IQML and ESPRIT to the new cost function is dealt with in Section 3.7, and simulation results are included in Section 3.8. It is sketched in Section 3.9 how the proposed estimator can be applied when the signal is composed of several portions which are known up to a scaling factor. Section 3.10 is concerned with a modification of the data model, so that it takes into account the propagation of the signal through a FIR channel. It is assumed that the arrivals are uniformly spaced, so only the first time delay needs to be determined. It is shown in Section 3.11 that the IQML algorithm can be applied in this case as well, and the time delay estimate is obtained by rooting a polynomial. Simulation results for the FIR channel are provided in Section 3.12. Finally, conclusions are drawn in Section 3.13.

## 3.2 Data Model

The data model employed in the first part of this chapter coincides exactly with the general model presented in Section 2.5.1. The principal equations are written below to facilitate the reading (for more details refer to the previous chapter). If an arbitrary $m$ element array receives $d$ scaled and delayed replicas of a known signal $s(t)$, the baseband array output can be expressed as the following $m \times 1$ vector:

$$\mathbf{y}\,[n] = \mathbf{A}\,\mathbf{s}\,[n, \boldsymbol{\tau}] + \mathbf{e}\,[n]\ , \tag{3.1}$$

where

$$\boldsymbol{\tau} = [\tau_0 \ \ \cdots \ \ \tau_{d-1}]^T \qquad d \times 1 \tag{3.2}$$

$$\mathbf{A} = [\boldsymbol{\alpha}_0 \ \ \cdots \ \ \boldsymbol{\alpha}_{d-1}] \qquad m \times d \tag{3.3}$$

$$\mathbf{s}[n, \boldsymbol{\tau}] = \left[\ s\,(nT_s - \tau_0) \quad s\,(nT_s - \tau_1) \quad \cdots \quad s\,(nT_s - \tau_{d-1})\ \right]^T \quad d \times 1\ . \tag{3.4}$$

The sampling period is $T_s$, $\boldsymbol{\alpha}_k \in \mathcal{C}^m$ and $\tau_k$ are the spatial signature and time delay of the $k$th arrival, and $\mathbf{e}[n] \in \mathcal{C}^m$ represents additive noise and all other disturbing terms. If $N$ samples are collected from the array, they all may be grouped together into the following $m \times N$ matrix equation:

$$\mathbf{Y} = \big[\mathbf{y}[1] \ \ \mathbf{y}[2] \ \ \cdots \ \ \mathbf{y}[N]\big] = \mathbf{A}\,\mathbf{S}\,(\boldsymbol{\tau}) + \mathbf{E}\ , \tag{3.5}$$

where $\mathbf{S}\,(\boldsymbol{\tau}) \in \mathcal{C}^{d \times N}$ and $\mathbf{E} \in \mathcal{C}^{m \times N}$ are formed identically to $\mathbf{Y}$.

Rather than parameterizing the array response $\boldsymbol{\alpha}_k$ in terms of one or more DOAs, we treat it as an unstructured deterministic vector. Note also that we assume that the received signal can be described by discrete arrivals with distinct delays. This is obviously an approximation, especially in the multipath rich environments often encountered in wireless communications. In situations where temporally and spatially diffuse arrivals are present, the above model is still quite reasonable since arrivals that have nearly the same delay $\tau$ (i.e., arrivals whose delays are

separated by less than the resolution of the estimator, due for example to a cluster of closely spaced scatterers) can be grouped together into a single term. The temporal spread in a given cluster and the total number of clusters $d$ will then depend on the bandwidth of the transmitted signal; the wider the signal bandwidth, the more clusters that may be necessary. The singular values of the data matrix $\mathbf{Y}$ formed from several snapshots of data can be used to determine $d$ for a given scenario.

This approach is advantageous from a modeling and estimation point of view, as it leads to algorithms with a more reasonable computational cost. In a fully parameterized model, the spatial signature would be decomposed as

$$\boldsymbol{\alpha}_k = \sum_{i=1}^{d_k} \alpha_{i,k} \mathbf{a}(\theta_{i,k}) \ , \tag{3.6}$$

where $\mathbf{a}(\theta)$ represents the far-field array response to a unit amplitude plane wave arriving from DOA $\theta$, and $d_k$, $\alpha_{i,k}$ and $\theta_{i,k}$ denote the total number of multipaths associated with arrival $k$, their complex amplitudes, and their DOAs, respectively. While perhaps more concise than assuming an unstructured $\boldsymbol{\alpha}_k$ (unless $d_k$ is large), such a model requires in general a more complicated estimator due its non-linear dependence on the DOA parameters. In addition, estimation of the DOAs necessitates that the array response $\mathbf{a}(\theta)$ be accurately calibrated, which is a problematic assumption. For these reasons, we feel that the use of an unstructured spatial response model leads to a much more practical approach. If DOA information is needed (e.g., in forming transmit beamformer weights for downlink communication in frequency division duplex communications systems), the directions can be determined from the estimated spatial signatures using a simple least-squares fit, provided that $d_k$ is not too large (i.e., $d_k < (m+1)/2$). See [Swi98a, Xu95] for more information on this approach.

Errors in the above model, together with the effects of background noise and co-channel interference, are all lumped together in the error term $\mathbf{e}[n]$. The CCI contribution to $\mathbf{e}[n]$ could be parameterized in some way, e.g., as several delayed versions of certain signal or as a finite alphabet sequence. However, taking the CCI structure into account in this way will lead to a search over a larger set of parameters which are of no interest, such as the finite alphabet sequences transmitted by the interferers. Instead of such a computationally demanding strategy, we model the CCI contribution, along with additive noise and model errors, as complex Gaussian. This assumption is primarily for modeling purposes, and allows us to develop a metric that takes the spatial covariance of the CCI into account. Thus, $\mathbf{e}[n]$ is modeled as a complex, circularly-symmetric, zero-mean Gaussian process. For simplicity the process is assumed to be temporally white. However, as in, e.g., [Li95, Ced96, Swi98b, Vib97, Ast99b, Dlu89, Liu98a, Mol98], the CCI is accounted for by modeling the process as *spatially* colored with an arbitrary unknown correlation matrix (assumption (**A2**) in Section 2.5.1):

$$\mathrm{E}\left\{\mathbf{e}[n]\mathbf{e}^*[l]\right\} = \mathbf{Q}\,\delta_{n,l} \ . \tag{3.7}$$

While such a model for $\mathbf{e}[n]$ is clearly only approximate, it captures the most significant effects of the noise and interference, and leads to tractable algorithms. The Gaussian hypothesis may be justified from different points of view. The usual one relies on the Central Limit Theorem based on the fact that many sources contribute to $\mathbf{e}[n]$, or it can simply be said that it is model that is expected to work. From a practical standpoint, assuming that the noise is Gaussian allows to deal with the ML estimator analytically. Although the resulting estimator is not optimum (or at least ML) unless the interferers are Gaussian, it is able to combat directional interferers independently of their particular statistics. As a result, we believe that the model used in this chapter offers an excellent compromise between model realism and computational complexity.

With the above mathematical model in hand, we can succinctly state the problem addressed in this work:

> **Problem P1** – Given $N$ snapshots of data in the matrix $\mathbf{Y}$ described by equations (3.1)-(3.5) and (3.7), estimate the spatial signatures $\mathbf{A}$ and time delays $\boldsymbol{\tau}$ of the arrivals, as well as the spatial covariance $\mathbf{Q}$ of the noise and interference.

As a final modeling issue, note that in the above discussion we have implicitly assumed that $d$, the number of rays or clusters (or also the length of the FIR channels in Sections 3.10–3.11), is known. Determining $d$ is a non-trivial problem that is beyond the scope of this thesis. A number of possibilities exist, including simple rank tests on $\mathbf{Y}$, use of the Minimum Description Length (MDL) [Ris78, Wax85] or Akaike's criterion (AIC) [Aka74], sequential tests based on the asymptotic distribution of a given criterion function [Vib91b, Ott93, Wu94, Pel98a] [Ran99, chapter 5], robust bootstrap techniques [Vib99], among many others.

## 3.3 Maximum Likelihood Estimator

Let $p(\cdot|\mathbf{Q})$ denote the probability density function (pdf) of a complex Gaussian vector with zero mean and covariance $\mathbf{Q}$. Under the previous model for $\mathbf{e}[n]$, the negative log-likelihood function[1] for $N$ observations of $\mathbf{y}[n]$ is given by

$$f_N(\boldsymbol{\tau}, \mathbf{A}, \mathbf{Q}) = -\sum_{n=1}^{N} \ln p\left(\mathbf{y}[n] - \mathbf{A}\mathbf{s}[n, \boldsymbol{\tau}] \,|\mathbf{Q}\right) \ . \tag{3.8}$$

The subscript $N$ is used to explicitly denote the number of data samples used to form the criterion. The maximum likelihood estimates of the parameters are those values that minimize (3.8). Making use of the expression for the complex Gaussian pdf [Kay93] and neglecting irrelevant additive and multiplicative constants, we obtain

$$f_N(\boldsymbol{\tau}, \mathbf{A}, \mathbf{Q}) = \ln|\mathbf{Q}| + \mathrm{Tr}\left\{\mathbf{C}(\boldsymbol{\tau}, \mathbf{A})\,\mathbf{Q}^{-1}\right\} \ , \tag{3.9}$$

[1] The likelihood function is simply the probability density function considered as a function of the parameters.

where

$$\mathbf{C}(\boldsymbol{\tau},\mathbf{A}) = \hat{\mathbf{R}}_{yy} - \mathbf{A}\hat{\mathbf{R}}_{ys}^{*}(\boldsymbol{\tau}) - \hat{\mathbf{R}}_{ys}(\boldsymbol{\tau})\mathbf{A}^{*} + \mathbf{A}\hat{\mathbf{R}}_{ss}(\boldsymbol{\tau})\mathbf{A}^{*} \tag{3.10}$$

$$\hat{\mathbf{R}}_{yy} = \frac{1}{N}\mathbf{Y}\mathbf{Y}^{*} \tag{3.11}$$

$$\hat{\mathbf{R}}_{ys}(\boldsymbol{\tau}) = \frac{1}{N}\mathbf{Y}\mathbf{S}^{*}(\boldsymbol{\tau}) \tag{3.12}$$

$$\hat{\mathbf{R}}_{ss}(\boldsymbol{\tau}) = \frac{1}{N}\mathbf{S}(\boldsymbol{\tau})\mathbf{S}^{*}(\boldsymbol{\tau})\ . \tag{3.13}$$

The minimization of (3.9) with respect to $\mathbf{Q}$ and $\mathbf{A}$ may be performed explicitly. Using standard matrix calculus results (see e.g., [Gra81, Bre78]), the gradient of the criterion with respect to $\mathbf{Q}$ is easily shown to be

$$\frac{\partial f_N(\boldsymbol{\tau},\mathbf{A},\mathbf{Q})}{\partial \mathbf{Q}} = \mathbf{Q}^{-1} - \mathbf{Q}^{-1}\mathbf{C}(\boldsymbol{\tau},\mathbf{A})\mathbf{Q}^{-1}\ , \tag{3.14}$$

from which it is clear that the ML estimate of $\mathbf{Q}$ is given by[2]

$$\hat{\mathbf{Q}}_{ML}(\boldsymbol{\tau},\mathbf{A}) = \mathbf{C}(\boldsymbol{\tau},\mathbf{A})\ . \tag{3.15}$$

Replacing $\mathbf{Q}$ in (3.9) with (3.15) and neglecting the resulting constant term yields

$$f_N(\boldsymbol{\tau},\mathbf{A}) = \ln\left|\hat{\mathbf{R}}_{yy} - \mathbf{A}\hat{\mathbf{R}}_{ys}^{*}(\boldsymbol{\tau}) - \hat{\mathbf{R}}_{ys}(\boldsymbol{\tau})\mathbf{A}^{*} + \mathbf{A}\hat{\mathbf{R}}_{ss}(\boldsymbol{\tau})\mathbf{A}^{*}\right| \tag{3.16}$$

$$= \ln\Big|\hat{\mathbf{R}}_{yy} - \hat{\mathbf{R}}_{ys}(\boldsymbol{\tau})\hat{\mathbf{R}}_{ss}^{-1}(\boldsymbol{\tau})\hat{\mathbf{R}}_{ys}^{*}(\boldsymbol{\tau}) + \Big(\mathbf{A} - \hat{\mathbf{R}}_{ys}(\boldsymbol{\tau})\hat{\mathbf{R}}_{ss}^{-1}(\boldsymbol{\tau})\Big)\hat{\mathbf{R}}_{ss}\Big(\mathbf{A} - \hat{\mathbf{R}}_{ys}(\boldsymbol{\tau})\hat{\mathbf{R}}_{ss}^{-1}(\boldsymbol{\tau})\Big)^{*}\Big| \tag{3.17}$$

$$\geq \ln\left|\hat{\mathbf{R}}_{yy} - \hat{\mathbf{R}}_{ys}(\boldsymbol{\tau})\hat{\mathbf{R}}_{ss}^{-1}(\boldsymbol{\tau})\hat{\mathbf{R}}_{ys}^{*}(\boldsymbol{\tau})\right|\ , \tag{3.18}$$

where in the second equation we have added and subtracted the term

$$\hat{\mathbf{R}}_{ys}(\boldsymbol{\tau})\hat{\mathbf{R}}_{ss}^{-1}(\boldsymbol{\tau})\hat{\mathbf{R}}_{ys}^{*}(\boldsymbol{\tau})\ .$$

We have used in writing (3.18) that the determinant is a nondecreasing function. This means that for any positive definite matrix $\mathbf{G}$ and any non-negative definite matrix $\Delta\mathbf{G}$, the determinant satisfies

$$\begin{aligned}|\mathbf{G} + \Delta\mathbf{G}| &= \left|\mathbf{G}(\mathbf{I} + \mathbf{G}^{-1}\Delta\mathbf{G})\right| \\ &= |\mathbf{G}|\left|\mathbf{I} + \mathbf{G}^{-1}\Delta\mathbf{G}\right| \\ &\geq |\mathbf{G}|\ ,\end{aligned}$$

since the eigenvalues of $\mathbf{I} + \mathbf{G}^{-1}\Delta\mathbf{G}$ are $\geq 1$. Note that the equality only holds for $\Delta\mathbf{G} = \mathbf{0}$. For every $\boldsymbol{\tau}$, the lower bound of (3.18) is clearly achieved if $\mathbf{A} = \hat{\mathbf{R}}_{ys}(\boldsymbol{\tau})\hat{\mathbf{R}}_{ss}^{-1}(\boldsymbol{\tau})$, so the ML estimates of $\mathbf{A}$ and $\mathbf{Q}$ may be expressed as

$$\hat{\mathbf{A}}_{ML}(\boldsymbol{\tau}) = \hat{\mathbf{R}}_{ys}(\boldsymbol{\tau})\hat{\mathbf{R}}_{ss}^{-1}(\boldsymbol{\tau}) \tag{3.19}$$

$$\hat{\mathbf{Q}}_{ML}(\boldsymbol{\tau}) = \hat{\mathbf{R}}_{yy} - \hat{\mathbf{R}}_{ys}(\boldsymbol{\tau})\hat{\mathbf{R}}_{ss}^{-1}(\boldsymbol{\tau})\hat{\mathbf{R}}_{ys}^{*}(\boldsymbol{\tau})\ . \tag{3.20}$$

[2]We assume that $N \geq m + d$ so that the matrix $\mathbf{C}(\boldsymbol{\tau},\mathbf{A})$ is invertible with probability one.

Although it is not explicitly adverted above, it is unequivocal that in order to obtain the ML estimates of $\mathbf{A}$ and $\mathbf{Q}$, (3.19)-(3.20) have to be evaluated at the ML estimate of the delays. The resulting criterion for $\boldsymbol{\tau}$ is then

$$f_N(\boldsymbol{\tau}) = \ln \left| \hat{\mathbf{R}}_{yy} - \hat{\mathbf{R}}_{ys}(\boldsymbol{\tau}) \hat{\mathbf{R}}_{ss}^{-1}(\boldsymbol{\tau}) \hat{\mathbf{R}}_{ys}^{*}(\boldsymbol{\tau}) \right| = \ln \left| \hat{\mathbf{Q}}_{ML}(\boldsymbol{\tau}) \right| \ . \tag{3.21}$$

Thus, the maximum likelihood estimate of the spatial signatures, $\hat{\mathbf{A}}_{ML}(\boldsymbol{\tau})$, is given by a least squares fit to the data, and the ML estimate of the spatial noise covariance, $\hat{\mathbf{Q}}_{ML}(\boldsymbol{\tau})$, is simply the sample covariance of the residuals. The delays for which the determinant of the sample covariance of the residuals is minimized are the estimates of the propagation delays.

Using the following standard properties of the matrix determinant:

$$|\mathbf{XZ}| = |\mathbf{X}| \cdot |\mathbf{Z}| \tag{3.22}$$

$$|\mathbf{I} - \mathbf{XZ}| = |\mathbf{I} - \mathbf{ZX}| \ , \tag{3.23}$$

where $\mathbf{X}$ and $\mathbf{Z}$ are appropriately dimensioned matrices, it is straightforward to show that

$$f_N(\boldsymbol{\tau}) = \ln \left| \hat{\mathbf{R}}_{yy} \right| + \ln \left| \mathbf{I} - \hat{\mathbf{R}}_{yy}^{-1} \hat{\mathbf{R}}_{ys}(\boldsymbol{\tau}) \hat{\mathbf{R}}_{ss}^{-1}(\boldsymbol{\tau}) \hat{\mathbf{R}}_{ys}^{*}(\boldsymbol{\tau}) \right| \tag{3.24}$$

$$= \ln \left| \hat{\mathbf{R}}_{yy} \right| + \ln \left| \mathbf{I} - \hat{\mathbf{R}}_{yy}^{-\frac{1}{2}} \hat{\mathbf{R}}_{ys}(\boldsymbol{\tau}) \hat{\mathbf{R}}_{ss}^{-1}(\boldsymbol{\tau}) \hat{\mathbf{R}}_{ys}^{*}(\boldsymbol{\tau}) \hat{\mathbf{R}}_{yy}^{-\frac{1}{2}} \right| \tag{3.25}$$

$$\triangleq \ln \left| \hat{\mathbf{R}}_{yy} \right| + \ln |\mathbf{I} - \mathbf{B}_N(\boldsymbol{\tau})| \ , \tag{3.26}$$

where we have defined $\mathbf{B}_N(\boldsymbol{\tau})$ in an obvious way. Note that the first term involving the determinant of $\hat{\mathbf{R}}_{yy}$ can be ignored when minimizing with respect to $\boldsymbol{\tau}$ since it is parameter independent. We will define $V_N(\boldsymbol{\tau})$ as the criterion obtained by ignoring the first term:

$$V_N(\boldsymbol{\tau}) = \ln |\mathbf{I} - \mathbf{B}_N(\boldsymbol{\tau})| \ .$$

Consequently, the proposed maximum likelihood synchronization approach can be summarized as in Table 3.1. Some properties of the algorithm are discussed below.

### 3.3.1 Consistency

The consistency of the ML time delay estimator follows from the fact that as $N \to \infty$, $V_N(\boldsymbol{\tau})$ converges with probability one and uniformly in $\boldsymbol{\tau}$ to its limiting value $V_\infty(\boldsymbol{\tau})$, which is minimized by the true values of the time delays (if certain condition is satisfied), denoted by the vector $\check{\boldsymbol{\tau}}$. In this section and in all the following ones involving asymptotic results, it is assumed that assumption (**A1**), presented in Section 2.5.1, is satisfied.

Now, we prove that the limiting criterion is minimized by the true delays. By (2.21), the

$$\hat{\boldsymbol{\tau}}_{ML} = \arg\min_{\boldsymbol{\tau}} V_N(\boldsymbol{\tau}) \tag{3.27}$$

$$= \arg\min_{\boldsymbol{\tau}} \ln|\mathbf{I} - \mathbf{B}_N(\boldsymbol{\tau})| \tag{3.28}$$

$$\mathbf{B}_N(\boldsymbol{\tau}) = \hat{\mathbf{R}}_{yy}^{-\frac{1}{2}} \hat{\mathbf{R}}_{ys}(\boldsymbol{\tau}) \hat{\mathbf{R}}_{ss}^{-1}(\boldsymbol{\tau}) \hat{\mathbf{R}}_{ys}^{*}(\boldsymbol{\tau}) \hat{\mathbf{R}}_{yy}^{-\frac{1}{2}} \tag{3.29}$$

$$\hat{\mathbf{A}}_{ML}(\boldsymbol{\tau}_{ML}) = \hat{\mathbf{R}}_{ys}(\hat{\boldsymbol{\tau}}_{ML}) \hat{\mathbf{R}}_{ss}^{-1}(\hat{\boldsymbol{\tau}}_{ML}) \tag{3.30}$$

$$\hat{\mathbf{Q}}_{ML}(\boldsymbol{\tau}_{ML}) = \hat{\mathbf{R}}_{yy} - \hat{\mathbf{R}}_{ys}(\hat{\boldsymbol{\tau}}_{ML}) \hat{\mathbf{R}}_{ss}^{-1}(\hat{\boldsymbol{\tau}}_{ML}) \hat{\mathbf{R}}_{ys}^{*}(\hat{\boldsymbol{\tau}}_{ML}) \tag{3.31}$$

Table 3.1: Summary of the Maximum Likelihood Synchronization Algorithm for Spatially Colored Noise and Interference.

limiting value of the cost function is

$$\begin{aligned} V_\infty(\boldsymbol{\tau}) &= \ln \left| \mathbf{I} - \mathbf{R}_{yy}^{-\frac{1}{2}} \mathbf{A} \mathbf{C}_{ss}(\check{\boldsymbol{\tau}}, \boldsymbol{\tau}) \mathbf{C}_{ss}^{-1}(\boldsymbol{\tau}, \boldsymbol{\tau}) \mathbf{C}_{ss}^{*}(\check{\boldsymbol{\tau}}, \boldsymbol{\tau}) \mathbf{A}^{*} \mathbf{R}_{yy}^{-\frac{1}{2}} \right| \\ &= \ln \left| \mathbf{I} - \mathbf{R}_{yy}^{-\frac{1}{2}} \mathbf{A} \mathbf{C}_{ss}(\check{\boldsymbol{\tau}}, \check{\boldsymbol{\tau}}) \mathbf{A}^{*} \mathbf{R}_{yy}^{-\frac{1}{2}} \right. \\ &\left. + \mathbf{R}_{yy}^{-\frac{1}{2}} \mathbf{A} \left( \mathbf{C}_{ss}(\check{\boldsymbol{\tau}}, \check{\boldsymbol{\tau}}) - \mathbf{C}_{ss}(\check{\boldsymbol{\tau}}, \boldsymbol{\tau}) \mathbf{C}_{ss}^{-1}(\boldsymbol{\tau}, \boldsymbol{\tau}) \mathbf{C}_{ss}^{*}(\check{\boldsymbol{\tau}}, \boldsymbol{\tau}) \right) \mathbf{A}^{*} \mathbf{R}_{yy}^{-\frac{1}{2}} \right| \end{aligned} \tag{3.32}$$

where $\mathbf{R}_{yy}$ is the limiting value of $\hat{\mathbf{R}}_{yy}$ and the $k,l$-th element of the matrix $\mathbf{C}_{ss}(\boldsymbol{\tau}, \boldsymbol{\lambda})$ is $c_{ss}(\lambda_l - \tau_k)$ (recall that $c_{ss}(\tau)$ was defined in (2.20)). At this point we have to use that the determinant is a nondecreasing function, and that the matrix

$$\mathbf{M}(\check{\boldsymbol{\tau}}, \boldsymbol{\tau}) = \mathbf{C}_{ss}(\check{\boldsymbol{\tau}}, \check{\boldsymbol{\tau}}) - \mathbf{C}_{ss}(\check{\boldsymbol{\tau}}, \boldsymbol{\tau}) \mathbf{C}_{ss}^{-1}(\boldsymbol{\tau}, \boldsymbol{\tau}) \mathbf{C}_{ss}^{*}(\check{\boldsymbol{\tau}}, \boldsymbol{\tau})$$

is non-negative definite because it is the Schur complement of $\mathbf{C}_{ss}(\boldsymbol{\tau}, \boldsymbol{\tau})$ in the following matrix [Hor85]:

$$\begin{bmatrix} \mathbf{C}_{ss}(\boldsymbol{\tau}, \boldsymbol{\tau}) & \mathbf{C}_{ss}^{*}(\check{\boldsymbol{\tau}}, \boldsymbol{\tau}) \\ \mathbf{C}_{ss}(\check{\boldsymbol{\tau}}, \boldsymbol{\tau}) & \mathbf{C}_{ss}(\check{\boldsymbol{\tau}}, \check{\boldsymbol{\tau}}) \end{bmatrix} = \lim_{N \to \infty} \frac{1}{N} \sum_{N} \begin{bmatrix} \mathbf{s}[n, \boldsymbol{\tau}] \\ \mathbf{s}[n, \check{\boldsymbol{\tau}}] \end{bmatrix} \begin{bmatrix} \mathbf{s}^{*}[n, \boldsymbol{\tau}] & \mathbf{s}^{*}[n, \check{\boldsymbol{\tau}}] \end{bmatrix}, \tag{3.33}$$

which is clearly non-negative definite. Therefore, the limiting cost function satisfies

$$V_\infty(\boldsymbol{\tau}) \geq \ln \left| \mathbf{I} - \mathbf{R}_{yy}^{-\frac{1}{2}} \mathbf{A} \mathbf{C}_{ss}(\check{\boldsymbol{\tau}}, \check{\boldsymbol{\tau}}) \mathbf{A}^{*} \mathbf{R}_{yy}^{-\frac{1}{2}} \right| = V_\infty(\check{\boldsymbol{\tau}}) \tag{3.34}$$

The equality in (3.34) holds if the Schur complement $\mathbf{M}(\check{\boldsymbol{\tau}}, \boldsymbol{\tau})$ is zero. This is only possible for $\boldsymbol{\tau} = \check{\boldsymbol{\tau}}$ if the following *non-ambiguity condition* is fulfilled: The matrix $\mathbf{C}_{ss}(\widetilde{\boldsymbol{\tau}}, \widetilde{\boldsymbol{\tau}})$ is positive definite for any vector $\widetilde{\boldsymbol{\tau}}$ of length $2d$ whose elements are all distinct. This condition recalls the one presented in [Vib95] for the estimation of directions of arrival with large arrays. The consistency of $\hat{\mathbf{A}}_{ML}$ and $\hat{\mathbf{Q}}_{ML}$ follows immediately from (3.30)-(3.31) and the consistency of $\hat{\boldsymbol{\tau}}_{ML}$.

### 3.3.2 Cramér-Rao Bound

Since the ML estimates of all of the parameters are consistent, they will also be asymptotically (large $N$, hereafter) efficient (i.e., their asymptotic covariance coincides with the Cramér-Rao bound (CRB)) [Leh83, section 6.4]. The CRB for the time delays is (Appendix 3.A)

$$\mathbf{CRB}^{-1}(\boldsymbol{\tau}) = 2\,\mathrm{Re}\left\{\left(\mathbf{D}(\boldsymbol{\tau})\,\mathbf{P}^{\perp}_{\mathbf{S}^*(\boldsymbol{\tau})}\,\mathbf{D}^*(\boldsymbol{\tau})\right) \odot \left(\mathbf{A}^*\,\mathbf{Q}^{-1}\,\mathbf{A}\right)^T\right\} \tag{3.35}$$

where

$$\mathbf{D}(\boldsymbol{\tau}) = \left[\begin{array}{ccc} \mathbf{d}\,(\tau_0) & \cdots & \mathbf{d}\,(\tau_{d-1}) \end{array}\right]^T \tag{3.36}$$

$$\mathbf{d}\,(\tau_i) = -\left[\begin{array}{ccc} \frac{d\,s(t)}{d\,t}\Big|_{T_s-\tau_i} & \cdots & \frac{d\,s(t)}{d\,t}\Big|_{NT_s-\tau_i} \end{array}\right]^T \tag{3.37}$$

$$\mathbf{P}^{\perp}_{\mathbf{S}^*(\boldsymbol{\tau})} = \mathbf{I} - \mathbf{P}_{\mathbf{S}^*(\boldsymbol{\tau})} = \mathbf{I} - \mathbf{S}^*(\boldsymbol{\tau})\left(\mathbf{S}(\boldsymbol{\tau})\mathbf{S}^*(\boldsymbol{\tau})\right)^{-1}\mathbf{S}(\boldsymbol{\tau})\,. \tag{3.38}$$

### 3.3.3 Computation of the Estimates

The complicated non-linear dependence of $V_N$ on $\boldsymbol{\tau}$, especially due to the presence of the determinant, implies that a multidimensional search is the only method that can be used to find the estimates. Although the search might be implemented in more sophisticated ways than brute force evaluation of the cost function on a multidimensional grid (using, for example, gradient methods, expectation-maximization, or alternating projections), a more computationally efficient solution is still desirable.

A simpler solution is possible if the interference and noise are assumed to be spatially white (e.g., no CCI). Under this assumption, the criterion reduces to a trace rather than determinant operation. By transforming the data to the frequency domain, an iterative solution based on the so-called IQML (Iterative Quadratic Maximum Likelihood) [Bre86] or MODE [Sto90c, Sto90b] can be used. The computational advantage of these techniques results because the cost function depends linearly on the signal projection matrix $\mathbf{P}_{\mathbf{S}^*(\boldsymbol{\tau})}$. By reparameterizing the matrix $\mathbf{P}_{\mathbf{S}^*(\boldsymbol{\tau})}$ according to the coefficients of a certain polynomial, and assuming a previous estimate of these coefficients is available, the dependence of $\mathbf{P}_{\mathbf{S}^*(\boldsymbol{\tau})}$ on some trial coefficients and hence the cost function become quadratic. The quadratic optimization problem is then solved in closed form (see [Swi98a] for details).

The ML cost function for both spatially and temporally white noise is

$$f^w_N(\boldsymbol{\tau}) = -\mathrm{Tr}\left\{\hat{\mathbf{R}}_{ys}(\boldsymbol{\tau})\,\hat{\mathbf{R}}^{-1}_{ss}(\boldsymbol{\tau})\,\hat{\mathbf{R}}^*_{ys}(\boldsymbol{\tau})\right\} = -\frac{1}{N}\mathrm{Tr}\left\{\mathbf{Y}\,\mathbf{P}_{\mathbf{S}^*(\boldsymbol{\tau})}\,\mathbf{Y}^*\right\} \tag{3.39}$$

which satisfies the condition of linear dependence on $\mathbf{P}_{\mathbf{S}^*(\boldsymbol{\tau})}$ stated above. Note that (3.39) is equal up to an additive constant to $\mathrm{Tr}\left\{\hat{\mathbf{Q}}_{ML}(\boldsymbol{\tau})\right\}$, while for unknown correlated noise the cost function is $\left|\hat{\mathbf{Q}}_{ML}(\boldsymbol{\tau})\right|$. Both criteria are measures of the "magnitude" of the correlation

matrix of the residuals. In the white-noise case, the measure is equal to the arithmetic mean of the eigenvalues of $\hat{\mathbf{Q}}_{ML}(\boldsymbol{\tau})$, whereas the geometric mean is used in the correlated-noise case. Although it might not be expected at first glance, the change of the trace for the determinant, or the arithmetic mean for the geometric mean results in a drastic improvement of the performance of estimator in the presence of CCI. On the other hand, this change also results in a "increased non-linearity" of the cost function. Moreover, the performance of the ML cost function for unknown correlated noise does not undergo asymptotically any deterioration with respect to the ML criterion for white noise when the received noise is indeed spatially white. The proof of this statement is evident from the derivation of the CRB in Appendix 3.A. This result is virtually valid also in the finite-sample case, as illustrated in [Sec99b], given the proximity between the finite-sample performance of the estimator and the CRB, which can be also observed in Section 3.8.

As pointed out in [Ast99b], the cost function $f_N^w(\boldsymbol{\tau})$ is equal to minus the energy of the spatial signatures' estimates, $\hat{\mathbf{A}}_{ML}(\boldsymbol{\tau})$, in the norm of $\hat{\mathbf{R}}_{ss}^{-1}(\boldsymbol{\tau})$. Actually, $f_N^w(\boldsymbol{\tau})$ can be viewed as a extension of the MEDLL [Nee93a, Nee94] when an antenna array is used. The author of the MEDLL does not propose any computational efficient method for the optimization, apart from an approach based on the alternating projection paradigm. Futhermore, in the MEDLL the amplitudes are not eliminated analytically. This fact increases the number of parameters of the final cost function, and makes the convergence problems more severe.

The important issue is that the condition of linear dependence on $\mathbf{P}_{\mathbf{S}^*(\boldsymbol{\tau})}$ is not fulfilled by the ML cost function for unknown correlated noise in (3.28) due to the determinant operation. Consequently, an IQML-like algorithm cannot be directly applied to (3.28). The main goal of this chapter is to present and analyze a cost function that is asymptotically equivalent to the original ML criterion (3.28), but that is linear in the signal projection matrix and, therefore makes possible the computation of the estimates using an IQML approach.

## 3.4 An Asymptotically Equivalent Estimator

We propose computing the delay estimates as the minimizing arguments of the following criterion function:

$$g_N\left(\boldsymbol{\tau}, \mathbf{W}_{\text{op}}\right) = -\text{Tr}\left\{\mathbf{W}_{\text{op}}\, \mathbf{B}_N(\boldsymbol{\tau})\right\} \tag{3.40}$$

where

$$\mathbf{W}_{\text{op}} \triangleq \left(\mathbf{I} - \mathbf{B}_N\left(\check{\boldsymbol{\tau}}\right)\right)^{-1} \tag{3.41}$$

and $\mathbf{B}_N(\check{\boldsymbol{\tau}})$ is defined as in (3.29). A proof that this criterion yields asymptotically efficient delay estimates is given below.

### 3.4.1 Proof of the Asymptotic Equivalence

To begin, we note that it can be shown that the estimates obtained with (3.40) are consistent. The proof is similar to that in Section 3.3.1 and will be omitted. The only difference is that the nondecreasing property of the trace, instead of that of the determinant, is employed. We will now establish the asymptotic equivalence between

$$\hat{\boldsymbol{\tau}}_1 = \arg\min_{\boldsymbol{\tau}} \; V_N(\boldsymbol{\tau}) \tag{3.42}$$

$$\hat{\boldsymbol{\tau}}_2 = \arg\min_{\boldsymbol{\tau}} \; g_N\left(\boldsymbol{\tau}, \mathbf{W}_{\text{op}}\right) \; , \tag{3.43}$$

which means that

$$\hat{\boldsymbol{\tau}}_2 = \hat{\boldsymbol{\tau}}_1 + o_p\left(N^{-1/2}\right) \; , \tag{3.44}$$

A sufficient condition for (3.44) to hold is that [Ott93]

$$g_N^i\left(\check{\boldsymbol{\tau}}, \mathbf{W}_{\text{op}}\right) = V_N^i\left(\check{\boldsymbol{\tau}}\right) + o_p\left(N^{-1/2}\right) \tag{3.45}$$

$$g_N^{ij}\left(\check{\boldsymbol{\tau}}, \mathbf{W}_{\text{op}}\right) = V_N^{ij}\left(\check{\boldsymbol{\tau}}\right) + o_p\left(1\right) \tag{3.46}$$

where the superscript $(\cdot)^i$ denotes the derivative with respect to $\tau_i$. A double superscript denotes the corresponding second derivatives.

The proof of (3.45) is immediate since

$$V_N^i\left(\check{\boldsymbol{\tau}}\right) = -\text{Tr}\left\{\left(\mathbf{I} - \mathbf{B}_N\left(\check{\boldsymbol{\tau}}\right)\right)^{-1} \mathbf{B}_N^i\left(\check{\boldsymbol{\tau}}\right)\right\} = g_N^i\left(\check{\boldsymbol{\tau}}, \mathbf{W}_{\text{op}}\right) \; . \tag{3.47}$$

The second derivatives also satisfy the equivalence condition (3.46) because

$$\begin{aligned} V_N^{ij}\left(\check{\boldsymbol{\tau}}\right) = & -\text{Tr}\left\{\left(\mathbf{I} - \mathbf{B}_N\left(\check{\boldsymbol{\tau}}\right)\right)^{-1} \mathbf{B}_N^{ij}\left(\check{\boldsymbol{\tau}}\right)\right\} \\ & +\text{Tr}\left\{\left(\mathbf{I} - \mathbf{B}_N\left(\check{\boldsymbol{\tau}}\right)\right)^{-1} \mathbf{B}_N^i\left(\check{\boldsymbol{\tau}}\right)\left(\mathbf{I} - \mathbf{B}_N\left(\check{\boldsymbol{\tau}}\right)\right)^{-1} \mathbf{B}_N^j\left(\check{\boldsymbol{\tau}}\right)\right\} \\ = & \; g_N^{ij}\left(\check{\boldsymbol{\tau}}, \mathbf{W}_{\text{op}}\right) \\ & +\text{Tr}\left\{\left(\mathbf{I} - \mathbf{B}_N\left(\check{\boldsymbol{\tau}}\right)\right)^{-1} \mathbf{B}_N^i\left(\check{\boldsymbol{\tau}}\right)\left(\mathbf{I} - \mathbf{B}_N\left(\check{\boldsymbol{\tau}}\right)\right)^{-1} \mathbf{B}_N^j\left(\check{\boldsymbol{\tau}}\right)\right\} \end{aligned} \tag{3.48}$$

and the last term in (3.48) is (at least) $o_p\left(1\right)$ since, as shown in Appendix 3.B, $\mathbf{B}_N^i\left(\check{\boldsymbol{\tau}}\right) = O_p\left(N^{-1/2}\right)$.

### 3.4.2 Calculation of the Weighting Matrix

The weighting matrix $\mathbf{W}_{\text{op}}$ appearing in the proposed cost function depends on the true value of the delays, and hence is unknown. However, it is a standard result that we can replace it with a consistent estimate $\hat{\mathbf{W}}$ without affecting the asymptotic properties of the delay estimates. If $\hat{\boldsymbol{\tau}}$ is a consistent estimate of $\check{\boldsymbol{\tau}}$, then we can construct the *practical* weighting matrix as

$$\hat{\mathbf{W}} = \left(\mathbf{I} - \mathbf{B}_N\left(\hat{\boldsymbol{\tau}}\right)\right)^{-1} \; . \tag{3.49}$$

The estimates obtained from $g_N(\boldsymbol{\tau}, \mathbf{W}_{\text{op}})$ and $g_N(\boldsymbol{\tau}, \hat{\mathbf{W}})$ are asymptotically equivalent because the derivatives of these cost functions satisfy conditions similar to those stated in (3.45) and (3.46). The proof is immediate since $\hat{\mathbf{W}} = \mathbf{W}_{\text{op}} + o_p(1)$ (by the definition of consistency), $g_N^i(\check{\boldsymbol{\tau}}, \mathbf{W}_{\text{op}}) = O_p\left(N^{-1/2}\right)$ and $g_N^{ij}(\check{\boldsymbol{\tau}}, \mathbf{W}_{\text{op}}) = O_p(1)$. It is worth remarking that the *practical* cost function admits the following expression:

$$g_N(\boldsymbol{\tau}, \hat{\mathbf{W}}) = -\text{Tr}\left\{\hat{\mathbf{Q}}^{-1/2}\,\hat{\mathbf{R}}_{ys}(\boldsymbol{\tau})\,\hat{\mathbf{R}}_{ss}^{-1}(\boldsymbol{\tau})\,\hat{\mathbf{R}}_{ys}^{*}(\boldsymbol{\tau})\,\hat{\mathbf{Q}}^{-1/2}\right\} \tag{3.50}$$

since

$$\mathbf{B}_N(\hat{\boldsymbol{\tau}}) = \mathbf{I} - \hat{\mathbf{R}}_{yy}^{-1/2}\,\hat{\mathbf{Q}}\,\hat{\mathbf{R}}_{yy}^{-1/2} \tag{3.51}$$

$$\hat{\mathbf{Q}} = \hat{\mathbf{R}}_{yy} - \hat{\mathbf{R}}_{ys}(\hat{\boldsymbol{\tau}})\,\hat{\mathbf{R}}_{ss}^{-1}(\hat{\boldsymbol{\tau}})\,\hat{\mathbf{R}}_{ys}^{*}(\hat{\boldsymbol{\tau}}) \tag{3.52}$$

Note that $\hat{\mathbf{Q}}$ is a consistent estimate of the correlation matrix of the noise. The criterion in (3.50) above resembles the one in the white-noise case (3.39); the difference is that now the signals are prewhitened using an estimate of the noise correlation. While the function in (3.50) could have been derived using purely heuristic reasoning, the development followed herein has allowed us to prove the equivalence between (3.50) and the original criterion (3.28), which would have been difficult to do from a simple inspection of those cost functions. More iterations of the estimator (that is, using the time-delay estimates obtained from $g_N(\boldsymbol{\tau}, \hat{\mathbf{W}})$ to compute a new weighting matrix, which is substituted back into $g_N$ and then new estimates are calculated, ...) do not improve the large sample accuracy of the estimates, since $g_N(\boldsymbol{\tau}, \hat{\mathbf{W}})$ already provides asymptotically efficient estimates. Besides, interestingly enough, simulation results have shown that the additional iterations do not improve the performance either in the finite-sample case.

The consistent estimate of the time delays, $\hat{\boldsymbol{\tau}}$, needed to construct $\hat{\mathbf{W}}$ can be obtained as the minimizing argument of

$$h_N(\boldsymbol{\tau}) \triangleq g_N(\boldsymbol{\tau}, \mathbf{I}) = -\text{Tr}\left\{\mathbf{B}_N(\boldsymbol{\tau})\right\} \tag{3.53}$$

$$= -\text{Tr}\left\{\hat{\mathbf{R}}_{yy}^{-1/2}\,\hat{\mathbf{R}}_{ys}(\boldsymbol{\tau})\,\hat{\mathbf{R}}_{ss}^{-1}(\boldsymbol{\tau})\,\hat{\mathbf{R}}_{ys}^{*}(\boldsymbol{\tau})\,\hat{\mathbf{R}}_{yy}^{-1/2}\right\}, \tag{3.54}$$

in which the unknown weighting matrix is replaced by the identity, which amounts to prewhitening the signals according to the total correlation matrix $\hat{\mathbf{R}}_{yy}$ instead of the correlation of the noise, as done in (3.50). Again, the proof of the consistency of $h_N(\boldsymbol{\tau})$ is similar to that in Section 3.3.1 and will be omitted. Note that the criterion $f_N^w(\boldsymbol{\tau})$ obtained for spatially white noise also provides consistent estimates. Nevertheless, as illustrated in the simulations of Section 3.8, its variance will be much larger than that of the estimates obtained with (3.54) when the noise is not spatially white since $f_N^w(\boldsymbol{\tau})$ makes no attempt to prewhiten the signals. Therefore, there is no advantage in employing $f_N^w(\boldsymbol{\tau})$ instead of $h_N(\boldsymbol{\tau})$ (apart from a slightly reduced computational complexity), and the latter is preferred.

## 3.5 Systematic Derivation

In Section 3.4, rather than deriving the new estimator, we nearly postulated it. And the simple conditions of Section 3.4.1 served to prove its asymptotic efficiency. A more systematic approach would have been the following one. As stated above, the premise that a cost function has to satisfy in order to allow the application of IQML is that the dependence on $\mathbf{P}_{\mathbf{S}^*(\boldsymbol{\tau})}$ and, hence, on $\mathbf{B}_N(\boldsymbol{\tau})$ has to be linear. Then, $g_N(\boldsymbol{\tau}, \mathbf{W})$ defined as in (3.40), where $\mathbf{W}$ is a positive definite Hermitic matrix, is a logical choice since it is the most general linear function of the elements of $\mathbf{B}_N(\boldsymbol{\tau})$. Again, the proof that the estimates are consistent for any choice of $\mathbf{W}$ follows closely that of Section 3.3.1. The next step is to compute the asymptotic covariance of the estimates obtained from $g_N(\boldsymbol{\tau}, \mathbf{W})$ as a function of the weighting matrix, which we denote as $\mathbf{C}(\mathbf{W})$. It is a well known result that [Söd89]

$$N\mathbf{C}(\mathbf{W}) = \mathbf{H}^{-1}\,\mathbf{G}\,\mathbf{H}^{-1} \tag{3.55}$$

where

$$\mathbf{G} = \lim_{N\to\infty} N\,\mathrm{E}\left\{g'(\check{\boldsymbol{\tau}}, \mathbf{W})\ \left(g'(\check{\boldsymbol{\tau}}, \mathbf{W})\right)^T\right\} \tag{3.56}$$

$$\mathbf{H} = \lim_{N\to\infty} g''(\check{\boldsymbol{\tau}}, \mathbf{W})\ , \tag{3.57}$$

and $g'$ and $g''$ denote the gradient and the Hessian of $g(\boldsymbol{\tau}, \mathbf{W})$. The Hessian and the covariance of the gradient are given by (proof in Appendix 3.C)

$$\mathbf{H} = \frac{2}{N}\,\mathrm{Re}\left\{\left(\mathbf{D}\,\mathbf{P}^{\perp}_{\mathbf{S}^*}\,\mathbf{D}^*\right) \odot \left(\mathbf{A}^*\,\mathbf{R}_{yy}^{-1/2}\,\mathbf{W}\,\mathbf{R}_{yy}^{-1/2}\,\mathbf{A}\right)^T\right\} \tag{3.58}$$

$$\mathbf{G} = \frac{2}{N}\,\mathrm{Re}\left\{\left(\mathbf{D}\,\mathbf{P}^{\perp}_{\mathbf{S}^*}\,\mathbf{D}^*\right) \odot \left(\mathbf{A}^*\,\mathbf{R}_{yy}^{-1/2}\,\mathbf{W}\,\mathbf{R}_{yy}^{-1/2}\,\mathbf{Q}\,\mathbf{R}_{yy}^{-1/2}\,\mathbf{W}\,\mathbf{R}_{yy}^{-1/2}\,\mathbf{A}\right)^T\right\} \tag{3.59}$$

where $\mathbf{D}$, which was defined in (3.36), and $\mathbf{S}$ are evaluated at $\check{\boldsymbol{\tau}}$. Using a straightforward modification of [Sto90a, Lemma A.2] (see also [Swi92, Theorem 5.1]) we get

$$\mathbf{C}(\mathbf{W}) \geq \frac{1}{2}\,\mathrm{Re}\left\{\left(\mathbf{D}(\check{\boldsymbol{\tau}})\ \mathbf{P}^{\perp}_{\mathbf{S}^*(\check{\boldsymbol{\tau}})}\,\mathbf{D}^*(\check{\boldsymbol{\tau}})\right) \odot \left(\mathbf{A}^*\,\mathbf{Q}^{-1}\,\mathbf{A}\right)^T\right\}^{-1}\ . \tag{3.60}$$

Note that the right-hand expression of (3.60) is exactly the CRB, as written in (3.35). To minimize $\mathbf{C}(\mathbf{W})$, it would be sufficient to find a $\mathbf{W}$ for which the equality was obtained in (3.60). It is clear that this happens for

$$\mathbf{W}_{\min} = \mathbf{R}_{yy}^{1/2}\,\mathbf{Q}^{-1}\,\mathbf{R}_{yy}^{1/2}\ . \tag{3.61}$$

This result is perfectly coherent with the optimum weights defined by (3.41), since $\mathbf{W}_{\mathrm{op}} = \mathbf{W}_{\min} + o_p(1)$ and, as stated above, a term of order $o_p(1)$ in the weighting matrix does not affect the asymptotic accuracy of the estimator. For the simple case of $d = 1$, $\mathbf{W} = \mathbf{I}$ also yields the minimum variance. This is a logical result since, for $d = 1$, it is verified that $V_N(\tau_0) = \ln(1 + g_N(\tau_0, \mathbf{I}))$.

## 3.6 Heuristic Derivations

In this section, three different heuristic ways of deriving the new cost function $g_N(\boldsymbol{\tau}, \hat{\mathbf{W}})$ are presented. These approaches do not intend to be rigorous proofs. However, they are rather general and may thus be of interest for other problems as well.

### 3.6.1 Series Expansion of the Logarithm

Note that

$$\begin{aligned}\mathbf{B}_N(\boldsymbol{\tau}) &= \hat{\mathbf{R}}_{yy}^{-\frac{1}{2}}\hat{\mathbf{R}}_{ys}(\boldsymbol{\tau})\hat{\mathbf{R}}_{ss}^{-1}(\boldsymbol{\tau})\hat{\mathbf{R}}_{ys}^{*}(\boldsymbol{\tau})\hat{\mathbf{R}}_{yy}^{-\frac{1}{2}} \\ &= \underbrace{(\mathbf{Y}\mathbf{Y}^*)^{-1/2}\mathbf{Y}\mathbf{S}^*(\boldsymbol{\tau})\left(\mathbf{S}(\boldsymbol{\tau})\mathbf{S}^*(\boldsymbol{\tau})\right)^{-1}\mathbf{S}(\boldsymbol{\tau})}_{\mathbf{X}} \cdot \underbrace{\mathbf{Y}^*(\mathbf{Y}\mathbf{Y}^*)^{-1/2}}_{\mathbf{Z}} .\end{aligned}$$

If we compare the above equation with

$$\begin{aligned}\mathbf{P}_{\mathbf{Y}^*}\mathbf{P}_{\mathbf{S}^*(\boldsymbol{\tau})} &= \mathbf{Y}^*\left(\mathbf{Y}\,\mathbf{Y}^*\right)^{-1}\mathbf{Y}\mathbf{S}^*(\boldsymbol{\tau})\left(\mathbf{S}(\boldsymbol{\tau})\,\mathbf{S}^*(\boldsymbol{\tau})\right)^{-1}\mathbf{S}(\boldsymbol{\tau}) \\ &= \underbrace{\mathbf{Y}^*(\mathbf{Y}\mathbf{Y}^*)^{-1/2}}_{\mathbf{Z}} \cdot \underbrace{(\mathbf{Y}\mathbf{Y}^*)^{-1/2}\mathbf{Y}\mathbf{S}^*(\boldsymbol{\tau})\left(\mathbf{S}(\boldsymbol{\tau})\mathbf{S}^*(\boldsymbol{\tau})\right)^{-1}\mathbf{S}(\boldsymbol{\tau})}_{\mathbf{X}} ,\end{aligned}$$

we see that $\mathbf{B}_N(\boldsymbol{\tau})$ and the product of the two projection matrices above must share the same non-zero eigenvalues. Thus, the eigenvalues of $\mathbf{B}_N(\boldsymbol{\tau})$ satisfy $0 \leq \lambda_i \leq 1$, or in the presence of noise $\lambda_i < 1$. Therefore, we can use the series expansion of the logarithm to express the original ML criterion as follows:

$$V_N(\boldsymbol{\tau}) = -\mathrm{Tr}\left\{\mathbf{B}_N(\boldsymbol{\tau})\right\} - \frac{1}{2}\mathrm{Tr}\left\{\mathbf{B}_N^2(\boldsymbol{\tau})\right\} - \frac{1}{3}\mathrm{Tr}\left\{\mathbf{B}_N^3(\boldsymbol{\tau})\right\} + \cdots . \tag{3.62}$$

The function $h_N(\boldsymbol{\tau})$, which we have proposed to use in obtaining the initial consistent estimates, is the first term of this expansion. Unlike many other estimation problems (see e.g., [Li95, Vib97, Zhe97], and Chapter 5 of this thesis), the first-order term is not asymptotically equivalent to the original function because $\lim_{N\to\infty}\mathbf{B}_N\left(\check{\boldsymbol{\tau}}\right) = \mathbf{I} - \mathbf{R}_{yy}^{-1/2}\mathbf{Q}\mathbf{R}_{yy}^{-1/2}$ is not equal to zero. The error in this first order approximation is "small" when all the eigenvalues of $\mathbf{Q}$ are large with respect to the power of the signals (e.g., the SNR regarding the spatially white noise is very poor). However, this situation will seldom be encountered in practice, where usually only some of eigenvalues of $\mathbf{Q}$ are large, due to the reception of directional interferers. In order to maintain not only consistency but also asymptotic efficiency, all of the terms in the expansion (3.62) must be kept. Since the second and higher-order terms are the ones that introduce the undesirable nonlinear dependence on the matrix $\mathbf{P}_{\mathbf{S}^*(\boldsymbol{\tau})}$, we decide to approximate them. The approximation is not done directly over $V_N(\boldsymbol{\tau})$, but over its derivative. If we differentiate (3.62) and replace $\mathbf{B}_N(\boldsymbol{\tau})$ by $\mathbf{B}_N(\hat{\boldsymbol{\tau}})$ in all the second and higher-order terms (this is justified since $\mathbf{B}_N^i\left(\check{\boldsymbol{\tau}}\right) = O_p\left(N^{-1/2}\right)$),

it results that

$$V_N^i(\boldsymbol{\tau}) \simeq -\mathrm{Tr}\left\{\mathbf{B}_N^i(\boldsymbol{\tau})\left(\mathbf{I}+\mathbf{B}_N(\hat{\boldsymbol{\tau}})+\mathbf{B}_N^2(\hat{\boldsymbol{\tau}})+\cdots\right)\right\} \tag{3.63}$$

$$= -\mathrm{Tr}\left\{\left(\mathbf{I}-\mathbf{B}_N(\hat{\boldsymbol{\tau}})\right)^{-1}\mathbf{B}_N^i(\boldsymbol{\tau})\right\} . \tag{3.64}$$

Thus we retrieve the new criterion presented in Section 3.4 since the value of $\boldsymbol{\tau}$ that minimizes $g_N(\boldsymbol{\tau}, \hat{\mathbf{W}})$ also nulls (3.64).

### 3.6.2 Eigenvalue Weighting

The derivative of the original ML criterion can be written as

$$V_N^i(\boldsymbol{\tau}) = -\sum_{k=1}^{m} \frac{\lambda_k^i(\boldsymbol{\tau})}{1-\lambda_k(\boldsymbol{\tau})} , \tag{3.65}$$

while the derivative of the cost function that provides only consistent estimates is

$$h_N^i(\boldsymbol{\tau}) = -\sum_{k=1}^{m} \lambda_k^i(\boldsymbol{\tau}) , \tag{3.66}$$

where $\lambda_k(\boldsymbol{\tau})$ are the eigenvalues of $\mathbf{B}_N(\boldsymbol{\tau})$. We notice that the difference between the estimator that is asymptotically efficient and the one that is not lies in an appropriate weighting of the eigenvalues. The second criterion (3.66) approaches the original one (3.65) when all the nonzero eigenvalues are much smaller than one, or when all of them have similar values. Again, this only happens in general if all the eigenvalues of $\mathbf{Q}$ are much larger than the power of the desired signals. A reasonable approach to approximating the optimal weighting would be to replace the eigenvalues $\lambda_k(\boldsymbol{\tau})$ in (3.65) by the eigenvalues of $\mathbf{B}_N(\hat{\boldsymbol{\tau}})$. Using (3.65) and the eigendecomposition $\mathbf{B}_N(\boldsymbol{\tau}) = \mathbf{U}(\boldsymbol{\tau})\,\boldsymbol{\Lambda}(\boldsymbol{\tau})\,\mathbf{U}^*(\boldsymbol{\tau})$, this approach results in

$$V_N(\boldsymbol{\tau}) \simeq -\mathrm{Tr}\left\{\left(\mathbf{I}-\boldsymbol{\Lambda}(\hat{\boldsymbol{\tau}})\right)^{-1}\boldsymbol{\Lambda}(\boldsymbol{\tau})\right\} \tag{3.67}$$

$$= -\mathrm{Tr}\left\{\mathbf{U}(\boldsymbol{\tau})\left(\mathbf{I}-\boldsymbol{\Lambda}(\hat{\boldsymbol{\tau}})\right)^{-1}\mathbf{U}^*(\boldsymbol{\tau})\,\mathbf{U}(\boldsymbol{\tau})\boldsymbol{\Lambda}(\boldsymbol{\tau})\mathbf{U}^*(\boldsymbol{\tau})\right\} \tag{3.68}$$

$$\simeq -\mathrm{Tr}\left\{\mathbf{U}(\hat{\boldsymbol{\tau}})\left(\mathbf{I}-\boldsymbol{\Lambda}(\hat{\boldsymbol{\tau}})\right)^{-1}\mathbf{U}^*(\hat{\boldsymbol{\tau}})\,\mathbf{B}_N(\boldsymbol{\tau})\right\} \tag{3.69}$$

$$= -\mathrm{Tr}\left\{\left(\mathbf{I}-\mathbf{B}_N(\hat{\boldsymbol{\tau}})\right)^{-1}\mathbf{B}_N(\boldsymbol{\tau})\right\} = g_N(\boldsymbol{\tau}, \hat{\mathbf{W}}) \tag{3.70}$$

which is the cost function proposed in Section 3.4.

Note that in the two approaches above the approximations are always carried out on the derivative of the ML cost function, and next the function $g_N(\boldsymbol{\tau}, \hat{\mathbf{W}})$ results by integration. If the approximations had been performed directly on the ML cost function, the resulting criterion would not have been asymptotically efficient.

### 3.6.3 Modified First Order Approximation

As stated above, a direct first-order approximation of the ML cost function does not yield an asymptotically efficient estimator. However, using a simple trick we can write the ML cost function as

$$\begin{aligned} V_N(\boldsymbol{\tau}) &= \ln|\mathbf{I}-\mathbf{B}_N(\hat{\boldsymbol{\tau}})+\mathbf{B}_N(\hat{\boldsymbol{\tau}})-\mathbf{B}_N(\boldsymbol{\tau})| \\ &= \ln|\mathbf{I}-\mathbf{B}_N(\hat{\boldsymbol{\tau}})|+\ln\left|\mathbf{I}+\left(\mathbf{I}-\mathbf{B}_N(\hat{\boldsymbol{\tau}})\right)^{-1}\left(\mathbf{B}_N(\hat{\boldsymbol{\tau}})-\mathbf{B}_N(\boldsymbol{\tau})\right)\right| \end{aligned} \tag{3.71}$$

Since $\lim_{N\to\infty}\left(\mathbf{B}_N(\hat{\boldsymbol{\tau}})-\mathbf{B}_N\left(\check{\boldsymbol{\tau}}\right)\right)=\mathbf{0}$ and $\mathbf{B}_N^i\left(\check{\boldsymbol{\tau}}\right)=O_p\left(N^{-1/2}\right)$, it is possible to maintain the asymptotic efficiency by only keeping the first-order term in the series expansion of (3.71), which is

$$V_N(\boldsymbol{\tau})\underset{\substack{\text{first order}\\ \text{term}}}{\simeq}\ln|\mathbf{I}-\mathbf{B}_N(\hat{\boldsymbol{\tau}})|+\mathrm{Tr}\left\{\hat{\mathbf{W}}\,\mathbf{B}_N(\hat{\boldsymbol{\tau}})\right\}-\mathrm{Tr}\left\{\hat{\mathbf{W}}\,\mathbf{B}_N(\boldsymbol{\tau})\right\}=c+g_N(\boldsymbol{\tau},\hat{\mathbf{W}})\,, \tag{3.72}$$

where $c$ is a constant, and $\hat{\mathbf{W}}$ was defined in (3.49). Once more, this coincides with the alternative function we have proposed.

## 3.7 Calculating the Estimates with IQML and ESPRIT

In this section we outline how the IQML and ESPRIT algorithms can be applied to the cost functions that have appeared in the previous sections. Since the objective in the preceding sections has been to reduce the complexity involved in a direct minimization of a multidimensional criterion, it does not make sense to optimize the new cost functions using a search; instead, the use of computationally efficient algorithms is more appropriate.

The general expression of the cost function we consider is that given in (3.40), which can be written as

$$g_N\left(\boldsymbol{\tau},\mathbf{W}\right)=-\frac{1}{N}\mathrm{Tr}\left\{\mathbf{W}^{1/2}\,\hat{\mathbf{R}}_{yy}^{-1/2}\,\mathbf{Y}\,\mathbf{P}_{\mathbf{S}^*(\boldsymbol{\tau})}\,\mathbf{Y}^*\,\hat{\mathbf{R}}_{yy}^{-1/2}\,\mathbf{W}^{1/2}\right\}\,. \tag{3.73}$$

Different criteria are obtained from different choices of the matrix $\mathbf{W}$. That is, if $\mathbf{W}$ is a consistent estimate of $\mathbf{W}_{\text{op}}$ in (3.41) then the asymptotically efficient estimator is obtained; if $\mathbf{W}$ is equal to the identity matrix or equal to $\hat{\mathbf{R}}_{yy}$ then the consistent estimator $h_N(\boldsymbol{\tau})$ or the white-noise estimator $f_N^w(\boldsymbol{\tau})$ result, respectively.

The IQML and ESPRIT algorithms work with a frequency representation of the data. This representation was already described in Section 2.5.2. However, the main equation are summarized below. If the $N$ temporal samples are transformed into the frequency domain using the DFT, the signals approximately satisfy the following relationship:

$$\mathbf{S}^*(\boldsymbol{\tau})=\mathbf{S}_\omega^*\,\mathbf{V}(\boldsymbol{\tau}) \tag{3.74}$$

where $\mathbf{S}_\omega$ is a diagonal matrix whose entries are the DFT of the vector samples $[s(T_s), \cdots, s(NT_s)]$, and

$$\mathbf{V}(\boldsymbol{\tau}) = \left[ \begin{array}{ccc} \mathbf{v}(\tau_0) & \cdots & \mathbf{v}(\tau_{d-1}) \end{array} \right] \tag{3.75}$$

$$\mathbf{v}(\tau_k) = \left[ \begin{array}{ccc} \exp(j\omega_1\tau_k) & \cdots & \exp(j\omega_N\tau_k) \end{array} \right]^T \tag{3.76}$$

$$\omega_i = \frac{2\pi}{NT_s}\left(i - 1 - \left\lfloor \frac{N}{2} \right\rfloor\right) . \tag{3.77}$$

Note that the same notation, $\mathbf{S}(\boldsymbol{\tau})$ and $\mathbf{Y}$, is used for both the time and frequency domain. Since the noise is assumed to be white in time, it is also white in frequency, so all of the estimators above can be applied in an identical fashion to the frequency rather than time samples.

### 3.7.1 IQML Algorithm

Let the elements of the vector $\mathbf{g} = [g_0 \ \cdots \ g_d]^T$ be taken from the coefficients of the polynomial

$$\mathcal{G}(z) = g_0 z^d + g_1 z^{d-1} + \cdots + g_d \tag{3.78}$$

whose roots are

$$\exp(j2\pi\tau_0/NT_s), \cdots, \exp(j2\pi\tau_{d-1}/NT_s) . \tag{3.79}$$

Since the roots lie on the unit circle, the coefficients satisfy the so-called conjugate symmetry constraint:

$$g_k = g_{d-k}^*, \quad k = 0, 1, \cdots, d . \tag{3.80}$$

The class of polynomials that satisfies (3.80) contains not only polynomials with roots on the unit circle, but also all polynomials with roots symmetrical (inverted and conjugated) with respect to the unit circle. Since the conjugate symmetry constraint on the coefficients is less restrictive than the unit norm constraint on the roots, some performance loss might occur when the cost function is parameterized by the coefficients $\mathbf{g}$ subject to (3.80), instead of the time delays $\boldsymbol{\tau}$. However, when evaluated in simulations concerning the problem of DOA estimation [Sto90c, Kri98], the performance degradation has been shown to be negligible in most cases. This can be explained by the fact that when the constraint in (3.80) is used, the roots stay on the unit circle for small perturbations in the coefficients (see [Sto88]). Thus, for a consistent estimator this reparameterization is asymptotically equivalent to a parameterization where the unit norm on the roots is included.

It is straightforward to prove the following equality of projection matrices [Swi98a]:

$$\mathbf{P}^{\perp}_{\mathbf{S}^*(\boldsymbol{\tau})} = \mathbf{P}_{\mathbf{S}_\omega^{-1}\mathbf{G}} = \mathbf{S}_\omega^{-1}\mathbf{G}\left(\mathbf{G}^*\mathbf{S}_\omega^{-*}\mathbf{S}_\omega^{-1}\mathbf{G}\right)^{-1}\mathbf{G}^*\mathbf{S}_\omega^{-*} \tag{3.81}$$

where the $N \times N-d$ Sylvester matrix $\mathbf{G}$ is given by

$$\mathbf{G} = \begin{bmatrix} g_d & g_{d-1} & \cdots & g_0 & 0 & & \\ 0 & g_d & g_{d-1} & \cdots & g_0 & 0 & \\ & \ddots & \ddots & \ddots & \ddots & \ddots & 0 \\ & & 0 & g_d & g_{d-1} & \cdots & g_0 \end{bmatrix}^* \tag{3.82}$$

Therefore, minimizing the cost function in (3.73) is equivalent to minimizing

$$\tilde{g}_N(\mathbf{g}, \mathbf{W}) = \frac{1}{N}\mathrm{Tr}\left\{ \mathbf{W}^{\frac{1}{2}} \hat{\mathbf{R}}_{yy}^{-\frac{1}{2}} \mathbf{Y}\, \mathbf{S}_\omega^{-1}\mathbf{G} \left(\mathbf{G}^* \mathbf{S}_\omega^{-*} \mathbf{S}_\omega^{-1} \mathbf{G}\right)^{-1} \mathbf{G}^* \mathbf{S}_\omega^{-*} \mathbf{Y}^* \hat{\mathbf{R}}_{yy}^{-\frac{1}{2}} \mathbf{W}^{\frac{1}{2}} \right\} \tag{3.83}$$

In the IQML (Iterative Quadratic Maximum Likelihood) algorithm the minimization of (3.83) is done iteratively. That is, the matrix $\left(\mathbf{G}_k^* \mathbf{S}_\omega^{-*} \mathbf{S}_\omega^{-1} \mathbf{G}_k\right)^{-1}$ is computed using a given estimate $\mathbf{g}_k$ and held fixed. Then, the resulting criterion is quadratic in $\mathbf{g}_k$ and can be solved in closed-form. Details on the implementation of this step subject to the conjugate symmetry constraint (3.80) and to a certain constraint that avoids the trivial solution (e.g., $\|\mathbf{g}_k\|_2 = 1$, or $\mathrm{Re}\{g_0\} = 1$) can be found in [Swi98a, Bre86, Hua94]. The resulting vector $\mathbf{g}_{k+1}$ is used to fix $\left(\mathbf{G}_{k+1}^* \mathbf{S}_\omega^{-*} \mathbf{S}_\omega^{-1} \mathbf{G}_{k+1}\right)^{-1}$, and the process is repeated until a certain convergence or failure criterion is satisfied (see Section 3.8.1).

If we want the matrix $\mathbf{W}$ to be a consistent estimate of $\mathbf{W}_{\mathrm{op}}$, then we have two iterative processes: the IQML algorithm itself and the computation of the matrix $\mathbf{W}$. Since these two processes can be coupled or not, we can choose two different approaches to implement the complete estimation procedure:

**A)** Coupled iterations

1. Initialize $k = 0$, $\mathbf{W}_0 = \mathbf{I}$ and $\mathbf{g}_0$ (see Section 3.8.1).
2. Do *only one* iteration of the IQML algorithm and obtain $\mathbf{g}_{k+1}$.
3. Compute $\boldsymbol{\tau}_{k+1}$ from $\mathbf{g}_{k+1}$ using (3.78)-(3.79).
4. Compute the weighting matrix $\mathbf{W}_{k+1}$ using $\boldsymbol{\tau}_{k+1}$ and expression (3.49). Substitute $\mathbf{W}_{k+1}$ in the cost function that is being minimized (3.83).
5. If the convergence / failure condition is satisfied, take the final estimate of the delays as $\hat{\boldsymbol{\tau}} = \boldsymbol{\tau}_{k+1}$. If not, set $k = k + 1$ and return to step 2.

**B)** Decoupled iterations

1. Initialize $\mathbf{W}_0 = \mathbf{I}$ and $\mathbf{g}_0$ (see Section 3.8.1).
2. Perform *all* iterations of the IQML algorithm until it converges or fails (not only one iteration as in the procedure **A**). The result is the vector $\mathbf{g}_1$, and the corresponding time-delay estimate $\boldsymbol{\tau}_1$ is obtained using (3.78)-(3.79).

3. Compute the weighting matrix $\mathbf{W}_1$ using $\boldsymbol{\tau}_1$ and expression (3.49). Introduce $\mathbf{W}_1$ in the cost function (3.83).
4. Again perform *all* iterations of the IQML algorithm until convergence or failure occurs. The result is the vector $\mathbf{g}_2$, and the corresponding time-delay estimate is the final estimate: $\hat{\boldsymbol{\tau}} = \boldsymbol{\tau}_2$.

As we will show in the simulation results, the method **A** presents a lower estimation error and requires less iterations of the IQML algorithm to converge than the method **B**. On the other hand, their computational loads are similar, since in the method **B** the weighting matrix is computed only once (but the total number of iterations is greater). Note that the decoupled iterations method is the one that stems directly from the theoretical results. That is, the delay estimation is divided into two stages: *i)* obtaining the consistent estimate, *ii)* obtaining the asymptotically efficient estimate. However, the coupled iteration method is a logical *ad hoc* modification of the decoupled one given the two iterative processes needed by the proposed estimator. The coupled iterations method does not stem directly from the theoretical study, but it happens to have certain advantages and is preferred in front of the decoupled one.

### 3.7.2 ESPRIT Algorithm

If $d < m$, $d < N$ and $\mathbf{A}$ is full column-rank, it is possible to exploit the Vandermonde structure of $\mathbf{V}(\boldsymbol{\tau})$ using the ESPRIT algorithm [Roy86]. The application of this method to time-delay estimation in the white-noise case is detailed in [Swi98a]. Given the similarity between the cost functions $f_N^w(\boldsymbol{\tau})$ in (3.39) and $g_N(\boldsymbol{\tau}, \mathbf{W})$ in (3.73), the extension of ESPRIT to the new criterion is immediate. In our case, the matrix $\mathbf{F} = \mathbf{Y}^* \hat{\mathbf{R}}_{yy}^{-1/2} \mathbf{W}^{1/2}$ plays exactly the same role as $\mathbf{Y}^*$ in the white-noise case.

Let $\mathbf{U}$ denote the $d$ singular vectors of $\mathbf{F}$ associated with the largest singular values. Next, $\mathbf{U}_1$ (resp. $\mathbf{U}_2$) is constructed by taking the first (resp. last) $N - \delta$ rows of $\mathbf{U}$. The diagonal matrices $\mathbf{S}_{\omega 1}$ and $\mathbf{S}_{\omega 2}$ are built from the first and last $N - \delta$ elements of the diagonal of $\mathbf{S}_\omega$, respectively. Let the $d \times d$ matrix $\boldsymbol{\Psi}$ be the solution of the following overdetermined system of linear equations:

$$\mathbf{S}_{\omega 1}^* \mathbf{U}_2 = \mathbf{S}_{\omega 2}^* \mathbf{U}_1 \boldsymbol{\Psi} \tag{3.84}$$

The time-delay estimates can be determined from the phase of the eigenvalues $\lambda_i$ of $\boldsymbol{\Psi}$ (see [Roy86, Swi98a]):

$$\hat{\tau}_i = \frac{N T_s \angle \lambda_i}{2\pi \delta} \quad i = 0, \cdots, d-1 \,. \tag{3.85}$$

The shift parameter $\delta$ must satisfy two conditions:

$$\delta \leq N - d \quad , \quad \delta < \frac{N T_s}{2 \max_i |\tau_i|} \tag{3.86}$$

The first one prevents the system (3.84) from being indefinite, while the second guarantees that the association between eigenvalues and delays is unique. It is possible to solve the system of equations (3.84) using either Least Squares (LS) or Total Least Squares (TLS) [Gol96].

## 3.8 Simulation Results

In this section we analyze the performance of the cost functions proposed above by means of numerical simulations. Our performance metric is the Root Mean Squared Error (RMSE) of the delay estimates produced by each algorithm. We calculate the RMSE for a wide variety of scenarios as a function of the number of samples $N$, the number of sensors $m$, the signal to interference ratio, the signal to noise ratio, and the relative delay and DOA of the multipath reflections.

### 3.8.1 Simulation Parameters

All simulations are conducted assuming that $d = 2$ delayed versions of a known signal are received by a uniform linear array with antennas spaced 0.5 wavelengths apart. This known signal is a concatenation of $M$ truncated and sampled Nyquist square-root raised cosine pulses[3]. Each pulse has a bandwidth equal to $(1+\varrho)/2T_c$, is truncated to the interval $[-3T_c, 3T_c]$, and the sampling period is $T_c/2$, so there are $L = 13$ samples in each pulse (see Figure 3.1). Note that $T_c$ acts simply as a normalization constant, and $\varrho$ is the roll-off factor which we set equal to 0.2. The use of this type of signal is of interest because each pulse may represent the output of the despreader at every symbol period in a DS-CDMA system (refer to Section 2.5.3 for further details).

The noise plus interference field in which the array operates consists of: *i)* spatially and temporally white Gaussian noise, and *ii)* a temporally white Gaussian interference at DOA $-30^o$ relative to the array broadside, which is responsible for the spatial correlation of the noise plus interference field. Both the noise and the interference are uncorrelated with the desired signal. The remaining scenario parameters, except when one of them is varied, are as follows: $m = 6$ antennas; $M = 3$ pulses constituting each signal; delays of the two signals equal to 0 and $0.4\,T_c$; DOAs of those signals: $0^o$, $10^o$, respectively; Signal to Noise Ratio (SNR) of the first signal[4]: 15.87 dB; Signal to Interference Ratio (SIR) of the first signal: $-3.13$ dB; the second signal is attenuated 3 dB with respect to the first, and they are in phase at the first sensor. In all cases, only the 7 DFT bins with the strongest signal content are employed by IQML and

[3] The expression of the derivative of the Nyquist square-root raised cosine pulse, which is needed to compute the CRB, has been included in Appendix 3 .D, since it presents some indeterminations that need special consideration.

[4] The power of the signals is averaged over all the observation window.

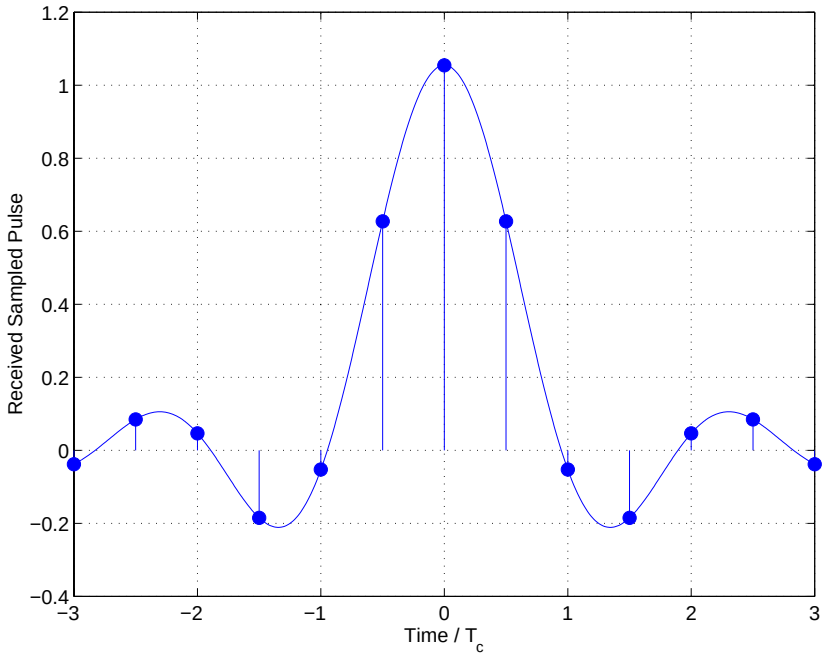


Figure 3.1: Samples of a single pulse and the underlying analog signal.

ESPRIT for estimation of the time delays.

In the figures below, we show the RMSE of the estimate of the time-delay of the first signal (the time-delay estimate of the second signal behaves similarly) obtained from different cost functions and optimization algorithms. The RMSEs are computed from 500 Monte Carlo realizations of the noise and interference, and they are compared to the CRB given by (3.35). Each curve in the figures corresponds to one of the following methods:

1. Asymptotically efficient estimator $g_N(\boldsymbol{\tau}, \hat{\mathbf{W}})$ given by (3.50). The minimization is carried out using IQML, with the weight matrix $\hat{\mathbf{W}}$ recomputed at every IQML iteration (i.e., the coupled iteration method **A** of Section 3.7.1).

2. Consistent estimator $g_N(\boldsymbol{\tau}, \mathbf{I})$ given by (3.54). The estimates are calculated using LS-ESPRIT, since we have observed that in this case ESPRIT somewhat surprisingly yields a lower RMSE than IQML.

3. ML estimator in spatially white noise $f_N^w(\boldsymbol{\tau})$ given by (3.39), with the estimates obtained via IQML as in [Swi98a].

4. Asymptotically efficient estimator $g_N(\boldsymbol{\tau}, \hat{\mathbf{W}})$ given by (3.50). The minimization is carried out using IQML twice, but the matrix $\hat{\mathbf{W}}$ is computed after the first IQML has converged (i.e., the decoupled iteration method **B** in Section 3.7.1). The performance of this method is shown only in Figure 3.2, and it is referred to as IQML "2 iterations".

Only the RMSEs are plotted because these four methods are essentially unbiased (i.e., their biases are much smaller than their standard deviations). The initial value of $\hat{\mathbf{W}}$ used in methods 1 and 4 above is the identity matrix. In these methods and also in method 3, the matrix $\mathbf{G}^*\mathbf{S}_\omega^{-*}\mathbf{S}_\omega^{-1}\mathbf{G}$ appearing in the IQML algorithm is initialized using estimates obtained with ESPRIT. We have noticed that the alternative of initializing this matrix to the identity results in an increased RMSE. In all cases, LS-ESPRIT is used since the more complicated TLS-ESPRIT does not provide an appreciable performance improvement. The displacement between the two data structures in ESPRIT is $\delta = 2$. IQML is implemented with the quadratic constraint $\|\mathbf{g}\|_2 = 1$, since it seems to give better results than the linear constraint $\mathrm{Re}\{g_0\} = 1$. The IQML iterations are terminated when either of the following is satisfied:

- $\|\mathbf{g}_k - \mathbf{g}_{k-1}\|_2 < \epsilon = 10^{-4}$. (Any value of $\epsilon$ between $10^{-2}$ and $10^{-4}$ provides essentially the same performance.)
- the number of iterations $> 50$

### 3.8.2 Effect of the Number of Samples

The finite-sample and asymptotic performance of the four methods above is illustrated in Figure 3.2. As predicted by the theoretical study, the RMSE of the proposed cost functions (methods 1 and 4) tend to the CRB as the number of samples (equivalently, as the number of pulses) increases. Although both methods are asymptotically efficient, method 1 shows a lower RMSE than method 4 for a small number of samples (e.g., the former attains the CRB for 4 or more pulses, whereas the latter needs at least 7 pulses). Another advantage of method 1 over method 4 is that fewer iterations of IQML are required for convergence. For instance, when the number of received pulses is 3, the number of iterations required by method 1 is $5.59 \pm 0.93$ (mean $\pm$ standard deviation), while method 4 needs $7.66 \pm 1.18$ iterations. All the same, both methods have converged in all the runs. Though the number of iterations varies depending on the scenario, in the vast majority of the cases we have simulated it is less than 15 and the difference between method 1 and 4 is approximately constant. Thus, the computational time required for the optimization is reduced by several orders of magnitude thanks to the use of IQML and ESPRIT instead of minimizing (3.28) or (3.50) via a search.

Since method 1 has some advantages over method 4, the former is used for the rest of the simulations. The small difference between its RMSE and the CRB visible in Figures 3.3-3.7 occurs because the method has not achieved its asymptotic behavior for signals formed by only 3 pulses. Also as predicted by the theoretical study, method 2 does not attain the CRB, but performs much better than the estimator designed for the white-noise case (method 3). This occurs because method 2 (cost function $g_N(\boldsymbol{\tau}, \mathbf{I})$) takes into account the spatial correlation of the noise field, though not in an optimal way. It is worth remarking that, because of its simplicity

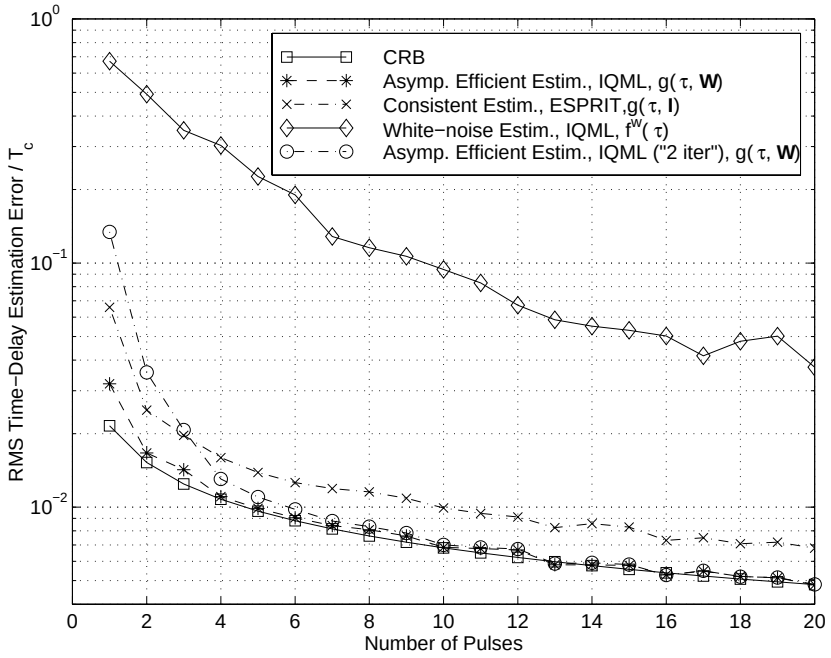


Figure 3.2: RMSE of the proposed estimators as a function of the number of training pulses. Parameters: $\check{\theta}_0 = 0^{\rm o}$, $\check{\theta}_1 = 10^{\rm o}$, $\check{\theta}_i = -30^{\rm o}$, $\check{\tau}_0 = 0$, $\check{\tau}_1 = 0.4T_c$, $m = 6$ antennas, $\mathrm{SNR}_0 = 15.87\,\mathrm{dB}$, $\mathrm{SIR}_0 = -3.13\,\mathrm{dB}$, $\mathrm{SNR}_0/\mathrm{SNR}_1 = 3\,\mathrm{dB}$.

(only ESPRIT is applied) and its low RMSE, method 2 is an excellent initialization scheme for the asymptotically efficient estimators based on IQML. The RMSE obtained with the white-noise estimator is plotted for comparison purposes, and the severe degradation that it undergoes when the noise field is spatially correlated is evident in all the simulations.

### 3.8.3 Effect of the Number of Sensors

Results showing the effect of varying the number of sensors are given in Figure 3.3. In all cases, method 1 outperforms method 2, and both are clearly superior to the white-noise estimator. For the number of sensors shown in the figure, the CRB decreases slightly faster than $1/m$. Now, however, the RMSE of the estimates obtained with $g_N(\boldsymbol{\tau}, \hat{\mathbf{W}})$ does not approach the CRB as the number of sensors increases. This behavior coincides with two well-known results in sensor array processing: As the data grows in a dimension different from the dimension in which the parameters are estimated, *i)* the deterministic ML estimator is not asymptotically efficient [Sto90a, Sto89], and *ii)* the IQML algorithm is inconsistent [Sto97] and its RMSE does not necessarily decrease [Li98]. Moreover, in our problem another deleterious effect is added; namely, the estimation errors of the covariance matrices $\hat{\mathbf{R}}_{yy}$ or $\hat{\mathbf{Q}}$ increase as the number of antennas increases for a fixed number of samples.

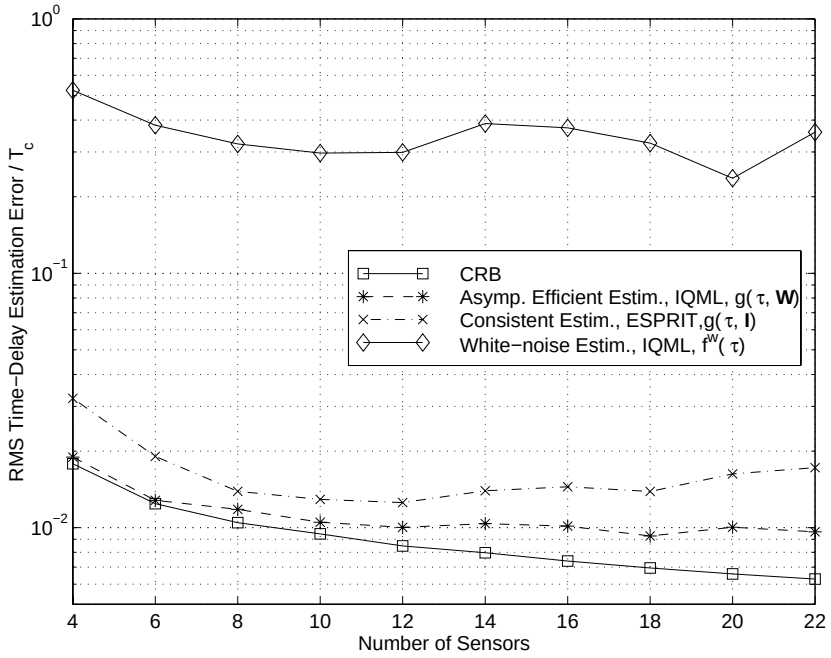


Figure 3.3: RMSE of the proposed estimators as a function of the number of sensors. Parameters: $\check{\theta}_0 = 0^{\rm o}$, $\check{\theta}_1 = 10^{\rm o}$, $\check{\theta}_i = -30^{\rm o}$, $\check{\tau}_0 = 0$, $\check{\tau}_1 = 0.4\,T_c$, $M = 3$ pulses, $\mathrm{SNR}_0 = 15.87\,\mathrm{dB}$, $\mathrm{SIR}_0 = -3.13\,\mathrm{dB}$, $\mathrm{SNR}_0/\mathrm{SNR}_1 = 3\,\mathrm{dB}$.

Another effect is that the number of iterations needed by IQML to converge increases with the number of sensors. Although beyond the scope of this thesis, it is worth noting that the performance of the method 4, which is the most sensitive to the increase of the array size, can be improved for a large number of antennas using a low-rank modification of the signal matrix similar to that in the MODE and WSF (weighted subspace fitting) algorithms. That is, the term $\mathbf{Z} = \mathbf{Y}^* \hat{\mathbf{R}}_{yy}^{-1/2}\, \hat{\mathbf{W}}\, \hat{\mathbf{R}}_{yy}^{-1/2}\, \mathbf{Y}$ appearing in $g(\boldsymbol{\tau}, \hat{\mathbf{W}})$ can be replaced by $\hat{\mathbf{E}}\, \tilde{\boldsymbol{\Lambda}}\, \hat{\mathbf{E}}^*$, where $\hat{\mathbf{E}}$ represents the eigenvectors of $\mathbf{Z}$ associated with the $d$ largest eigenvalues, and $\tilde{\boldsymbol{\Lambda}}$ is a certain diagonal weighting matrix [Sto90c, Ott93, Vib91a]. The study of the performance using the low-rank matrix is left as a topic for future research.

### 3.8.4 Effect of the SIR and SNR

The objective of the first simulation, whose results are given in Figure 3.4, is to show that the RMSE of the consistent and asymptotically efficient estimators proposed herein are robust against arbitrarily strong interferers. Therefore, they are valid approaches for time-delay estimation in interference-limited situations, such as most mobile communication systems. Note that the estimator designed for a white-noise scenario completely fails for $\mathrm{SIR} < -10\,\mathrm{dB}$. Next, observe in Figure 3.5 the effect of varying the power of the white noise. As it could be expected,

the improvement obtained using $g_N(\boldsymbol{\tau}, \mathbf{W})$ and $g_N(\boldsymbol{\tau}, \mathbf{I})$ instead of $f_N^w(\boldsymbol{\tau})$ is increasingly more significant as the SNR increases. Similarly, the superiority of the asymptotically efficient estimator to the consistent estimator becomes slightly more noticeable for high SNR. Actually, this behavior was justified theoretically in Sections 3.6.1 and 3.6.2, where the condition needed by the consistent estimator to approach the exact ML method was presented.

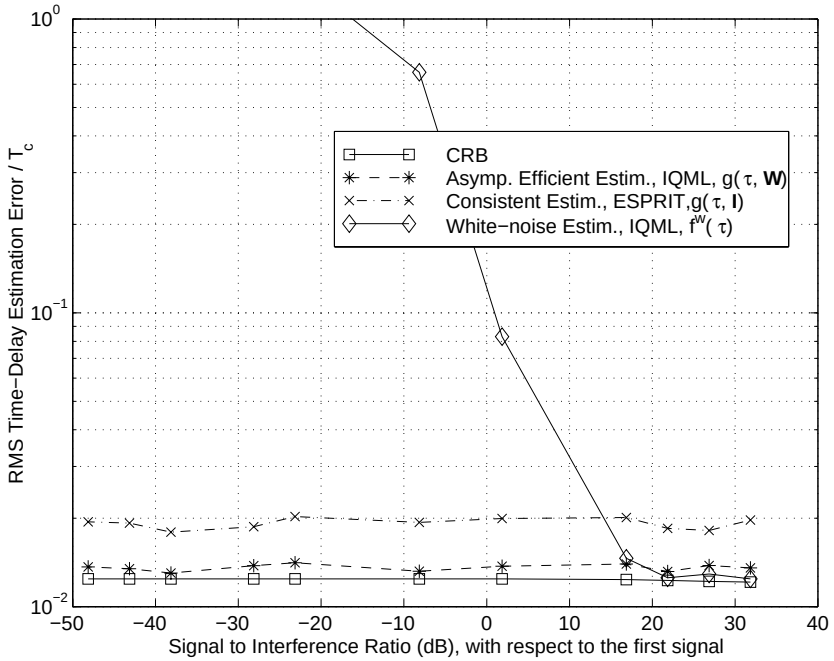


Figure 3.4: RMSE of the proposed estimators as a function of the interference power. Parameters: $\check{\theta}_0 = 0^{\text{o}}$, $\check{\theta}_1 = 10^{\text{o}}$, $\check{\theta}_i = -30^{\text{o}}$, $\check{\tau}_0 = 0$, $\check{\tau}_1 = 0.4\,T_c$, $m = 6$ antennas, $M = 3$ pulses, $\text{SNR}_0 = 15.87\,\text{dB}$, $\text{SNR}_0/\text{SNR}_1 = 3\,\text{dB}$.

### 3.8.5 Closely Spaced Signals

In Figures 3.6 and 3.7, we investigate the ability of the different methods to resolve closely-spaced signals in the temporal and spatial domains. As with all time-delay estimators that do not assume parameterized spatial signatures, the CRB grows without limit as the relative delay of the signals decreases. We observe that the estimator we have proposed is always very close to the CRB, except for the case of relative delays smaller than $0.1T_c$. However, this range of delays lacks practical interest because reliable unbiased delay estimates cannot be expected for any method; i.e., in this range the best achievable standard deviation for any unbiased estimator is larger than half the time-delay separation between the two signals [Vib91b]. It is remarkable that the RMSE can be largely reduced in this range of delays by allowing a small bias for the estimates, as shown in Chapter 4.

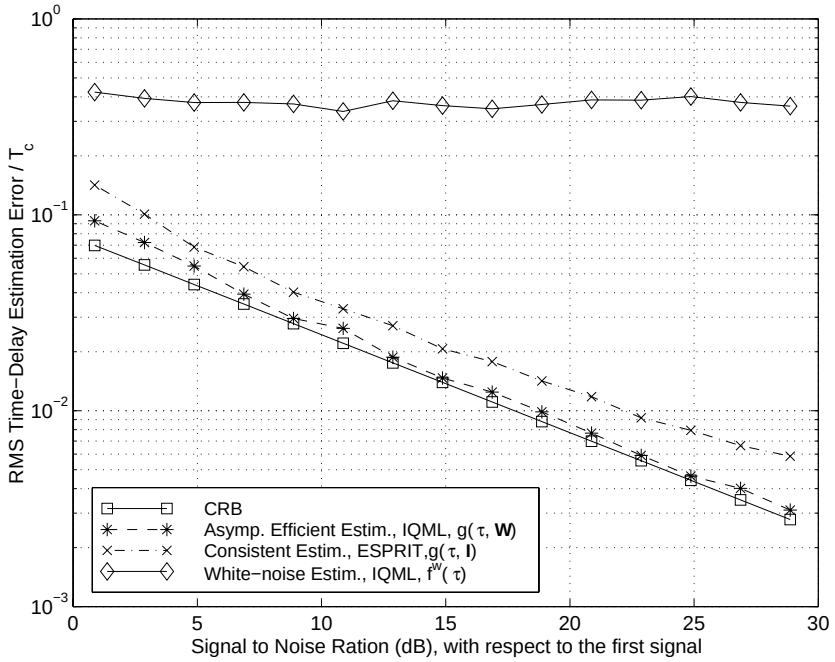


Figure 3.5: RMSE of the proposed estimators as a function of the white-noise power. Parameters: $\check{\theta}_0 = 0^{\text{o}}$, $\check{\theta}_1 = 10^{\text{o}}$, $\check{\theta}_i = -30^{\text{o}}$, $\check{\tau}_0 = 0$, $\check{\tau}_1 = 0.4\,T_c$, $m = 6$ antennas, $M = 3$ pulses, $\text{SIR}_0 = -3.13$ dB, $\text{SNR}_0/\text{SNR}_1 = 3$ dB.

When the DOA separation of the signals is smaller than the beamwidth of the sensor array (in our case, about $9^{\text{o}}$ at -3dB), the CRB increases as the DOA separation decreases; but it does not tend to infinity as in the case of delay separation. Also when the DOA separation is smaller than the beamwidth, ESPRIT undergoes a severe degradation because the matrix $\mathbf{A}$ tends to be rank deficient. However, the performance of the proposed method is always very close to the CRB, even though it is initialized with ESPRIT.

### 3.8.6 Performance Using a Search

We have also analyzed the RMSEs obtained when the criteria $V_N(\boldsymbol{\tau})$ in (3.28), $g_N(\boldsymbol{\tau}, \hat{\mathbf{W}})$ in (3.50), $g_N(\boldsymbol{\tau}, \mathbf{I})$ in (3.54), and $f_N^w(\boldsymbol{\tau})$ in (3.39) are minimized using a search. We have observed that direct minimization of $V_N(\boldsymbol{\tau})$ and $g_N(\boldsymbol{\tau}, \hat{\mathbf{W}})$ and method 1 all yield nearly the same RMSE even for a small number of samples (see Figure 3.8). Therefore, the new cost function we have proposed, besides being asymptotically efficient, does not entail any degradation in the finite-sample case with respect to the exact ML estimator (3.28). Moreover, the minimization using IQML does not introduce any impairment with respect to the use of a search. Secondly, the minimization of $g_N(\boldsymbol{\tau}, \mathbf{I})$ by means of a search or using ESPRIT (i.e., method 2) results in approximately the same RMSE. On the contrary, the RMSE obtained from the minimization

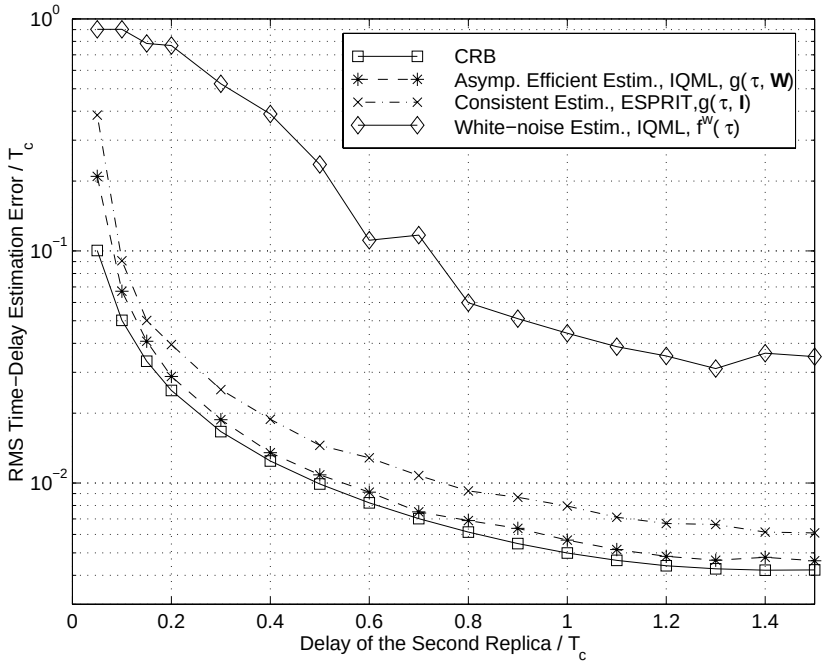


Figure 3.6: RMSE of the proposed estimators as a function of time-delay separation. Parameters: $\check{\theta}_0 = 0^{\rm o}$, $\check{\theta}_1 = 10^{\rm o}$, $\check{\theta}_i = -30^{\rm o}$, $\check{\tau}_0 = 0$, $m = 6$ antennas, $M = 3$ pulses, $\mathrm{SNR}_0 = 15.87\,\mathrm{dB}$, $\mathrm{SIR}_0 = -3\,\mathrm{dB}$, $\mathrm{SNR}_0/\mathrm{SNR}_1 = 3\,\mathrm{dB}$.

of $f_N^w(\boldsymbol{\tau})$ using a search is slightly smaller than that obtained using IQML (i.e., method 3). Numerical results supporting these last claims are provided in Figure 3.9.

## 3.9 Use of Multiple Incoherent Bursts

The asymptotically efficient approximation to the exact ML estimator proposed in this chapter also serves to simplify the ML estimator obtained when the data is constituted by multiple "incoherent bursts". This situation consists in that the received signals can be divided into several portions or "bursts". The waveform of the desired signals is known during any of those portions, but the signals are multiplied by different unknown constants in each portion, so the waveform is not known along the whole observation interval. The data corresponding to the $l$th burst is represented by the following $m \times L$ matrix

$$\mathbf{Y}_l = \gamma_l \, \mathbf{A} \, \mathbf{S}(\boldsymbol{\tau}) + \mathbf{E}_l \qquad l = 1 \ldots M' \,, \tag{3.87}$$

where $M'$ is the number of bursts, and $\{\gamma_l\}$ are the unknown constants multiplying the corresponding portions of the signal. Since the spatial signatures are unstructured, we can arbitrarily fix the value of one of those constants, e.g., we fix $\gamma_1 = 1$. The assumption of multiple incoherent bursts may be suitable to model the despread signals when the transmitted symbols are

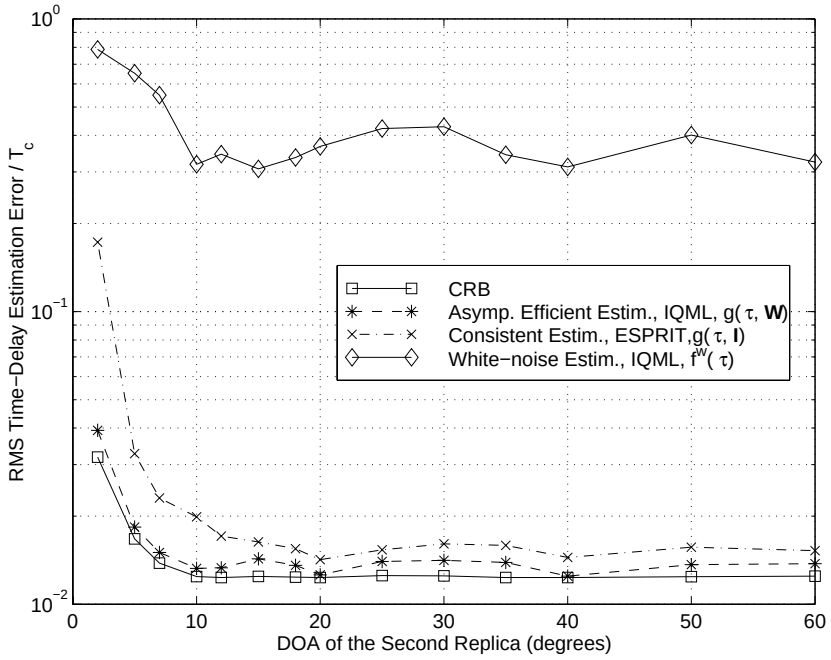


Figure 3.7: RMSE of the proposed estimators as a function of DOA separation. Parameters: $\check{\theta}_0 = 0^{\rm o}$, $\check{\theta}_i = -30^{\rm o}$, $\check{\tau}_0 = 0$, $\check{\tau}_1 = 0.4\,T_c$, $m = 6$ antennas, $M = 3$ pulses, $\mathrm{SNR}_0 = 15.87\,\mathrm{dB}$, $\mathrm{SIR}_0 = -3.13\,\mathrm{dB}$, $\mathrm{SNR}_0/\mathrm{SNR}_1 = 3\,\mathrm{dB}$.

unknown. It is clear that the model in (3.87) is equivalent to that in (2.43) when the symbols are unknown (making an evident identification between $\mathbf{S}(\boldsymbol{\tau})$ and $\mathbf{G}(\boldsymbol{\tau})$). Another situation where the use of multiple bursts is appropriate arises when the Doppler frequency is not small compared with the reciprocal of the observation interval. In this case, the whole observation interval may be divided into several portions, in such a way that the amplitudes can be taken as constant during each portion. Thus, the carrier-phase shift produced by the Doppler frequency from portion to portion is modeled by the coefficients $\{\gamma_l\}$.

The spatial correlation matrix of the noise in the $l$th interval is named $\mathbf{Q}_l$. This matrix may be either equal or not for all the bursts, depending on the degree of variability of the scenario. For instance, if the variation of the number, DOA or power of the interferences is slow with respect to the observation interval, it is logical that the correlation matrix be the same for all the bursts.

The application of the ML principle to (3.87) does not lead to an estimator in which $\mathbf{A}$ and $\{\gamma_l\}$ can be eliminated analytically in an easy manner, and the estimator does not seem to admit an approximation similar to the one presented in Section 3.4. To circumvent this problem, we make a simplifying assumption. It consists in considering that the matrices of spatial signatures are arbitrary at each burst, so they are not necessarily related by a multiplicative constant.

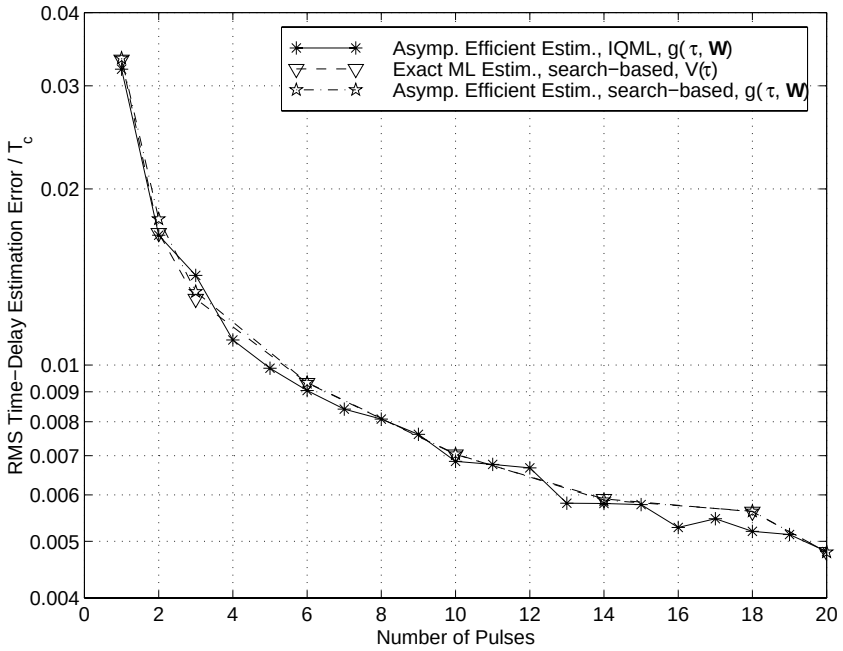


Figure 3.8: Comparison with the search-based estimators. Parameters: $\check{\theta}_0 = 0^{\rm o}$, $\check{\theta}_1 = 10^{\rm o}$, $\check{\theta}_i = -30^{\rm o}$, $\check{\tau}_0 = 0$, $\check{\tau}_1 = 0.4\,T_c$, $m = 6$ antennas, $\mathrm{SNR}_0 = 15.87\,\mathrm{dB}$, $\mathrm{SIR}_0 = -3.13\,\mathrm{dB}$, $\mathrm{SNR}_0/\mathrm{SNR}_1 = 3\,\mathrm{dB}$.

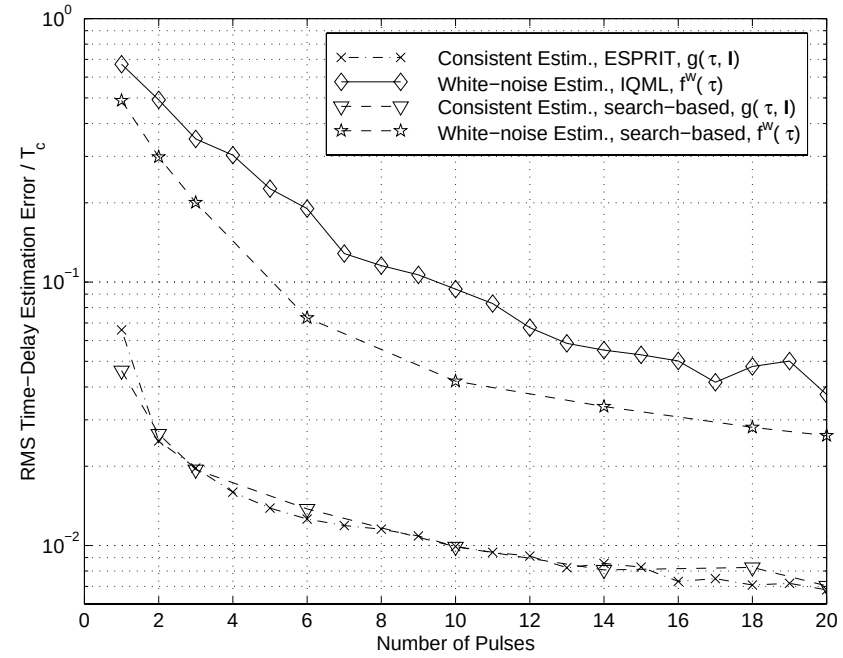


Figure 3.9: Comparison with the search-based estimators. Parameters: $\check{\theta}_0 = 0^{\rm o}$, $\check{\theta}_1 = 10^{\rm o}$, $\check{\theta}_i = -30^{\rm o}$, $\check{\tau}_0 = 0$, $\check{\tau}_1 = 0.4\,T_c$, $m = 6$ antennas, $\mathrm{SNR}_0 = 15.87\,\mathrm{dB}$, $\mathrm{SIR}_0 = -3.13\,\mathrm{dB}$, $\mathrm{SNR}_0/\mathrm{SNR}_1 = 3\,\mathrm{dB}$.

Therefore, the model that we adopt in order to apply the ML approach is

$$\mathbf{Y}_l = \mathbf{A}_l\,\mathbf{S}(\boldsymbol{\tau}) + \mathbf{E}_l \qquad l = 1 \ldots M' \ . \tag{3.88}$$

If the correlation matrices of the noise are the same for all the bursts, the ML cost function to be minimized is

$$f(\boldsymbol{\tau}) = \ln \left| \mathbf{Y}_1\,\mathbf{Y}_1^* + \ldots + \mathbf{Y}_{M'}\,\mathbf{Y}_{M'}^* - \mathbf{Y}_1\,\mathbf{P}_{\mathbf{S}^*(\boldsymbol{\tau})}\,\mathbf{Y}_1^* - \ldots - \mathbf{Y}_{M'}\,\mathbf{P}_{\mathbf{S}^*(\boldsymbol{\tau})}\,\mathbf{Y}_{M'}^* \right| \ . \tag{3.89}$$

The derivation is omitted because it follows closely the steps of that in Section 3.3. The minimization of this function is computationally expensive. However, using the results of Sections 3.4–3.6, it is reasonable to consider the following approximate criterion

$$g(\boldsymbol{\tau}) = -\mathrm{Tr}\left\{ \mathbf{P}_{\mathbf{S}^*(\boldsymbol{\tau})} \left( \mathbf{Y}_1^*\,\hat{\mathbf{Q}}^{-1}\,\mathbf{Y}_1 + \ldots + \mathbf{Y}_{M'}^*\,\hat{\mathbf{Q}}^{-1}\,\mathbf{Y}_{M'} \right) \right\} \ , \tag{3.90}$$

where $\hat{\mathbf{Q}}$ is an estimate of the noise correlation matrix. The interesting feature is that $g(\boldsymbol{\tau})$ admits the use of the IQML algorithm, since it depends linearly on $\mathbf{P}_{\mathbf{S}^*(\boldsymbol{\tau})}$, and also the use of the ESPRIT algorithm (by performing an eigendecomposition of the matrix between parentheses in (3.90)).

Similar results are obtained when the noise correlation matrices differ from burst to burst. In this case, it is again straightforward to show that the ML criterion is

$$f(\boldsymbol{\tau}) = \ln \left| \mathbf{Y}_1\,\mathbf{Y}_1^* - \mathbf{Y}_1\,\mathbf{P}_{\mathbf{S}^*(\boldsymbol{\tau})}\,\mathbf{Y}_1^* \right| + \ldots + \ln \left| \mathbf{Y}_{M'}\,\mathbf{Y}_{M'}^* - \mathbf{Y}_{M'}\,\mathbf{P}_{\mathbf{S}^*(\boldsymbol{\tau})}\,\mathbf{Y}_{M'}^* \right| \ . \tag{3.91}$$

Approximating each term in (3.91) according to the results in Sections 3.4–3.6 yields

$$g(\boldsymbol{\tau}) = -\mathrm{Tr}\left\{ \mathbf{P}_{\mathbf{S}^*(\boldsymbol{\tau})} \left( \mathbf{Y}_1^*\,\hat{\mathbf{Q}}_1^{-1}\,\mathbf{Y}_1 + \ldots + \mathbf{Y}_{M'}^*\,\hat{\mathbf{Q}}_{M'}^{-1}\,\mathbf{Y}_{M'} \right) \right\} \ , \tag{3.92}$$

where $\hat{\mathbf{Q}}_l$ is an estimate of the noise correlation matrix during the $l$th interval.

The ML estimators of (3.89) and (3.91) are not asymptotically efficient as $M' \to \infty$, because the number of unknowns increases linearly with $M'$ (the estimates of $\mathbf{A}_l$ will not be consistent). Indeed, the performance analysis of Sections 3.3–3.4 is only valid when the number of samples per burst (for a fixed number of bursts) tends to infinity. Similarly, the approximations of (3.89) and (3.91) by (3.90) and (3.92), respectively, cannot be claimed to be (asymptotically) equivalent as $M' \to \infty$. They are simply *ad hoc* approximations which offer a computational advantage. An open research topic is the study of the time delay estimation problem when a stochastic model for the spatial signatures is used. That is, instead of treating the spatial signatures are deterministic quantities, the rows of $\mathbf{A}_l$ are considered as random vectors drawn from a Gaussian distribution with $d \times d$ correlation matrix $\mathbf{R}_A$. Then, the problem is to estimate $\mathbf{R}_A$ in place of the particular value of the spatial signatures. It is probable that the ML estimator derived for that signal model be asymptotically efficient as the number of bursts increases (assuming that the noise correlation is the same for all the bursts). In relation to this, it would be also

interesting to analyze if there exist some low-rank modification (e.g., similar to the MODE or subspace weighting methods) of the matrix $\mathbf{Y}_1^* \hat{\mathbf{Q}}^{-1} \mathbf{Y}_1 + \ldots + \mathbf{Y}_{M'}^* \hat{\mathbf{Q}}^{-1} \mathbf{Y}_{M'}$ that makes the estimator $g(\boldsymbol{\tau})$ in (3.90) asymptotically (in $M'$) efficient.

## 3.10 Data Model for FIR Channels

In this and the following two sections, we consider a slight variation of the problem (**P1**) presented in Section 3.2 that results when a small but significant modification to the signal model is used. In this approach, the effect of the multipath channel is modeled as a finite impulse response (FIR) filter with order $d$. Thus, as an alternative to (3.4), consider the following definition for $\mathbf{s}[n,\tau]$:

$$\mathbf{s}[n,\tau] = \left[ \begin{array}{cccc} s\left(nT_s - \tau\right) & s\left(nT_s - \tau - T_0\right) & \cdots & s\left(nT_s - \tau - (d-1)\,T_0\right) \end{array} \right]^T \qquad d \times 1\,, \quad (3.93)$$

where $T_0$ is the temporal spacing of the FIR channel and can be freely chosen, together with $d$, when setting up the model. In order to further differentiate the model employed herein from that in previous sections, the matrix of spatial signatures $\mathbf{A}$ is replaced by a channel matrix named $\mathbf{H}$. Therefore, the set of received samples is written as

$$\mathbf{Y} = \mathbf{H}\,\mathbf{S}\,(\tau) + \mathbf{E}\,, \quad (3.94)$$

where the $n$th column of $\mathbf{S}\,(\tau)$ is $\mathbf{s}[n,\tau]$. The $k$th row of $\mathbf{H}$ contains the FIR filter coefficients for the channel separating the source and the $k$th antenna. That is, the $m \times d$ matrix $\mathbf{H}$ represents the single-input-multiple-output (SIMO) channel for the signal of interest. A motivation for this model arises from the fact that sometimes receivers combine the different rays of the signals using a RAKE structure before detecting the symbols. The RAKE structure is indeed a bank of filters with a fixed delay (typically the inverse of the signal bandwidth or a fraction thereof) between consecutive taps, that is to say, it is a FIR filter. Hence, it seems logical to extend this structure also to the timing synchronization.

The scalar time delay parameter $\tau$ is referred to as *frame* delay in order to differentiate it from the *propagation* delays in the model of (3.4). For the model of (3.93), we word the problem statement as follows:

> **Problem P2** – Given $N$ snapshots of data in the matrix $\mathbf{Y}$ described by equations (3.93), (3.94), and (3.7), estimate the FIR channel matrix $\mathbf{H}$ and frame delay $\tau$ of the signal, as well as the spatial covariance $\mathbf{Q}$ of the noise and interference.

Although in the FIR case the effects of temporal oversampling or a pulse shaping filter (for digitally modulated signals) could be factored into the channel matrix $\mathbf{H}$, we will assume that the

elements of $\mathbf{s}[n,\tau]$ are samples of the continuous modulated waveform $s(t)$ rather than discrete symbols (this applies to the model in (3.4) as well). As such, the matrix $\mathbf{H}$ only describes the propagation effects of the channel, and $\tau$ is a continuous-valued variable. This assumption is somewhat different than that made in [Ast99b] and in other work on blind equalization of FIR channels (e.g., [Ton94, Slo94, Mou95, Tug95, Din97]).

A relation between the FIR model in (3.94) and the model used for the estimation of the delays of several replicas can be established. In the latter, the contribution of the signals is expressed as $\mathbf{A}\,\tilde{\mathbf{S}}(\boldsymbol{\tau})$, as shown in (3.1)-(3.5). Now, we consider that the number of columns of $\mathbf{A}$ (i.e., the number of rows of $\tilde{\mathbf{S}}(\boldsymbol{\tau})$) is $d'$. Assuming that the underlying signal $s(t)$ is band-limited and $T_0$ satisfies the Nyquist criterion, the $k,l$th element of $\tilde{\mathbf{S}}(\boldsymbol{\tau})$ can be expressed approximately as a linear combination of the $l$th-column elements of $\mathbf{S}\,(\tau)$ [Laa96]. Therefore, there exists a $d' \times d$ interpolating matrix $\mathbf{J}$ such that

$$\tilde{\mathbf{S}}(\boldsymbol{\tau}) \approx \mathbf{J}\,\mathbf{S}\,(\tau)\ . \tag{3.95}$$

For (3.95) to be exact in a general case, the number of columns of rows of $\mathbf{S}\,(\tau)$, that is $d$, should be infinite. However, very good approximations can be obtained for a finite $d$ [Laa96]. Therefore, we can write $\mathbf{A}\,\tilde{\mathbf{S}}(\boldsymbol{\tau}) \approx \mathbf{A}\,\mathbf{J}\,\mathbf{S}\,(\tau)$, and identifying the channel matrix as $\mathbf{H} = \mathbf{A}\,\mathbf{J}$, the relation between the FIR model and the multiple-delays model becomes apparent.

The CRB for the problem at hand can be readily obtained from the derivation in Appendix 3.A. It suffices to express the delays' vector as

$$\boldsymbol{\tau} = \left[\ \tau \quad \tau + T_0 \quad \ldots \quad \tau + (d-1)T_0\ \right]^T\ , \tag{3.96}$$

and apply the chain rule for the derivative (taking into account that the elements of the Fisher information matrix (FIM) are minus the expectation of the Hessian of the log-likelihood function). Thus, the FIM of the signal parameters

$$\boldsymbol{\eta}_s = \left[\ \mathrm{Re}\left\{\mathrm{vec}\left\{\mathbf{H}\right\}\right\}^T \quad \mathrm{Im}\left\{\mathrm{vec}\left\{\mathbf{H}\right\}\right\}^T \quad \tau\ \right]^T \tag{3.97}$$

is

$$\mathbf{FIM}\left(\boldsymbol{\eta}_s\right) = \left[\begin{array}{cc|c} \mathrm{Re}\left\{\mathbf{F}_1\right\} & -\mathrm{Im}\left\{\mathbf{F}_1\right\} & \mathrm{Re}\left\{\mathbf{F}_3\,\mathbf{1}\right\} \\ \mathrm{Im}\left\{\mathbf{F}_1\right\} & \mathrm{Re}\left\{\mathbf{F}_1\right\} & \mathrm{Im}\left\{\mathbf{F}_3\,\mathbf{1}\right\} \\ \hline \mathrm{Re}\left\{\mathbf{F}_3\,\mathbf{1}\right\}^T & \mathrm{Im}\left\{\mathbf{F}_3\,\mathbf{1}\right\}^T & \mathrm{Re}\left\{\mathbf{1}^T\,\mathbf{F}_2\,\mathbf{1}\right\} \end{array}\right]\ , \tag{3.98}$$

where $\mathbf{F}_1$, $\mathbf{F}_2$ and $\mathbf{F}_3$ are defined as in (3.113)–(3.115) (with the change of $\mathbf{A}$ by $\mathbf{H}$). Hence, the CRB for the frame delay is

$$\begin{aligned} \mathrm{CRB}^{-1}\left(\tau\right) &= 2\cdot\mathbf{1}^T\left(\left(\mathbf{D}(\boldsymbol{\tau})\,\mathbf{P}^{\perp}_{\mathbf{S}^*(\boldsymbol{\tau})}\,\mathbf{D}^*(\boldsymbol{\tau})\right)\odot\left(\mathbf{H}^*\,\mathbf{Q}^{-1}\,\mathbf{H}\right)^T\right)\mathbf{1} \\ &= 2\,\mathrm{Tr}\left\{\left(\mathbf{D}(\boldsymbol{\tau})\,\mathbf{P}^{\perp}_{\mathbf{S}^*(\boldsymbol{\tau})}\,\mathbf{D}^*(\boldsymbol{\tau})\right)\left(\mathbf{H}^*\,\mathbf{Q}^{-1}\,\mathbf{H}\right)\right\}. \end{aligned} \tag{3.99}$$

## 3.11 Polynomial Rooting Approach

The mathematical approach to the exact ML estimator and the asymptotically equivalent one for problems (**P1**) and (**P2**) is identical. Therefore, the derivations throughout Sections 3.3–3.5 apply for both problems; the only difference is that for (**P2**), $\boldsymbol{\tau}$ is a scalar variable. As a result, the ML criterion for the frame delay requires only a one-dimensional search, and thus is not overly burdensome. However, we find interesting to propose an algorithm that provides the frame delay estimate by rooting a low-order polynomial. Such an algorithm may be useful, for instance, in applications where fast feedforward synchronization is needed (e.g., burst transmissions).

The polynomial rooting-algorithm stems from a modification of the IQML algorithm. According to the results of this chapter, we are concerned with the minimization of

$$g_N(\tau, \mathbf{W}) = -\frac{1}{N}\mathrm{Tr}\left\{\mathbf{W}^{1/2}\,\hat{\mathbf{R}}_{yy}^{-1/2}\,\mathbf{Y}\,\mathbf{P}_{\mathbf{S}^*(\tau)}\,\mathbf{Y}^*\,\hat{\mathbf{R}}_{yy}^{-1/2}\,\mathbf{W}^{1/2}\right\} . \tag{3.100}$$

for a certain weighting matrix $\mathbf{W}$. Similarly to (3.74)–(3.77), the frequency representation of the signal satisfies

$$\mathbf{S}^*(\tau) = \mathbf{S}_\omega^*\,\mathbf{V}(\tau) , \tag{3.101}$$

where

$$\mathbf{V}(\tau) = \left[\begin{array}{cccc} \mathbf{v}(\tau) & \mathbf{v}(\tau+T_0) & \ldots & \mathbf{v}(\tau+(d-1)T_0) \end{array}\right] . \tag{3.102}$$

The criterion in (3.100) can be expressed as a function of $x \triangleq \exp(j2\pi\tau/(NT_s))$, resulting in a polynomial in $x$ of order $2N-2$, since the matrix $(\mathbf{V}^*(\tau)\,\mathbf{S}_\omega\,\mathbf{S}_\omega^*\,\mathbf{V}(\tau))$ that appears in the projection matrix does not depend on $\tau$. Instead of this approach, we describe below a method that leads to the rooting of polynomials of order $2d$, and it is natural that $d \ll N$.

As in the IQML algorithm, let the elements of the vector $\mathbf{g} = [1\; g_1\; \cdots\; g_d]^T$ be taken from the coefficients of the polynomial

$$\mathcal{G}(z) = z^d + g_1\,z^{d-1} + \cdots + g_d = \prod_{n=0}^{d-1}(z - x\,r^n) , \tag{3.103}$$

where $r \triangleq \exp(j2\pi T_0/(NT_s))$. Let us also define

$$\boldsymbol{\Omega} = \mathbf{S}_\omega^{-*}\,\mathbf{Y}^*\,\hat{\mathbf{R}}_{yy}^{-1/2}\,\mathbf{W}^{1/2}/\sqrt{N} \tag{3.104}$$

$$\boldsymbol{\Upsilon} = \left(\mathbf{G}^*\,\mathbf{S}_\omega^{-*}\,\mathbf{S}_\omega^{-1}\,\mathbf{G}\right)^{-1} , \tag{3.105}$$

The matrix $\mathbf{G}$ was defined (3.82). Using the same reasoning as in Section 3.7.1, minimizing (3.100) is equivalent to minimizing

$$\tilde{g}(\mathbf{g}, \mathbf{W}) = \mathrm{Tr}\left\{\boldsymbol{\Omega}^*\,\mathbf{G}\,\boldsymbol{\Upsilon}\,\mathbf{G}^*\,\boldsymbol{\Omega}\right\} . \tag{3.106}$$

It can be readily shown starting from (3.103) that vector $\mathbf{g}$ satisfies

$$\mathbf{g} = \mathbf{K}\,\mathbf{t}\,(x)\ , \tag{3.107}$$

where $\mathbf{K}$ is a diagonal matrix whose elements are the coefficients of the polynomial $\mathcal{G}(z)$ for the case $x = 1$, and

$$\mathbf{t}\,(x) = \left[\ 1 \quad x \quad \ldots \quad x^d\ \right]^T\ . \tag{3.108}$$

Therefore, if the term $\boldsymbol{\Upsilon}$ is held fixed, the cost function in (3.106) can be written as a polynomial in $x$ of order $2d$, as follows:

$$\tilde{g}\,(x, \mathbf{W}) = \mathbf{t}^T\,(1/x)\ \mathbf{K}^*\,\mathbf{C}\,\mathbf{K}\,\mathbf{t}\,(x) \tag{3.109}$$

for some matrix $\mathbf{C}$ obtained from $\boldsymbol{\Omega}$ and $\boldsymbol{\Upsilon}$ (see Appendix 3.E). The minimum of $\tilde{g}\,(x, \mathbf{W})$ on the unit circle is computed by first finding the roots of its derivative. Next, (3.109) is evaluated at the set of roots that lie on the unit circle, and the one giving the minimum is selected. Using this root and the definition of $x$, the delay estimate is easily obtained. This procedure is repeated until certain convergence or failure conditions are satisfied (e.g., in the simulations these conditions are: change in $x$ smaller than $10^{-4}$, number of iterations larger than 50). At each iteration, the matrix $\boldsymbol{\Upsilon}$ is recomputed using the previous estimate of $x$; and in the first iteration, $\boldsymbol{\Upsilon}$ is taken equal to the identity. An essential feature of this algorithm is that the inverse matrix operation required by the computation of $\boldsymbol{\Upsilon}$ needs to be calculated only once, and this can be done *off-line*. The matrix to be inverted depends exclusively on some design parameters, and the update of $\boldsymbol{\Upsilon}$ at each iteration only involves the left- and right-hand product of a fixed matrix by diagonal ones that solely depend on $x$ (see Appendix 3.E).

## 3.12 Simulation Results for FIR Channels

In this section, we analyze and compare with the CRB the performance of several estimators for the FIR model. Specifically, we consider the exact ML estimator, its asymptotically equivalent approximation presented in this chapter, and the ML estimator derived under the assumption of white noise. The cost function of the first one is minimized by means of a search. Whereas, the polynomial rooting algorithm proposed in the previous section is applied to the latter two. Under the white-noise assumption, the weighting matrix is $\mathbf{W} = \hat{\mathbf{R}}_{yy}^{1/2}$. In the case of the approximate estimator for colored noise, we have chosen to update the matrix $\mathbf{W}$ at each iteration of the algorithm using (3.49) and (3.96). That is to say, we use the coupled iteration procedure **A** described in Section 3.7.1.

The characteristics of the signal scenario essentially coincide with those in Section 3.8.1. A few parameters are different, and their default values are described below. The signals are formed

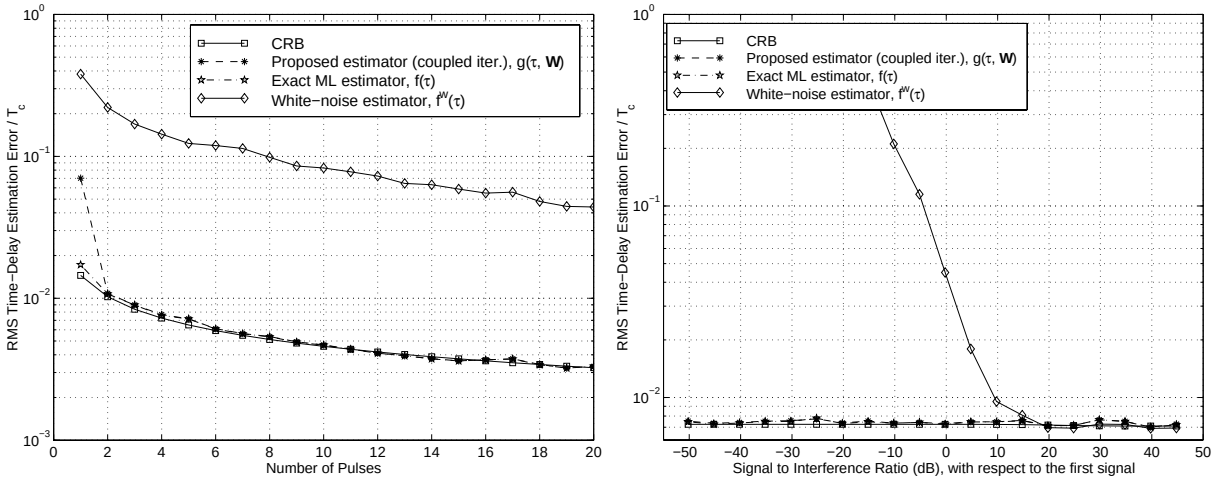


(a) $\mathrm{SIR}_0 = -7.2\,\mathrm{dB}$ (b) $M = 4$ pulses

Figure 3.10: RMSE of several estimators as a function of the number of training pulses and the interference power. Parameters: $\breve{\theta}_0 = 0^{\mathrm{o}}$, $\breve{\theta}_1 = 10^{\mathrm{o}}$, $\breve{\theta}_i = -30^{\mathrm{o}}$, $\breve{\tau}_0 = 0$, $\breve{\tau}_1 = 0.5\,T_c$, $m = 6$ antennas, $d = 2$, $\mathrm{SNR}_0 = 13.8\,\mathrm{dB}$, $\mathrm{SNR}_0/\mathrm{SNR}_1 = 3\,\mathrm{dB}$, $T_0 = 0.5T_c$.

by the concatenation of $M = 4$ pulses. Each square-root raised cosine pulse is truncated to the interval $[-5T_c, 5T_c]$, so it consists of $L = 21$ samples. The delays of the two arrivals are $\breve{\tau}_0 = 0$ and $\breve{\tau}_1 = 0.5T_c$. The signal to noise ratio for the first (strongest) ray is $\mathrm{SNR}_0$=13.8dB, which is lower than that used in Section 3.8.1 because the length of the pulses has been increased. This effect together with an increase of the interference power itself reduces the signal to interference ratio to $\mathrm{SIR}_0 = -7.2$dB. Finally, the model assumes that the temporal spacing of the FIR channel is $T_0 = 0.5T_c$, and the number of taps is $d = 2$ (excepting in Figure 3.11b).

In Figure 3.10a, the performance of the different estimators in the absence of model errors (i.e., $T_0 = \breve{\tau}_1 - \breve{\tau}_0$ and the length of the FIR filter $d$ is equal to the number of arrivals) versus the length of the signal is illustrated. The RMSEs of the exact ML estimator and the proposed approximation reach the CRB for small sample sizes. This fact proves that neither the cost function $g(\tau, \hat{\mathbf{W}})$ itself nor the subsequent minimization using the polynomial rooting approach entail a significant degradation with respect to the exact search-based ML estimator. Moreover, the number of iterations required by proposed algorithm is rather modest. For instance, when the number of received pulses is 4, the number of iterations is $8.41 \pm 2.77$ (mean $\pm$ standard deviation), and the algorithm converged in all realizations. Figure 3.10b bears out that the methods that take into account the spatial correlation of the interference are practically insensitive to the CCI level, whenever enough degrees of freedom are available. On the other hand, under the rather usual assumption of white noise, the resulting estimator is deteriorated for signal to interference ratios below 10dB. In Figure 3.11a, we investigate the performance of the estimator when the number of taps of the model is $d = 4$ and the delay difference between the signal arrivals, $\breve{\tau}_1 - \breve{\tau}_0$, does not necessarily coincide with the spacing of the FIR channel, $T_0$.

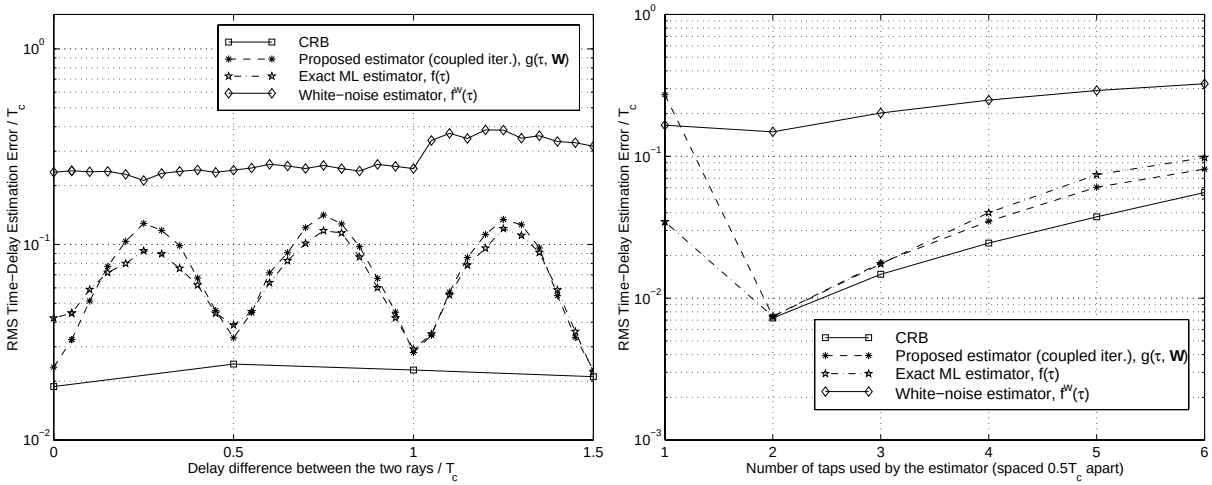


(a) $d = 4$ taps in the model (b) $\check{\tau}_1 = 0.5T_c$

Figure 3.11: RMSE of several estimators as a function of the delay separation of the two arrivals and the number of taps of the model. Parameters: $\check{\theta}_0 = 0^{\text{o}}$, $\check{\theta}_1 = 10^{\text{o}}$, $\check{\theta}_i = -30^{\text{o}}$, $\check{\tau}_0 = 0$, $M = 4$ pulses, $m = 6$ antennas, $\text{SNR}_0 = 13.8\,\text{dB}$, $\text{SIR}_0 = -7.2\,\text{dB}$, $\text{SNR}_0/\text{SNR}_1 = 3\,\text{dB}$, $T_0 = 0.5T_c$.

As expected, the RMSE presents minima when the former is a multiple of the latter. In the other cases, the model in (3.94) is only approximate, which results in a higher RMSE. Finally, increasing the length of the FIR filter beyond the necessary minimum ($d = 2$ in this case) impairs the performance, as shown in Figure 3.11b.

## 3.13 Concluding Remarks

Synchronization and time delay estimation are important components of many signal processing, navigation and communications systems. This chapter has focused on how multiple receive antennas can be efficiently used in interference-limited scenarios in order to estimate the time delays of multiple replicas of a known signal. The spatial selectivity of the array provides an additional dimension in which to differentiate the desired signal from the noise and interference. Under the assumption that the noise and CCI are spatially colored but temporally white Gaussian processes, and that the spatial signatures are unstructured, the maximum likelihood solution to the time delay estimation problem was derived. It was proven that the ML estimator is consistent and asymptotically efficient. However, the resulting concentrated criterion for the delays is highly non-linear, and not conducive to simple minimization procedures. Using various systematic and heuristic techniques, it was shown how the optimal ML criterion could be approximated by a simpler cost function that was shown to provide asymptotically equivalent (and hence statistically efficient) delay estimates. The form of the new criterion lends itself to minimization by the IQML algorithm, an iterative approach that avoids the need for gradient-

based or exhaustive searches. The existence of simple yet accurate initialization schemes based on ESPRIT or identity weightings makes the approach viable for practical implementation. Two different procedures to implement the IQML algorithm in the new cost function were discussed. The one that updates the noise correlation matrix at each iteration of the IQML algorithm is preferred. A number of simulation studies were presented that demonstrate the performance advantage of the proposed technique over related delay estimators, and also analyze its optimality in the finite-sample case. Finally, the new cost function was also applied to the estimation of the frame delay in a FIR channel. In this case, an appropriate formulation of the matrix that spans the subspace orthogonal to the signals reduces each iteration of the IQML algorithm to the rooting of a polynomial, being its order equal to the length of the FIR channel.

## Appendix 3.A Derivation of the Cramér-Rao Bound

The Cramér-Rao Bound can be derived using directly its definition [Kay93], as done in [Sto89], or using the Bangs-Slepian's formula [Ban71, Kay93]. We follow herein the second approach because it makes the derivation somewhat easier. According to the Bangs-Slepian's formula, and using equations (3.1)–(3.4), the $k,l$th element of the Fisher Information Matrix (FIM), which is the inverse of the CRB matrix, is

$$[\mathbf{FIM}]_{kl} = N \operatorname{Tr}\left\{\mathbf{Q}^{-1}\,\mathbf{Q}^{k}\,\mathbf{Q}^{-1}\,\mathbf{Q}^{l}\right\} + 2\,\operatorname{Re}\left\{\sum_{n=1}^{N}\left(\boldsymbol{\mu}^{k}\,(n)\right)^{*}\mathbf{Q}^{-1}\boldsymbol{\mu}^{l}\,(n)\right\}\,, \tag{3.110}$$

where $\boldsymbol{\mu}(n) = \mathbf{A}\,\mathbf{s}[n,\boldsymbol{\tau}]$ and $(\cdot)^{k}$ denotes the derivative with respect to the $k$th parameter. Since $\boldsymbol{\mu}(n)$ and $\mathbf{Q}$ depend on different parameters, the FIM is block diagonal with respect to the signal parameters

$$\boldsymbol{\eta}_s = \left[\begin{array}{cccccccc} \operatorname{Re}\{\boldsymbol{\alpha}_0\}^T & \ldots & \operatorname{Re}\{\boldsymbol{\alpha}_{d-1}\}^T & \operatorname{Im}\{\boldsymbol{\alpha}_0\}^T & \ldots & \operatorname{Im}\{\boldsymbol{\alpha}_{d-1}\}^T & \boldsymbol{\tau}^T \end{array}\right]^T \tag{3.111}$$

and the noise parameters (i.e., the real and imaginary parts of the elements of $\mathbf{Q}$). Therefore, the CRB for the signal parameters is the inverse of the corresponding $(2m+1)d \times (2m+1)d$ block of the FIM, which is partitioned as follows

$$\mathbf{FIM}\,(\boldsymbol{\eta}_s) = \left[\begin{array}{cc|c} \operatorname{Re}\{\mathbf{F}_1\} & -\operatorname{Im}\{\mathbf{F}_1\} & \operatorname{Re}\{\mathbf{F}_3\} \\ \operatorname{Im}\{\mathbf{F}_1\} & \operatorname{Re}\{\mathbf{F}_1\} & \operatorname{Im}\{\mathbf{F}_3\} \\ \hline \operatorname{Re}\{\mathbf{F}_3\}^T & \operatorname{Im}\{\mathbf{F}_3\}^T & \operatorname{Re}\{\mathbf{F}_2\} \end{array}\right]^{-1}. \tag{3.112}$$

The blocks of this matrix are computed using the last term of (3.110). After straightforward but lengthy calculations, we get

$$\mathbf{F}_1 = 2\ (\mathbf{S}^c(\boldsymbol{\tau})\,\mathbf{S}^T(\boldsymbol{\tau})) \otimes \mathbf{Q}^{-1} \tag{3.113}$$

$$\mathbf{F}_2 = 2\ (\mathbf{D}^c(\boldsymbol{\tau})\,\mathbf{D}^T(\boldsymbol{\tau})) \odot \left(\mathbf{A}^*\,\mathbf{Q}^{-1}\,\mathbf{A}\right) \tag{3.114}$$

$$\mathbf{F}_3 = \begin{bmatrix} 2\,\mathbf{Q}^{-1}\,\mathbf{A}\,\mathrm{diag}\left\{\mathbf{s}^*\left(\tau_0\right)\,\mathbf{D}^T(\boldsymbol{\tau})\right\} \\ \vdots \\ 2\,\mathbf{Q}^{-1}\,\mathbf{A}\,\mathrm{diag}\left\{\mathbf{s}^*\left(\tau_{d-1}\right)\,\mathbf{D}^T(\boldsymbol{\tau})\right\} \end{bmatrix}, \tag{3.115}$$

where $\mathbf{D}(\boldsymbol{\tau})$ was defined in (3.36), and

$$\mathbf{s}\left(\tau_i\right) = \begin{bmatrix} s\left(T_s - \tau_i\right) & s\left(2T_s - \tau_i\right) & \ldots & s\left(NT_s - \tau_i\right) \end{bmatrix}^T. \tag{3.116}$$

Next, we need the following two results, valid for non-singular matrices:

$$\begin{bmatrix} \mathrm{Re}\left\{\mathbf{X}\right\} & -\mathrm{Im}\left\{\mathbf{X}\right\} \\ \mathrm{Im}\left\{\mathbf{X}\right\} & \mathrm{Re}\left\{\mathbf{X}\right\} \end{bmatrix}^{-1} = \begin{bmatrix} \mathrm{Re}\left\{\mathbf{X^{-1}}\right\} & -\mathrm{Im}\left\{\mathbf{X^{-1}}\right\} \\ \mathrm{Im}\left\{\mathbf{X^{-1}}\right\} & \mathrm{Re}\left\{\mathbf{X^{-1}}\right\} \end{bmatrix} \tag{3.117}$$

$$(\mathbf{X} \otimes \mathbf{Z})^{-1} = \mathbf{X}^{-1} \otimes \mathbf{Z}^{-1}\,. \tag{3.118}$$

The proofs can be found in [Sto89, Appendix E] and [Gra81], respectively. The CRB for the time delays is the $d \times d$ trailing block of the inverse of $\mathbf{FIM}\left(\boldsymbol{\eta}_s\right)$. Using the well known formula of the inverse of a partitioned matrix and (3.117), this CRB can be written as

$$\begin{aligned} \mathbf{CRB}^{-1}(\boldsymbol{\tau}) &= \mathrm{Re}\left\{\mathbf{F}_2\right\} - \mathrm{Re}\left\{\mathbf{F}_3\right\}^T\,\mathrm{Re}\left\{\mathbf{F}_1^{-1}\right\}\,\mathrm{Re}\left\{\mathbf{F}_3\right\} + \mathrm{Re}\left\{\mathbf{F}_3\right\}^T\,\mathrm{Im}\left\{\mathbf{F}_1^{-1}\right\}\,\mathrm{Im}\left\{\mathbf{F}_3\right\} \\ &\quad - \mathrm{Im}\left\{\mathbf{F}_3\right\}^T\,\mathrm{Im}\left\{\mathbf{F}_1^{-1}\right\}\,\mathrm{Re}\left\{\mathbf{F}_3\right\} - \mathrm{Im}\left\{\mathbf{F}_3\right\}^T\,\mathrm{Re}\left\{\mathbf{F}_1^{-1}\right\}\,\mathrm{Im}\left\{\mathbf{F}_3\right\} \qquad (3.119) \\ &= \mathrm{Re}\left\{\mathbf{F}_2\right\} - \mathrm{Re}\left\{\mathbf{F}_3^*\,\mathbf{F}_1^{-1}\,\mathbf{F}_3\right\} \qquad (3.120) \end{aligned}$$

Taking into account (3.118) in the computation of $\mathbf{F}_1^{-1}$, and also the structure of $\mathbf{F}_3$, we obtain

$$\begin{aligned} \mathbf{CRB}^{-1}(\boldsymbol{\tau}) &= \mathrm{Re}\left\{\mathbf{F}_2\right\} - 2\sum_{i=0}^{d-1}\sum_{j=0}^{d-1}\mathrm{Re}\Bigg\{\left[\left(\mathbf{S}^c(\boldsymbol{\tau})\,\mathbf{S}^T(\boldsymbol{\tau})\right)^{-1}\right]_{i,j}\mathrm{diag}\Big\{\mathbf{D}^c(\boldsymbol{\tau})\mathbf{s}\left(\tau_i\right)\Big\} \\ &\qquad \cdot\left(\mathbf{A}^*\,\mathbf{Q}^{-1}\,\mathbf{A}\right)\mathrm{diag}\big\{\mathbf{s}^*\left(\tau_j\right)\,\mathbf{D}^T(\boldsymbol{\tau})\big\}\Bigg\} \qquad (3.121) \\ &= \mathrm{Re}\left\{\mathbf{F}_2\right\} - 2\sum_{i=0}^{d-1}\sum_{j=0}^{d-1}\mathrm{Re}\Bigg\{\left(\mathbf{A}^*\,\mathbf{Q}^{-1}\,\mathbf{A}\right) \\ &\qquad \odot\left(\left(\mathbf{D}^c(\boldsymbol{\tau})\mathbf{s}\left(\tau_i\right)\right)\left[\left(\mathbf{S}^c(\boldsymbol{\tau})\,\mathbf{S}^T(\boldsymbol{\tau})\right)^{-1}\right]_{i,j}\left(\mathbf{s}^*\left(\tau_j\right)\mathbf{D}^T(\boldsymbol{\tau})\right)\right) \qquad (3.122) \\ &= 2\,\mathrm{Re}\Big\{\left(\mathbf{D}^c(\boldsymbol{\tau})\,\mathbf{D}^T(\boldsymbol{\tau})\right)\odot\left(\mathbf{A}^*\,\mathbf{Q}^{-1}\,\mathbf{A}\right)\Big\} \\ &\quad - 2\,\mathrm{Re}\Big\{\left(\mathbf{D}^c(\boldsymbol{\tau})\mathbf{S}^T(\boldsymbol{\tau})\left(\mathbf{S}^c(\boldsymbol{\tau})\,\mathbf{S}^T(\boldsymbol{\tau})\right)^{-1}\mathbf{S}^c(\boldsymbol{\tau})\,\mathbf{D}^T(\boldsymbol{\tau})\right)\odot\left(\mathbf{A}^*\,\mathbf{Q}^{-1}\,\mathbf{A}\right)\Big\}, \\ &\qquad (3.123) \end{aligned}$$

where (3.122) is obtained from (3.121) by making use of the property: $\mathrm{diag}(\mathbf{x})\,\mathbf{z} = \mathbf{x} \odot \mathbf{z}$, valid for arbitrary vectors of the same length. Finally, it is evident that equation (3.123) is identical to (3.35) since $\mathbf{CRB}(\boldsymbol{\tau})$ is a symmetric matrix.

## Appendix 3.B Asymptotic Order of the Derivative of B

In this appendix we compute the order of the convergence in probability of the matrix $\mathbf{B}_N^i(\check{\boldsymbol{\tau}})$. Using (3.5), (3.11)–(3.13), (3.29), and the expression for the derivative of a projection matrix [Ott93]

$$\mathbf{P}_{\mathbf{S}^*}^i = \mathbf{P}_{\mathbf{S}^*}^{\perp} \left(\mathbf{S}^*\right)^i \left(\mathbf{S}^*\right)^{\dagger} + (\cdots)^* \ , \tag{3.124}$$

we get

$$\mathbf{B}_N^i(\check{\boldsymbol{\tau}}) = \frac{1}{N} \hat{\mathbf{R}}_{yy}^{-1/2}\, \mathbf{E}\, \mathbf{P}_{\mathbf{S}^*}^{\perp} \left(\mathbf{S}^*\right)^i \mathbf{A}^* \hat{\mathbf{R}}_{yy}^{-1/2} + (\cdots)^* \tag{3.125}$$

$$+ \frac{1}{N} \hat{\mathbf{R}}_{yy}^{-1/2}\, \mathbf{E}\, \mathbf{P}_{\mathbf{S}^*}^{\perp} \left(\mathbf{S}^*\right)^i \left(\mathbf{S}^*\right)^{\dagger} \mathbf{E}^* \hat{\mathbf{R}}_{yy}^{-1/2} + (\cdots)^* \ , \tag{3.126}$$

where all functions of $\boldsymbol{\tau}$ are evaluated at $\check{\boldsymbol{\tau}}$, the relation $\mathbf{S}\mathbf{P}_{\mathbf{S}^*}^{\perp} = \mathbf{0}$ has been used, and the notation $(\cdots)^*$ means that the same expression appears again transposed and conjugated. In order to obtain an asymptotic expression, the matrix $\hat{\mathbf{R}}_{yy}$ is replaced by $\mathbf{R}_{yy}$ and the terms in (3.126) are neglected since they converge faster to zero than those in (3.125). Thus, we can write up to first order

$$\mathbf{B}_N^i(\check{\boldsymbol{\tau}}) \approx \frac{1}{N} \mathbf{R}_{yy}^{-1/2}\, \mathbf{E}\, \mathbf{P}_{\mathbf{S}^*}^{\perp} \left(\mathbf{S}^*\right)^i \mathbf{A}^* \mathbf{R}_{yy}^{-1/2} + (\cdots)^* \ . \tag{3.127}$$

The correlation between the $k,l$th element of $\mathbf{B}_N^i(\check{\boldsymbol{\tau}})$ and the $r,s$th element of $\mathbf{B}_N^j(\check{\boldsymbol{\tau}})$ for any value $k, l, r, s = 1, \cdots, m$ and $i, j = 0, \cdots, d-1$ is

$$\Psi_{\mathbf{B}^i}(k,l,r,s;i,j) \triangleq \mathrm{E}\left\{ \left[\mathbf{B}_N^i(\check{\boldsymbol{\tau}})\right]_{k,l} \left[\mathbf{B}_N^j(\check{\boldsymbol{\tau}})\right]_{r,s}^* \right\} = \tag{3.128}$$

$$= \frac{1}{N^2} \left[\mathbf{R}_{yy}^{-\frac{1}{2}}\right]_{:,s}^* \mathbf{A}\, \mathbf{S}^j\, \mathbf{P}_{\mathbf{S}^*}^{\perp} \mathrm{E}\left\{ \mathbf{E}^* \left[\mathbf{R}_{yy}^{-\frac{1}{2}}\right]_{:,r} \left[\mathbf{R}_{yy}^{-\frac{1}{2}}\right]_{:,k}^* \mathbf{E} \right\} \mathbf{P}_{\mathbf{S}^*}^{\perp} \left(\mathbf{S}^*\right)^i \mathbf{A}^* \left[\mathbf{R}_{yy}^{-\frac{1}{2}}\right]_{:,l}$$

$$+ \frac{1}{N^2} \left[\mathbf{R}_{yy}^{-\frac{1}{2}}\right]_{:,k}^* \mathbf{A}\, \mathbf{S}^i\, \mathbf{P}_{\mathbf{S}^*}^{\perp} \mathrm{E}\left\{ \mathbf{E}^* \left[\mathbf{R}_{yy}^{-\frac{1}{2}}\right]_{:,l} \left[\mathbf{R}_{yy}^{-\frac{1}{2}}\right]_{:,s}^* \mathbf{E} \right\} \mathbf{P}_{\mathbf{S}^*}^{\perp} \left(\mathbf{S}^*\right)^j \mathbf{A}^* \left[\mathbf{R}_{yy}^{-\frac{1}{2}}\right]_{:,r} \ .$$

The expectation of the terms containing twice $\mathbf{E}$ or $\mathbf{E}^*$ is zero, because the noise is circularly symmetric, and hence it has not been written in (3.128). For the noise model that we have considered,

$$\mathrm{E}\left\{ \mathbf{E}^* \left[\mathbf{R}_{yy}^{-\frac{1}{2}}\right]_{:,r} \left[\mathbf{R}_{yy}^{-\frac{1}{2}}\right]_{:,k}^* \mathbf{E} \right\} = \mathbf{I} \left( \left[\mathbf{R}_{yy}^{-\frac{1}{2}}\right]_{:,k}^* \mathbf{Q} \left[\mathbf{R}_{yy}^{-\frac{1}{2}}\right]_{:,r} \right) = \mathbf{I} \left[\mathbf{R}_{yy}^{-\frac{1}{2}}\, \mathbf{Q}\, \mathbf{R}_{yy}^{-\frac{1}{2}}\right]_{k,r} \ . \tag{3.129}$$

This result and the fact that each row of $\mathbf{S}$ only depends on one variable yield

$$\Psi_{\mathbf{B}'}(k,l,r,s;i,j) = \frac{1}{N^2}\left[\mathbf{R}_{yy}^{-\frac{1}{2}}\,\mathbf{Q}\,\mathbf{R}_{yy}^{-\frac{1}{2}}\right]_{k,r}\left[\mathbf{R}_{yy}^{-\frac{1}{2}}\mathbf{A}\right]_{s,j}\left[\mathbf{A}^*\,\mathbf{R}_{yy}^{-\frac{1}{2}}\right]_{i,l}\left(\mathbf{d}^T(\tau_j)\,\mathbf{P}^{\perp}_{\mathbf{S}^*}\mathbf{d}^c(\tau_i)\right)+\cdots \tag{3.130}$$

where the second term has been omitted because it can be readily obtained from the first one and (3.128) by an appropriate change of subscripts. Vector $\mathbf{d}(\tau)$ was defined in (3.37). Since we have assumed that $s(t)$ is a finite-average-power signal and is sampled above the Nyquist rate, the order of $\mathbf{d}^T(\tau_j)\,\mathbf{P}^{\perp}_{\mathbf{S}^*}\mathbf{d}^c(\tau_i)$ is $O(N)$. Therefore, the correlation (3.128) of the elements of $\mathbf{B}_N(\check{\boldsymbol{\tau}})^i$ is $O\left(N^{-1}\right)$, which completes the proof that $\mathbf{B}_N^i(\check{\boldsymbol{\tau}}) = O_p\left(N^{-1/2}\right)$.

## Appendix 3.C Hessian and Covariance of the Gradient

We need the following expression for the second derivative of a projection matrix [Ott93]

$$\begin{aligned}\mathbf{P}^{ij}_{\mathbf{S}^*} =& -\mathbf{P}^{\perp}_{\mathbf{S}^*}(\mathbf{S}^*)^j(\mathbf{S}^*)^{\dagger}(\mathbf{S}^*)^i(\mathbf{S}^*)^{\dagger} - \left((\mathbf{S}^*)^{\dagger}\right)^*(\mathbf{S})^i\,\mathbf{P}^{\perp}_{\mathbf{S}^*}(\mathbf{S}^*)^j(\mathbf{S}^*)^{\dagger} + \mathbf{P}^{\perp}_{\mathbf{S}^*}(\mathbf{S}^*)^{ij}(\mathbf{S}^*)^{\dagger}\\ &+\mathbf{P}^{\perp}_{\mathbf{S}^*}(\mathbf{S}^*)^i(\mathbf{S}\mathbf{S}^*)^{-1}(\mathbf{S})^j\,\mathbf{P}^{\perp}_{\mathbf{S}^*} - \mathbf{P}^{\perp}_{\mathbf{S}^*}(\mathbf{S}^*)^i(\mathbf{S}^*)^{\dagger}(\mathbf{S}^*)^j(\mathbf{S}^*)^{\dagger} + (\cdots)^*\ ,\end{aligned} \tag{3.131}$$

where the notation $(\ldots)^*$ means that the same expression appears again transposed. Next, using (3.5), (3.11)-(3.13), (3.29), we get

$$\lim_{N\to\infty}\mathbf{B}_N^{ij}(\check{\boldsymbol{\tau}}) = -\frac{1}{N}\,\mathbf{R}_{yy}^{-1/2}\,\mathbf{A}\,\mathbf{S}^i\,\mathbf{P}^{\perp}_{\mathbf{S}^*}\,(\mathbf{S}^*)^j\,\mathbf{A}\,\mathbf{R}_{yy}^{-1/2} + (\ldots)^*\ , \tag{3.132}$$

where all functions of $\boldsymbol{\tau}$ are evaluated at $\check{\boldsymbol{\tau}}$, and the relation $\mathbf{S}\mathbf{P}^{\perp}_{\mathbf{S}^*} = \mathbf{0}$ has been used. Only the contribution of the signal, and not that of the noise, appears in (3.132) because this expression is a limit for $N$ tending to infinity. Then, the $i,j$th element of the limiting Hessian of $g_N(\boldsymbol{\tau},\mathbf{W})$ is

$$[\mathbf{H}]_{ij} = \frac{1}{N}\,\mathrm{Tr}\left\{\mathbf{S}^i\,\mathbf{P}^{\perp}_{\mathbf{S}^*}\,(\mathbf{S}^*)^j\,\mathbf{A}^*\,\mathbf{R}_{yy}^{-1/2}\,\mathbf{W}\,\mathbf{R}_{yy}^{-1/2}\,\mathbf{A} + (\ldots)^*\right\}\ . \tag{3.133}$$

The fact that each row of $\mathbf{S}(\boldsymbol{\tau})$ only depends on one time delay, in such a way that only the $i,j$th element of $\mathbf{S}^i\,\mathbf{P}^{\perp}_{\mathbf{S}^*}\,(\mathbf{S}^*)^j$ is non-zero, yields

$$[\mathbf{H}]_{ij} = \frac{2}{N}\,\mathrm{Re}\left\{\left[\mathbf{D}\,\mathbf{P}^{\perp}_{\mathbf{S}^*}\,\mathbf{D}^*\right]_{i,j}\left[\mathbf{A}^*\,\mathbf{R}_{yy}^{-1/2}\,\mathbf{W}\,\mathbf{R}_{yy}^{-1/2}\,\mathbf{A}\right]_{j,i}\right\}\ . \tag{3.134}$$

The $i,j$th element of the covariance of the gradient is

$$[\mathbf{G}]_{i,j} = \lim_{N\to\infty} N\,\mathrm{E}\left\{\mathrm{Tr}\left\{\mathbf{W}\,\mathbf{B}_N^i(\check{\boldsymbol{\tau}})\right\}\,\mathrm{Tr}\left\{\mathbf{W}^*\,\left(\mathbf{B}_N^j(\check{\boldsymbol{\tau}})\right)^*\right\}\right\} \tag{3.135}$$

$$= \sum_{k=1}^{m}\sum_{l=1}^{m}\sum_{r=1}^{m}\sum_{s=1}^{m}[\mathbf{W}]_{l,k}\,[\mathbf{W}]^*_{s,r}\lim_{N\to\infty} N\,\mathrm{E}\left\{\left[\mathbf{B}_N^i(\check{\boldsymbol{\tau}})\right]_{k,l}\left[\mathbf{B}_N^j(\check{\boldsymbol{\tau}})\right]^*_{r,s}\right\} \tag{3.136}$$

$$= \sum_{k=1}^{m}\sum_{l=1}^{m}\sum_{r=1}^{m}\sum_{s=1}^{m}[\mathbf{W}]_{l,k}\,[\mathbf{W}]^*_{s,r}\,N\,\Psi_{\mathbf{B}'}(k,l,r,s;i,j)\ , \tag{3.137}$$

where we have used the definition of the asymptotic correlation $\Psi_{\mathbf{B}'}$ in (3.128). Finally, using equation (3.130) and expressing the summations as matrix products, we obtain

$$[\mathbf{G}]_{i,j} = \frac{2}{N} \operatorname{Re} \left\{ \left[ \mathbf{D}\, \mathbf{P}^{\perp}_{\mathbf{S}^*}\, \mathbf{D}^* \right]_{i,j} \left[ \mathbf{A}^* \, \mathbf{R}_{yy}^{-1/2} \, \mathbf{W} \, \mathbf{R}_{yy}^{-1/2} \, \mathbf{Q} \, \mathbf{R}_{yy}^{-1/2} \, \mathbf{W} \, \mathbf{R}_{yy}^{-1/2} \, \mathbf{A} \right]_{j,i} \right\} . \tag{3.138}$$

## Appendix 3.D Derivative of the Nyquist Square-Root Raised-Cosine Pulse

It is well known that the expression of the Nyquist square-root raised-cosine pulse of bandwidth $(1+\varrho)/2T$, where $\varrho$ is the roll-off factor, is

$$g(t) = \frac{1}{\sqrt{T}} \frac{\sin\left((1-\varrho)\,\pi t/T\right) + 4\varrho t \cos\left((1+\varrho)\,\pi t/T\right)/T}{\left(1-(4\varrho t/T)^2\right)\pi t/T} . \tag{3.139}$$

Simple calculations lead to the expression of the derivative

$$\begin{aligned} g'(t) = \frac{d\,g(t)}{d\,t} =& \frac{1}{\sqrt{T}} \frac{(1-\varrho)\,\pi \cos\left((1-\varrho)\,\pi t/T\right)/T}{\left(1-(4\varrho t/T)^2\right)\pi t/T} \\ &+ \frac{1}{\sqrt{T}} \frac{\sin\left((1-\varrho)\,\pi t/T\right)\left(32\varrho^2\pi t^2/T^3 - \left(1-(4\varrho t/T)^2\right)\pi/T\right)}{\left(1-(4\varrho t/T)^2\right)^2 (\pi t/T)^2} \\ &- \frac{1}{\sqrt{T}} \frac{4\varrho\,(1+\varrho)\sin\left((1+\varrho)\,\pi t/T\right)/T}{1-(4\varrho t/T)^2} \\ &+ \frac{1}{\sqrt{T}} \frac{128\varrho^3 t \cos\left((1+\varrho)\,\pi t/T\right)/\left(\pi T^2\right)}{\left(1-(4\varrho t/T)^2\right)^2} . \end{aligned} \tag{3.140}$$

When programming (3.140) in a computer, care has to be taken with the indeterminations, which are located at the points $t = 0, \pm T/(4\varrho)$. Computing directly the limits of (3.140) seems a formidable task. Instead, we will compute the limits starting from the numerator and denominator of $g(t)$. To this end, we use the following result. If $f(t)$ and $h(t)$ are arbitrary functions such that

$$z(t) = \frac{f(t)}{h(t)}, \qquad f(t_0) = h(t_0) = 0 \tag{3.141}$$

then

$$\lim_{t\to t_0} \frac{d\,z(t)}{d\,t} = \frac{1}{2} \frac{f''(t_0)\,h'(t_0) - f'(t_0)\,h''(t_0)}{\left(h'(t_0)\right)^2} . \tag{3.142}$$

Thus, it can be easily shown that

$$g'(0) = 0 \tag{3.143}$$

$$\begin{aligned} g'\left(\pm T/(4\varrho)\right) = \pm \frac{\varrho}{\sqrt{2T}T\pi} \Big( & \left(2\pi - 4\varrho\pi - 12\varrho - \pi^2\right) \sin\left(\pi/(4\varrho)\right) \\ & + \left(\pi^2 + 2\pi - 4\varrho\pi + 12\varrho\right) \cos\left(\pi/(4\varrho)\right) \Big) . \end{aligned} \tag{3.144}$$

## Appendix 3.E Structure of Matrices C and $\boldsymbol{\Upsilon}$

The cost function in (3.106) can be written as

$$\tilde{g}\left(\mathbf{g},\mathbf{W}\right)=\sum_{n=1}^{m}\left[\boldsymbol{\Omega}\right]_{:,n}^{*}\,\mathbf{G}\,\boldsymbol{\Upsilon}\,\mathbf{G}^{*}\,\left[\boldsymbol{\Omega}\right]_{:,n}\;. \tag{3.145}$$

Given the structure of matrix $\mathbf{G}$ in (3.82), it is satisfied that

$$\mathbf{G}^{*}\,\left[\boldsymbol{\Omega}\right]_{:,n}=\bar{\boldsymbol{\Omega}}_{n}\,\mathbf{g}\;, \tag{3.146}$$

where

$$\bar{\boldsymbol{\Omega}}_{n}\triangleq\begin{bmatrix}\left[\boldsymbol{\Omega}\right]_{d+1,n} & \left[\boldsymbol{\Omega}\right]_{d,n} & \cdots & \left[\boldsymbol{\Omega}\right]_{1,n}\\ \left[\boldsymbol{\Omega}\right]_{d+2,n} & \left[\boldsymbol{\Omega}\right]_{d+1,n} & \cdots & \left[\boldsymbol{\Omega}\right]_{2,n}\\ \vdots & \vdots & \vdots & \vdots\\ \left[\boldsymbol{\Omega}\right]_{N,n} & \left[\boldsymbol{\Omega}\right]_{N-1,n} & \cdots & \left[\boldsymbol{\Omega}\right]_{N-d,n}\end{bmatrix}\qquad (N-d)\times(d+1)\;. \tag{3.147}$$

Therefore, we get

$$\tilde{g}\left(\mathbf{g},\mathbf{W}\right)=\mathbf{g}^{*}\,\underbrace{\left(\sum_{n=0}^{m}\bar{\boldsymbol{\Omega}}_{n}^{*}\,\boldsymbol{\Upsilon}\,\bar{\boldsymbol{\Omega}}_{n}\right)}_{\mathbf{C}}\,\mathbf{g}\;. \tag{3.148}$$

Next, we consider the structure of matrix $\boldsymbol{\Upsilon}$ defined in (3.105). Using the definition of matrix $\mathbf{G}$, the factorization of vector $\mathbf{g}$ according to (3.107), and the fact that $x$ is on the unit circle, it is straightforward to prove that $\boldsymbol{\Upsilon}$ can be decomposed as

$$\boldsymbol{\Upsilon}\left(x\right)=\boldsymbol{\Sigma}\left(x\right)\,\boldsymbol{\Upsilon}_{1}\,\boldsymbol{\Sigma}^{*}\left(x\right)\;, \tag{3.149}$$

where $\boldsymbol{\Upsilon}_{1}$ is the value of $\boldsymbol{\Upsilon}$ for $x=1$, and

$$\boldsymbol{\Sigma}\left(x\right)=\mathrm{diag}\left\{1,\,x,\,\ldots,\,x^{N-d-1}\right\}\;. \tag{3.150}$$

# Chapter 4

# Time Delay and Carrier Phase Estimation of One Replica with Known Steering Vector

The goal of the estimators presented in this chapter is to take advantage of one particularity of GNSS systems, which consists in that the direction-of-arrival (DOA) of the line-of-sight signal (LOSS) may be known a priori. Based on this fact, a simplified and approximate model for the received signal is proposed. In this model, all disturbing signals are gathered together into a Gaussian term with unknown spatial correlation. The maximum likelihood (ML) estimator of the time delay and carrier phase of the LOSS is derived from the simplified model, and some possible implementations thereof are analyzed.

The chapter is organized as follows. Section 4.1 sets up and justifies the simplified signal model on which the rest of the chapter is based. In Section 4.2, the ML estimator is derived. Other related estimators obtained from slightly different assumptions are reviewed. Closed form and iterative algorithms for computing the ML estimates are presented in Sections 4.3 and 4.4, respectively. In the latter, the relationship between the ML estimator and a certain hybrid beamformer is explored. Section 4.5 reports on some simulation experiments, which show the performance of the proposed methods in a large variety of scenarios. The sensitivity of the proposed ML estimator to errors in the assumed steering vector of the LOSS is analyzed is Section 4.6. A modification of the ML estimator that takes into account the presence of calibration or pointing errors is presented in Section 4.7, and simulation results concerning the effects of such errors can be found in Section 4.8. Finally, Section 4.9 contains our conclusions.

## 4.1 Simplified Signal Model

In this section, a simplified signal model for the received signals is described. Not only is this model justified by practical considerations, but also by the fact that the knowledge of the steering vector of the direct signal does not provide a significant performance improvement of the estimators based on more complex models, and however this additional information increases the complexity of such estimators.

We start by considering the same model as the one employed in the previous chapter. That it to say, when an antenna array composed of $m$ elements arranged in an arbitrary geometry receives $d$ copies of a known signal $s(t)$, the baseband array output is

$$\mathbf{y}[n] = \mathbf{A}\,\mathbf{s}[n, \boldsymbol{\tau}] + \mathbf{e}[n] \tag{4.1}$$

$$= \boldsymbol{\alpha}_0\, s(nT_s - \tau_0) + \mathbf{A}_r\,\mathbf{s}_r[n, \boldsymbol{\tau}_r] + \mathbf{e}[n]\ , \tag{4.2}$$

where

$$\boldsymbol{\tau} = [\tau_0 \ \cdots \ \tau_{d-1}]^T \qquad d \times 1 \tag{4.3}$$

$$\mathbf{A} = [\boldsymbol{\alpha}_0 \ \cdots \ \boldsymbol{\alpha}_{d-1}] \qquad m \times d \tag{4.4}$$

$$\mathbf{s}[n, \boldsymbol{\tau}] = \left[\ s(nT_s - \tau_0) \quad s(nT_s - \tau_1) \quad \cdots \quad s(nT_s - \tau_{d-1})\ \right]^T \qquad d \times 1\ . \tag{4.5}$$

The sampling period is denoted by $T_s$. $\boldsymbol{\alpha}_k$ and $\tau_k$ are the spatial signature and time delay of the $k$th arrival, and $\mathbf{e}[n]$ represents the background noise and all other interfering terms. In (4.2), the contribution of the line-of-sight signal (LOSS) is separated from that of the reflections. The subscript 0 stands for the LOSS; whereas the subscript $r$ corresponds to the reflections, which are the $1, \ldots, (d-1)$th replicas. Thus, the definition of $\mathbf{A}_r$, $\boldsymbol{\tau}_r$ and $\mathbf{s}_r[n, \boldsymbol{\tau}_r]$ flows directly from (4.3)–(4.5).

A particularity of GNSS systems, which we seek to exploit in this chapter, is that the receiver has very accurate estimates of its own position and the satellite position. Therefore, the DOA of the direct signal can be computed beforehand, and assuming that the antenna array is calibrated, it is possible to know the steering vector (or spatial signature) of the LOSS up to a scaling factor. We will assume that the following relation holds

$$\boldsymbol{\alpha}_0 = \alpha_0\, \mathbf{a}_0\ , \tag{4.6}$$

where $\mathbf{a}_0$ is the known steering vector of the LOSS and $\alpha_0$ is an unknown complex amplitude. The attitude (or orientation) of the antenna array is also needed for the computation of $\mathbf{a}_0$, but this information is available in most cases. The way in which it is obtained depends on the particular application. It is apparent that in a static array, which may be found for instance in differential reference stations, knowing the attitude does not represent any difficulty. In a dynamic array, it usually requires the use of an attitude sensor or data from the navigation unit.

However, in aeronautical applications the attitude is mostly available. Even in very adverse multipath scenarios, the inaccuracies of the satellite and receiver positions, which are at most on the order of a few tens or a hundred of meters, result in negligible errors in the calculation of the DOA of the LOSS because the distance between the receiver and the satellites is about 20000 km. Moreover, it will be proven in Section 4.6 and Section 4.8 that the ML estimator proposed in this chapter is robust to errors in the steering vector of the LOSS. For all these reasons, assuming that $\mathbf{a}_0$ is known is fully justified in the problem under consideration, and this hypothesis has also been made in other work, such as in [Zol95, Moe96b, Ray98, Hat98, Fan98]. Indeed, having the knowledge of the DOA of the direct signal is not a situation that is found only in GNSS systems. For instance, in a radar system, one of the parameters of interest is the distance to the target, whose angular location is approximately given by the transmit direction of the radar.

Now, we analyze the effect that the knowledge of $\mathbf{a}_0$ has over the Cramér-Rao Bound (CRB). To this end, the spatial signatures of the reflections $\mathbf{A}_r$ are treated as arbitrary deterministic vectors. Following the common thread along this thesis (assumption (**A2**) in Section 2.5.1), $\mathbf{e}[n]$ is considered to be a complex, circularly symmetric Gaussian vector, which is zero-mean, spatially white, uncorrelated with the signal terms in (4.2), and has an arbitrary unknown spatial correlation:

$$\mathrm{E}\left\{\mathbf{e}[n]\mathbf{e}^*[l]\right\} = \mathbf{Q}\,\delta_{n,l}\,. \tag{4.7}$$

We also assume that $N$ samples of the signals are collected. The CRB for the signal model in (4.2) with the additional information in (4.6) is derived in Appendix 4.A. On the other hand, for the case in which the knowledge of $\mathbf{a}_0$ is not available and, hence, $\boldsymbol{\alpha}_0$ is treated as an unstructured vector, the CRB was derived in Section 3.3.2 and Appendix 3.A. In Figure 4.1, we compare the CRBs for the time delay of the direct signal in both cases. The description of the signals employed in obtaining these results can be found in Section 4.5.1, and the corresponding parameters are detailed in the caption of the figure. Although this figure is only a particular example, it summarizes the main features that we want to highlight. It has been observed that both CRBs (the one that takes into account the knowledge of $\mathbf{a}_0$ and the one that does not) are generally very close, nearly indistinguishable. In particular, it can be shown starting from (4.124) that when $\mathbf{a}_0$ is orthogonal to the columns of $\mathbf{A}_r$ (in the norm of $\mathbf{Q}^{-1}$) both CRBs for the time delay of the direct signal are identical (a similar result for DOA estimation was presented in [Li93]). There exists a slight difference between the CRBs solely when the DOA of the direct signal is very close to one of the reflections, as it happens in the scenario of Figure 4.1, where the DOA separation is only $5^{\mathrm{o}}$. Therefore, the knowledge of $\mathbf{a}_0$ does not supply essential information and does not allow to improve significantly the performance of the estimator. A different situation arises when, besides the spatial signature, the modulus of the amplitude $|\alpha_0|$ is known. As shown in Figure 4.1, the CRB is greatly reduced and does not tend to infinity as

the delays approach one another. However, this situation is not addressed in this thesis.

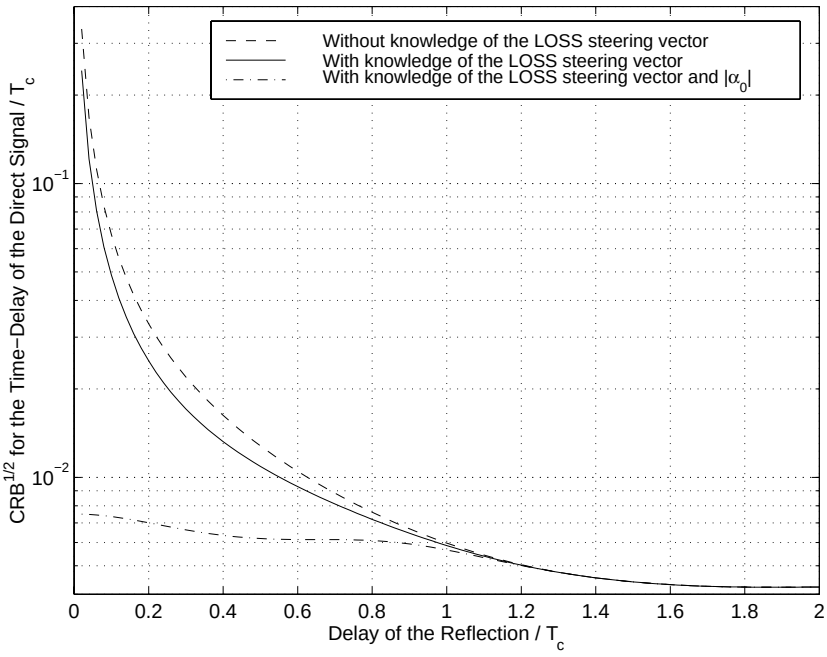


Figure 4.1: Cramér-Rao Bound for the time-delay of the LOSS as a function of the delay of the reflection. Different types of additional information are considered. Parameters: $\check{\theta}_0 = 0^{\text{o}}$, $\check{\tau}_0 = 0$, $\check{\theta}_1 = 5^{\text{o}}$, $\check{\alpha}_0/\check{\alpha}_1 = \sqrt{2}$, $M = 3$ pulses, $m = 6$ antennas, $\text{SNR}_0 = 15.87\,\text{dB}$.

Moreover, the ML estimator for the model in (4.2) with the constraint in (4.6) is highly non-linear and requires computationally expensive minimization algorithms since the IQML-based algorithm presented in the previous chapter cannot be applied in this case. This ML estimator can readily be derived starting from (3.17). Since an overall objective of this work is to avoid multidimensional searches, and given the tiny improvement to be expected with respect to the estimators in Chapter 3, we conclude that it is not worth introducing the knowledge of $\mathbf{a}_0$ into the model in (4.2). Instead, we propose to use this additional information to simplify the model itself. In the simplified model (as opposed to the detailed model in (4.2)) the contribution of the reflections is included into the error term (or "equivalent" noise) $\mathbf{e}[n]$. Hence, the array output can be expressed as

$$\mathbf{y}[n] = \alpha_0\, \mathbf{a}_0\, s\,(nT_s - \tau_0) + \mathbf{e}[n]\;, \tag{4.8}$$

which amounts to considering that $d = 1$ in (4.2). The vector $\mathbf{a}_0$ acts as a spatial reference to the LOSS, which allows to identify if from among all the other components. This fact provides additional support for separating the contribution of the direct signal from that of the rest. On the other hand, if the spatial signature of the LOSS were unknown, it would not be possible to select which component is modeled by the first term on the right-hand side of (4.8), and which

ones are modeled by $\mathbf{e}[n]$.

The complexity of the estimators based on detailed signal models (i.e., those that take explicitly into account the presence of reflections, such as (4.2)) proceeds from the fact that an important effort is devoted to estimating the parameters of the reflections (a review of these estimators can be found in Section 2.3). In the simplified model, however, only the parameters that are essential for a GNSS application (i.e., the delay and the amplitude of the LOSS) remain explicitly. Note that the argument of $\alpha_0$ is the carrier phase. The estimation of the reflections' parameters is avoided by lumping all the reflections together in the equivalent noise term. Such a "non-parametric modeling" of the reflections presents also the advantage that $d$ need not be known or estimated, and hence the estimators derived from the simplified model are not restricted to scenarios involving a discrete number of reflections (or clusters of reflections). It is worth remarking that the synchronization of the direct signal is a problem of interest in the downlink of a satellite communication system as well, since the signal that propagates through the direct path does not suffer from severe fading.

The statistical model considered for $\mathbf{e}[n]$ in the simplified signal model coincides with the one stated above in this section (see equation (4.7) and the paragraph preceding this equation). The matrix $\mathbf{Q}$ attempts to model the directional or spatial characteristics of both the interferences and the multipath components. Indeed, it is the fact that the correlation matrix is unknown and has to be estimated what will make the estimator capable of using the diversity introduced by the antenna array to discriminate the signals in the spatial dimension, despite the approximate modeling of $\mathbf{e}[n]$. The simplification of the signal model is clearly at the expense of a certain mismatch between the model and the actual received signal, because none of the previous assumptions about the equivalent noise is necessarily satisfied in a real scenario, and this could result in a certain impairment (increased bias and/or variance) of the estimates. Clearly, the weakest assumption is that $\mathbf{e}[n]$ is uncorrelated with the direct signal, which actually does not occur when $\mathbf{e}[n]$ contains the contribution of (coherent) reflections. The failure of this assumption will bias the estimates as it will be shown by the numerical results. The Gaussian hypothesis for the equivalent noise is of interest because it allows to simplify analytically the ML estimator presented in this chapter. Moreover, the Gaussian hypothesis is not crucial as far as the ability of the estimator to mitigate spatially the undesired signals is concerned, since this ability is retained independently of the actual statistics of the noise plus interference. The extension to non-circularly symmetric noise consists simply in working with an observation vector formed by stacking the real and imaginary parts of $\mathbf{y}[n]$ on top of one another. The estimator presented in the next section can be modified to take into account this situation, but there is not any proof or experimental evidence that this strategy leads to better performance (similar assertions were reported [Ran99, chapters 2 and 4] for somewhat related problems). All the same, the use of the simplified signal model is completely justified from a practical standpoint since it allows to derive simple algorithms whose performance is excellent, as it is shown by the

results in Section 4.5, although no a priori claims to the optimality of the estimates can be made in the general case.

The estimators proposed in this chapter mitigate the effects of the reflections in accordance with their contribution to the correlation matrix of the equivalent noise. At this point, it is necessary to recall that in the systems under consideration the received power of the direct signal and its reflections is more than 10 or 20dB below the white noise level (see Section 2.4). If the correlation matrix were computed before the despreading, the contribution of the reflections to that matrix would be imperceptible compared with that of the white noise and interferences (which are generally stronger than the white noise), and it would be impossible to infer any spatial information about the reflected replicas from that correlation matrix. In other words, if the estimators proposed herein were applied to the signals before the despreading, they would be insensitive to the reflections, and they would be able to cancel only powerful interferences, as happens in [Zol95, Moe96b, Moe96a, Hat98, Myr00]. Since our overall objective is to use the spatial dimension to mitigate both the multipath components and the interferences, some kind of preprocessing (prior to the techniques proposed in this chapter) that increases the signal-to-noise ratio (SNR) of the desired signal is mandatory. The increase of the SNR may be achieved by means of the despreading process of the DS-SS signals, as it was detailed in Section 2.5.3. Nonetheless, the derivation and formulation of the different techniques presented in the following sections are independent of the particular way in which $\mathbf{y}[n]$ and $s(t)$ are obtained.

The $N$ samples of $\mathbf{y}[n]$ in (4.8) collected during an observation interval may be arranged into the following $m \times N$ matrix

$$\mathbf{Y} = \left[\mathbf{y}\left[1\right] \;\; \mathbf{y}\left[2\right] \;\; \cdots \;\; \mathbf{y}\left[N\right]\right] = \alpha_0 \, \boldsymbol{a}_0 \, \boldsymbol{s}^T\left(\tau_0\right) + \mathbf{E} \; , \tag{4.9}$$

where $\mathbf{E}$ is formed identically to $\mathbf{Y}$ and we have defined the signal vector

$$\mathbf{s}\left(\tau\right) = \left[ \; s\left(T_s - \tau\right) \;\; s\left(2T_s - \tau\right) \;\; \ldots \;\; s\left(NT_s - \tau\right) \; \right]^T \; . \tag{4.10}$$

## 4.2 Maximum Likelihood Time Delay and Carrier Phase Estimator

The problem addressed in this section may be stated as follows: given the collection of data $\mathbf{Y}$ modeled by (4.9), the vector $\mathbf{a}_0$ and the signal $s(t)$, estimate the unknown parameters $\tau_0$, $\alpha_0$ and $\mathbf{Q}$. To this end, the maximum likelihood principle is applied [Sch90]. The reciprocal of the likelihood function[1] of the data is

$$\Lambda_1\left(\tau_0, \alpha_0, \mathbf{Q}\right) = \left|\mathbf{Q}\right| \exp\left\{ \; \mathrm{Tr}\left\{\mathbf{Q}^{-1}\,\mathbf{C}\left(\tau_0, \alpha_0\right)\right\} \; \right\} , \tag{4.11}$$

[1]Parameter-independent additive or multiplicative constants in the cost functions are neglected throughout the chapter.

where

$$\mathbf{C}\left(\tau_0, \alpha_0\right) = \frac{1}{N}\left(\mathbf{Y} - \alpha_0\,\mathbf{a}_0\,\mathbf{s}^T\left(\tau_0\right)\right)\left(\mathbf{Y} - \alpha_0\,\mathbf{a}_0\,\mathbf{s}^T\left(\tau_0\right)\right)^* \ . \tag{4.12}$$

The dimensionality of the parameter space can be reduced to one by eliminating analytically all the unknowns except for $\tau_0$. The gradient of (4.11) with respect to $\mathbf{Q}$ is [Mag99]

$$\frac{\partial\,\Lambda_1\left(\tau_0, \alpha_0, \mathbf{Q}\right)}{\partial\,\mathbf{Q}} = \Lambda_1\left(\tau_0, \alpha_0, \mathbf{Q}\right)\left(\mathbf{Q}^{-1} - \mathbf{Q}^{-1}\,\mathbf{C}\left(\tau_0, \alpha_0\right)\,\mathbf{Q}^{-1}\right) \ . \tag{4.13}$$

The value of $\mathbf{Q}$ that nulls (4.13) and also the ML estimate (as long as it is evaluated at the ML estimates of $\tau_0$ and $\alpha_0$), is given by

$$\hat{\mathbf{Q}}_{ML} = \mathbf{C}\left(\tau_0, \alpha_0\right) \ , \tag{4.14}$$

where we have assumed that $N \geq m+1$ in order that $\mathbf{C}\left(\tau_0, \alpha_0\right)$ be invertible with probability one.

Let us define the following sample correlations

$$\hat{\mathbf{R}}_{yy} = \frac{1}{N}\,\mathbf{Y}\,\mathbf{Y}^* \qquad\qquad \hat{\mathbf{r}}_{ys}\left(\tau_0\right) = \frac{1}{N}\,\mathbf{Y}\,\mathbf{s}^c\left(\tau_0\right) \tag{4.15}$$

$$\hat{P}_s = \frac{1}{N}\,\mathbf{s}^*\left(\tau_0\right)\,\mathbf{s}\left(\tau_0\right) \qquad\qquad \hat{\mathbf{W}}\left(\tau_0\right) = \hat{\mathbf{R}}_{yy} - \hat{P}_s^{-1}\,\hat{\mathbf{r}}_{ys}\left(\tau_0\right)\,\hat{\mathbf{r}}_{ys}^*\left(\tau_0\right) \ . \tag{4.16}$$

The matrix $\hat{\mathbf{W}}\left(\tau_0\right)$ is an unstructured estimate of the noise correlation matrix $\mathbf{Q}$. It is referred to as unstructured because, unlike $\mathbf{C}\left(\tau_0, \alpha_0\right)$, it does not use the knowledge of the spatial signature of the LOSS. Substituting (4.14) into (4.11) yields the following concentrated inverse likelihood function

$$\Lambda_2\left(\tau_0, \alpha_0\right) = \left|\hat{\mathbf{R}}_{yy} - \alpha_0\,\mathbf{a}_0\,\hat{\mathbf{r}}_{ys}^*\left(\tau_0\right) - \alpha_0^*\,\hat{\mathbf{r}}_{ys}\left(\tau_0\right)\,\mathbf{a}_0^* + \left|\alpha_0\right|^2\,\hat{P}_s\,\mathbf{a}_0\,\mathbf{a}_0^*\right| \tag{4.17}$$

$$= \left|\hat{\mathbf{W}}\left(\tau_0\right) + \left(\alpha_0\,\mathbf{a}_0 - \hat{\mathbf{r}}_{ys}\left(\tau_0\right)\,\hat{P}_s^{-1}\right)\,\hat{P}_s\,\left(\alpha_0\,\mathbf{a}_0 - \hat{\mathbf{r}}_{ys}\left(\tau_0\right)\,\hat{P}_s^{-1}\right)^*\right| \tag{4.18}$$

$$= \left|\hat{\mathbf{W}}\left(\tau_0\right)\right| \cdot \left(1 + \hat{P}_s\,\left(\alpha_0\,\mathbf{a}_0 - \hat{\mathbf{r}}_{ys}\left(\tau_0\right)\,\hat{P}_s^{-1}\right)^*\,\hat{\mathbf{W}}^{-1}\left(\tau_0\right)\,\left(\alpha_0\,\mathbf{a}_0 - \hat{\mathbf{r}}_{ys}\left(\tau_0\right)\,\hat{P}_s^{-1}\right)\right) . \tag{4.19}$$

Equation (4.19) stems directly from the standard properties of the determinant (3.22) and (3.23). Note that the problem addressed in Chapter 3 would have led to a cost function equal to the determinant in (4.19). Now, thanks to the knowledge of $\mathbf{a}_0$, the resulting cost function also depends on the second term in that equation. A straightforward minimization of (4.19) with respect to $\alpha_0$ results in the ML estimate of the LOSS amplitude:

$$\boxed{\hat{\alpha}_{0,ML} = \left.\frac{\mathbf{a}_0^*\ \hat{\mathbf{W}}^{-1}\left(\tau_0\right)\,\hat{\mathbf{r}}_{ys}\left(\tau_0\right)}{\hat{P}_s\,\mathbf{a}_0^*\ \hat{\mathbf{W}}^{-1}\left(\tau_0\right)\,\mathbf{a}_0}\right|_{\tau_0=\hat{\tau}_{0,ML}} \ .} \tag{4.20}$$

Note that this expression has to be evaluated at $\hat{\tau}_{0,ML}$, which is the ML estimate of $\tau_0$. Thanks to the invariance principle of the ML estimates [Sch90, Kay93], the ML estimate of the carrier phase is directly the argument of $\hat{\alpha}_{0,ML}$. After plain but lengthy calculations, in which (4.20) is substituted into (4.19) and $\hat{\mathbf{W}}^{-1}(\tau_0)$ is expanded using the matrix inversion lemma, i.e.,

$$\hat{\mathbf{W}}^{-1}(\tau_0) = \hat{\mathbf{R}}_{yy}^{-1} + \frac{\hat{\mathbf{R}}_{yy}^{-1}\,\hat{\mathbf{r}}_{ys}(\tau_0)\,\hat{\mathbf{r}}_{ys}^{*}(\tau_0)\,\hat{\mathbf{R}}_{yy}^{-1}}{\hat{P}_s - \hat{\mathbf{r}}_{ys}^{*}(\tau_0)\,\hat{\mathbf{R}}_{yy}^{-1}\,\hat{\mathbf{r}}_{ys}(\tau_0)}\,, \tag{4.21}$$

the criterion in (4.19) can be expressed as a function of only $\tau_0$:

$$\Lambda_3(\tau_0) = \Lambda_2(\tau_0, \hat{\alpha}_{0,ML}) = \left|\hat{\mathbf{R}}_{yy}\right| \cdot \left(1 - \hat{\alpha}_{0,ML}^{*}\,\hat{\mathbf{r}}_{ys}^{*}\,\hat{\mathbf{R}}_{yy}^{-1}\,\mathbf{a}_0\right) \tag{4.22}$$

$$= \left|\hat{\mathbf{R}}_{yy}\right| \cdot \left(1 + \frac{\left|\mathbf{a}_0^{*}\,\hat{\mathbf{R}}_{yy}^{-1}\,\hat{\mathbf{r}}_{ys}(\tau_0)\right|^2}{\left(\hat{P}_s - \hat{\mathbf{r}}_{ys}^{*}(\tau_0)\,\hat{\mathbf{R}}_{yy}^{-1}\,\hat{\mathbf{r}}_{ys}(\tau_0)\right)\left(\mathbf{a}_0^{*}\,\hat{\mathbf{R}}_{yy}^{-1}\,\mathbf{a}_0\right)}\right)^{-1}. \tag{4.23}$$

Therefore, the ML estimate of the time delay, that is to say the value that minimizes $\Lambda_3(\tau_0)$, is

$$\hat{\tau}_{0,ML} = \arg\max_{\tau_0} \Lambda_{ML}(\tau_0) \tag{4.24}$$

$$\triangleq \arg\max_{\tau_0} \frac{\left|\mathbf{a}_0^{*}\,\hat{\mathbf{R}}_{yy}^{-1}\,\hat{\mathbf{r}}_{ys}(\tau_0)\right|^2}{\hat{P}_s - \hat{\mathbf{r}}_{ys}^{*}(\tau_0)\,\hat{\mathbf{R}}_{yy}^{-1}\,\hat{\mathbf{r}}_{ys}(\tau_0)}\,. \tag{4.25}$$

The computation of the ML estimates only involves the search of the maximum of the one-dimensional (1-D) function $\Lambda_{ML}(\tau_0)$, so the complexity is comparable to that of the well-known single-sensor matched filter approach. Moreover, this ML estimator is applicable in the same way in the presence of any type (specular or diffuse) of multipath, which is an important advantage with respect to methods based on the detailed model in (4.2). An expression analogous to (4.25) was already presented in [Swi98b] for a similar problem: the estimation of the direction-of-arrival and the Doppler frequency of a desired signal in a noise field with unknown spatial correlation.

If the received signal is exactly described by the simplified model (4.8) and the assumption (**A1**) in Section 2.5.1 holds, the limiting or asymptotic (large $N$ throughout the chapter) expression of the cost function in (4.25) is

$$\frac{\left|\mathbf{a}_0^{*}\,\mathbf{R}_{yy}^{-1}\,\boldsymbol{\alpha}_0\right|^2 \left|c_{ss}(\tau_0 - \check{\tau}_0)\right|^2}{P_s - \boldsymbol{\alpha}_0^{*}\,\mathbf{R}_{yy}^{-1}\,\boldsymbol{\alpha}_0\,\left|c_{ss}(\tau_0 - \check{\tau}_0)\right|^2} \tag{4.26}$$

with probability one. $\check{\tau}_0$ denotes the true value of the delay, and $P_s = c_{ss}(0)$ and $\mathbf{R}_{yy}$ represent the limiting values of the corresponding quantities. It is clear that (4.26) is maximum at $\tau_0 = \check{\tau}_0$, since the numerator and denominator are maximum and minimum, respectively, at this value of the delay. Subsequently, the consistency of $\hat{\alpha}_{0,ML}$ and $\hat{\mathbf{Q}}_{ML}$ follows from (4.20) and (4.14), and

the consistency of $\hat{\tau}_{0,ML}$. Therefore, if the model (4.8) holds exactly, the ML estimators of $\mathbf{Q}$, $\alpha_0$ and $\tau_0$ are also asymptotically efficient [Leh83, section 6.4]. A direct proof of the asymptotic efficiency of $\hat{\tau}_{0,ML}$ is also provided in Section 4.6.

Below, we analyze the asymptotic expression of the cost function in (4.25) when the actual received signal follows the "detailed" signal model in (4.1)–(4.5), being $\check{\boldsymbol{\tau}}$ the true value of the delays. Besides, we assume that the signal-to-noise ratio (SNR) is high. This analysis does not intend to be a rigorous study, but only a way to gain insight into the ML cost function.

First, the denominator of (4.25) can be written as

$$\frac{\hat{P}_s}{\left|\hat{\mathbf{R}}_{yy}\right|}\left|\hat{\mathbf{R}}_{yy}\right|\cdot\left(1-\frac{1}{\hat{P}_s}\,\hat{\mathbf{r}}_{ys}^{*}\left(\tau_0\right)\,\hat{\mathbf{R}}_{yy}^{-1}\,\hat{\mathbf{r}}_{ys}\left(\tau_0\right)\right)=\frac{\hat{P}_s}{\left|\hat{\mathbf{R}}_{yy}\right|}\left|\hat{\mathbf{W}}\left(\tau_0\right)\right|\ . \tag{4.27}$$

Under the detailed model hypothesis, the limiting value of (4.27) is

$$\frac{c_{ss}\left(0\right)}{\left|\mathbf{R}_{yy}\right|}\left|\mathbf{R}_{yy}-\mathbf{A}\,\mathbf{C}_{ss}\left(\check{\boldsymbol{\tau}},\tau_0\right)\,c_{ss}^{-1}\left(0\right)\,\mathbf{C}_{ss}^{*}\left(\check{\boldsymbol{\tau}},\tau_0\right)\,\mathbf{A}^{*}\right| \tag{4.28}$$

with probability one. $\mathbf{C}_{ss}\left(\boldsymbol{\tau},\boldsymbol{\lambda}\right)$ is a matrix whose $k,l$-th element is $c_{ss}\left(\lambda_l-\tau_k\right)$, and

$$\mathbf{R}_{yy}=\mathbf{A}\,\mathbf{C}_{ss}\left(\check{\boldsymbol{\tau}},\check{\boldsymbol{\tau}}\right)\,\mathbf{A}^{*}+\mathbf{Q}\ . \tag{4.29}$$

If we define

$$\mathbf{M}\left(\check{\boldsymbol{\tau}},\tau_0\right)=\mathbf{C}_{ss}\left(\check{\boldsymbol{\tau}},\check{\boldsymbol{\tau}}\right)-\mathbf{C}_{ss}\left(\check{\boldsymbol{\tau}},\tau_0\right)\,c_{ss}^{-1}\left(0\right)\,\mathbf{C}_{ss}^{*}\left(\check{\boldsymbol{\tau}},\tau_0\right)\ , \tag{4.30}$$

then the second determinant in (4.28) can be expressed as

$$\left|\mathbf{Q}+\mathbf{A}\,\mathbf{M}\left(\check{\boldsymbol{\tau}},\tau_0\right)\,\mathbf{A}^{*}\right|=\left|\mathbf{Q}\right|\,\left|\mathbf{I}+\mathbf{A}^{*}\,\mathbf{Q}^{-1}\,\mathbf{A}\,\mathbf{M}\left(\check{\boldsymbol{\tau}},\tau_0\right)\right| \tag{4.31}$$

$$\approx\left|\mathbf{Q}\right|\,\left|\mathbf{A}^{*}\,\mathbf{Q}^{-1}\,\mathbf{A}\right|\,\left|\mathbf{M}\left(\check{\boldsymbol{\tau}},\tau_0\right)\right|\ . \tag{4.32}$$

The approximation in (4.32) is based on the assumption of high SNR. Note that for this approximation to be valid, $\mathbf{A}^{*}\,\mathbf{Q}^{-1}\,\mathbf{A}$ has to be full-rank. The matrix $\mathbf{M}\left(\check{\boldsymbol{\tau}},\tau_0\right)$ is the Schur complement of $c_{ss}\left(0\right)$ in

$$\mathbf{C}_{ss}\left(\boldsymbol{\tau}_a,\boldsymbol{\tau}_a\right)=\left[\begin{array}{c|c}\mathbf{C}_{ss}\left(\check{\boldsymbol{\tau}},\check{\boldsymbol{\tau}}\right) & \mathbf{C}_{ss}\left(\check{\boldsymbol{\tau}},\tau_0\right)\\ \hline \mathbf{C}_{ss}^{*}\left(\check{\boldsymbol{\tau}},\tau_0\right) & c_{ss}\left(0\right)\end{array}\right]\ , \tag{4.33}$$

where $\boldsymbol{\tau}_a=\left[\check{\boldsymbol{\tau}}^{T}\ \tau_0\right]^{T}$. Since $c_{ss}\left(0\right)$ is strictly greater than zero, $\mathbf{M}\left(\check{\boldsymbol{\tau}},\tau_0\right)$ is singular if and only if $\mathbf{C}_{ss}\left(\boldsymbol{\tau}_a,\boldsymbol{\tau}_a\right)$ is singular. At this point, we need to consider that the following mild non-ambiguity condition of the "time manifold" is satisfied: the matrix $\mathbf{C}\left(\tilde{\boldsymbol{\tau}},\tilde{\boldsymbol{\tau}}\right)$ is non-singular (positive definite) for any vector $\tilde{\boldsymbol{\tau}}$ of length $d+1$ whose elements are all distinct. Therefore, equation (4.32) is zero when $\mathbf{C}_{ss}\left(\tilde{\boldsymbol{\tau}},\tilde{\boldsymbol{\tau}}\right)$ is singular; and this can only happen when $\tau_0$ coincides with any of the elements of $\check{\boldsymbol{\tau}}$, since the elements of $\check{\boldsymbol{\tau}}$ are all distinct.

In the second place, we analyze the asymptotic expression of the numerator of (4.25). Applying the matrix inversion lemma to (4.29) yields

$$\mathbf{R}_{yy}^{-1} = \mathbf{Q}^{-1} - \mathbf{Q}^{-1}\,\mathbf{A}\,\left(\mathbf{C}_{ss}^{-1}\left(\check{\boldsymbol{\tau}},\check{\boldsymbol{\tau}}\right) + \mathbf{A}^{*}\,\mathbf{Q}^{-1}\,\mathbf{A}\right)^{-1}\,\mathbf{A}^{*}\,\mathbf{Q}^{-1} \tag{4.34}$$

$$= \mathbf{Q}^{-1} - \mathbf{Q}^{-1}\,\mathbf{A}\,\left(\mathbf{A}^{*}\,\mathbf{Q}^{-1}\,\mathbf{A}\right)^{-1}\,\left(\mathbf{I} + \mathbf{C}_{ss}^{-1}\left(\check{\boldsymbol{\tau}},\check{\boldsymbol{\tau}}\right)\,\left(\mathbf{A}^{*}\,\mathbf{Q}^{-1}\,\mathbf{A}\right)^{-1}\right)^{-1}\,\mathbf{A}^{*}\,\mathbf{Q}^{-1}\,. \tag{4.35}$$

In (4.35), we have again implicitly considered that $\mathbf{A}^{*}\,\mathbf{Q}^{-1}\,\mathbf{A}$ is non-singular. Taking into account that the SNR is high, we perform the following Taylor expansion

$$\left(\mathbf{I} + \mathbf{C}_{ss}^{-1}\left(\check{\boldsymbol{\tau}},\check{\boldsymbol{\tau}}\right)\,\left(\mathbf{A}^{*}\,\mathbf{Q}^{-1}\,\mathbf{A}\right)^{-1}\right)^{-1} \approx \mathbf{I} - \mathbf{C}_{ss}^{-1}\left(\check{\boldsymbol{\tau}},\check{\boldsymbol{\tau}}\right)\,\left(\mathbf{A}^{*}\,\mathbf{Q}^{-1}\,\mathbf{A}\right)^{-1}\,. \tag{4.36}$$

After substituting this expansion into (4.35), we get

$$\begin{aligned}\mathbf{R}_{yy}^{-1} \approx\ & \mathbf{Q}^{-1} - \mathbf{Q}^{-1}\,\mathbf{A}\,\left(\mathbf{A}^{*}\,\mathbf{Q}^{-1}\,\mathbf{A}\right)^{-1}\,\mathbf{A}^{*}\,\mathbf{Q}^{-1} \\ & - \mathbf{Q}^{-1}\,\mathbf{A}\,\left(\mathbf{A}^{*}\,\mathbf{Q}^{-1}\,\mathbf{A}\right)^{-1}\,\mathbf{C}_{ss}^{-1}\left(\check{\boldsymbol{\tau}},\check{\boldsymbol{\tau}}\right)\,\left(\mathbf{A}^{*}\,\mathbf{Q}^{-1}\,\mathbf{A}\right)^{-1}\,\mathbf{A}^{*}\,\mathbf{Q}^{-1}\,.\end{aligned} \tag{4.37}$$

Using this approximation of $\mathbf{R}_{yy}^{-1}$ for high SNR, the asymptotic expression of the numerator of $\Lambda_{ML}\left(\tau_0\right)$ is

$$\frac{1}{\left|\alpha_0\right|^2}\,\left|\mathbf{e}_1^{T}\,\mathbf{C}_{ss}^{-1}\left(\check{\boldsymbol{\tau}},\check{\boldsymbol{\tau}}\right)\,\mathbf{C}_{ss}\left(\check{\boldsymbol{\tau}},\tau_0\right)\right|^2\,, \tag{4.38}$$

where $\mathbf{e}_i$ is a vector whose $i$-th element is 1 and the others are zero. The maximum of (4.38) is not in general attained at the true delay of the LOSS. However, the important property is that equation (4.38) is different from zero at $\tau_0 = \check{\tau}_0$, and zero at $\tau_0 = \check{\tau}_k$ for $k = 1, \ldots, d-1$. This statement comes readily from the fact that

$$\mathbf{C}_{ss}\left(\check{\boldsymbol{\tau}},\check{\boldsymbol{\tau}}\right) = \left[\begin{array}{cccc}\mathbf{C}_{ss}\left(\check{\boldsymbol{\tau}},\check{\tau}_0\right) & \mathbf{C}_{ss}\left(\check{\boldsymbol{\tau}},\check{\tau}_1\right) & \cdots & \mathbf{C}_{ss}\left(\check{\boldsymbol{\tau}},\check{\tau}_{d-1}\right)\end{array}\right] \tag{4.39}$$

and, hence, $\mathbf{C}_{ss}^{-1}\left(\check{\boldsymbol{\tau}},\check{\boldsymbol{\tau}}\right)\,\mathbf{C}_{ss}\left(\check{\boldsymbol{\tau}},\check{\tau}_k\right) = \mathbf{e}_{k+1}$.

To sum up, the limiting expressions of both the numerator and denominator of $\Lambda_{ML}\left(\tau_0\right)$ approximated for high SNR cancel at the true delays of the reflections (i.e., at $\tau_0 = \check{\tau}_k$ for $k = 1, \ldots, d-1$); whereas only the denominator is zero at the true delay of the direct signal (i.e., at $\tau_0 = \check{\tau}_0$). This behavior of the numerator and denominator occurs thanks to the presence of the matrix $\mathbf{R}_{yy}^{-1}$. This matrix appears in the ML cost function because the correlation of the noise has been assumed to be unknown. When the noise is considered spatially white the resulting cost functions are $\Lambda_{WH}\left(\tau_0\right)$ and $\Lambda_{WH-TE}\left(\tau_0\right)$, which are presented in the next section in equations (4.43) and (4.44). The asymptotic value of these two costs functions is independent of the SNR, and they do not present the interesting properties of the numerator and denominator of the $\Lambda_{ML}\left(\tau_0\right)$.

### 4.2.1 Related Estimators

The performance of the ML estimators above will be compared in Section 4.5 with that of other methods. In this section, we outline four different estimators that are obtained from simplifying considerations about the signal model or from an ad-hoc reasoning. The first of these estimators stems from the assumption that the steering vector of the LOSS is arbitrary and unknown, along with the model (4.8). The minimization of (4.19) with respect to $(\alpha_0\,\mathbf{a}_0)$ is trivial, and therefore ML time-delay estimate using only temporal reference is

$$\hat{\tau}_{0,TE} = \arg\max_{\tau_0} \Lambda_{TE}\left(\tau_0\right) \triangleq \arg\max_{\tau_0} \frac{\hat{\mathbf{r}}_{ys}^{*}\left(\tau_0\right)\,\hat{\mathbf{R}}_{yy}^{-1}\,\hat{\mathbf{r}}_{ys}\left(\tau_0\right)}{\hat{P}_s}\,. \tag{4.40}$$

It is worth noting that $\Lambda_{TE}\left(\tau_0\right)$ is the sum of the $m$ single-sensor ML time-delay estimators obtained from each of the antennas, having previously whitened the signals according to the inverse of the total correlation matrix. Indeed, this is the ML estimator derived in Chapter 3 for the particular case of $d = 1$. An alternative expression that provides insights into this estimator is

$$\Lambda_{TE}\left(\tau_0\right) = \frac{\mathbf{s}^{T}\left(\tau_0\right)\,\mathbf{P}_{\mathbf{Y}^*}\,\mathbf{s}^{c}\left(\tau_0\right)}{\mathbf{s}^{T}\left(\tau_0\right)\,\mathbf{s}^{c}\left(\tau_0\right)}\,, \tag{4.41}$$

where $\mathbf{P}_{\mathbf{Y}^*} = \mathbf{Y}^{*}\left(\mathbf{Y}\,\mathbf{Y}^{*}\right)^{-1}\mathbf{Y}$. Expression (4.41) implies that $\hat{\tau}_{0,TE}$ is estimated as the delay that yields the vector $\mathbf{s}^{c}\left(\tau_0\right)$ closest to the column span of $\mathbf{Y}^{*}$.

The second method rests on the same simplified model as the ML estimator proposed in this chapter, but with the additional assumption that the noise is spatially white. In this method, the vector $\mathbf{a}_0$ is considered again to be known. The derivation of the ML estimates when $\mathbf{Q}$ is replaced by $\sigma^2\,\mathbf{I}$ is simple and yields

$$\hat{\alpha}_{0,WH} = \left.\frac{\mathbf{a}_0^{*}\,\hat{\mathbf{r}}_{ys}\left(\tau_0\right)}{\hat{P}_s\,\mathbf{a}_0^{*}\,\mathbf{a}_0}\right|_{\tau_0=\hat{\tau}_{0,WH}} \tag{4.42}$$

$$\hat{\tau}_{0,WH} = \arg\max_{\tau_0} \Lambda_{WH}\left(\tau_0\right) \triangleq \arg\max_{\tau_0} \frac{\left|\mathbf{a}_0^{*}\,\hat{\mathbf{r}}_{ys}\left(\tau_0\right)\right|^2}{\hat{P}_s}\,. \tag{4.43}$$

On the other hand, if the steering vector is unknown, the resulting time-delay estimator is

$$\hat{\tau}_{0,WH-TE} = \arg\max_{\tau_0} \Lambda_{WH-TE}\left(\tau_0\right) \triangleq \arg\max_{\tau_0} \frac{\hat{\mathbf{r}}_{ys}^{*}\left(\tau_0\right)\,\hat{\mathbf{r}}_{ys}\left(\tau_0\right)}{\hat{P}_s}\,. \tag{4.44}$$

The last approach involves spatially filtering the received signals using the classical minimum variance or Capon's beamformer (MVB) :

$$\hat{\mathbf{w}}_{MV} = \frac{\hat{\mathbf{R}}_{yy}^{-1}\,\mathbf{a}_0}{\mathbf{a}_0^{*}\,\hat{\mathbf{R}}_{yy}^{-1}\,\mathbf{a}_0} \tag{4.45}$$

At first glance, this may seem a logical solution and it has been proposed for the problem under consideration in some works, such as [Zol95] and [Hat98]. If the ML criterion is applied to the output signal of the beamformer ($\mathbf{y}_{MV}^T = \hat{\mathbf{w}}_{MV}^* \mathbf{Y}$), the resulting estimates are

$$\hat{\alpha}_{0,MV} = \left. \frac{\mathbf{a}_0^* \hat{\mathbf{R}}_{yy}^{-1} \hat{\mathbf{r}}_{ys}(\tau_0)}{\hat{P}_s \mathbf{a}_0^* \hat{\mathbf{R}}_{yy}^{-1} \mathbf{a}_0} \right|_{\tau_0 = \hat{\tau}_{0,MV}} \tag{4.46}$$

$$\hat{\tau}_{0,MV} = \arg\max_{\tau_0} \Lambda_{MV}(\tau_0) \triangleq \arg\max_{\tau_0} \frac{\left| \mathbf{a}_0^* \hat{\mathbf{R}}_{yy}^{-1} \hat{\mathbf{r}}_{ys}(\tau_0) \right|^2}{\hat{P}_s} . \tag{4.47}$$

It is interesting to note that the ML criterion proposed in this chapter can be expressed as a function of the ML criterion using only temporal information and the cost function based on the MVB:

$$\Lambda_{ML}(\tau_0) = \frac{\Lambda_{MV}(\tau_0)}{1 - \Lambda_{TE}(\tau_0)} . \tag{4.48}$$

Nonetheless, simulation results will show that the estimates obtained from $\Lambda_{ML}(\tau_0)$ largely outperform those obtained from $\Lambda_{MV}(\tau_0)$ and $\Lambda_{TE}(\tau_0)$ separately. Substituting (4.21) into (4.20) yields an equivalent expression for the ML amplitude estimate:

$$\hat{\alpha}_{0,ML} = \left. \frac{\mathbf{a}_0^* \hat{\mathbf{R}}_{yy}^{-1} \hat{\mathbf{r}}_{ys}(\tau_0)}{\hat{P}_s \mathbf{a}_0^* \hat{\mathbf{R}}_{yy}^{-1} \mathbf{a}_0 - \left( \hat{\mathbf{r}}_{ys}^*(\tau_0) \hat{\mathbf{R}}_{yy}^{-1} \hat{\mathbf{r}}_{ys}(\tau_0) \right) \left( \mathbf{a}_0^* \hat{\mathbf{R}}_{yy}^{-1} \mathbf{a}_0 \right) + \left| \mathbf{a}_0^* \hat{\mathbf{R}}_{yy}^{-1} \hat{\mathbf{r}}_{ys}(\tau_0) \right|^2} \right|_{\tau_0 = \hat{\tau}_{0,ML}} . \tag{4.49}$$

It is clear that the amplitude estimates obtained from the ML and MV criteria would satisfy the following relations

$$\begin{aligned} |\hat{\alpha}_{0,ML}| &\geq |\hat{\alpha}_{0,MV}| \\ \angle\hat{\alpha}_{0,ML} &= \angle\hat{\alpha}_{0,MV} \end{aligned} \qquad \text{if} \quad \hat{\tau}_{0,MV} = \hat{\tau}_{0,ML} . \tag{4.50}$$

If this were the case (namely, if $\hat{\tau}_{0,MV} = \hat{\tau}_{0,ML}$), the carrier phase measurements obtained with both criteria would be exactly the same. However, in reality the errors of $\hat{\tau}_{0,MV}$ are much larger than those of $\hat{\tau}_{0,ML}$, as it will be shown in Section 4.5, what makes the estimator $\hat{\alpha}_{0,MV}$ perform generally worse than $\hat{\alpha}_{0,ML}$. In a different framework, an ML amplitude estimator similar to (4.20), named APES (Amplitude and Phase EStimator) was proposed in [Li96], and compared in [Jak00] with an estimator based on the Capon's beamformer, like (4.46), for the spectral estimation problem.

## 4.3 Closed Form Algorithms

It may be useful for certain practical designs even to eliminate the 1-D maximization involved by (4.25), and several strategies can be devised to achieve such objective. The standard approach

consists in searching the zero-crossing of the derivative of $\Lambda_{ML}(\tau_0)$, which is approximated as

$$\frac{d\,\Lambda_{ML}(\tau_0)}{d\,\tau_0} \approx \frac{\Lambda_{ML}(\tau_0+\delta\,T_c)-\Lambda_{ML}(\tau_0-\delta\,T_c)}{2\delta\,T_c}\,, \tag{4.51}$$

where usually $\delta \in (0,1)$. This approximation of the derivative may be used as the controlling error signal of a timing closed loop and, hence, may appropriate for a feedback implementation [Spi77, Sim85]. This scheme, which shares the same idea as the DLL, was studied in [Sec97b]. In this section, we present two algorithms that bring forward, in our opinion, a more interesting contribution than that provided by the derivative approximation and that are valid for feedforward designs.

### 4.3.1 Polynomial-Rooting in the Frequency Domain

In this technique, the linear phase dependence on the delay of the frequency-domain representation of the signal is exploited. If the $N$ temporal samples are transformed into the frequency domain using the DFT, the signal vector approximately satisfies the following relation (see Section 2.5.2 for further details)

$$\mathbf{s}(\tau_0) = \mathrm{e}^{j\,\phi}\,\mathbf{S}_\omega\,\mathbf{u}\left(\exp\left(-j\,2\pi\tau_0/\left(NT_s\right)\right)\right)\,, \tag{4.52}$$

where $\mathbf{S}_\omega$ is a diagonal matrix whose elements are the DFT of $[s(T_s),\, s(2T_s), \ldots, s(NT_s)]$, and

$$\phi = \frac{2\pi\tau_0}{NT_s}\lfloor N/2\rfloor\,, \tag{4.53}$$

$$\mathbf{u}(z) = \left[\begin{array}{ccccc} 1 & z & z^2 & \ldots & z^{N-1}\end{array}\right]^T\,. \tag{4.54}$$

Since the DFT is a unitary transform, the ML estimator presented in Section 4.2 can be applied identically in the frequency domain. Therefore, considering that at this point the matrix $\mathbf{Y}$ contains the frequency samples of the signals and that the relationship (4.52) is exact, the ML cost function in (4.25) can be expressed as the quotient of $(2N-2)$th order polynomials evaluated on the unit circle as follows

$$\Lambda_{ML}(\tau_0) = \Lambda_{MLF}(z)\,\big|_{z=\exp(j\,2\pi\tau_0/NT_s)}\,, \tag{4.55}$$

where we have defined

$$\Lambda_{MLF}(z) \triangleq \frac{\mathbf{u}^T(z^{-1})\,\mathbf{S}_\omega\,\mathbf{Y}^*\,\hat{\mathbf{R}}_{yy}^{-1}\,\mathbf{a}_0\,\mathbf{a}_0^*\,\hat{\mathbf{R}}_{yy}^{-1}\,\mathbf{Y}\,\mathbf{S}_\omega^*\,\mathbf{u}(z)}{\mathbf{u}^T(z^{-1})\,\mathbf{S}_\omega\,\left(N\,\mathbf{I}-\mathbf{Y}^*\,\hat{\mathbf{R}}_{yy}^{-1}\,\mathbf{Y}\right)\mathbf{S}_\omega^*\,\mathbf{u}(z)}\,. \tag{4.56}$$

Finding the values that null the derivative of $\Lambda_{ML}(\tau_0)$ can be replaced by finding the values that null the derivative of $\Lambda_{MLF}(z)$ since

$$\frac{d\;\Lambda_{ML}(\tau_0)}{d\,\tau_0} = j\,\frac{2\pi}{NT_s}\,\exp\left(j\frac{2\pi\tau_0}{NT_s}\right)\,\frac{d\;\Lambda_{MLF}(z)}{d\,z}\bigg|_{z=\exp(j\,2\pi\tau_0/NT_s)}\,. \tag{4.57}$$

Therefore, the maximization of $\Lambda_{ML}(\tau_0)$ amounts to rooting a $(4N-6)$th order polynomial, named $p(z)$, which is the numerator of the derivative of $\Lambda_{MLF}(z)$ with respect to $z$. The polynomial $p(z)$ can be computed in closed form. Only the subset of roots lying on the unit circle is considered. After evaluating the cost function $\Lambda_{MLF}(z)$ at the elements of this subset, the one yielding the maximum is selected and designated $\hat{z}_0$. Then, the time-delay estimate is

$$\hat{\tau}_{0,MLF} = \frac{N\,T_s}{2\pi}\,\angle\hat{z}_0\ . \tag{4.58}$$

It may be argued that the order of the polynomial $p(z)$ can be large. However, there exist computationally efficient rooting algorithms for high-order polynomials; see, e.g., [Pre95, Hot99, Hot00] and references therein. Moreover, simulation results have shown that the absolute value of the coefficients of $p(z)$ spans several orders of magnitude (usually about 15), and only a very small portion of the coefficients is representative (see Section 4.5 for further details). Consequently, $p(z)$ can be truncated and also decimated so as to retain only its significant coefficients, and then the order of the resulting polynomial is largely reduced.

### 4.3.2 Linearization of the Signal Vector

The basis of the algorithm presented in this section is a piecewise linear approximation of the vector $\mathbf{s}(\tau_0)$. Let us divide the range of uncertainty[2] of $\tau_0$ into intervals of length $T_0$, so that we can write $\tau_0 = (p+\delta)\,T_0$, where $p$ is an integer and $\delta \in [0,1)$. Using a first-order Taylor expansion, the signal vector can be expressed in each interval $\tau_0 \in \big[p\,T_0, (p+1)\,T_0\big)$ as

$$\mathbf{s}(\tau_0) \approx \mathbf{s}(p\,T_0) + \delta\,T_0\ \left.\frac{d\,\mathbf{s}(\tau)}{d\,\tau}\right|_{\tau=p\,T_0} \tag{4.59}$$

or, using a piecewise linear interpolation, as

$$\mathbf{s}(\tau_0) \approx (1-\delta)\ \mathbf{s}(p\,T_0) + \delta\,\mathbf{s}\big((p+1)\,T_0\big)\ . \tag{4.60}$$

Some numerical examples concerning the selection of the value of $T_0$, which has to be small enough to assure that the errors in (4.59) and (4.60) are not excessive, are shown in Section 4.5. Both approximations become exact when the *received* chip-shaping pulse is triangular. This is the case, for instance, when the *transmitted* chip-shaping pulse is rectangular, and it is filtered with a rectangular matched filter before applying of the estimation algorithm, as in [Str96, Par96b, Zhe97, Liu98a, Ben98, Liu98b]. This situation could be encountered in a GPS receiver, because GPS satellites transmit nearly rectangular pulses given that the chip rate $(1/T_c)$ of the C/A code is 1.023Mchips/s and the bandwidth is about 20MHz. What is more important is that

[2]The range of possible delays is usually on the order of or smaller than two times the chip interval, $2T_c$, because it is assumed that previous coarse synchronization has been achieved or a previous time-delay estimate is available.

simulation results have shown that the approximations above also yield satisfactory results for rounder pulses, such as Nyquist pulses. Consequently, even though those approximations may seem not to have a sound foundation, they allow the derivation of an algorithm with practical interest.

In the sequel, we only consider the expression (4.60) and we define

$$\mathbf{V}(p) = \left[ \begin{array}{cc} \mathbf{s}(\tau_0) & \mathbf{s}\big((p+1)\,T_0\big) \end{array} \right] \quad \text{and} \quad \boldsymbol{\mu}(\delta) = \left[ \begin{array}{cc} 1-\delta & \delta \end{array} \right]^T . \tag{4.61}$$

These definitions are trivially modified in order to use the approximation (4.59). Substituting (4.60) into (4.25) and using (4.61) yield the following expression of the ML cost function

$$\Lambda_{MLL}(\delta, p) \triangleq \frac{P(\delta, p)}{Q(\delta, p)} = \frac{\boldsymbol{\mu}^T(\delta)\ \mathbf{V}^T(p)\ \mathbf{Y}^*\,\hat{\mathbf{R}}_{yy}^{-1}\,\mathbf{a}_0\,\mathbf{a}_0^*\,\hat{\mathbf{R}}_{yy}^{-1}\,\mathbf{Y}\ \mathbf{V}^c(p)\ \boldsymbol{\mu}(\delta)}{\boldsymbol{\mu}^T(\delta)\ \mathbf{V}^T(p)\ \Big(N\,\mathbf{I} - \mathbf{Y}^*\,\hat{\mathbf{R}}_{yy}^{-1}\,\mathbf{Y}\Big)\ \mathbf{V}^c(p)\ \boldsymbol{\mu}(\delta)}\,, \tag{4.62}$$

which is, for a fixed interval $p$, a quotient of second-order polynomials in $\delta$. Therefore, the local extrema of the ML function in the $p$th interval are the roots of the quadratic polynomial

$$R(\delta, p) = \frac{d\,P(\delta, p)}{d\,\delta}\,Q(\delta, p) - \frac{d\,Q(\delta, p)}{d\,\delta}\,P(\delta, p) \tag{4.63}$$

which are real and belong to the interval $[0, 1)$. Since the absolute maximum of the cost function has to be either one of the local extrema or one of the points between intervals, the algorithm for finding the absolute maximum is as follows

1. Let $\Omega$ be the set of pairs $\big\{(p_{\min}, \delta = 0), (p_{\min+1}, \delta = 0), \ldots, (p_{\max}, \delta = 0)\big\}$, where $\{p_{\min}, \ldots, p_{\max}\}$ correspond to the intervals of length $T_0$ needed to cover the range of uncertainty of $\tau_0$.
2. For each value of $p = p_{\min}, \ldots, p_{\max}$
   a. Find the roots $\delta_1$ and $\delta_2$ of $R(\delta, p)$.
   b. If any root $\delta_i$ $(i = 1, 2)$ belongs to $[0, 1)$, then add the pair $(p, \delta_i)$ to $\Omega$.
3. Evaluate $\Lambda_{MLL}(\delta, p)$ at all the elements in $\Omega$, and choose the pair $\Big(\hat{\delta}, \hat{p}\Big)$ that yields the maximum cost. Finally, form the estimate of the time-delay as $\hat{\tau}_{0,MLL} = \Big(\hat{p} + \hat{\delta}\Big)\,T_0$.

Table 4.1: Algorithm based on the linearization of the signal vector.

## 4.4 Iterative Algorithm: Hybrid Beamforming

In this section, the equivalence between the maximum likelihood estimation and a specific type of beamforming is presented. Not only does this equivalence shed light on the performance of the systematic, yet non-intuitive, ML estimators of the code (4.25) and carrier (4.20) phases presented above, but it is also the basis for an iterative realization of those ML estimators. From the beamforming viewpoint, the cost function to be optimized has a clear interpretation, and can be written without the need for a probabilistic description of the data. These are the reasons why according to the beamforming approach it is easier to understand how the signals received at different antennas are processed in order to mitigate the effects of the undesired components. However, no a priori claims to the optimality of the estimates obtained from that approach can be done. On the other hand, the maximum likelihood principle provides a procedure to obtain optimum estimates (in the sense that usually they are asymptotically efficient) based on a probabilistic setting, but sometimes it fails in giving an understandable interpretation on how the signals are processed. This is exactly what happens with the ML estimators studied above, especially with the expression (4.25).

First, we prove the equivalence between the ML and the beamforming approaches, and then we present the iterative algorithm. The mean squared error (MSE) between the output of a beamformer with weights $\mathbf{w}$ and the reference signal $\alpha_0\,\mathbf{s}\,(\tau_0)$ is

$$J_1\,(\mathbf{w},\alpha_0,\tau_0) = \frac{1}{N}\left\|\mathbf{w}^*\,\mathbf{Y} - \alpha_0\,\mathbf{s}^T\,(\tau_0)\,\right\|_2^2 . \tag{4.64}$$

Even though expression (4.64) recalls the one that is minimized in the design of a conventional temporal-reference beamformer, there is an important difference: In (4.64) the reference signal is not completely known, but it is parameterized by the delay of the direct signal ($\tau_0$), which has to be estimated together with the optimum weight vector. If (4.64) were minimized with the constraint $|\alpha_0|^2 = 1/\hat{P}_s$, the resulting criterion for the delay would be $\Lambda_{TE}\,(\tau_0)$. However, since the steering vector of the line-of-sight signal is known, we will impose a spatial constraint on $\mathbf{w}$ in order to force the beamformer to always point this signal. This is how the beamformer is made to extract the direct signal and not any other reflection. Thus, the optimum weight vector ($\hat{\mathbf{w}}_{hMSE}$), and the estimates of the amplitude ($\hat{\alpha}_{0,hMSE}$) and the delay ($\hat{\tau}_{0,hMSE}$) obtained with the new criterion are the solutions of the following constrained optimization problem:

$$\hat{\mathbf{w}}_{hMSE},\,\hat{\alpha}_{0,hMSE},\,\hat{\tau}_{0,hMSE} = \arg\min_{\mathbf{w},\alpha_0,\tau_0} J_1\,(\mathbf{w},\alpha_0,\tau_0) \tag{4.65}$$

$$\text{subject to} \qquad \mathbf{w}^*\,\mathbf{a}_0 = 1\,. \tag{4.66}$$

Note that, due to the spatial constraint, now it is not convenient to fix the value of the amplitude. The resulting $\hat{\mathbf{w}}_{hMSE}$ is a hybrid beamformer, because it is derived using both temporal and spatial references [Hon87]. Also note that no assumptions about the spatial or statistical

properties of the noise have been needed to phrase this new problem. It is straightforward that the amplitude that minimizes the cost $J_1$ for fixed $\mathbf{w}$ and $\tau_0$ is

$$\hat{\alpha}_{0,\,hMSE} = \frac{\mathbf{w}^*\,\hat{\mathbf{r}}_{ys}\,(\tau_0)}{\hat{P}_s}\,, \tag{4.67}$$

which substituted into (4.64) and using (4.16) results in[3]

$$J_2\,(\mathbf{w},\tau_0) = \frac{1}{N}\left\|\mathbf{w}^*\,\left(\mathbf{Y} - \frac{\mathbf{r}_{ys}\,(\tau_0)}{\hat{P}_s}\,\mathbf{s}^T\,(\tau_0)\right)\right\|_2^2 = \mathbf{w}^*\;\hat{\mathbf{W}}\,(\tau_0)\;\mathbf{w}\;. \tag{4.68}$$

The weight vector for which (4.68) is minimized with the constraint in (4.66), for a fixed $\tau_0$, is

$$\hat{\mathbf{w}}_{hMSE} = \frac{\hat{\mathbf{W}}^{-1}\,(\tau_0)\;\mathbf{a}_0}{\mathbf{a}_0^*\,\hat{\mathbf{W}}^{-1}\,(\tau_0)\;\mathbf{a}_0}\;. \tag{4.69}$$

After replacing $\mathbf{w}$ in (4.68) with (4.69) and using the identity (4.21), we get the expression of the MSE that has to be minimized in order to obtain $\hat{\tau}_{0,hMSE}$:

$$J_{hMSE}\,(\tau_0) = \frac{1}{\mathbf{a}_0^*\,\hat{\mathbf{W}}^{-1}\,(\tau_0)\;\mathbf{a}_0} = \frac{1}{\mathbf{a}_0^*\,\hat{\mathbf{R}}_{yy}^{-1}\,\mathbf{a}_0 + \Lambda_{ML}\,(\tau_0)}\;. \tag{4.70}$$

This expression proves that the ML and the beamforming approaches yield identical time delay estimates, i.e., $\hat{\tau}_{0,hMSE} = \hat{\tau}_{0,ML}$. The proof of the equivalence concludes by noting that, after substituting (4.69) into (4.67), the amplitude estimates are also identical, i.e., $\hat{\alpha}_{0,hMSE} = \hat{\alpha}_{0,ML}$.

In order to derive an iterative version of the ML estimator, the mean squared error in (4.64) subject to the spatial constraint in (4.66) is minimized with respect to each parameter in an order different from the one followed above (the estimates obtained with this second approach are differentiated using $(\cdot)^\bullet$). First, the optimum beamformer for given $\tau_0$ and $\alpha_0$ is computed, which is denoted by $\hat{\mathbf{w}}^\bullet_{hMSE}$. Applying the Lagrange's multipliers technique, it is easily shown that

$$\hat{\mathbf{w}}^\bullet_{hMSE}\,(\tau_0,\alpha_0) = \alpha_0^*\,\hat{\mathbf{w}}_{TE}\,(\tau_0) + \beta\,(\tau_0,\alpha_0)\;\hat{\mathbf{w}}_{MV} \tag{4.71}$$

$$\beta\,(\tau_0,\alpha_0) = 1 - \alpha_0^*\,\mathbf{a}_0^*\,\hat{\mathbf{R}}_{yy}^{-1}\,\hat{\mathbf{r}}_{ys}\,(\tau_0)\;\;, \tag{4.72}$$

where the minimum variance (or spatial-reference) beamformer $\hat{\mathbf{w}}_{MV}$ was defined in (4.45), and the temporal-reference beamformer $\hat{\mathbf{w}}_{TE}$ is

$$\hat{\mathbf{w}}_{TE}\,(\tau_0) = \hat{\mathbf{R}}_{yy}^{-1}\,\hat{\mathbf{r}}_{ys}\,(\tau_0)\;\;. \tag{4.73}$$

The hybrid beamformer $\hat{\mathbf{w}}^\bullet_{hMSE}$, which is a weighted linear combination of the minimum MSE beamformer calculated with only the temporal reference ($\hat{\mathbf{w}}_{TE}$) and the minimum variance or Capon's beamformer calculated with only the spatial reference ($\hat{\mathbf{w}}_{MV}$), performs much better than its two components in scenarios with multipath propagation. While the hybrid beamformer

[3]The matrix $\hat{\mathbf{W}}\,(\tau_0)$ was defined in (4.16).

tries to attenuate the reflections of the GNSS signal, the MV beamformer combines destructively the reflections with the direct signal attempting to minimize the total power (it suffers the so-called desired-signal cancellation phenomenon), and the temporal-reference beamformer may tend to combine constructively the reflections with the direct signal in order to increase the total signal-to-noise-plus-interference ration (SNIR) of the GNSS components. Note that if the coefficient $\beta(\tau_0, \alpha_0)$, which multiplies the MVB, is evaluated at the ML estimate of the amplitude, then it is proportional to the inverse ML function $\Lambda_3(\tau_0)$ in (4.22). In the second place, the time delay and amplitude estimates are the values that minimize $J_1(\hat{\mathbf{w}}^{\bullet}_{hMSE}, \alpha_0, \tau_0)$. Considering that the hybrid beamformer is fixed, i.e., not taking into account the dependence of $\hat{\mathbf{w}}^{\bullet}_{hMSE}$ on $\tau_0$ or $\alpha_0$, it is straightforward that the estimates are

$$\hat{\tau}^{\bullet}_{0,hMSE} = \arg\max_{\tau_0} \frac{\left|\mathbf{y}_h^T \mathbf{s}^c(\tau_0)\right|^2}{\hat{P}_s} \tag{4.74}$$

$$\hat{\alpha}^{\bullet}_{0,hMSE} = \left.\frac{\mathbf{y}_h^T \mathbf{s}^c(\tau_0)}{\hat{P}_s}\right|_{\tau_0=\hat{\tau}^{\bullet}_{0,hMSE}}, \tag{4.75}$$

where $\mathbf{y}_h^T = \hat{\mathbf{w}}^{\bullet H}_{hMSE}\mathbf{Y}$ is the beamformer output. Estimating $\tau_0$ and $\alpha_0$ from the signal $\mathbf{y}_h$ is actually the process realized by any GNSS receiver, since the beamformer output can be considered to be the signal received by a single *equivalent* antenna. Consequently, the estimators in (4.74) and (4.75) could be replaced by any of the single-sensor methods implemented in conventional receivers, such as the DLL [Par96a] or the MEDLL [Nee94, Lax97], even though in this case the resulting estimates may not be the ML ones any longer. At this point, the formulation of an iterative algorithm for the computation of the hybrid beamformer, and the time delay and amplitude estimates is immediate, and it is summarized by the following steps:

1. Choose an initial value of the beamformer $\mathbf{w}^{0)}$. With the available information, the *delay-and-sum* beamformer is a convenient choice: $\mathbf{w}^{0)} = \mathbf{a}_0 / (\mathbf{a}_0^* \mathbf{a}_0)$.
2. For $k = 1, 2, 3, \ldots$
   a. Determine the new estimates $\hat{\tau}_0^{k)}$ and $\hat{\alpha}_0^{k)}$ from the output of the beamformer $\mathbf{w}^{k-1)}$. This estimates can be obtained using (4.74) and (4.75), or any other algorithm.
   b. Update the beamformer using equation (4.71), that is, $\mathbf{w}^{k)} = \mathbf{w}^{\bullet}_{hMSE}\left(\hat{\tau}_0^{k)}, \hat{\alpha}_0^{k)}\right)$.

Table 4.2: Iterative estimation algorithm based on the hybrid beamforming.

This algorithm can be applied either in block-mode or adaptively. In the former, the itera-

tions are carried out using fixed batches of data, one after another; while in the latter, the data received up to a given instant are used to adaptively update $\hat{\mathbf{R}}_{yy}$ and $\hat{\mathbf{r}}_{ys}$ in the step 2b, and to compute the estimates in the step 2a. Following this last approach, the calculation of the weight vector in (4.71) could be also done adaptively by employing the LMS or RLS algorithms [Hay96], and also the GSLC (Generalized Side Lobe Canceller) structure [Joh93]. As a result, the iterative algorithm presented herein admits of a large number of practical implementations. We will only focus in the next section on the performance of the algorithm when applied in block-mode, for coherence with the whole of the thesis; and the possible implementations, which are related to specific designs, are left outside the scope of this work. Finally, it is remarkable that the relationship between the ML estimator and the hybrid beamformer described in this section offers an interesting view of the estimation process, since it separates in two different, yet coupled, stages the spatial filtering and the temporal processing.

## 4.5 Simulation Results

In order to gain clear insight into the ML estimator, and its closed-form and iterative variants proposed in the preceding sections, their performance is evaluated and compared with that of other techniques in two types of scenarios. In the first, a wide-band (i.e., temporally white) interference is received; in the second, the effect of the multipath propagation is addressed. The LOSS, and temporally and spatially white noise are present in all cases.

### 4.5.1 Simulation Parameters

The input signal $\mathbf{s}(\tau_0)$ to the estimators is the concatenation of $M$ truncated and sampled Nyquist square-root raised cosine pulses. Each pulse has a bandwidth equal to $(1+\varrho)/2T_c$ and is truncated to the interval $[-3T_c, 3T_c]$. The sampling period is $T_s = T_c/2$, so there are 13 samples in each pulse and the total number of samples is $N = 13\,M$ (see Figure 3.1). The roll-off factor $\varrho$ is set equal to 0.2. The choice of this pulse is of interest because it is the one proposed for the future system GNSS2 [Sch98a]. Each pulse in $\mathbf{s}(\tau_0)$ is often called *finger*, and represents a portion of the result of filtering a DS-SS signal with a code-matched filter. It is assumed that the length of this filter is one symbol period $T$. Therefore, the vector $\mathbf{s}(\tau_0)$ is not a continuous part of the matched filter output, but only the concatenation of those portions spaced $T$ seconds apart, in which the alignment error between the code of the received DS-SS signal and the local code is within $\pm 3\,T_c$. Note that the matched filter does not include the chip-shaping waveform, but only the effect of the pseudo-random code, that is, the sequence of chips (see Section 2.5.3 for further details). All results are calculated by averaging 500 Monte Carlo runs, and the simulation conditions, except when one of them is varied, are as follows:

- The observation interval comprises $M = 3$ pulses.
- The array is uniform and linear (only for simplicity), with $m = 6$ antennas spaced half wavelength apart.
- The DOA of the LOSS is $\check{\theta}_0 = 0^{\rm o}$ relative to the array broadside. The delay of LOSS is taken as $\check{\tau}_0 = 0$.
- The SNR for the LOSS averaged over all the observation window is 15.87dB, which is equivalent to 24dB when it is averaged only over the $T_c$–length intervals containing the maximum of each Nyquist pulse. This value of SNR is obtained with an usual set of system parameters, such as a Carrier-to-Noise spectral density (CNo) of 44dB-Hz, and a chip rate and spreading factor equal to those of the GPS system: $1/T_c = 1.023\,$Mchips/s, $P = 20460\,$chips/bit.
- The interference, when it is present, arrives from DOA $\check{\theta}_i = -30^{\rm o}$. The Signal-to-Interference Ratio (SIR) for the LOSS, averaged over all the observation window is -3.13dB, which means that the interference is 19dB above the noise level.
- The specular reflection, when it is present, arrives from DOA $\check{\theta}_1 = 10^{\rm o}$, it is attenuated $-3$dB and delayed $\check{\tau}_1 = 0.25\,T_c$ or $0.4\,T_c$ with respect to the LOSS; and both signals are in phase at the first antenna.

In many of the figures below, there are some lines designated "CRB for the detailed model" (CRB-D) and the "CRB for the simplified model" (CRB-S). The first refers to the Cramér-Rao Bound (CRB) derived under the model in (4.2), while the second one is derived under the model in (4.8). Both of them assume that steering vector of the LOSS, $\mathbf{a}_0$, is known, and they coincide when no reflections are received. The CRB-D is derived in Appendix 4.A, and the derivatives of Nyquist pulses can be found in Appendix 3.D. The CRB-S is given by expressions (4.126)-(4.128). However, in order to compute the CRB-S, not only is the contribution of the noise plus interference included in the matrix $\mathbf{Q}$ like it is done for the CRB-D, but also the contribution of the reflections. This way of computing $\mathbf{Q}$ amounts to considering that the reflections are uncorrelated with the LOSS, but this does not happen with the actual received signals (the reflections are uncorrelated with the direct signal when the delay or Doppler differences are large compared with $T_c$ or the inverse of the observation interval, respectively).

It is important to remark that the results obtained with the frequency-domain polynomial-rooting algorithm described in Section 4.3.1 have not been included in the figures because there is no appreciable difference between them and those obtained with the exact ML estimator in (4.25). In the implementation of the polynomial-rooting algorithm, the polynomial $p(z)$ has been truncated and decimated, neglecting the coefficients $\{p_i\}$ that satisfy $10\log(|p_i/p_{\max}|) < -45$, where $p_{\max}$ is the coefficient with the largest modulus. Typically, the number of retained

coefficients has been approximately 25. This similarity of the results signifies that neither the approximation (4.52) nor the reduction of the polynomial order involve a sensible performance impairment. As an example, a realization of the polynomial coefficients is shown in Figure 4.2.

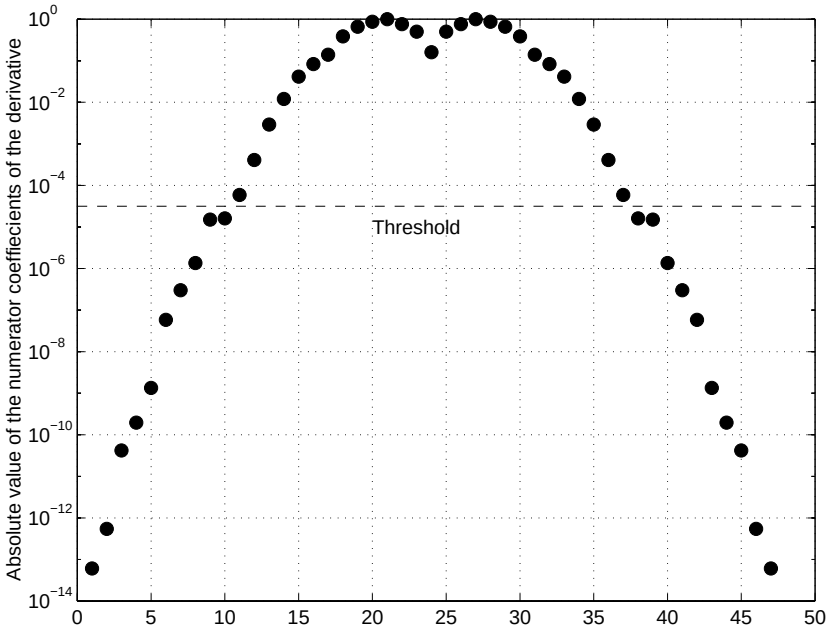


Figure 4.2: One realization of the coefficients of $p(z)$. Parameters: $\check{\theta}_0 = 0^{\mathrm{o}}$, $\check{\theta}_i = -30^{\mathrm{o}}$, $\check{\tau}_0 = 0$, $m = 6$ antennas, $M = 1$ pulse, $\mathrm{SNR}_0 = 15.87\,\mathrm{dB}$, $\mathrm{SIR}_0 = -3.13\,\mathrm{dB}$.

### 4.5.2 Interference Effects

First, we consider that one interference is received apart from the LOSS and the noise. Only the errors in the time delay and carrier phase estimates are considered, because these are the two essential parameters in a GNSS receiver. In the absence of reflections, all methods are essentially unbiased, i.e., their biases are negligible as compared to their standard deviations (STD). Therefore, the Root Mean Squared Error (RMSE) coincides with the STD for all practical purposes, and suffices to characterize the accuracy attainable with each method. The RMSEs of different estimators as a function of the number of pulses $M$ (equivalently, as a function of the number of samples $N$) are plotted in Figure 4.3. In particular, we consider the ML estimator (MLE) in (4.20) and (4.25), the estimator based on the MV beamformer (MVBE) in (4.46) and (4.47), and the ML estimator derived under the white-noise hypothesis (ML-WHE) in (4.42) and (4.43). It is observed that only the MLE attains the CRB for the time delay, and this is achieved for a small (5 or more) number of pulses. For shorter signals, there is a slight deterioration, which causes the tiny difference between the RMSE of the MLE and the CRB present in many of the next figures. The MVBE performs as well as the MLE with regard to the carrier phase

estimation and both attain the CRB (at least for the number of antennas used in Figure 4.3), but it performs much worse as far as the estimation of the time delay is concerned. It will be proven in Section 4.6 that the time delay RMSE of the MVBE really tends to the CRB but, as shown by the results, it has a very unsatisfactory finite-sample behavior, and needs too large a number of samples to reach the CRB. On the other hand, the MLE lacks particular finite-sample characteristics, since it attains the asymptotic behavior practically from the beginning. It is interesting to remark that the MLE does not inherit the poor performance of the MVBE even though the cost function of the MVBE ($\Lambda_{MV}(\tau_0)$) is the numerator of the ML cost function ($\Lambda_{ML}(\tau_0)$), see equation (4.48). The ML-WHE is severely degraded by the interference. The use of this estimator is equivalent to filtering the signals with the *delay-and-sum* beamformer, which comes down to attenuating the interference in -12.5dB. It is shown in Figure 4.4 that for a high number of antennas, the MLE and the MVBE become separated from their asymptotic behavior. While the MLE is reasonably close to the CRB up to 12 antennas approximately (for a total number of samples equal to $N = 39$), the MVB-based estimators of the time delay and the carrier phase follow the CRB only up to 2 and 8 antennas, respectively, and moreover they diverge much faster than the MLE.

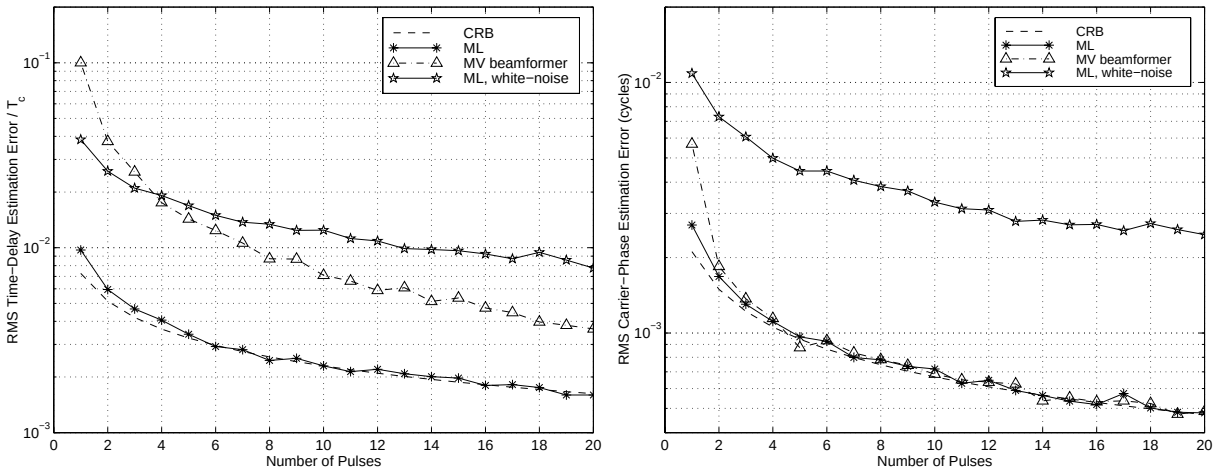


(a) Time-Delay RMSE. (b) Carrier-Phase RMSE.

Figure 4.3: Effect of varying the observation length of the signal. Parameters: $\check{\theta}_0 = 0^{\circ}$, $\check{\tau}_0 = 0$, $\check{\theta}_i = -30^{\circ}$, $m = 6$ antennas, $\mathrm{SNR}_0 = 15.87\,\mathrm{dB}$, $\mathrm{SIR}_0 = -3.13\mathrm{dB}$.

Note that results regarding the ML estimator with only temporal reference (ML-TEE), which was introduced in (4.40), have not been included in Figures 4.3a–4.4a since they virtually coincide with those of the MLE. This means that, in the absence of reflections, the temporal information (i.e., the shape of $\mathbf{s}(\tau_0)$) suffices to discriminate the LOSS from the noise and interference. This fact is corroborated by the interference nulling capabilities of the different beamformers. In Figure 4.5, the attenuation applied to the interference with respect to the LOSS is shown for the MVB in (4.45), and for the temporal-reference (TRB) and hybrid (HB) beamformers in

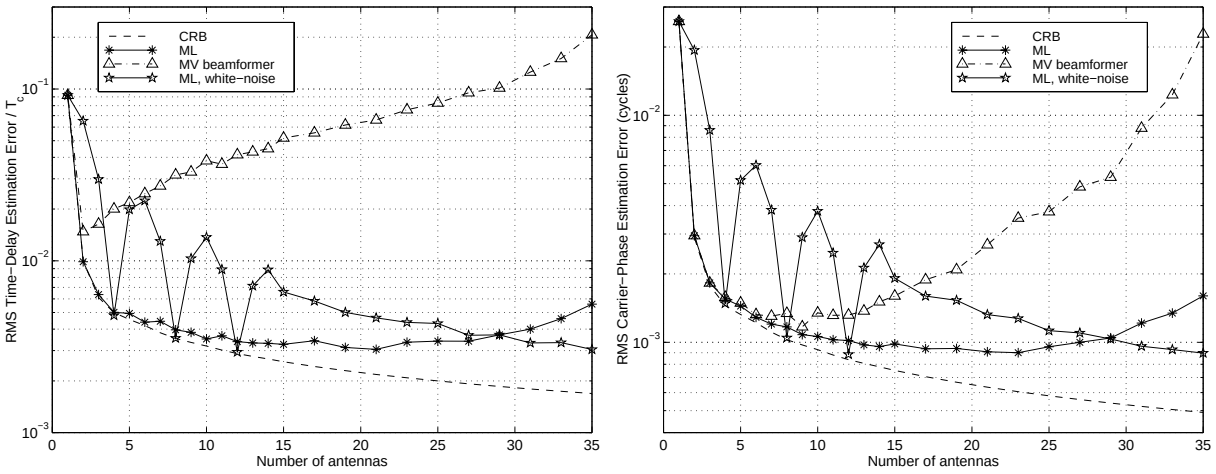


(a) Time-Delay RMSE.

(b) Carrier-Phase RMSE.

Figure 4.4: Effect of varying the number of antennas. Parameters: $\check{\theta}_0 = 0^{\text{o}}$, $\check{\tau}_0 = 0$, $\check{\theta}_i = -30^{\text{o}}$, $M = 3$ pulses, $\text{SNR}_0 = 15.87\,\text{dB}$, $\text{SIR}_0 = -3.13\text{dB}$.

(4.73) and (4.71), respectively. The hybrid beamformer is computed after 25 iterations of the algorithm presented in Table 4.2. Simulation results have shown that the algorithm typically converges in less than 10 iterations in the scenario under consideration. Two different TRBs are considered indeed. One is simply obtained at the end of the iterative process involved in computing the hybrid beamformer. The other is calculated by applying (4.73) with the time-delay estimate provided by the ML-TEE. Both TRBs and the HB result in the same attenuation, which means that the additional spatial information ($\mathbf{a}_0$) employed by the HB does not result in a performance improvement. It is known that the MVB is optimum with perfectly averaged correlation matrices (i.e., with an infinite number of samples), but Figure 4.5 shows again that it performs poorly in the finite-sample case, being the difference of the attenuations larger than 20dB with respect the TRB and HB. This result is coherent with the analysis carried out in [Wax96a] and is also related to the results in [Har00].

The effect of varying the power of the interference for two sizes of the antenna array is investigated in Figure 4.6. The MLE and MVBE are nearly insensitive to the SIR, although the former always outperforms the latter, especially as for the time delay estimation. The RMSE of the MVBE with 6 antennas is lower than that with 10. This occurs because the minimum variance beamformer is limited by its finite-sample effects, which makes necessary to increase the number of samples proportionally to the number of antennas in order to maintain the same performance [Wax96a]. The ML-WHE undergoes a rapid degradation when the SIR $<$ 10dB, so it is not a convenient method to operate in a scenario with arbitrarily strong interferers. Therefore, it is clear from all the results above that the assumption of an unknown noise correlation matrix is appropriate for deriving an ML estimator that greatly mitigates the interferences and achieves the best possible performance, given by the CRB.

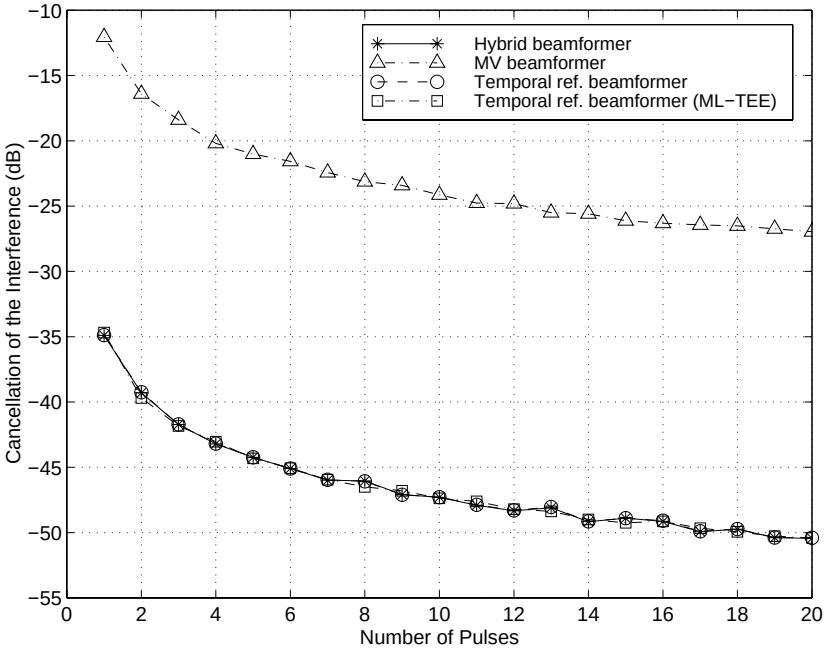


Figure 4.5: Comparison of the interference cancellation capability of different beamformers for different lengths of the signal. Parameters: $\breve{\theta}_0 = 0^{\mathrm{o}}$, $\breve{\tau}_0 = 0$, $\breve{\theta}_i = -30^{\mathrm{o}}$, $m = 6$ antennas, $\mathrm{SNR}_0 = 15.87\,\mathrm{dB}$, $\mathrm{SIR}_0 = -3.13\mathrm{dB}$, 25 iterations.

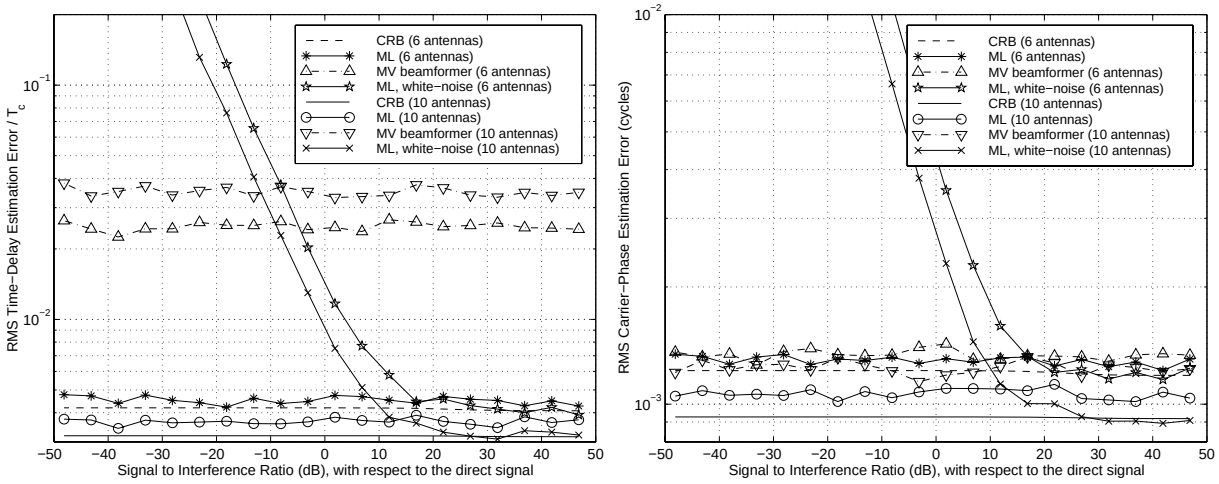


(a) Time-Delay RMSE. (b) Carrier-Phase RMSE.

Figure 4.6: Study of robustness against interference. Parameters: $\breve{\theta}_0 = 0^{\mathrm{o}}$, $\breve{\tau}_0 = 0$, $\breve{\theta}_i = -30^{\mathrm{o}}$, $m = 6$ antennas, $\mathrm{SNR}_0 = 15.87\,\mathrm{dB}$, $M = 3$ pulses.

Figure 4.7 compares the linearization-based algorithm proposed in Section 4.3.2 with the exact MLE for different values of the *linearization spacing*, $T_0$. It is shown that values of $T_0$ up to $T_c/2$ can be used without a significant performance impairment despite the round shape of

the Nyquist pulses.

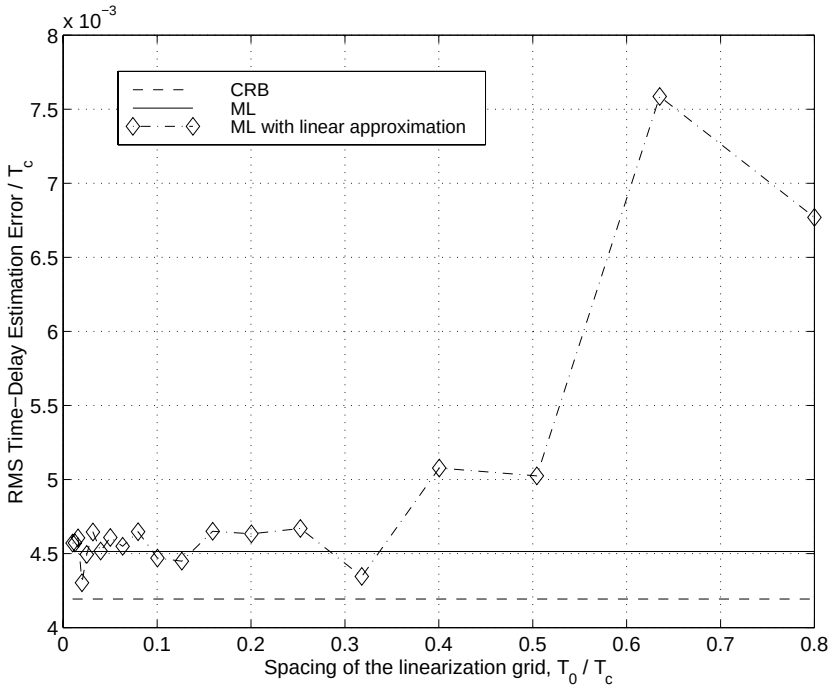


Figure 4.7: Performance of the algorithm based on the linear interpolation of the signal vector as a function of the interpolation grid spacing, and in the presence of one interference. Parameters: $\check{\theta}_0 = 0^{\text{o}}$, $\check{\tau}_0 = 0$, $\check{\theta}_i = -30^{\text{o}}$, $M = 3$ pulses, $m = 6$ antennas, $\text{SNR}_0 = 15.87\,\text{dB}$, $\text{SIR}_0 = -3.13\text{dB}$, 25 iterations.

### 4.5.3 Multipath Effects

In the second set of simulations, the specular reflection is received instead of the interference, and hence all the estimators are in general biased. A rather usual way of assessing the robustness of a certain technique against multipath propagation is to evaluate the biases produced by a single reflection as a function of its delay separation with respect to the LOSS. These results are shown in Figure 4.8. As expected, the ML-WHE provides severely biased estimates (the method derived under the white-noise hypothesis and without knowledge of $\mathbf{a}_0$ performs even worse). It is well known that single-sensor methods are seriously impaired by multipath, and therefore the poor performance of the ML-WHE is readily justified by the fact that it comes down to a single-sensor ML estimator in which the reflection has been previously attenuated $-4.2\text{dB}$ using the *delay-and-sum* beamformer. The range of reflection delays that cause a significant time delay bias can be shortened by employing the ML-TEE. However, a very important reduction of the magnitude of the bias is only achieved with the MLE proposed in this chapter. Its performance regarding the carrier phase bias is also excellent, even though the LOSS and the reflection arrive

from close directions-of-arrival. Thanks to the use of temporal and spatial information, the MLE is able to model a large part of the contribution of the reflection with the unknown noise correlation matrix. This part of the reflection is considered as an uncorrelated interference, and therefore it is attenuated. Obviously, how large is the portion of the reflection modeled as an interference depends on the degree of correlation with the LOSS, and this is a function of the delay separation between the two signals. In fact, for separations larger than $0.6\,T_c$, the MLE is capable of cancelling nearly completely the contribution of the reflection to the extent that the estimates are practically unbiased. Results illustrating the bias of the MLE as a function of the reflection delay for different array sizes and directions-of-arrival of the reflection are given in Figure 4.9.

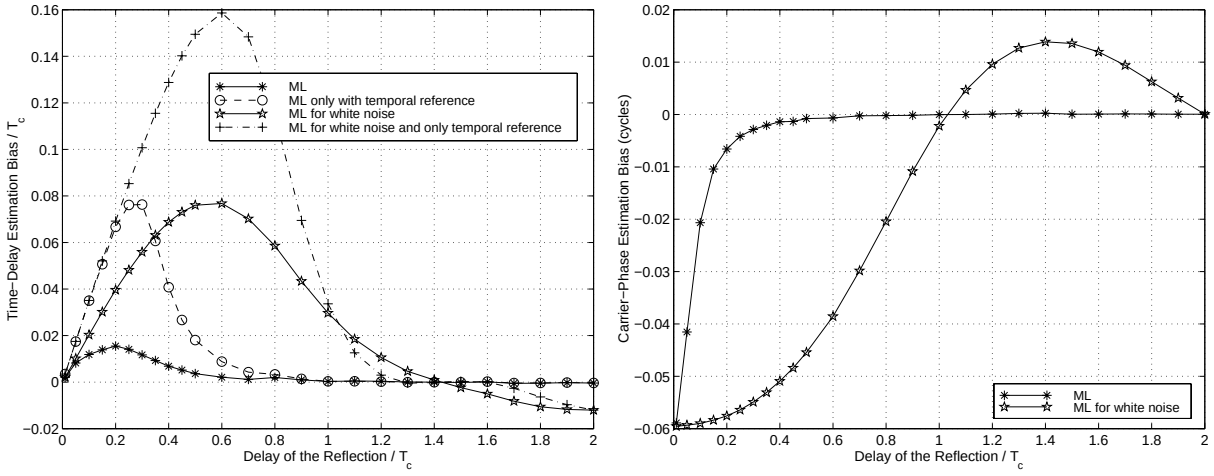


(a) Time-Delay Bias. (b) Carrier-Phase Bias.

Figure 4.8: Bias of several estimators produced by a specular reflection as a function of its delay relative to the direct signal. Parameters: $\breve{\theta}_0 = 0^{\mathrm{o}}$, $\breve{\tau}_0 = 0$, $\breve{\theta}_1 = 10^{\mathrm{o}}$, $\breve{\alpha}_0/\breve{\alpha}_1 = \sqrt{2}$, $M = 3$ pulses, $m = 6$ antennas, $\mathrm{SNR}_0 = 15.87\,\mathrm{dB}$.

Next, the RMSEs as a function of the reflection delay are represented in Figure 4.10. Although the estimators are biased, the comparison with the CRB-D is still meaningful in the sense that the CRB-D represents the best performance that can be achieved with more complex unbiased estimators based on the detailed model. The CRB-S is only meaningful for large delays ($T_c$ or greater) of the reflection, since in these cases the degree of correlation between the reflection and the LOSS is small. Note also that for delays $\breve{\tau}_1 > T_c$, it is satisfied that CRB-D $<$ CRB-S. This inequality means that it should be possible to obtain in this range of delays a slight performance improvement by exploiting the temporal structure of the reflection, given that the LOSS and the reflection arrive from very close DOAs. If the angular separation is larger, approximately $\left|\breve{\theta}_1 - \breve{\theta}_0\right| > 15^{\mathrm{o}}$, the two CRBs practically coincide which means that the temporal structure of the reflection need not be exploited when $\breve{\tau}_1 > T_c$. The RMSE of the MLE is smaller than that of the other methods, and tends to the CRB-S for large delays, which

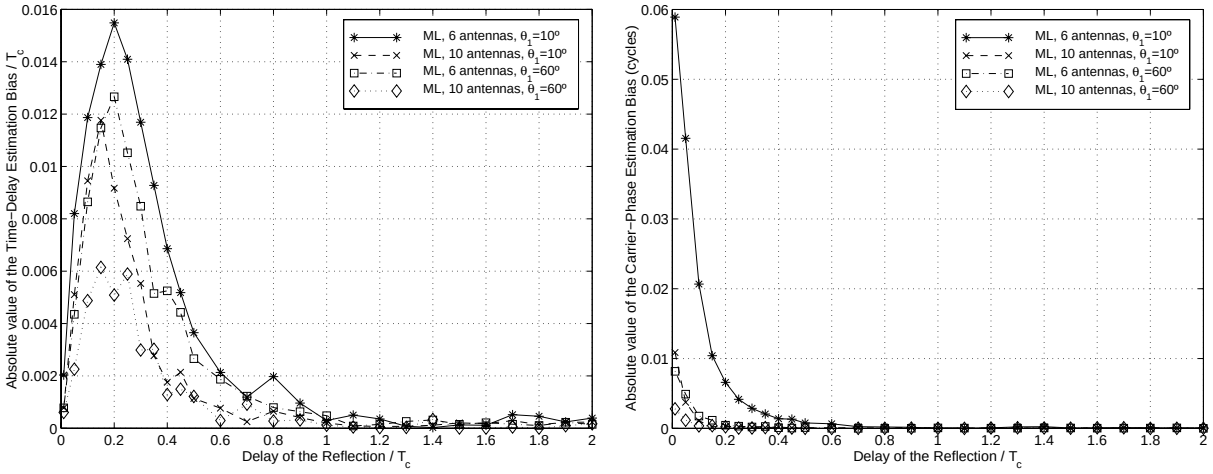


(a) Time-Delay Bias. (b) Carrier-Phase Bias.

Figure 4.9: Bias produced by a specular reflection as a function of its delay, for different number of antennas and different angular separations. Parameters: $\check{\theta}_0 = 0^{\mathrm{o}}$, $\check{\tau}_0 = 0$, $\check{\alpha}_0/\check{\alpha}_1 = \sqrt{2}$, $M = 3$ pulses, $\mathrm{SNR}_0 = 15.87\,\mathrm{dB}$.

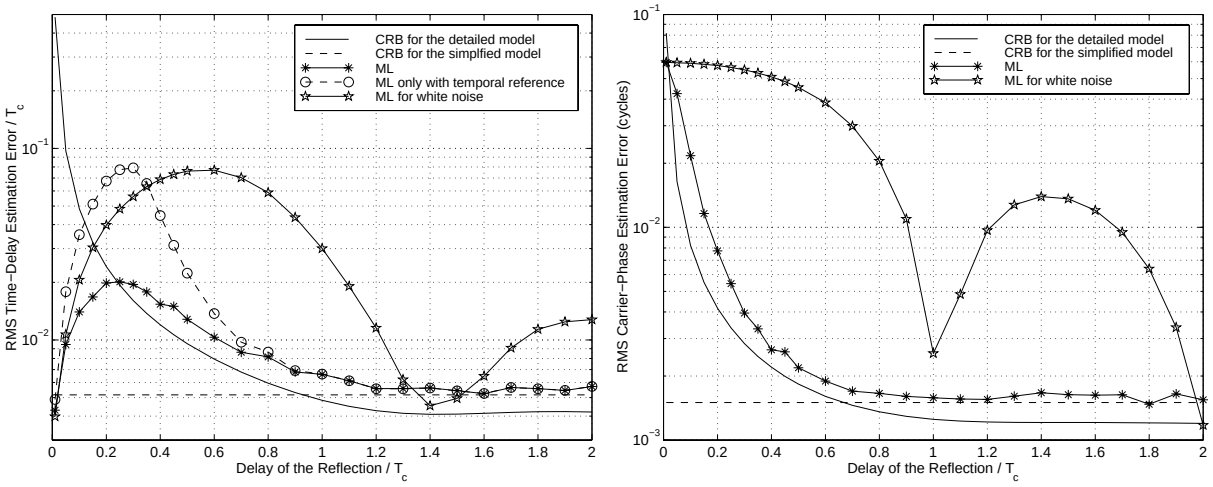


(a) Time-Delay RMSE. (b) Carrier-Phase RMSE.

Figure 4.10: RMSE as a function of the delay of the reflection with respect to the direct signal. Parameters: $\check{\theta}_0 = 0^{\mathrm{o}}$, $\check{\tau}_0 = 0$, $\check{\theta}_1 = 10^{\mathrm{o}}$, $\check{\alpha}_0/\check{\alpha}_1 = \sqrt{2}$, $M = 3$ pulses, $m = 6$ antennas, $\mathrm{SNR}_0 = 15.87\,\mathrm{dB}$.

is logical since the MLE does not profit from the temporal structure of the reflection. On the other hand, the RMSE of the MLE nearly reaches the CRB-D if $\check{\tau}_1 < T_c$ as regards the time delay, or $\check{\tau}_1 < 0.7T_c$ as regards the carrier phase, which is a rather surprising result. However, the RMSE does not go to infinity when the delay spacing tends to zero, as it happens with the CRB-D. This is an apparent advantage of the MLE proposed herein with respect to more complex unbiased estimators. By allowing a small bias, the RMSE may be smaller than the CRB-D for very closely-spaced reflections, as it is clear especially in Figure 4.10a. As a result,

although the simplified model is only an approximate one when reflections are received, as stated in Section 4.1, it makes possible the derivation of an ML estimator whose performance is very close to that of other more complex methods that estimate the parameters of the reflections. Besides, the MLE offers a reasonable trade-off between bias and RMSE for highly coherent (i.e., very small relative delay) reflections. Using the results of [Her96], future work may go deeply into this trade-off. That is to say, it may be interesting to investigate the maximum reduction of the variance that can be obtained at the expense of a certain bias gradient.

The results obtained with the minimum variance beamformer have not been included in Figures 4.8 and 4.10 because the MVBE fails in scenarios with multipath propagation. For instance, if $\check{\tau}_1 = 0.2\,T_c$, the time-delay bias is about $0.5T_c$. A similar result will be observed in Figure 4.15a. The failure of the MVBE can also be explained in view of Figure 4.11a, where the cancellation of the reflection provided by different beamformers is shown. For small delays, the MVB amplifies the reflection. The hybrid beamformer presents the higher cancellation, which increases with the separation between the LOSS and the reflection, and it is closely followed by the TRB computed in the iterative process of Table 4.2 (100 iterations are realized). It is significant that the HB attains an attenuation of $-15$dB when the reflection delay $\check{\tau}_1$ is only $0.2T_c$. On the other hand, the TRB computed with the ML-TEE estimates performs worse than the TRB in the iterative process. The explanation of this difference may be that the latter can be thought as being computed with the delay estimates provided by the MLE (as it will be proven by convergence study in Figures 4.18 and 4.19), and these estimates outperform those provided by the ML-TEE, as shown in Figures 4.8 and 4.10.

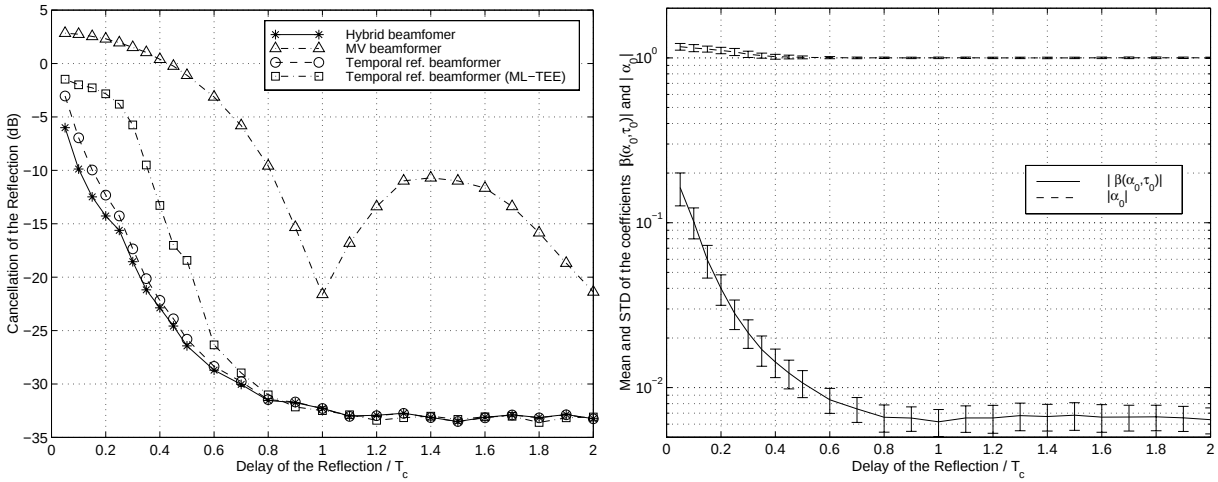


(a) Reflection cancellation with different beamformers.

(b) Meam values and standard deviations of the combining coefficients in the hybrid beamformer.

Figure 4.11: Analysis of different beamformers as a function of the relative delay of the reflection. Parameters: $\check{\theta}_0 = 0^o$, $\check{\tau}_0 = 0$, $\check{\theta}_1 = 10^o$, $\check{\alpha}_0/\check{\alpha}_1 = \sqrt{2}$, $M = 3$ pulses, $m = 6$ antennas, $\mathrm{SNR}_0 = 15.87\,\mathrm{dB}$, 100 iterations.

Recall that the hybrid beamformer is computed as a linear combination of other two beamformers, see equation (4.71). The mean of the absolute value of the coefficients in this linear combination (i.e., $|\alpha_0|$ and $|\beta(\tau_0, \alpha_0)|$) is plotted in Figure 4.11b as a function of the reflection delay. The variability of these coefficients is indicated by the vertical lines, whose length is equal to twice the standard deviation. Again, 100 iterations of the hybrid beamformer algorithm are performed; and the true value of the amplitude is $\check{\alpha}_0 = 1$. The coefficient $|\beta(\tau_0, \alpha_0)|$ is between one and two magnitude orders smaller than the estimated $|\alpha_0|$, and decreases along with the reflection delay. This means that in the hybrid beamformer, the contribution of the TRB predominates. The contribution of the MVB is especially small when the reflection is separated more than $0.7T_c$.

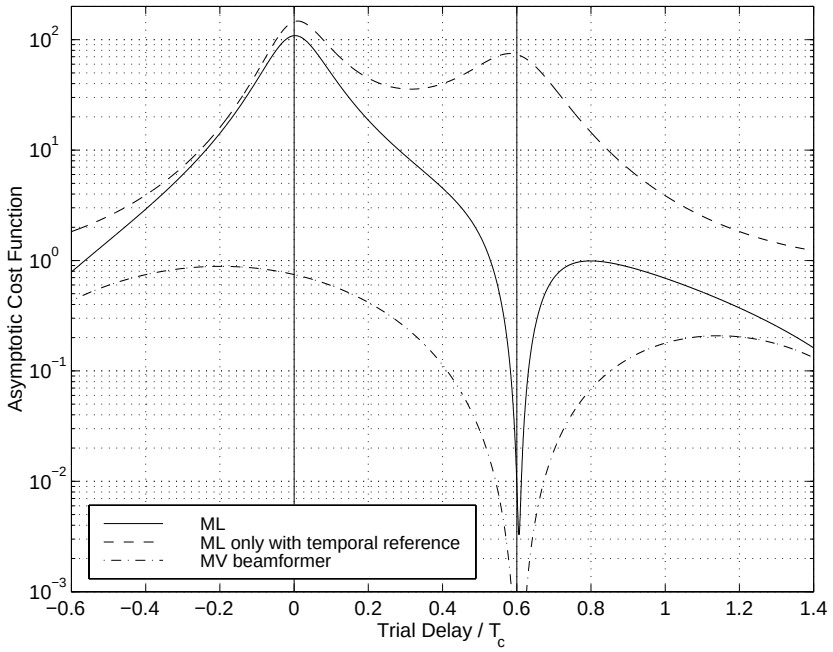


Figure 4.12: Asymptotic shape of the cost functions. Parameters: $\check{\theta}_0 = 0^{\text{o}}$, $\check{\tau}_0 = 0$, $\check{\theta}_1 = 10^{\text{o}}$, $\check{\tau}_1 = 0.6\,T_c$, $\check{\alpha}_0/\check{\alpha}_1 = \sqrt{2}$, $M = \infty$ pulses, $m = 6$ antennas, $\text{SNR}_0 = 15.87\,\text{dB}$.

To gain insight into why the MLE (or the HB) is preferred to both the ML-TEE (or the TRB) and the MVBE, the shape of the cost functions $\Lambda_{ML}(\tau_0)$, $(1 - \Lambda_{TE}(\tau_0))^{-1}$ and $\Lambda_{MV}(\tau_0)$ is compared in Figure 4.12. In this simulation, we have considered that $\check{\tau}_1 = 0.6\,T_c$ and that the number of samples is infinite (i.e., the asymptotic cost functions are plotted). The ML-TEE is capable of discriminating the LOSS and the reflection, since it presents a peak for each signal. On the other hand, the MVBE is fairly flat in the vicinity of $\check{\tau}_0$, and presents a deep null at $\check{\tau}_1$. These results, therefore, corroborate the theoretical analysis carried out in Section 4.2. The MLE inherits the best characteristics of the ML-TEE and the MVBE, which are combined according to (4.48). The MVBE selects the appropriate peak of the ML-TEE (namely, the one corresponding to the LOSS) and places a null at the peak corresponding to the reflection. Thus,

the MLE presents a single peak located near the delay of the direct signal. Note that the position of the maximum of MLE is mainly given by the position of the corresponding peak of ML-TEE. Nonetheless, the maximum of MLE is slightly closer to $\check{\tau}_0$ than that of ML-TEE. At the same time, the maximum of MVBE is far from $\check{\tau}_0$, which results in the unsatisfactory performance of the MVBE, as commented above. This large error of the MVBE, however, does not affect the MLE, since the goal of the MVBE is simply to identify the contribution of the LOSS in the cost function of the ML-TEE.

In Figure 4.13, we examine the dependence of the time delay and carrier phase biases upon the DOA of the reflection. Unlike the previous simulations, at each DOA the maximum absolute bias for all possible phase shifts between the reflection and the LOSS is plotted, and this is referred to as "worst bias". The overall trend of the bias of MLE is to decrease as the angular separation of the reflection increases, but it is also influenced by the shape of the reception pattern of the *delay-and-sum* beamformer. On the other hand, the time delay bias of ML-TEE is nearly constant, except for very small angular separations. It is also remarkable the large superiority of the MLE to the ML-WHE as regards the carrier phase bias. Note that we have considered a highly correlated reflection with a delay $\check{\tau}_1 = 0.25\,T_c$. This is the most unfavorable situation for the MLE as far as the time delay estimate is concerned, but not for the ML-WHE, which experiences the largest bias for $\check{\tau}_1$ around $0.5T_c$ (see Figure 4.8a). Consequently, it can be concluded from Figures 4.8, 4.9 and 4.13 that the MLE reduces the bias to nearly insignificant levels (although this level depends on the particular GNSS application), as long as the reflection is not spatially *and* temporally very close to the LOSS.

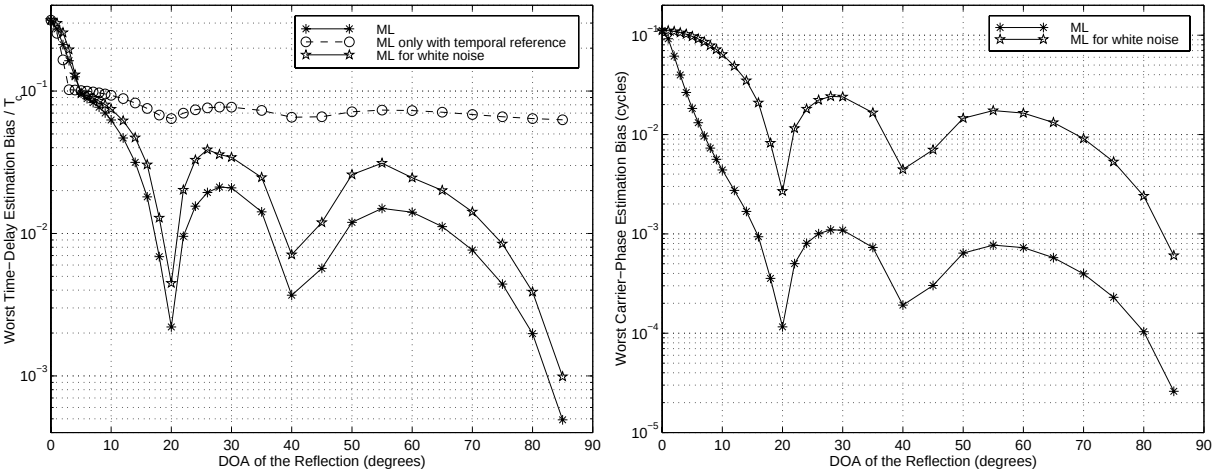


(a) "Worst" Time-Delay Bias.

(b) "Worst" Carrier-Phase Bias.

Figure 4.13: Dependence of the bias on the angular separation between the reflection and the direct signal. Parameters: $\check{\theta}_0 = 0^{\mathrm{o}}$, $\check{\tau}_0 = 0$, $\check{\tau}_1 = 0.25\,T_c$, $|\check{\alpha}_0|/|\check{\alpha}_1| = \sqrt{2}$, $M = \infty$ pulses, $m = 6$ antennas, $\mathrm{SNR}_0 = 15.87\,\mathrm{dB}$.

Figure 4.14 compares the biases for different sizes of the antenna array. It also proves that

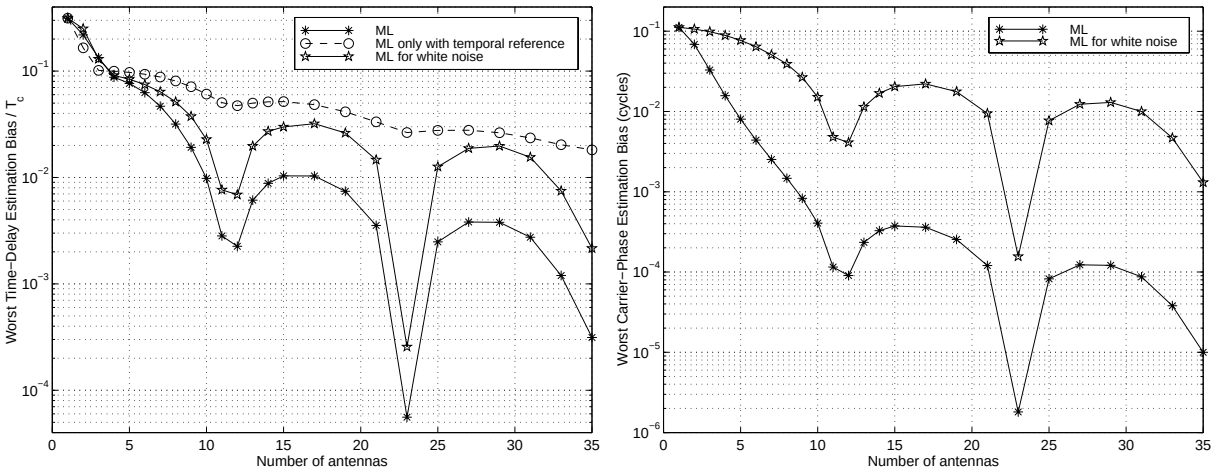


(a) "Worst" Time-Delay Bias.

(b) "Worst" Carrier-Phase Bias.

Figure 4.14: Dependence of the bias produced by one specular reflection upon the size of the antenna array. Parameters: $\check{\theta}_0 = 0^{\text{o}}$, $\check{\tau}_0 = 0$, $\check{\theta}_1 = 10^{\text{o}}$, $\check{\tau}_1 = 0.25\,T_c$, $M = \infty$ pulses, $|\check{\alpha}_0|/|\check{\alpha}_1| = \sqrt{2}$, $\text{SNR}_0 = 15.87\,\text{dB}$.

a substantial reduction of the biases can be achieved by using a moderate number of antennas. For instance, the time-delay and carrier-phase mean errors of the MLE can be reduced in more than one and two orders of magnitude, respectively, with respect to the single-sensor case by employing a 10-sensor array. The MLE clearly outperforms the other estimators, and the bias of the ML-TEE decreases slowly with the number of antennas.

To complete the study of the estimators, their performance as a function of the SNR (averaged over all the observation window) is illustrated in Figures 4.15–4.16. As the SNR becomes very small, the performance of all the algorithms tends to be the same because the reflection turns out to be irrelevant with respect to the contribution of the noise, and hence the use of the ML-WHE (*delay-and-sum* beamformer) becomes the best solution. This also explains that the RMSE of all the estimators approaches the CRB-S for very low SNR. The bias of the ML-WHE is constant, which results in an irreducible floor-level in the RMSE for high signal-to-noise ratios. It is corroborated that the performance of the MVBE is absolutely unsatisfactory in virtually all the range of SNR, since the time delay bias is about $-0.45\,T_c$ for moderate or high SNR. Although the carrier phase bias of the MVBE is not so high, its carrier phase RMSE also presents an irreducible floor-level. An important characteristic appreciable in these figures is that the MLE and the ML-TEE are asymptotically in SNR unbiased. Note that the RMSE of the MLE (also that of the ML-TEE) tends to the CRB derived for the detailed signal model as the SNR increases. As stated above, this is a remarkable and quite surprising result, because the MLE is derived starting from the simplified model of the signals, and hence does not estimate the parameters of the reflections. Nonetheless, the RMSE of the MLE is smaller than that of the ML-TEE in all the range of SNR, thanks mainly to its reduced bias. The bias of the MLE

starts decreasing at SNR=0dB, which contrasts with the 20dB required by the ML-TEE. Unlike in the absence of reflections, now the spatial reference $\mathbf{a}_0$ to the LOSS is essential to improve the performance (especially to reduce the bias) of the estimates; see e.g., Figures 4.8a, 4.11a, 4.13a, 4.14a, and 4.15a.

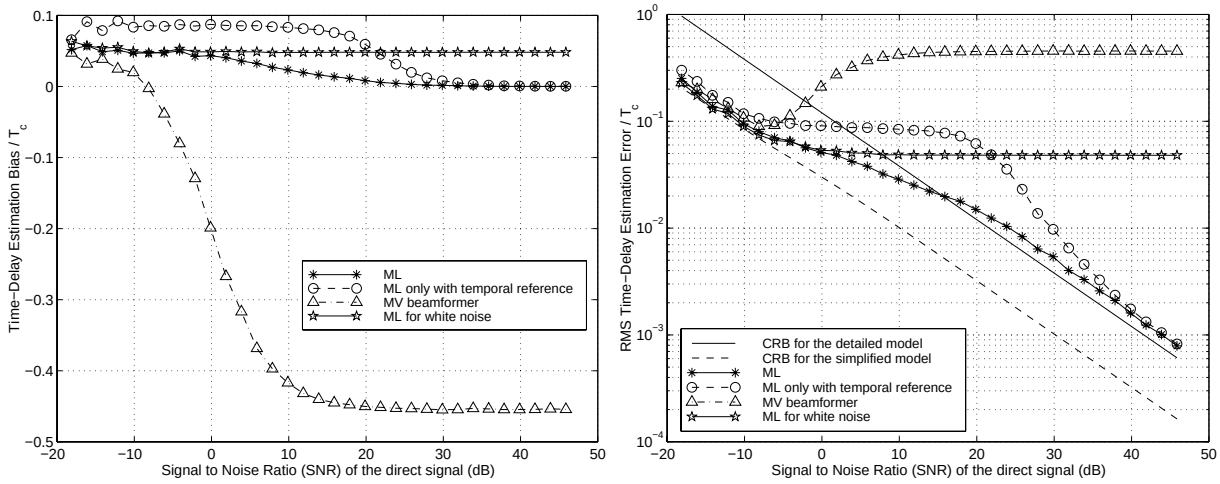


(a) Time-Delay Bias.

(b) Time-Delay RMSE.

Figure 4.15: Performance of the proposed ML time-delay estimator as a function of the SNR (averaged over all the observation window) in the presence of one specular reflection. Parameters: $\check{\theta}_0 = 0^{\text{o}}$, $\check{\tau}_0 = 0$, $\check{\theta}_1 = 10^{\text{o}}$, $\check{\tau}_1 = 0.25\,T_c$, $\check{\alpha}_0/\check{\alpha}_1 = \sqrt{2}$, $M = 3$ pulses, $m = 6$ antennas.

The performance of the linearization-based algorithm (Table 4.1) in the presence of one reflection is examined in Figure 4.17. While the standard deviation of the estimates is nearly insensitive to the value of $T_0$, the bias increases with this parameter. A maximum value of $T_0$ about $T_c/5$ can be employed without an excessive penalty in the RMSE. This value is smaller than the maximum value ($T_c/2$) that was possible in a reflection-free scenario (Figure 4.7), and seems reasonable given the shape of the Nyquist pulses. Therefore, assuming an uncertainty range of the delay equal to $2T_c$ and that $T_0 = T_c/5$, the estimation process can be reduced to the simple rooting of 10 second-order polynomials.

The convergence of the estimates obtained with the iterative hybrid-beamforming algorithm in Section 4.4 is investigated in Figures 4.18–4.19. Moreover, Figure 4.20 illustrates the evolution of the reflection cancellation achieved by the HB and its two constituting components, together with the evolution of the combining coefficients corresponding to the MVB and TRB (i.e., $\beta(\tau_0, \alpha_0)$ and $\alpha_0$). The simulations are carried out for two different delays of the reflection, $0.4\,T_c$ and $T_c$. Figures 4.18–4.19 show that the mean and standard deviation of the estimates obtained with the iterative algorithm tend to those of the ML estimates. As a matter of fact, not only is this a property valid for the mean and standard deviation, but also at every realization the estimates provided by the iterative algorithm tend to the ML estimates, although this is not shown in the figures below. Therefore, the iterative hybrid beamformer is really a valid

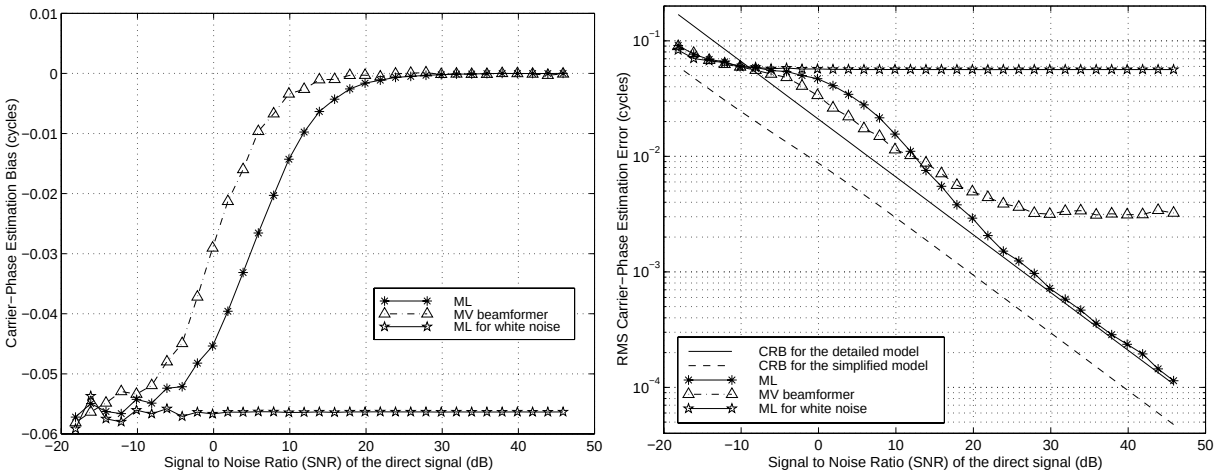


(a) Carrier-Phase Bias. (b) Carrier-Phase RMSE.

Figure 4.16: Performance of the proposed ML carrier-phase estimator as a function of the SNR (averaged over all the observation window) in the presence of one specular reflection. Parameters: $\check{\theta}_0 = 0^{\text{o}}$, $\check{\tau}_0 = 0$, $\check{\theta}_1 = 10^{\text{o}}$, $\check{\tau}_1 = 0.25\,T_c$, $\check{\alpha}_0/\check{\alpha}_1 = \sqrt{2}$, $M = 3$ pulses, $m = 6$ antennas.

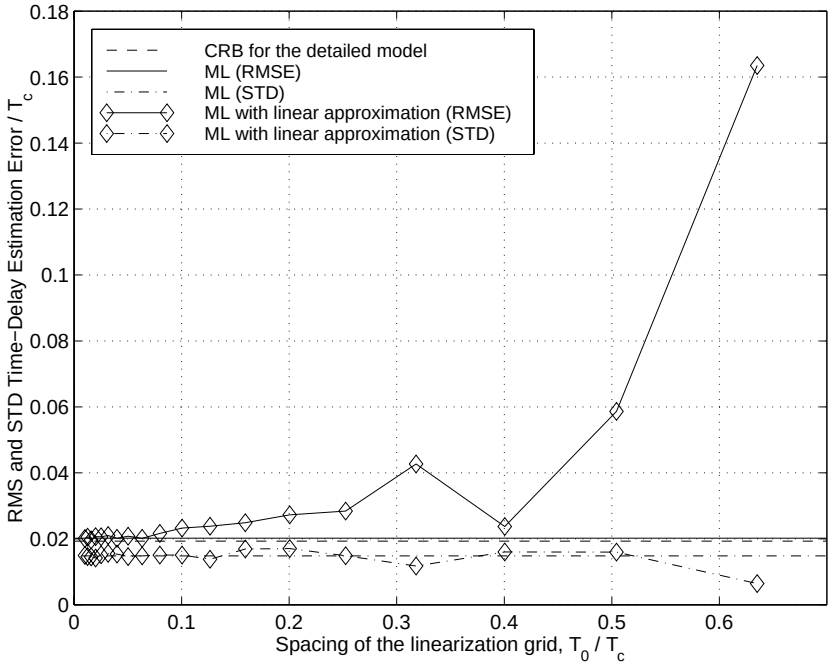


Figure 4.17: Performance of the algorithm based on the linear interpolation of the signal vector as a function of the interpolation grid spacing, and in the presence of one specular reflection. Parameters: $\check{\theta}_0 = 0^{\text{o}}$, $\check{\tau}_0 = 0$, $\check{\theta}_1 = 10^{\text{o}}$, $\check{\tau}_1 = 0.25\,T_c$, $\check{\alpha}_0/\check{\alpha}_1 = \sqrt{2}$, $M = 3$ pulses, $m = 6$ antennas, $\text{SNR}_0 = 15.87\,\text{dB}$.

implementation of the exact MLE. It is observed that the carrier phase converges faster than the time delay (note the different scaling of the horizontal axis in Figures 4.18–4.19), and also that

the smaller the delay separation of the reflection, the slower the convergence. The convergence speed is important during the acquisition stage, but not during the tracking operation of the receiver (unless the scenario is rapidly variant). Despite the similar reflection cancellation offered by the HB and the TRB (Figure 4.20a), the knowledge of $\mathbf{a}_0$ is essential since it makes the iterative computation of the hybrid beamformer converge to the extraction of the parameters of the LOSS. If the hybrid beamformer were replaced by the temporal-reference beamformer, the iterative algorithm might converge to the parameters of one of the reflections. This fact is related to the number of local maxima in the cost functions of the MLE and ML-TEE, as shown in Figure 4.12.

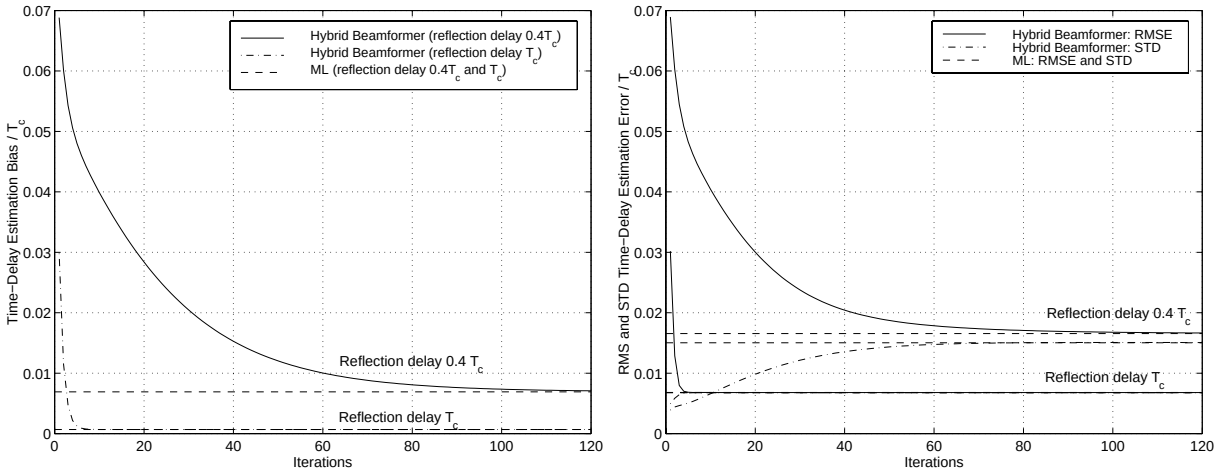


(a) Time-Delay Bias.

(b) Time-Delay RMSE and STD.

Figure 4.18: Convergence of the time delay estimates along the iterative algorithm in the presence of one specular reflection. Parameters: $\breve{\theta}_0 = 0^{\mathrm{o}}$, $\breve{\tau}_0 = 0$, $\breve{\theta}_1 = 10^{\mathrm{o}}$, $\breve{\tau}_1 = 0.4\,T_c$, $T_c$, $\breve{\alpha}_0/\breve{\alpha}_1 = \sqrt{2}$, $M = 3$ pulses, $m = 6$ antennas, $\mathrm{SNR}_0 = 15.87\,\mathrm{dB}$

The goal of the last simulation, whose results are plotted in Figure 4.21, is to show that the MLE method proposed in this chapter also performs satisfactorily in the presence of a large number of reflections (or diffuse reflections). In particular, ten reflections are received, and their parameters are described in Table 4.3 (the LOSS and all the reflections are in phase at the first antenna). Although the delays of the reflections cover all the range between $0.1\,T_c$ and $T_c$ and the array (6 antennas) does not have enough degrees of freedom to cancel all the reflections, the MLE is able to mitigate to a large extend their contributions. The time delay bias of the MLE is lower than $0.02\,T_c$, and also lower than the bias of the ML-TEE and the ML-WHE. The estimate provided by the HB starts from the value obtained with the *delay-and-sum* beamformer and reaches the ML estimate. Also in such a complex scenario, the iterative algorithm based on the HB converges to the ML solution.

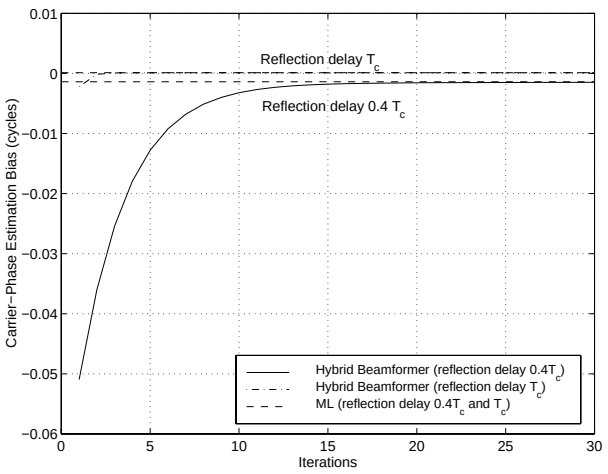


(a) Carrier-Phase Bias.

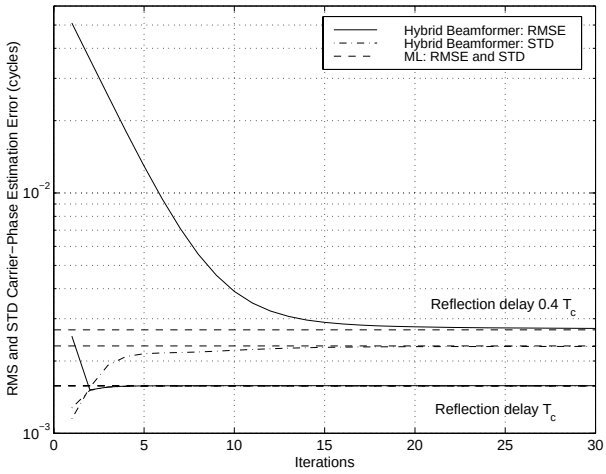


(b) Carrier-Phase RMSE and STD.

Figure 4.19: Convergence of the carrier phase estimates along the iterative algorithm in the presence of one specular reflection. Parameters: Identical to Figure 4.18.

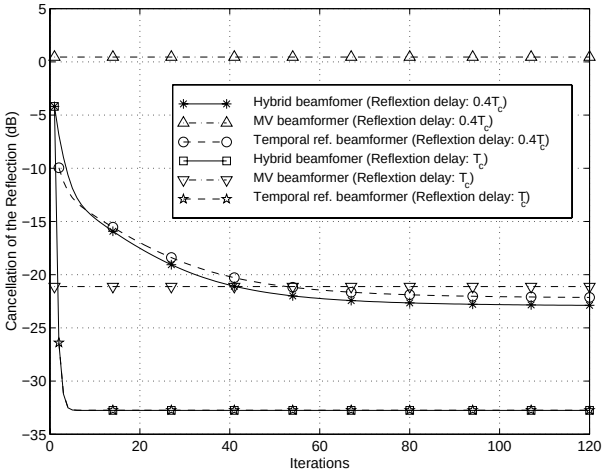


(a) Reflection cancellation of the hybrid beamformer and its two components.

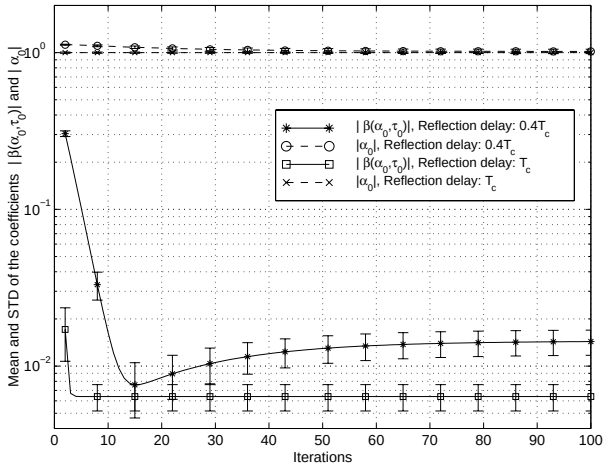


(b) Mean values and standard deviations of the combining coefficients in the hybrid beamformer.

Figure 4.20: Convergence of the hybrid beamformer along the iterative algorithm in the presence of one specular reflection. Parameters: Identical to Figure 4.18.

## 4.6 Asymptotic Variance of the Maximum–Likelihood Time Delay Estimator

The effect of calibration or pointing errors is a subject of primary interest in any method that relies on the a priori knowledge of a steering vector, such as the ML estimator presented in Section 4.2. We will derive here the asymptotic variance of the time delay estimates obtained with that method, that is to say, obtained using the cost function $\Lambda_{ML}(\tau_0)$ in (4.25). To this

| Delay/$T_c$ | 0.1 | 0.2 | 0.3 | 0.4 | 0.5 | 0.6 | 0.7 | 0.8 | 0.9 | 1 |
|---|---|---|---|---|---|---|---|---|---|---|
| DOA (degrees) | 60 | -30 | -60 | 30 | -10 | 10 | -40 | 40 | 75 | -25 |
| Attenuation (dB) | -4.5 | -5 | -5.5 | -6 | -6.5 | -7 | -7.5 | -8 | -8.5 | -9 |

Table 4.3: Parameters of the diffuse reflections.

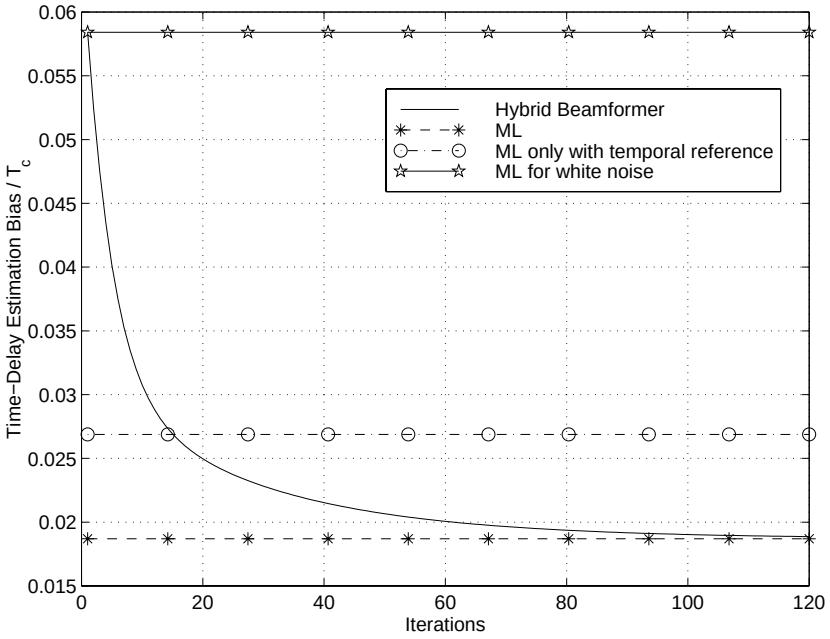


Figure 4.21: Performance of the ML estimator and convergence of the time delay estimates obtained from the iterative hybrid beamformer in an scenario with multiple reflections. Parameters: $\check{\theta}_0 = 0^{\text{o}}$, $\check{\tau}_0 = 0$, $M = 3$ pulses, $m = 6$ antennas, $\text{SNR}_0 = 15.87\,\text{dB}$, and the parameters of the reflections are in Table 4.3.

end, we assume that the received signal satisfies the simplified model set up in Section 4.1, but with a small difference. In other words, no reflection is present and the actual received signal is

$$\mathbf{y}[n] = \boldsymbol{\alpha}_0 \, s\left(nT_s - \tau_0\right) + \mathbf{e}[n]. \tag{4.76}$$

Now, $\boldsymbol{\alpha}_0$ is the actual spatial signature of the direct signal, whereas $\mathbf{a}_0$ will denote the nominal or a priori steering vector assumed by the receiver. The vector $\mathbf{a}_0$ need not be proportional to $\boldsymbol{\alpha}_0$, that is to say, only in the absence of pointing or calibration errors, $\mathbf{a}_0$ and $\boldsymbol{\alpha}_0$ are parallel.

In order to derive the asymptotic variance associated with the cost function $\Lambda_{ML}\left(\tau_0\right)$, we firstly obtain the asymptotic variances corresponding to $\Lambda_{TE}\left(\tau_0\right)$ and $\Lambda_{MV}\left(\tau_0\right)$, which were defined in equation (4.40) and (4.47), respectively. For any of these three functions (denoted by

$\Lambda_t(\tau_0)$ in general), the asymptotic variance of the time delay estimates is given by [Söd89]

$$N\,\sigma_t^2 = \frac{g_t}{h_t^2}\,, \tag{4.77}$$

where

$$g_t = \lim_{\mathbf{N}\to\infty} N\,\mathrm{E}\left\{\left(\Lambda_t'(\check{\tau}_0)\right)^2\right\} \tag{4.78}$$

$$h_t = \lim_{\mathbf{N}\to\infty} \Lambda_t''(\check{\tau}_0)\,, \tag{4.79}$$

where $\Lambda_t'$ and $\Lambda_t''$ denote the first and the second derivative of the cost function, respectively.

Since the function $\Lambda_{TE}(\tau_0)$ can also be expressed as

$$\Lambda_{TE}(\tau_0) = \frac{1}{N}\,\mathrm{Tr}\left\{\hat{\mathbf{R}}_{yy}^{-1/2}\,\mathbf{Y}\,\mathbf{P}_{\mathbf{s}^c(\tau_0)}\,\mathbf{Y}^*\,\hat{\mathbf{R}}_{yy}^{-1/2}\right\}\,, \tag{4.80}$$

using the results of Section 3.5, it is immediate that[4]

$$g_{TE} = \frac{2}{N}\left(\mathbf{d}^*(\check{\tau}_0)\,\mathbf{P}^{\perp}_{\mathbf{s}(\check{\tau}_0)}\,\mathbf{d}(\check{\tau}_0)\right)\left(\boldsymbol{\alpha}_0^*\,\mathbf{R}_{yy}^{-1}\,\mathbf{Q}\,\mathbf{R}_{yy}^{-1}\,\boldsymbol{\alpha}_0\right) \tag{4.81}$$

$$h_{TE} = -\frac{2}{N}\left(\mathbf{d}^*(\check{\tau}_0)\,\mathbf{P}^{\perp}_{\mathbf{s}(\check{\tau}_0)}\,\mathbf{d}(\check{\tau}_0)\right)\left(\boldsymbol{\alpha}_0^*\,\mathbf{R}_{yy}^{-1}\,\boldsymbol{\alpha}_0\right)\,, \tag{4.82}$$

and hence

$$\sigma_{TE}^2 = \frac{\boldsymbol{\alpha}_0^*\,\mathbf{R}_{yy}^{-1}\,\mathbf{Q}\,\mathbf{R}_{yy}^{-1}\,\boldsymbol{\alpha}_0}{2\left(\mathbf{d}^*(\check{\tau}_0)\,\mathbf{P}^{\perp}_{\mathbf{s}(\check{\tau}_0)}\,\mathbf{d}(\check{\tau}_0)\right)\left(\boldsymbol{\alpha}_0^*\,\mathbf{R}_{yy}^{-1}\,\boldsymbol{\alpha}_0\right)^2} \tag{4.83}$$

$$= \frac{1}{2\left(\mathbf{d}^*(\check{\tau}_0)\,\mathbf{P}^{\perp}_{\mathbf{s}(\check{\tau}_0)}\,\mathbf{d}(\check{\tau}_0)\right)\left(\boldsymbol{\alpha}_0^*\,\mathbf{Q}^{-1}\,\boldsymbol{\alpha}_0\right)}\,. \tag{4.84}$$

Equation (4.84) is derived from (4.83) by taking into account that for the simplified model $\mathbf{R}_{yy} = P_s\,\boldsymbol{\alpha}_0\,\boldsymbol{\alpha}_0^* + \mathbf{Q}$ and by applying the matrix inversion lemma to this matrix. Note that $\sigma_{TE}^2$ coincides with the CRB presented in (4.126).

The asymptotic variance of the gradient and Hessian of $\Lambda_{MV}(\tau_0)$ are derived in Appendix 4.B, and they are

$$g_{MV} = \frac{2}{N}\left(\mathbf{d}^*(\check{\tau}_0)\,\mathbf{P}^{\perp}_{\mathbf{s}(\check{\tau}_0)}\,\mathbf{d}(\check{\tau}_0)\right)\left|\mathbf{a}_0^*\,\mathbf{R}_{yy}^{-1}\,\boldsymbol{\alpha}_0\right|^2\left(\mathbf{a}_0^*\,\mathbf{R}_{yy}^{-1}\,\mathbf{Q}\,\mathbf{R}_{yy}^{-1}\,\mathbf{a}_0\right) \tag{4.85}$$

$$h_{MV} = -\frac{2}{N}\left(\mathbf{d}^*(\check{\tau}_0)\,\mathbf{P}^{\perp}_{\mathbf{s}(\check{\tau}_0)}\,\mathbf{d}(\check{\tau}_0)\right)\left|\mathbf{a}_0^*\,\mathbf{R}_{yy}^{-1}\,\boldsymbol{\alpha}_0\right|^2\,. \tag{4.86}$$

Therefore, the variance of the estimates obtained with the MVB is

$$\sigma_{MV}^2 = \frac{\mathbf{a}_0^*\,\mathbf{R}_{yy}^{-1}\,\mathbf{Q}\,\mathbf{R}_{yy}^{-1}\,\mathbf{a}_0}{2\left(\mathbf{d}^*(\check{\tau}_0)\,\mathbf{P}^{\perp}_{\mathbf{s}(\check{\tau}_0)}\,\mathbf{d}(\check{\tau}_0)\right)\left|\mathbf{a}_0^*\,\mathbf{R}_{yy}^{-1}\,\boldsymbol{\alpha}_0\right|^2}\,. \tag{4.87}$$

[4] Recall that $\mathbf{d}(\tau_0) = \frac{d\,\mathbf{s}(\tau_0)}{d\,\tau_0}$.

If $\mathbf{a}_0$ is parallel to $\boldsymbol{\alpha}_0$, then $\sigma^2_{MV}$ coincides with the CRB. However, $\sigma^2_{MV}$ is extremely sensitive to errors in $\mathbf{a}_0$. When this vector has a component orthogonal to $\boldsymbol{\alpha}_0$, this component lies in the noise subspace of $\mathbf{R}_{yy}$, and hence the numerator of (4.87) rapidly increases. Defining $\chi \triangleq P_s\, \boldsymbol{\alpha}_0^* \, \mathbf{Q}^{-1}\, \boldsymbol{\alpha}_0$, we arrive at the following alternative expression

$$\sigma^2_{MV} = \frac{1}{2\, \left( \mathbf{d}^* \left( \check{\tau}_0 \right) \, \mathbf{P}^{\perp}_{\mathbf{s}(\check{\tau}_0)} \, \mathbf{d} \left( \check{\tau}_0 \right) \right)} \left[ \frac{\mathbf{a}_0^* \, \mathbf{Q}^{-1} \, \mathbf{a}_0}{\left| \mathbf{a}_0^* \, \mathbf{Q}^{-1} \, \boldsymbol{\alpha}_0 \right|^2} \left( 1 + \chi \right)^2 - P_s \left( 2 + \chi \right) \right] , \tag{4.88}$$

which makes clear the high sensitivity to errors in $\mathbf{a}_0$ since $\chi$ is a measure of the SNR and usually it is $\chi \gg 1$. This result is coherent with the results in [Wax96b].

The computation of the asymptotic variance of the estimates obtained with $\Lambda_{ML}\left(\tau_0\right)$ using (4.77) together with the expression of this cost function in (4.25) seems to be too cumbersome. Instead, we will take advantage of the expression (4.48), which relates $\Lambda_{ML}\left(\tau_0\right)$ to $\Lambda_{TE}\left(\tau_0\right)$ and $\Lambda_{MV}\left(\tau_0\right)$. Using this relationship, we get

$$\Lambda'_{ML}\left(\check{\tau}_0\right) = \frac{\Lambda'_{MV}\left(\check{\tau}_0\right)\, \left(1 - \Lambda_{TE}\left(\check{\tau}_0\right)\right) + \Lambda_{MV}\left(\check{\tau}_0\right)\, \Lambda'_{TE}\left(\check{\tau}_0\right)}{\left(1 - \Lambda_{TE}\left(\check{\tau}_0\right)\right)^2} \tag{4.89}$$

$$\begin{aligned} \Lambda''_{ML}\left(\check{\tau}_0\right) = \left(1 - \Lambda_{TE}\left(\check{\tau}_0\right)\right)^{-4} \Big[ & \left(1 - \Lambda_{TE}\left(\check{\tau}_0\right)\right)^2 \left( \Lambda''_{MV}\left(\check{\tau}_0\right)\, \left(1 - \Lambda_{TE}\left(\check{\tau}_0\right)\right) + \Lambda_{MV}\left(\check{\tau}_0\right)\, \Lambda''_{TE}\left(\check{\tau}_0\right) \right) \\ & + 2\, \left( \Lambda'_{MV}\left(\check{\tau}_0\right)\, \left(1 - \Lambda_{TE}\left(\check{\tau}_0\right)\right) + \Lambda_{MV}\left(\check{\tau}_0\right)\, \Lambda'_{TE}\left(\check{\tau}_0\right) \right) \left(1 - \Lambda_{TE}\left(\check{\tau}_0\right)\right)\, \Lambda'_{TE}\left(\check{\tau}_0\right) \Big] . \end{aligned} \tag{4.90}$$

Since $\Lambda'_{TE}\left(\check{\tau}_0\right)$ and $\Lambda'_{MV}\left(\check{\tau}_0\right)$ are terms of order $O_p\left(N^{-1/2}\right)$, the asymptotic Hessian of the ML function is

$$h_{ML} = \frac{h_{MV}\, \left(1 - \bar{\Lambda}_{TE}\left(\check{\tau}_0\right)\right) + \bar{\Lambda}_{MV}\left(\check{\tau}_0\right)\, h_{TE}}{\left(1 - \bar{\Lambda}_{TE}\left(\check{\tau}_0\right)\right)^2} , \tag{4.91}$$

where

$$\bar{\Lambda}_{TE}\left(\check{\tau}_0\right) \triangleq \lim_{N \to \infty} \Lambda_{TE}\left(\check{\tau}_0\right) = P_s\, \boldsymbol{\alpha}_0^* \, \mathbf{R}_{yy}^{-1} \, \boldsymbol{\alpha}_0 \tag{4.92}$$

$$\bar{\Lambda}_{MV}\left(\check{\tau}_0\right) \triangleq \lim_{N \to \infty} \Lambda_{MV}\left(\check{\tau}_0\right) = P_s\, \left| \mathbf{a}_0^* \, \mathbf{R}_{yy}^{-1} \, \boldsymbol{\alpha}_0 \right|^2 . \tag{4.93}$$

Similarly, the asymptotic variance of the gradient is

$$g_{ML} = \frac{\left(1 - \bar{\Lambda}_{TE}\left(\check{\tau}_0\right)\right)^2\, g_{MV} + g_{TE}\, \bar{\Lambda}^2_{MV}\left(\check{\tau}_0\right) + 2\, \left(1 - \bar{\Lambda}_{TE}\left(\check{\tau}_0\right)\right)\, \bar{\Lambda}_{MV}\left(\check{\tau}_0\right)\, g_{TE,MV}}{\left(1 - \bar{\Lambda}_{TE}\left(\check{\tau}_0\right)\right)^4} , \tag{4.94}$$

where the term

$$g_{TE,MV} = \lim_{N \to \infty} N\, \mathrm{E}\left\{ \Lambda'_{TE}\left(\check{\tau}_0\right)\, \Lambda'_{MV}\left(\check{\tau}_0\right) \right\} \tag{4.95}$$

is computed in Appendix 4.B. After lengthy expansions of $h_{ML}$ and $g_{ML}$ using (4.81), (4.82), (4.85), (4.86), (4.92), (4.93) and (4.95), the following expression for the asymptotic variance of the ML estimates results:

$$\sigma^2_{ML} = \frac{g_{ML}}{N\, h^2_{ML}} = \frac{\mathbf{a}_0^* \, \mathbf{Q}^{-1} \, \mathbf{a}_0}{2\, \left( \mathbf{d}^* \left( \check{\tau}_0 \right) \, \mathbf{P}^{\perp}_{\mathbf{s}(\check{\tau}_0)} \, \mathbf{d} \left( \check{\tau}_0 \right) \right)\, \left| \mathbf{a}_0^* \, \mathbf{Q}^{-1} \, \boldsymbol{\alpha}_0 \right|^2} . \tag{4.96}$$

The variance $\sigma^2_{ML}$ coincides with the CRB when $\mathbf{a}_0$ is parallel to $\boldsymbol{\alpha}_0$. The interesting result herein is that $\sigma^2_{ML}$, unlike $\sigma^2_{MV}$, is not very sensitive to errors in $\mathbf{a}_0$, even though $\Lambda_{MV}(\tau_0)$ is the numerator of $\Lambda_{ML}(\tau_0)$. The sensitivity of $\sigma^2_{ML}$ is independent of the SNR and is simply given by the array beam-pattern in the norm of $\mathbf{Q}^{-1}$. The ML estimator presented in [Swi98b] for the estimation of the Doppler frequency and DOA of the direct signal was shown to be, however, very sensitive to calibration errors. This behavior is seemingly in contradiction with the analysis in this section and with the numerical results presented in Section 4.8. The study of such disparity constitutes an open issue which is beyond the scope of this thesis. Nevertheless, we can point out some reasons that might justify those different behaviors. The estimator in [Swi98b] that undergoes a severe deterioration due to calibration errors is the one that performs a 2-D search over the DOA and the Doppler of the desired signal. If the 2-D search is, however, replaced by two 1-D searches (first the Doppler is estimated, and next the DOA), the effect of calibration errors is quite small. In our case, the ML estimator is computed for a fixed steering vector $\mathbf{a}_0$, and solely a 1-D search over the time delay is performed. This approach is somewhat similar to the approach in [Swi98b] based on the two 1-D searches, and both approaches are rather insensitive to errors in $\mathbf{a}_0$. On the other hand, the performance of the estimator in [Swi98b] that requires a 2-D search is not necessarily comparable to the performance 1-D ML estimator used in this chapter. This explanation hints that the results presented herein and in the aforementioned paper need not be contradictory. In the second place, note that the results in [Swi98b] and Section 4.8 consider different types of error. While in [Swi98b] calibration errors are generated by adding to the nominal response of the array a Gaussian vector with *iid* components; in Section 4.8, errors in the nominal DOA of the direct signal are considered.

## 4.7 Reducing the Sensitivity to Errors in the LOSS Steering Vector

Although the ML estimator presents an inherent low sensitivity to errors in the nominal steering vector of the direct signal, it might be worth investigating methods in order to further improve its robustness. Moreover, the analysis carried out in the previous section is not valid when reflections are received, so it does not guarantee that the ML estimator is robust in this case as well. Simulation results will show, however, that the ML estimator is rather insensitive to errors in $\mathbf{a}_0$ also in the presence of reflections.

In this section, we address the problem of designing an estimator that assumes that the steering vector of the LOSS is close to a nominal one. Let us consider that this steering vector is parameterized by an unknown nuisance/perturbation real parameter[5] $\rho$. That is to say, the steering vector is $\mathbf{a}(\rho)$, in such a way that $\mathbf{a}(0) = \mathbf{a}_0$ is the nominal vector. It is possible to

[5]The extension to the multi-parameter case is not difficult but obscures the exposition.

deal with the nuisance parameter following two approaches. The first, usually referred to as autocalibration, attempts to estimate the value of $\rho$ that optimizes a given criterion [Vib94, Er94, Ast98]. On the other hand, in the second approach a probability density function (pdf) is assigned to the nuisance parameter, and a certain criterion is averaged over the distribution of the parameter [Rib97, Bel00]. We are going to apply this second approach to the ML time delay estimator. The expression of $\Lambda_{ML}(\tau_0)$ in (4.25) is not appropriate because it does not include the contribution of all terms containing $\mathbf{a}_0$. Instead, a more convenient expression for the ML criterion is the following Rayleigh quotient

$$\Lambda^{\bullet}_{ML}(\tau_0;\rho) = \frac{\mathbf{a}^*(\rho)\,\hat{\mathbf{W}}^{-1}(\tau_0)\,\mathbf{a}(\rho)}{\mathbf{a}^*(\rho)\,\hat{\mathbf{R}}_{yy}^{-1}\,\mathbf{a}(\rho)}\,, \tag{4.97}$$

where $\hat{\mathbf{W}}(\tau_0)$ was defined in (4.16). It is apparent that $\Lambda^{\bullet}_{ML}(\tau_0;\rho)$ is exactly the reciprocal of the second factor in (4.23).

The cost function averaged over the uncertainty in the steering vector is

$$\Psi(\tau_0) = \mathrm{E}_{\rho}\left\{\Lambda^{\bullet}_{ML}(\tau_0;\rho)\right\}\,. \tag{4.98}$$

This is the criterion to be maximized in order to estimate the time delay. In general, the expectation in (4.98) presents impassable obstacles. Since, in cases of practical interest, $\rho$ has zero mean and small variance $\sigma_\rho^2$, it is possible to derive an approximation of (4.98) regardless of the particular distribution of the nuisance parameter. To this end, the following second-order series expansions are employed:

$$\mathbf{a}(\rho) \approx \mathbf{a}_0 + \rho\,\mathbf{b}_0 + \frac{\rho^2}{2}\,\mathbf{h}_0 \qquad\qquad \frac{1}{1+x} \approx 1 - x + x^2\,, \tag{4.99}$$

where

$$\mathbf{b}_0 = \left.\frac{d\,\mathbf{a}(\rho)}{d\,\rho}\right|_{\rho=0} \qquad\qquad \mathbf{h}_0 = \left.\frac{d^2\,\mathbf{a}(\rho)}{d\rho^2}\right|_{\rho=0}\,. \tag{4.100}$$

Thus, an approximation of $\Psi(\tau_0)$ is obtained after developing $\Lambda^{\bullet}_{ML}(\tau_0;\rho)$ with (4.99). The resulting cost function is exact up to the second-order moment. A case with special interest is that in which the array is uniform and linear with antennas spaced $\delta$ wavelengths apart, and $\rho$ represents the pointing direction with respect to the nominal DOA, $\theta_0$. Then, the $p$th element of the steering vector is

$$[\mathbf{a}(\rho)]_p = e^{-j\,2\pi\delta\,\sin(\theta_0+\rho)}\,. \tag{4.101}$$

After lengthy but facile calculations, we get

$$\Psi(\tau_0) \approx \frac{\mathbf{a}_0^*\left(\hat{\mathbf{W}}^{-1}(\tau_0)\odot\mathbf{B}\right)\mathbf{a}_0}{\mathbf{a}_0^*\left(\hat{\mathbf{R}}_{yy}^{-1}\odot\mathbf{B}\right)\mathbf{a}_0}\left(1 + 4\,\sigma_\rho^2\,\frac{\mathrm{Re}^2\left\{\mathbf{a}_0^*\,\hat{\mathbf{R}}_{yy}^{-1}\,\mathbf{b}_0\right\}}{\left(\mathbf{a}_0^*\,\hat{\mathbf{R}}_{yy}^{-1}\,\mathbf{a}_0\right)^2}\right.$$
$$\left. - 4\,\sigma_\rho^2\,\frac{\mathrm{Re}\left\{\mathbf{a}_0^*\,\hat{\mathbf{R}}_{yy}^{-1}\,\mathbf{b}_0\right\}\mathrm{Re}\left\{\mathbf{a}_0^*\,\hat{\mathbf{W}}^{-1}(\tau_0)\,\mathbf{b}_0\right\}}{\left(\mathbf{a}_0^*\,\hat{\mathbf{R}}_{yy}^{-1}\,\mathbf{a}_0\right)\left(\mathbf{a}_0^*\,\hat{\mathbf{W}}^{-1}(\tau_0)\,\mathbf{a}_0\right)}\right)\,, \tag{4.102}$$

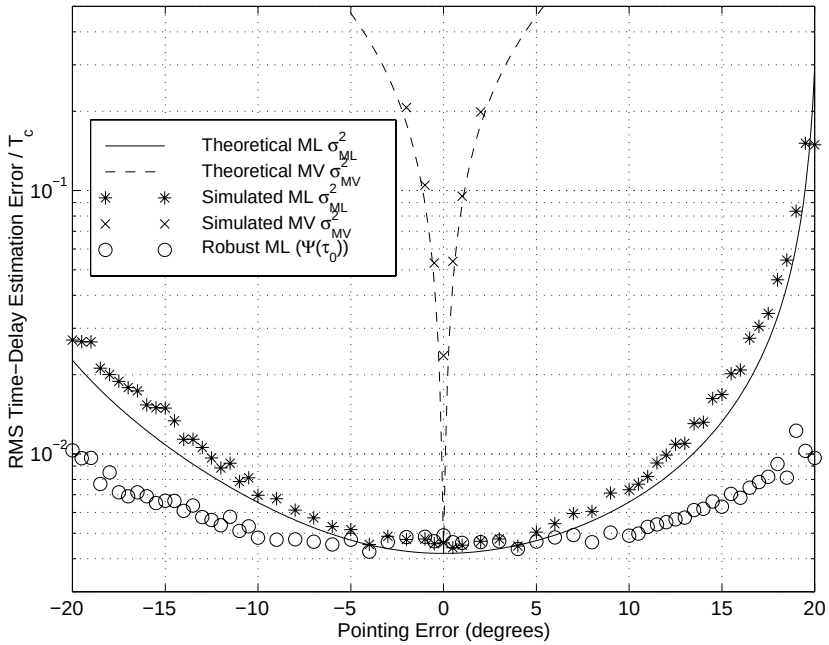


Figure 4.22: Effect of the pointing error on the time-delay RMSE when an interference is received. Parameters: $\check{\theta}_0 = 0^{\rm o}$, $\check{\tau}_0 = 0$, $\check{\theta}_i = -30^{\rm o}$, $M = 3$ pulses, $m = 6$ antennas, $\mathrm{SNR}_0 = 15.87\,\mathrm{dB}$, $\mathrm{SIR}_0 = -3.13\mathrm{dB}$, $\sigma_\rho = 8\pi/180$.

where we have assumed that the odd-order moments of the pdf of $\rho$ are zero, and the $p,q$th element of $\mathbf{B}$ is

$$[\mathbf{B}]_{p,q} = e^{-2\pi^2\delta^2\cos^2(\theta_0)\sigma_\rho^2(p-q)^2 + j\pi\delta\sigma_\rho^2\sin(\theta_0)(q-p)} \,. \tag{4.103}$$

Note that the terms in (4.102) of order $\sigma_\rho^2$ are exact, whereas only the components involving $\sigma_\rho^4$, $\sigma_\rho^6$, ... are approximated.

## 4.8 Simulation Results concerning the Effect of Pointing Errors in the LOSS Steering Vector

The characteristics of the signal scenario essentially coincide with those described in Section 4.5, and they are summarized in the figures' captions. Only the parameters that are different will be pointed out below. The robust estimator in (4.102) is designed using a standard deviation equal to $\sigma_\rho = 8\pi/180$; and $\rho$ symbolizes the direction-of-arrival relative to the nominal one. The pointing error, which is in the x-axis of the following figures, is defined as the difference between the nominal (or a priori) DOA and the true DOA of the direct signal, namely, $\theta_0 - \check{\theta}_0$. In the first experiment, a wide-band Gaussian interference impinging from a DOA equal to -30$^{\rm o}$ is received with a SIR of -3.13dB. This scenario satisfies the conditions for which the results in

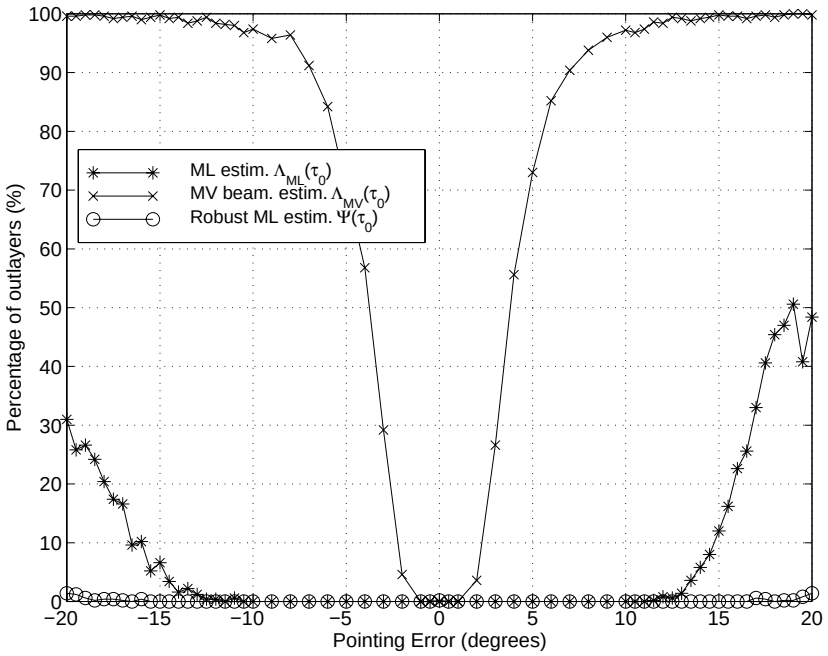


Figure 4.23: Effect of the pointing error on the number of outlayers when an interference is received. Parameters: Identical to Figure 4.22.

Section 4.6 were derived. The simulated (using 500 Monte Carlo runs) and theoretical RMSEs of the minimum variance beamformer-based estimator (MVBE) and the MLE are shown in Figure 4.22. Also the simulated RMSE of the robust estimator $\Psi(\tau_0)$ is presented in this figure. The probabilities of outlayers ($P_{out}$) of the same techniques are plotted in Figure 4.23. In the ML and robust methods, an estimate is considered to be an outlayer when its distance to the true value is greater than $\min\{0.5\,T_c, 6\sigma_t\}$, where $\sigma_t$ is the theoretical variance of the method under consideration as derived in Section 4.6. In the MVBE, the threshold for the outlayers is simply $0.5\,T_c$. It can be observed that the simulated RMSEs agree with the values predicted by (4.87) and (4.96). An exception is the MVBE in the absence of pointing errors, which has worse finite-sample performance that the ML approach, as it was already shown by the numerical results in Section 4.5. Furthermore, the RMSE and the $P_{out}$ of the MVBE undergo a severe degradation for tiny pointing errors, whereas the ML estimator tolerates errors even larger than $10^o$. The robust estimator still outperforms the ML method. The improvement is especially important in the probability of outlayers, since the $P_{out}$ of the robust method is smaller than 1.5% in all the $\pm 20^o$ simulated range of pointing errors.

In the second experiment, whose results are shown in Figures 4.24 and 4.25, a reflection is received instead of an interference. It arrives from a DOA of $30^o$, is attenuated -3dB and delayed $0.25\,T_c$ with respect to the LOSS; and both signals are in phase at the first antenna. Unlike in the first experiment, all the estimators are in general biased, so the difference between the

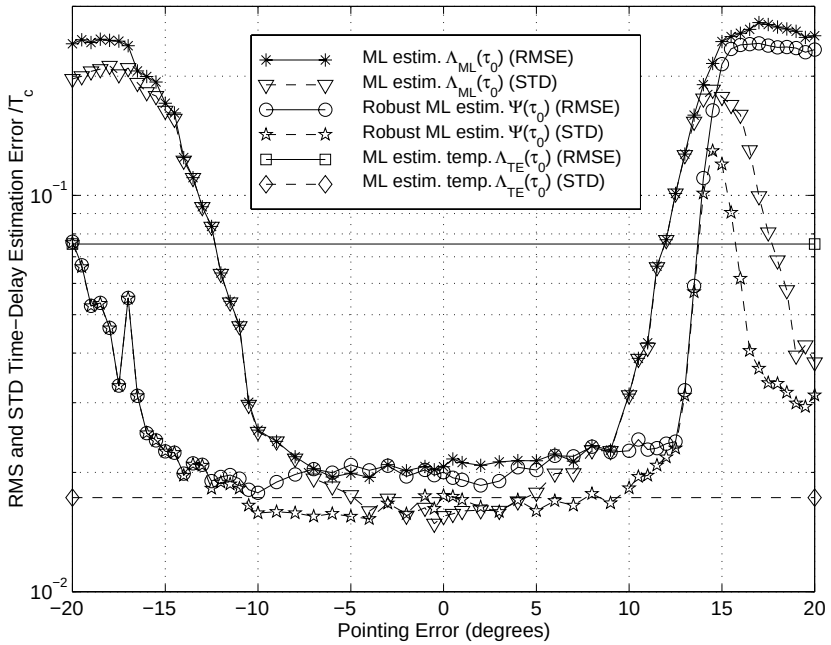


Figure 4.24: Time-delay standard deviation and RMSE as a function of the pointing error when a reflection is received. Parameters: $\check{\theta}_0 = 0^{\text{o}}$, $\check{\tau}_0 = 0$, $\check{\theta}_1 = 30^{\text{o}}$, $\check{\tau}_1 = 0.25\,T_c$, $\check{\alpha}_0/\check{\alpha}_1 = \sqrt{2}$, $M = 3$ pulses, $m = 6$ antennas, $\text{SNR}_0 = 15.87\,\text{dB}$, $\text{SIR}_0 = -3.13\text{dB}$, $\sigma_\rho = 8\pi/180$.

RMSE and the standard deviation (STD) gives information about the bias. To compute these metrics, the outlayers are removed, being the threshold $0.5\,T_c$. We have omitted the MVBE because it fails due to the multipath propagation. Even in the presence of the reflection, the performance of the ML estimator is virtually insensitive to errors up to $\pm 10^{\text{o}}$. This *flat region* is further extended for $5^{\text{o}}$ approximately using the robust estimator, whose $P_{out}$ is smaller than or equal to 1% in all the plotted range. Note that for pointing errors larger than $15^{\text{o}}$, the bias of the MLE and the MVBE approaches $0.25\,T_c$. This means that both methods tend to estimate the time delay of the reflection, what is a logical result since the nominal steering vector is closer to the steering vector of the reflection than to that of the direct signal.

## 4.9 Conclusions

An estimator of the time delay (pseudorange) and carrier phase of the line-of-sight signal received from a GNSS satellite has been proposed. The estimator is derived by applying the ML principle to a simplified and approximate signal model, in which all the signals other than the desired one are modeled as Gaussian term with unknown and arbitrary spatial correlation matrix. A particularity of many GNSS applications, consisting in that the direction-of-arrival of the direct

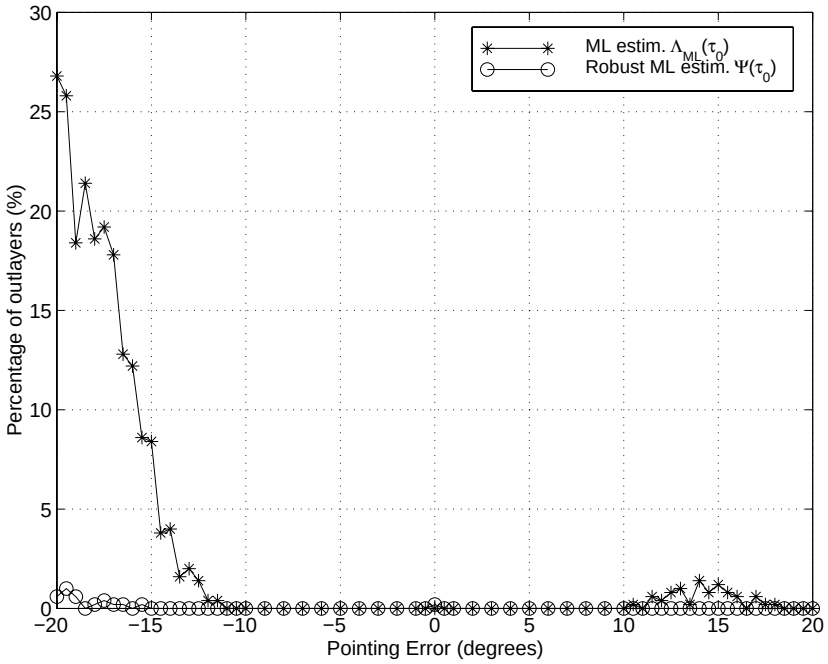


Figure 4.25: Number of outlayers as a function of the pointing error when a reflection is received. Parameters: Identical to Figure 4.24.

signal is known, is exploited by the estimator. As long as the antenna array is calibrated and has known attitude, the knowledge of this direction-of-arrival allows to compute beforehand the steering vector of the direct signal, which acts as a spatial reference to this signal and makes feasible the use of the simplified model. The estimator presented herein outperforms the estimators obtained with additional simplifying assumptions, such as that the noise field is spatially white or that the spatial signature of the direct signal is unknown. Actually, it is shown that the proposed ML cost function is the quotient between the ML cost function obtained at the output of the minimum variance beamformer and the ML cost function obtained without knowledge of the steering vector of the direct signal. Moreover, the performance of the ML estimator proposed in this chapter is very close in many situations to the best possible performance of more complex methods based on an exact description of the multipath channel. This is a remarkable result taking into account that the technique has low complexity because only the parameters of the line-of-sight signal are estimated. In particular, the ML estimator is robust against arbitrarily strong interferences and reduces in several orders of magnitude the errors produced by the reflections of the GNSS signal. This proves that although the simplified model is approximate in the presence of reflections, as long as it is combined with a spatial reference to the line-of-sight signal, it makes possible the derivation of an estimator that mitigates interference- and multipath-induced errors, and offers a reasonable trade-off between bias and RMSE for highly coherent reflections. Furthermore, this estimator is applicable identically in the presence of any type (specular or diffuse) of multipath, which is another advantage with respect

to methods based on the exact description of the multipath channel. Two polynomial-rooting algorithms for computing the time delay estimate have been presented. The first exploits the linear dependence on the delay of the signals' phase in the frequency domain, while the second employs a linear interpolation of the signal vector. It is also shown that the ML estimates can be computed from the output signal of a certain beamformer. This is a hybrid beamformer, which is computed iteratively. The resulting iterative algorithm provides an insight into the estimation problem and may be appropriate for a practical implementation. We have also shown that the ML time delay estimator, unlike the estimator based on the MVB, is inherently robust against errors in the nominal steering vector of the direct signal. Finally, a modification of this ML estimator that further extends the range of tolerable pointing errors has been presented. It is based on averaging the original estimator according to the uncertainty in the nominal steering vector.

## Appendix 4.A Cramér-Rao Bound with Knowledge of the LOSS Steering Vector

In this appendix, we derive the CRB for the model that assumes the knowledge of steering vector of the direct signal. In this case, the unknown signal parameters are

$$\boldsymbol{\eta}_s = \left[ \begin{array}{ccccccccc} |\alpha_0| & \varphi_0 & \mathrm{Re}\{\boldsymbol{\alpha}_1\}^T & \dots & \mathrm{Re}\{\boldsymbol{\alpha}_{d-1}\}^T & \mathrm{Im}\{\boldsymbol{\alpha}_1\}^T & \dots & \mathrm{Im}\{\boldsymbol{\alpha}_{d-1}\}^T & \boldsymbol{\tau}^T \end{array} \right]^T , \tag{4.104}$$

where $\varphi_0 = \angle\alpha_0$. The Fisher Information Matrix (FIM) is computed used the Bangs-Slepian's formula [Sch90, Section 6.7]. The FIM is block-diagonal with respect to the signal and noise parameters, so that only the block corresponding to $\boldsymbol{\eta}_s$ needs to be computed (see Appendix 3.A for further details). Let us first define

$$\mathbf{S}_r(\boldsymbol{\tau}_r) = \left[ \begin{array}{ccc} \mathbf{s}_r[1, \boldsymbol{\tau}_r] & \cdots & \mathbf{s}_r[N, \boldsymbol{\tau}_r] \end{array} \right] = \left[ \begin{array}{c} \mathbf{s}^T(\tau_1) \\ \vdots \\ \mathbf{s}^T(\tau_{d-1}) \end{array} \right] \qquad (d-1) \times N , \tag{4.105}$$

where $\mathbf{s}(\tau)$ was defined in (4.10), and

$$\mathbf{D}(\boldsymbol{\tau}) = \left[ \begin{array}{ccc} \mathbf{d}(\tau_0) & \cdots & \mathbf{d}(\tau_{d-1}) \end{array} \right]^T \tag{4.106}$$

$$\mathbf{d}(\tau) = \frac{d\,\mathbf{s}(\tau)}{d\,\tau} . \tag{4.107}$$

The signal parameters' block of the FIM can be partitioned as follows

$$\mathbf{FIM}\left(\boldsymbol{\eta}_s\right) = \left[\begin{array}{c|c|c} \mathbf{F}_1 & \mathbf{F}_2 & \mathbf{F}_3 \\ \hline \mathbf{F}_2^T & \mathbf{F}_4 & \mathbf{F}_5 \\ \hline \mathbf{F}_3^T & \mathbf{F}_5^T & \mathbf{F}_6 \end{array}\right], \tag{4.108}$$

where

$$\mathbf{F}_1 = \left[\begin{array}{cc} 2\left(\mathbf{s}^*\left(\tau_0\right)\mathbf{s}\left(\tau_0\right)\right)\left(\mathbf{a}_0^*\,\mathbf{Q}^{-0}\,\mathbf{a}_0\right) & 0 \\ 0 & 2\left(\mathbf{s}^*\left(\tau_0\right)\mathbf{s}\left(\tau_0\right)\right)\left(\boldsymbol{\alpha}_0^*\,\mathbf{Q}^{-0}\,\boldsymbol{\alpha}_0\right) \end{array}\right] \qquad 2\times 2 \tag{4.109}$$

$$\mathbf{F}_2 = \left[\begin{array}{c} 2\,\mathrm{Re}\left\{e^{-j\varphi_0}\,\left(\mathbf{s}^*\left(\tau_0\right)\,\mathbf{S}_r^T\left(\boldsymbol{\tau}_r\right)\right)\otimes\left(\mathbf{a}_0^*\,\mathbf{Q}^{-1}\right)\right\} \quad \cdots \\ 2\,\mathrm{Im}\left\{\left(\mathbf{s}^*\left(\tau_0\right)\,\mathbf{S}_r^T\left(\boldsymbol{\tau}_r\right)\right)\otimes\left(\boldsymbol{\alpha}_0^*\,\mathbf{Q}^{-1}\right)\right\} \\ \qquad -2\,\mathrm{Im}\left\{e^{-j\varphi_0}\,\left(\mathbf{s}^*\left(\tau_0\right)\,\mathbf{S}_r^T\left(\boldsymbol{\tau}_r\right)\right)\otimes\left(\mathbf{a}_0^*\,\mathbf{Q}^{-1}\right)\right\} \\ \qquad 2\,\mathrm{Re}\left\{\left(\mathbf{s}^*\left(\tau_0\right)\,\mathbf{S}_r^T\left(\boldsymbol{\tau}_r\right)\right)\otimes\left(\boldsymbol{\alpha}_0^*\,\mathbf{Q}^{-1}\right)\right\} \end{array}\right] \qquad 2\times 2m\left(d-1\right) \tag{4.110}$$

$$\mathbf{F}_3 = \left[\begin{array}{c} 2\,\mathrm{Re}\left\{e^{-j\varphi_0}\,\left(\mathbf{s}^*\left(\tau_0\right)\,\mathbf{D}^T\left(\boldsymbol{\tau}\right)\right)\odot\left(\mathbf{a}_0^*\,\mathbf{Q}^{-1}\,\mathbf{A}\right)\right\} \\ 2\,\mathrm{Im}\left\{\left(\mathbf{s}^*\left(\tau_0\right)\,\mathbf{D}^T\left(\boldsymbol{\tau}\right)\right)\odot\left(\boldsymbol{\alpha}_0^*\,\mathbf{Q}^{-1}\,\mathbf{A}\right)\right\} \end{array}\right] \qquad 2\times d \tag{4.111}$$

$$\mathbf{F}_4 = \left[\begin{array}{cc} 2\,\mathrm{Re}\left\{\left(\mathbf{S}_r^c\left(\boldsymbol{\tau}_r\right)\,\mathbf{S}_r^T\left(\boldsymbol{\tau}_r\right)\right)\otimes\mathbf{Q}^{-1}\right\} & -2\,\mathrm{Im}\left\{\left(\mathbf{S}_r^c\left(\boldsymbol{\tau}_r\right)\,\mathbf{S}_r^T\left(\boldsymbol{\tau}_r\right)\right)\otimes\mathbf{Q}^{-1}\right\} \\ 2\,\mathrm{Im}\left\{\left(\mathbf{S}_r^c\left(\boldsymbol{\tau}_r\right)\,\mathbf{S}_r^T\left(\boldsymbol{\tau}_r\right)\right)\otimes\mathbf{Q}^{-1}\right\} & 2\,\mathrm{Re}\left\{\left(\mathbf{S}_r^c\left(\boldsymbol{\tau}_r\right)\,\mathbf{S}_r^T\left(\boldsymbol{\tau}_r\right)\right)\otimes\mathbf{Q}^{-1}\right\} \end{array}\right]$$
$$2m\left(d-1\right)\times 2m\left(d-1\right) \tag{4.112}$$

$$\mathbf{F}_5 = \left[\begin{array}{c} 2\,\mathrm{Re}\left\{\left(\mathbf{Q}^{-1}\,\mathbf{A}\right)\,\mathrm{diag}\left(\mathbf{s}^*\left(\tau_1\right)\,\mathbf{D}^T\left(\boldsymbol{\tau}\right)\right)\right\} \\ \vdots \\ 2\,\mathrm{Re}\left\{\left(\mathbf{Q}^{-1}\,\mathbf{A}\right)\,\mathrm{diag}\left(\mathbf{s}^*\left(\tau_{d-1}\right)\,\mathbf{D}^T\left(\boldsymbol{\tau}\right)\right)\right\} \\ 2\,\mathrm{Im}\left\{\left(\mathbf{Q}^{-1}\,\mathbf{A}\right)\,\mathrm{diag}\left(\mathbf{s}^*\left(\tau_1\right)\,\mathbf{D}^T\left(\boldsymbol{\tau}\right)\right)\right\} \\ \vdots \\ 2\,\mathrm{Im}\left\{\left(\mathbf{Q}^{-1}\,\mathbf{A}\right)\,\mathrm{diag}\left(\mathbf{s}^*\left(\tau_{d-1}\right)\,\mathbf{D}^T\left(\boldsymbol{\tau}\right)\right)\right\} \end{array}\right] \qquad 2m\left(d-1\right)\times d \tag{4.113}$$

$$\mathbf{F}_6 = 2\,\mathrm{Re}\left\{\left(\mathbf{D}^c(\boldsymbol{\tau})\,\mathbf{D}^T(\boldsymbol{\tau})\right)\odot\left(\mathbf{A}^*\,\mathbf{Q}^{-1}\,\mathbf{A}\right)\right\} \qquad d\times d\,. \tag{4.114}$$

Using twice the formula of the inverse of a partitioned matrix, the CRB for the time delays can be written as

$$\mathbf{CRB}^{-1}(\boldsymbol{\tau}) = \mathbf{F}_6 - \left[\begin{array}{c|c} \mathbf{F}_3^T & \mathbf{F}_5^T \end{array}\right] \left[\begin{array}{c|c} \mathbf{F}_1 & \mathbf{F}_2 \\ \hline \mathbf{F}_2^T & \mathbf{F}_4 \end{array}\right]^{-1} \left[\begin{array}{c} \mathbf{F}_3 \\ \hline \mathbf{F}_5 \end{array}\right] \tag{4.115}$$

$$= \mathbf{F}_6 - \left[\begin{array}{c|c} \mathbf{F}_3^T & \mathbf{F}_5^T \end{array}\right] \cdot \left[\begin{array}{c|c} \left(\mathbf{F}_1 - \mathbf{F}_2\,\mathbf{F}_4^{-1}\,\mathbf{F}_2^T\right)^{-1} & -\left(\mathbf{F}_1 - \mathbf{F}_2\,\mathbf{F}_4^{-1}\,\mathbf{F}_2^T\right)^{-1}\,\mathbf{F}_2\,\mathbf{F}_4^{-1} \\ \hline -\mathbf{F}_4^{-1}\,\mathbf{F}_2^T\,\left(\mathbf{F}_1 - \mathbf{F}_2\,\mathbf{F}_4^{-1}\,\mathbf{F}_2^T\right)^{-1} & \mathbf{F}_4^{-1} + \mathbf{F}_4^{-1}\,\mathbf{F}_2^T\,\left(\mathbf{F}_1 - \mathbf{F}_2\,\mathbf{F}_4^{-1}\,\mathbf{F}_2^T\right)^{-1}\,\mathbf{F}_2\,\mathbf{F}_4^{-1} \end{array}\right] \left[\begin{array}{c} \mathbf{F}_3 \\ \hline \mathbf{F}_5 \end{array}\right] \tag{4.116}$$

$$= \mathbf{F}_6 - \mathbf{F}_5^T\,\mathbf{F}_4^{-1}\,\mathbf{F}_5 - \left(\mathbf{F}_3 - \mathbf{F}_2\,\mathbf{F}_4^{-1}\,\mathbf{F}_5\right)^T\,\left(\mathbf{F}_1 - \mathbf{F}_2\,\mathbf{F}_4^{-1}\,\mathbf{F}_2^T\right)^{-1}\,\left(\mathbf{F}_3 - \mathbf{F}_2\,\mathbf{F}_4^{-1}\,\mathbf{F}_5\right)\ . \tag{4.117}$$

The developments of Appendix 3.A can be easily applied to the term $\mathbf{F}_6 - \mathbf{F}_5^T\,\mathbf{F}_4^{-1}\,\mathbf{F}_5$, and hence it is expressed as

$$\mathbf{F}_6 - \mathbf{F}_5^T\,\mathbf{F}_4^{-1}\,\mathbf{F}_5 = 2\,\mathrm{Re}\left\{\left(\mathbf{D}^c(\boldsymbol{\tau})\,\mathbf{P}^{\perp}_{\mathbf{S}_r^T(\boldsymbol{\tau}_r)}\,\mathbf{D}^T(\boldsymbol{\tau})\right) \odot \left(\mathbf{A}^*\,\mathbf{Q}^{-1}\,\mathbf{A}\right)\right\}\ , \tag{4.118}$$

where $\mathbf{P}^{\perp}_{\mathbf{S}_r^T(\boldsymbol{\tau}_r)}$ is the orthogonal projector onto the orthogonal complement of the columns of $\mathbf{S}_r^T(\boldsymbol{\tau}_r)$. In order to derive appropriate expressions for the rest of the terms in (4.117), the following three identities along with (3.117)-(3.118) are used:

$$\begin{aligned} \mathrm{Re}\{\mathbf{X}\,\mathbf{Z}\,\mathbf{V}^*\} &= \mathrm{Re}\{\mathbf{X}\}\,\mathrm{Re}\{\mathbf{Z}\}\,\mathrm{Re}\{\mathbf{V}\}^T - \mathrm{Im}\{\mathbf{X}\}\,\mathrm{Im}\{\mathbf{Z}\}\,\mathrm{Re}\{\mathbf{V}\}^T \\ &\quad + \mathrm{Im}\{\mathbf{X}\}\,\mathrm{Re}\{\mathbf{Z}\}\,\mathrm{Im}\{\mathbf{V}\}^T + \mathrm{Re}\{\mathbf{X}\}\,\mathrm{Im}\{\mathbf{Z}\}\,\mathrm{Im}\{\mathbf{V}\}^T \qquad (4.119) \\ \mathrm{Im}\{\mathbf{X}\,\mathbf{Z}\,\mathbf{V}^*\} &= \mathrm{Im}\{\mathbf{X}\}\,\mathrm{Re}\{\mathbf{Z}\}\,\mathrm{Re}\{\mathbf{V}\}^T + \mathrm{Re}\{\mathbf{X}\}\,\mathrm{Im}\{\mathbf{Z}\}\,\mathrm{Re}\{\mathbf{V}\}^T \\ &\quad + \mathrm{Im}\{\mathbf{X}\}\,\mathrm{Im}\{\mathbf{Z}\}\,\mathrm{Im}\{\mathbf{V}\}^T - \mathrm{Re}\{\mathbf{X}\}\,\mathrm{Re}\{\mathbf{Z}\}\,\mathrm{Im}\{\mathbf{V}\}^T \qquad (4.120) \\ (\mathbf{X}\otimes\mathbf{Z})\,(\mathbf{U}\otimes\mathbf{V}) &= (\mathbf{X}\,\mathbf{U})\otimes(\mathbf{Z}\,\mathbf{V})\ , \qquad (4.121) \end{aligned}$$

which are valid for arbitrary matrices (with the appropriate dimensions). The proof of equation (4.121) can be found in [Gra81, Bre78]. After lengthy calculations, we get

$$\mathbf{F}_1 - \mathbf{F}_2\,\mathbf{F}_4^{-1}\,\mathbf{F}_2^T = 2\,\left(\mathbf{s}^*(\tau_0)\,\mathbf{P}^{\perp}_{\mathbf{S}_r^T(\boldsymbol{\tau}_r)}\,\mathbf{s}(\tau_0)\right)\,\left(\mathbf{a}_0^*\,\mathbf{Q}^{-1}\,\mathbf{a}_0\right)\,\left[\begin{array}{cc} 1 & 0 \\ 0 & |\alpha_0|^2 \end{array}\right] \tag{4.122}$$

$$\mathbf{F}_3 - \mathbf{F}_2\,\mathbf{F}_4^{-1}\,\mathbf{F}_5 = \left[\begin{array}{c} 2\,\mathrm{Re}\left\{e^{-j\varphi_0}\,\left(\mathbf{s}^*(\tau_0)\,\mathbf{P}^{\perp}_{\mathbf{S}_r^T(\boldsymbol{\tau}_r)}\,\mathbf{D}^T(\boldsymbol{\tau})\right) \odot \left(\mathbf{a}_0^*\,\mathbf{Q}^{-1}\,\mathbf{A}\right)\right\} \\ 2\,\mathrm{Re}\left\{\left(\mathbf{s}^*(\tau_0)\,\mathbf{P}^{\perp}_{\mathbf{S}_r^T(\boldsymbol{\tau}_r)}\,\mathbf{D}^T(\boldsymbol{\tau})\right) \odot \left(\boldsymbol{\alpha}^*\,\mathbf{Q}^{-1}\,\mathbf{A}\right)\right\} \end{array}\right]\ . \tag{4.123}$$

Finally, substituting (4.118), (4.122) and (4.123) into (4.117) yields

$$\begin{aligned} \mathbf{CRB}^{-1}(\boldsymbol{\tau}) &= 2\,\mathrm{Re}\left\{\left(\mathbf{D}^c(\boldsymbol{\tau})\,\mathbf{P}^{\perp}_{\mathbf{S}_r^T(\boldsymbol{\tau}_r)}\,\mathbf{D}^T(\boldsymbol{\tau})\right) \odot \left(\mathbf{A}^*\,\mathbf{Q}^{-1}\,\mathbf{A}\right)\right\} \\ &\quad - 2\,\left(\mathbf{s}^*(\tau_0)\,\mathbf{P}^{\perp}_{\mathbf{S}_r^T(\boldsymbol{\tau}_r)}\,\mathbf{s}(\tau_0)\right)^{-1}\,\left(\boldsymbol{\alpha}_0^*\,\mathbf{Q}^{-1}\,\boldsymbol{\alpha}_0\right)^{-1} \qquad (4.124) \\ &\quad \cdot \mathrm{Re}\left\{\left(\left(\mathbf{A}^*\,\mathbf{Q}^{-1}\,\boldsymbol{\alpha}_0\right) \odot \left(\mathbf{D}^c(\boldsymbol{\tau})\,\mathbf{P}^{\perp}_{\mathbf{S}_r^T(\boldsymbol{\tau}_r)}\,\mathbf{s}(\tau_0)\right)\right)\,\left(\left(\mathbf{s}^*(\tau_0)\,\mathbf{P}^{\perp}_{\mathbf{S}_r^T(\boldsymbol{\tau}_r)}\,\mathbf{D}^T(\boldsymbol{\tau})\right) \odot \left(\boldsymbol{\alpha}_0^*\,\mathbf{Q}^{-1}\,\mathbf{A}\right)\right)\right\}\ . \end{aligned}$$

A similar result to this one was reported in [Li93] for a somewhat dual problem: estimation of directions-of-arrival using the knowledge of the waveform of the desired signal in spatially and temporally white noise. Using (4.118), (4.122) and (4.123), an expression of the $2 \times 2$ upper-left block of the CRB matrix can also be derived since

$$\begin{aligned}\mathbf{CRB}^{-1}\left([|\alpha_0|,\, \varphi_0]\right) &= \mathbf{F}_1 - \mathbf{F}_2\,\mathbf{F}_4^{-1}\,\mathbf{F}_2^T \\ &\quad - \left(\mathbf{F}_3 - \mathbf{F}_2\,\mathbf{F}_4^{-1}\,\mathbf{F}_5\right)\,\left(\mathbf{F}_6 - \mathbf{F}_5^T\,\mathbf{F}_4^{-1}\,\mathbf{F}_5\right)^{-1}\,\left(\mathbf{F}_3 - \mathbf{F}_2\,\mathbf{F}_4^{-1}\,\mathbf{F}_5\right)^T\,. \end{aligned} \tag{4.125}$$

When $d = 1$, (4.124) adopts the following expression

$$\mathrm{CRB}^{-1}\left(\tau_0\right) = 2\,\left(\boldsymbol{\alpha}_0^*\,\mathbf{Q}^{-1}\,\boldsymbol{\alpha}_0\right)\,\left(\mathbf{d}^*\left(\tau_0\right)\,\mathbf{P}^{\perp}_{\mathbf{s}(\tau_0)}\,\mathbf{d}\left(\tau_0\right)\right)\,, \tag{4.126}$$

which coincides with the CRB obtained for a signal with unknown steering vector. In the case of $d = 1$, the CRB for the modulus and argument of the amplitude can also be easily obtained, and their expressions are

$$\mathrm{CRB}^{-1}\left(\varphi_0\right) = 2\,\left(\boldsymbol{\alpha}_0^*\,\mathbf{Q}^{-1}\,\boldsymbol{\alpha}_0\right)\,\left(\mathbf{s}^*\left(\tau_0\right)\,\mathbf{P}^{\perp}_{\mathbf{d}(\tau_0)}\,\mathbf{s}\left(\tau_0\right)\right)\,\left(1 - \frac{\mathrm{Re}^2\left\{\mathbf{s}^*\left(\tau_0\right)\,\mathbf{d}\left(\tau_0\right)\right\}}{\left\|\mathbf{s}\left(\tau_0\right)\right\|^2\,\left\|\mathbf{d}\left(\tau_0\right)\right\|^2}\right)^{-1} \tag{4.127}$$

$$\mathrm{CRB}^{-1}\left(|\alpha_0|\right) = 2\,\left(\mathbf{a}_0^*\,\mathbf{Q}^{-1}\,\mathbf{a}_0\right)\,\left(\mathbf{s}^*\left(\tau_0\right)\,\mathbf{P}^{\perp}_{\mathbf{d}(\tau_0)}\,\mathbf{s}\left(\tau_0\right)\right)\,\left(1 - \frac{\mathrm{Im}^2\left\{\mathbf{s}^*\left(\tau_0\right)\,\mathbf{d}\left(\tau_0\right)\right\}}{\left\|\mathbf{s}\left(\tau_0\right)\right\|^2\,\left\|\mathbf{d}\left(\tau_0\right)\right\|^2}\right)^{-1}\,. \tag{4.128}$$

## Appendix 4.B A Few Asymptotic Expressions

The cost function of the time delay estimator based on the minimum variance beamformer was presented in (4.47) and can also be written as

$$\Lambda_{MV}\left(\tau_0\right) = \frac{1}{N}\,\mathbf{a}_0^*\,\hat{\mathbf{R}}_{yy}^{-1}\,\mathbf{Y}\,\mathbf{P}_{\mathbf{s}^c(\tau_0)}\,\mathbf{Y}^*\,\hat{\mathbf{R}}_{yy}^{-1}\,\mathbf{a}_0\,. \tag{4.129}$$

Using the expression (3.131) of the second derivative of a projection matrix [Ott93] along with the model in (4.76), and retaining only the desired signal contribution because the limit $N \to \infty$ is performed, it is straightforward that

$$h_{MV} = -\frac{2}{N}\,\mathbf{a}_0^*\,\hat{\mathbf{R}}_{yy}^{-1}\,\boldsymbol{\alpha}_0\,\mathbf{d}^T\left(\check{\tau}_0\right)\,\mathbf{P}^{\perp}_{\mathbf{s}^c(\check{\tau}_0)}\,\mathbf{d}^c\left(\check{\tau}_0\right)\,\boldsymbol{\alpha}_0^*\,\hat{\mathbf{R}}_{yy}^{-1}\,\mathbf{a}_0\,. \tag{4.130}$$

The first derivative of the cost function can be written as

$$\begin{aligned}\Lambda'_{MV}\left(\check{\tau}_0\right) = \frac{2}{N}\,\mathrm{Re}\Bigg\{&\mathbf{a}_0^*\,\hat{\mathbf{R}}_{yy}^{-1}\,\boldsymbol{\alpha}_0\,\mathbf{d}^T\left(\check{\tau}_0\right)\,\mathbf{P}^{\perp}_{\mathbf{s}^c(\check{\tau}_0)}\,\mathbf{E}^*\,\hat{\mathbf{R}}_{yy}^{-1}\,\mathbf{a}_0 \\ &+ \frac{1}{N\,\hat{P}_s}\,\mathbf{a}_0^*\,\hat{\mathbf{R}}_{yy}^{-1}\,\mathbf{E}\,\mathbf{s}^c(\check{\tau}_0)\,\mathbf{d}^T\left(\check{\tau}_0\right)\,\mathbf{P}^{\perp}_{\mathbf{s}^c(\check{\tau}_0)}\,\mathbf{E}^*\,\hat{\mathbf{R}}_{yy}^{-1}\,\mathbf{a}_0\Bigg\}\,,\end{aligned} \tag{4.131}$$

where we have used the formula (3.124) of the first derivative of a projection matrix [Ott93]. In order to obtain asymptotic results, $\Lambda'_{MV}\left(\check{\tau}_0\right)$ can be approximated as

$$\Lambda'_{MV}\left(\check{\tau}_0\right) \approx \frac{2}{N}\,\mathrm{Re}\Bigg\{\mathrm{Tr}\left\{\mathbf{R}_{yy}^{-1}\,\mathbf{a}_0\,\mathbf{a}_0^*\,\mathbf{R}_{yy}^{-1}\,\boldsymbol{\alpha}_0\,\mathbf{d}^T\left(\check{\tau}_0\right)\,\mathbf{P}^{\perp}_{\mathbf{s}^c(\check{\tau}_0)}\,\mathbf{E}^*\right\}\Bigg\}\,. \tag{4.132}$$

Taking into account that noise is circularly symmetric, the variance of (4.132) is

$$g_{MV}/N = \frac{2}{N^2}\,\mathrm{Re}\Bigg\{ \sum_{r=1}^{m}\sum_{s=1}^{m} \left[\mathbf{R}_{yy}^{-1}\right]_{r,:}\, \mathbf{a}_0\, \mathbf{a}_0^*\, \mathbf{R}_{yy}^{-1}\, \boldsymbol{\alpha}_0\, \mathbf{d}^T\left(\check{\tau}_0\right)\, \mathbf{P}^{\perp}_{\mathbf{s}^c(\check{\tau}_0)}\, \underbrace{\mathrm{E}\left\{ \left[\mathbf{E}^*\right]_{:,r}\, \left[\mathbf{E}\right]_{s,:} \right\}}_{[\mathbf{Q}]_{s,r}\,\mathbf{I}} \cdot$$

$$\cdot\, \mathbf{P}^{\perp}_{\mathbf{s}^c(\check{\tau}_0)}\, \mathbf{d}^c(\check{\tau}_0)\, \boldsymbol{\alpha}_0^*\, \mathbf{R}_{yy}^{-1}\, \mathbf{a}_0\, \mathbf{a}_0^*\, \left[\mathbf{R}_{yy}^{-1}\right]_{:,s} \Bigg\} \tag{4.133}$$

$$= \frac{2}{N^2}\, \left(\mathbf{d}^T(\check{\tau}_0)\, \mathbf{P}^{\perp}_{\mathbf{s}^c(\check{\tau}_0)}\, \mathbf{d}^c(\check{\tau}_0)\right)\, \left|\mathbf{a}^*\, \mathbf{R}_{yy}^{-1}\, \boldsymbol{\alpha}_0\right|^2\, \mathrm{Re}\left\{ \sum_{r=1}^{m}\sum_{s=1}^{m} \left[\mathbf{R}_{yy}^{-1}\right]_{r,:}\, \mathbf{a}_0\, \left[\mathbf{Q}\right]_{s,r}\, \mathbf{a}_0^*\, \left[\mathbf{R}_{yy}^{-1}\right]_{:,s} \right\} \tag{4.134}$$

$$= \frac{2}{N^2}\, \left(\mathbf{d}^T(\check{\tau}_0)\, \mathbf{P}^{\perp}_{\mathbf{s}^c(\check{\tau}_0)}\, \mathbf{d}^c(\check{\tau}_0)\right)\, \left|\mathbf{a}^*\, \mathbf{R}_{yy}^{-1}\, \boldsymbol{\alpha}_0\right|^2\, \left(\mathbf{a}_0^*\, \mathbf{R}_{yy}^{-1}\, \mathbf{Q}\, \mathbf{R}_{yy}^{-1}\, \mathbf{a}_0\right)\ . \tag{4.135}$$

An approximate expression of the derivative of $\Lambda_{TE}\left(\tau_0\right)$ valid for deriving asymptotic results is

$$\Lambda'_{TE}(\check{\tau}_0) \approx \frac{2}{N}\,\mathrm{Re}\left\{ \mathrm{Tr}\left\{ \mathbf{R}_{yy}^{-1}\, \boldsymbol{\alpha}_0\, \mathbf{d}^T(\check{\tau}_0)\, \mathbf{P}^{\perp}_{\mathbf{s}^c(\check{\tau}_0)}\, \mathbf{E}^* \right\} \right\}\ , \tag{4.136}$$

which can be readily obtained from (4.80) using the same steps as those employed for $\Lambda'_{MV}\left(\tau_0\right)$, or from Appendix 3.B. Then, the asymptotic cross-covariance between the derivatives of the temporal-reference and the minimum-variance-beamforming criteria is given by

$$g_{TE,MV}/N = \frac{2}{N^2}\,\mathrm{Re}\Bigg\{ \sum_{r=1}^{m}\sum_{s=1}^{m} \left[\mathbf{R}_{yy}^{-1}\right]_{r,:}\, \boldsymbol{\alpha}_0\, \mathbf{d}^T(\check{\tau}_0)\, \mathbf{P}^{\perp}_{\mathbf{s}^c(\check{\tau}_0)}\, \mathrm{E}\left\{ \left[\mathbf{E}^*\right]_{:,r}\, \left[\mathbf{E}\right]_{s,:} \right\} \cdot$$

$$\cdot\, \mathbf{P}^{\perp}_{\mathbf{s}^c(\check{\tau}_0)}\, \mathbf{d}^c(\check{\tau}_0)\, \boldsymbol{\alpha}_0^*\, \mathbf{R}_{yy}^{-1}\, \mathbf{a}_0\, \mathbf{a}_0^*\, \left[\mathbf{R}_{yy}^{-1}\right]_{:,s} \Bigg\} \tag{4.137}$$

$$= \frac{2}{N^2}\, \left(\mathbf{d}^T(\check{\tau}_0)\, \mathbf{P}^{\perp}_{\mathbf{s}^c(\check{\tau}_0)}\, \mathbf{d}^c(\check{\tau}_0)\right)\, \mathrm{Re}\left\{ \boldsymbol{\alpha}_0^*\, \mathbf{R}_{yy}^{-1}\, \mathbf{a}_0\, \sum_{r=1}^{m}\sum_{s=1}^{m} \left[\mathbf{R}_{yy}^{-1}\right]_{r,:}\, \boldsymbol{\alpha}_0\, \left[\mathbf{Q}\right]_{s,r}\, \mathbf{a}_0^*\, \left[\mathbf{R}_{yy}^{-1}\right]_{:,s} \right\} \tag{4.138}$$

$$= \frac{2}{N^2}\, \left(\mathbf{d}^T(\check{\tau}_0)\, \mathbf{P}^{\perp}_{\mathbf{s}^c(\check{\tau}_0)}\, \mathbf{d}^c(\check{\tau}_0)\right)\, \mathrm{Re}\left\{ \left(\boldsymbol{\alpha}_0^*\, \mathbf{R}_{yy}^{-1}\, \mathbf{a}_0\right)\, \left(\mathbf{a}_0^*\, \mathbf{R}_{yy}^{-1}\, \mathbf{Q}\, \mathbf{R}_{yy}^{-1}\, \boldsymbol{\alpha}_0\right) \right\} \tag{4.139}$$

$$= \frac{2}{N^2}\, \left(\mathbf{d}^T(\check{\tau}_0)\, \mathbf{P}^{\perp}_{\mathbf{s}^c(\check{\tau}_0)}\, \mathbf{d}^c(\check{\tau}_0)\right)\, \frac{\left|\boldsymbol{\alpha}_0^*\, \mathbf{Q}^{-1}\, \mathbf{a}_0\right|^2}{\left(1 + P_s\, \boldsymbol{\alpha}_0^*\, \mathbf{Q}^{-1}\, \boldsymbol{\alpha}_0\right)^3}\ . \tag{4.140}$$

The last equation is obtained by applying the matrix inversion lemma to $\mathbf{R}_{yy} = P_s\, \boldsymbol{\alpha}_0\, \boldsymbol{\alpha}_0^* + \mathbf{Q}$.

# Chapter 5

# Code-Timing Synchronization in DS-CDMA Communication Systems Using Space-Time Diversity

In this chapter, the synchronization of a desired user transmitting a known training sequence in a direct-sequence (DS) asynchronous code-division multiple-access (CDMA) system is addressed. It is assumed that the receiver consists of an arbitrary antenna array and works in a near-far, frequency-nonselective, slowly fading channel. The estimator that we propose is derived by applying the maximum likelihood (ML) principle to a signal model in which the contribution of all the interfering components (e.g., multiple-access interference, external interference and noise) is modeled as a Gaussian term with an unknown and arbitrary space-time correlation matrix. A large sample approximation of the exact ML estimator is actually employed. The main contribution of this chapter is the fact that the estimator makes efficient use of the structure of the signals in both the space and time domains. The performance of the proposed estimator is compared with the Cramér-Rao Bound, and with the performance of other methods recently proposed that also employ an antenna array but only exploit the structure of the signals in one of the two domains, while using the other simply as a means of path diversity. It is shown that the use of the temporal and spatial structures is necessary to achieve synchronization in heavily loaded systems or in the presence of directional external interference.

## 5.1 Introduction

The importance in communication systems of near-far resistant timing synchronization techniques that are also robust to external interference was already addressed in Section 1.2. The

conventional approaches to timing acquisition and tracking in DS-CDMA systems are the *sliding correlator* and the delay lock loop (DLL), respectively [Hol90]. These approaches are only well suited for an additive white Gaussian noise channel. Extensions of the DLL which are appropriate for a frequency-selective channel were developed in [She95, She98]. Nevertheless, these modified loops are not able to combat the multiple-access interference (MAI). Several near-far resistant timing estimators have recently been proposed in the literature for a single-antenna receiver [Smi94, Str96, Zhe97, Ben96, Ben98, Öst99, Ert00, Ran00]. Some of them are derived from the maximum likelihood principle and require training sequences. Others exploit the eigenstructure of the correlation matrix of the received signals. While these last estimators do not need training sequences, their performance is poorer than that of the ML-based ones. In [Zhe97], a large sample ML estimator was proposed, and a comparison with many other methods revealed that the ML estimator is preferred for moderate or large lengths of the training sequence. Its performance can be largely improved for short training sequences using a structured estimate of the correlation matrix, as suggested in [Ben98, Ert00]. This approximate ML estimator has been extended to the case of frequency-selective channels in [Ert00, Ran00]. However, the resulting criterion involves a complex multidimensional search, and therefore iterative optimization algorithms (e.g., the expectation-maximization or the alternating-projection methods) are considered. The techniques presented in [Ben98, Ert00] are claimed to be exact maximum likelihood estimators. However, they are large-sample approximations. The lapse lies in assuming that the correlation matrix of the noise-plus-interference is known, when it was indeed unknown.

It is well known that detection performance in DS-CDMA can be greatly improved through the use of antenna arrays [Pau97, Muñ97, Mol98]. Similarly, the synchronization problem can also benefit from using multiple antennas, as shown in [Liu98a, Liu98b, Jak98a, Sen98]. Moreover, given the lack of temporal structure of wide-band (i.e., temporally white) external interferers, the use of an antenna array is mandatory to achieve robustness against this type of interferers. In this chapter, we propose a method for estimating the timing of a certain user that transmits a known training sequence. We will focus on the code synchronization because several algorithms for estimating the remaining parameters given reliable estimates of the code-timings exist [Xie93]. In fact, the expression of the ML estimates of the amplitudes and phases of the signals will be obtained as a by-product of the derivation of the timing estimator in Section 5.4.1. We assume that the receiver consists of an arbitrary antenna array that operates in a frequency-nonselective (or flat), slowly fading channel [Pro95]. Actually, the estimator proposed herein could also be used in frequency-selective channels, but we will restrict our analysis to the nonselective case for the sake of simplicity. Flat-fading channels are common in situations where the distance between the users and the base station is relatively small (e.g., in a microcell), or when the multipath is due to local scatterers near the remote user or the base station. Note that the availability of a training sequence is not a too stringent assumption, since most communications

systems transmit these sequences during certain intervals. Besides, once a reliable estimate of the timing is formed, the estimator can be switched to a decision-directed mode. The fact that the method estimates the parameters of only one user while retaining near-far resistance (i.e., belongs to the class of the so-called single-user estimators) is also of interest, because it leads to decentralized implementations and dramatically reduces the complexity with respect to methods that estimate the parameters of all users jointly (see, for instance, [Str96]).

In accordance with the connecting theme along this thesis, all signals excepting that of the desired user are modeled as a Gaussian component with an arbitrary and unknown correlation matrix. This idea has been used for the problem at hand in [Zhe97, Ben98, Liu98a, Jak98a, Sen98] among others; for Doppler and direction-of-arrival estimation in radar systems in [Swi98b]; and for time-delay estimation in a general framework and in navigation systems particularly (see the two previous chapters). An extension of [Zhe97, Ben98] for a multiple-sensor receiver can be found in [Liu98b]. However, as this extension assumes that the interfering signals are uncorrelated among antennas, it reduces to several single-sensor estimators applied in parallel to several independent channels. Hence the effect of the antenna array is only to increase the signal-to-noise ratio (SNR) and to provide diversity in order to combat the fading of the desired user's signal at different antennas (i.e., maximal ratio combining); but the array does not use the directional properties of the interfering signals in order to cancel them. Indeed, as pointed out by the authors themselves, the performance of the estimator in [Liu98b] cannot be significantly improved by increasing the number of antennas, when for fair comparisons with single-antenna methods, the interference power is proportional to the number of sensors used in the receiver. In a slowly fading environment, the assumption of uncorrelation among antennas is not appropriate at all, because the signals present definite spatial signatures, as it will be justified in the next section. This fact is exploited by the estimator proposed in [Liu98a]. Nevertheless, this estimator assumes that the interfering signals are white in the temporal domain, so only the spatial structure of the MAI is used to combat it. As a result, a prohibitively large number of antennas may be needed to achieve near-far resistance.

The significance of this chapter lies in that we consider a space-time correlation matrix for the disturbing signals, which allows both the temporal (provided by the codes) and spatial structure (provided by the antenna array) of the received signals to be exploited. The benefits in symbol detection of exploiting the joint space-time signature have been analyzed thoroughly in [Ast99a]. However, the use of the space-time signature in synchronization is an open issue. The method proposed herein extends and outperforms those presented in previous works. It will be shown that the use of the spatial and temporal structure of the interference is indispensable in achieving code synchronization in some scenarios, and this can be accomplished with a small number of antennas. Note that the technique in [Sen98] also takes into account the spatial and temporal structure of the interference. But it considers a frequency-selective channel and is limited to estimating the overall channel response, since the estimation of the time delays is

computationally too complex.

This chapter is organized as follows. In Section 5.2, the signal model is introduced. Section 5.3 justifies the essential assumption on which the estimator rests and compares it with those made in related work. The derivation of the ML estimator and some alternatives to improve the estimate of correlation matrix are presented in Section 5.4. Section 5.5 is concerned with the Cramér-Rao Bound for the problem at hand. Finally, numerical results are analyzed in Section 5.6; and Section 5.7 summarizes our conclusions.

## 5.2 Signal Model

Consider an asynchronous DS-CDMA system with $K$ users and an arbitrary receiving antenna array of $m$ sensors, which satisfies the standard narrow-band array condition common to many array signal processing problems. We assume a flat-fading channel, which means that for each user the time-delay differences between different propagation paths are negligible compared with the reciprocal of the signal bandwidth [Pro95]. For this channel, the received complex baseband signal (after down-conversion and chip-matched filtering) at the $l$th sensor is

$$y_l(t) = \sum_{k=1}^{K} \alpha_{l,k}\, q_k(t-\tau_k) + w_l(t) \qquad l = 1, 2...m \ , \tag{5.1}$$

where $\alpha_{l,k}$ is the complex fading coefficient for the $k$th user at the $l$th antenna, $\tau_k$ is the delay associated with the $k$th user, and $w_l(t)$ represents the thermal noise and all other external interferences. The expression in (5.1) and the development below would also be valid for the received signal before chip-matched filtering. However, we have not considered this case for coherence with the existing literature, and because dealing with the signals after filtering makes possible to work with transmitted rectangular chip-pulses in a natural way [Str96].

The term in (5.1) corresponding to the $k$th user is:

$$q_k(t) = \sum_{i=-1}^{M-1} d_k(i)\, p_k(t-iT) \ , \tag{5.2}$$

where

$$p_k(t) = \sum_{n=0}^{P-1} c_k(n)\, g(t-nT_c) \tag{5.3}$$

is the spreading waveform. The symbols $d_k(i)$ are transmitted at a rate $1/T$, constitute an *iid* sequence with variance $\sigma_d^2$, and are independent for different users. The length of the chip sequence $c_k(n)$ is $P = T/T_c$, the chip rate is $1/T_c$ and $g(t)$ represents an arbitrary chip-shaping waveform. The signal is observed during an interval of $M+1$ symbols ($T_{obs} = (M+1)T$), which is the length of the training sequence.

The coefficients $\alpha_{l,k}$ include the effects of the propagation, transmitted power, carrier phase and Doppler frequency. Their temporal evolution is characterized by the coherence time $T_{coh}$, which is defined as the time interval during which a given fading coefficient is highly correlated with itself, and it is in general inversely proportional to the maximum Doppler frequency [Pro95]. Since we consider a slowly fading channel (i.e., $T_{coh} \gg T_{obs}$), for the estimator derivation we will assume that the fading coefficients are constant during the observation interval, as in many other works (e.g., [Zhe97, Liu98a, Jak98a, Sen98, Ert00]). This assumption is for mathematical convenience, and it will be shown that the performance of the proposed estimator is also highly satisfactory in more realistic scenarios. The condition for slow fading places restrictions on the length of the training sequence $M$ and on the maximum Doppler frequency. However, these are mild restrictions, which are satisfied by the parameters in a large number of practical situations and do not represent a significant limitation of our approach, as shown by the numerical examples of Section 5.7. The relevant implication of having fairly constant fading coefficients during $T_{obs}$ is that the signals show rather definite spatial signatures, which can be used to differentiate the desired user's signal from the MAI and external interference. It is important to remark that this property holds independently of the statistical correlation between the fading coefficients at different antennas.

The signals in (5.1) are sampled at a rate $1/T_s = Q/T_c$, where $Q$ is an integer and is referred to as the oversampling factor. Each set of $P \cdot Q$ consecutive samples received at the $l$th antenna is stacked into a column vector:

$$\mathbf{y}_l(i) = \left[ \begin{array}{cccc} y_l(iT + T_s) & \ldots & y_l(iT + PQT_s) \end{array} \right]^T . \tag{5.4}$$

The sampling is completely asynchronous, and the single condition is that previous bit synchronization of the desired user has been achieved, i.e., $\tau_1 \in [0, T)$, where without loss of generality we have assumed that the first user is the desired one. If the duration of the transmitted chip-shaping waveform is $T_c$, or smaller, only two consecutive symbols from the desired user contribute to $\mathbf{y}_l(i)$. For instance, this occurs with rectangular chip-shaping transmitted pulses and is a good approximation for other pulse types as well. In any case, if the adjacent bits are also present in that vector due to the tails of the chip-shaping pulse, then their tiny contribution will be lumped together in the noise term, as justified in [Mad97]. Therefore, the desired contribution of the first user to the vector $\mathbf{y}_l(i)$ can be expressed as follows

$$\mathbf{y}_{l,1}(i) = \alpha_{l,1}\mathbf{A}^{(1)}(\tau_1)\,\mathbf{d}_1(i) \ , \tag{5.5}$$

where

$$\mathbf{d}_1(i) = \left[ \begin{array}{cc} d_1(i) & d_1(i-1) \end{array} \right]^T \tag{5.6}$$

$$\mathbf{A}^{(1)}(\tau_1) = \left[ \begin{array}{cc} \mathbf{a}_+^{(1)}(\tau_1) & \mathbf{a}_-^{(1)}(\tau_1) \end{array} \right] \tag{5.7}$$

$$\left[\mathbf{a}_+^{(1)}(\tau_1)\right]_r = p_1(rT_s - \tau_1) \qquad r = 1...PQ \tag{5.8}$$

$$\left[\mathbf{a}_-^{(1)}(\tau_1)\right]_r = p_1(rT_s + T - \tau_1) \qquad r = 1...PQ\ . \tag{5.9}$$

The matrix $\mathbf{A}^{(1)}(\tau_1)$ contains the temporal signatures of the desired user. To simplify our notation, in the sequel we will drop the superscript $(\cdot)^{(1)}$. At this point, we can write the received $PQ \times 1$ vector at the $l$th sensor as

$$\mathbf{y}_l(i) = \alpha_{l,1}\, \mathbf{A}(\tau_1)\, \mathbf{d}_1(i) + \mathbf{e}_l(i) \quad i = 0, 1...M-1\ . \tag{5.10}$$

The vector $\mathbf{e}_l(i)$ includes the MAI, the thermal noise, the possible contribution of the adjacent bits, and all other interferences.

## 5.3 Space-Time Model of the Interference

If the temporal vectors received from every antenna are stacked into a space-time $mPQ \times 1$ vector:

$$\mathbf{y}(i) = \left[ \begin{array}{cccc} \mathbf{y}_1^T(i) & \mathbf{y}_2^T(i) & ... & \mathbf{y}_m^T(i) \end{array} \right]^T\ , \tag{5.11}$$

then equation (5.10) can be rewritten in a compact form as

$$\mathbf{y}(i) = (\boldsymbol{\alpha} \otimes \mathbf{A}(\tau_1))\, \mathbf{d}_1(i) + \mathbf{e}(i)\ , \tag{5.12}$$

where $\mathbf{e}(i)$ is formed similarly to $\mathbf{y}(i)$, and

$$\boldsymbol{\alpha} = \left[ \begin{array}{cccc} \alpha_{1,1} & \alpha_{2,1} & ... & \alpha_{m,1} \end{array} \right]^T \tag{5.13}$$

is the spatial signature of the first user. As outlined in the introduction, we model $\mathbf{e}(i)$ as a zero-mean, circularly symmetric, complex Gaussian $mPQ \times 1$ vector, which is independent of $\mathbf{d}_1(i)$ and independent for different samples. Besides, it has an arbitrary and unknown space-time covariance matrix:

$$\mathrm{E}\{\mathbf{e}(i)\} = \mathbf{0} \qquad \mathrm{E}\{\mathbf{e}(i)\, \mathbf{e}^*(l)\} = \mathbf{Q}\, \delta_{i,l}\ . \tag{5.14}$$

There is no doubt that this model is only approximate. Nevertheless, it gathers the most significant effects of all the disturbing signals, and allows us to derive manageable algorithms.

The problem addressed in this chapter may be stated as follows. Estimate $\tau_1$, given the set of samples

$$\mathbf{Y} = \left[ \begin{array}{cccc} \mathbf{y}(0) & \mathbf{y}(1) & \cdots & \mathbf{y}(M-1) \end{array} \right] \tag{5.15}$$

and assuming that $\{c_1(n)\}_{n=0}^{P-1}$ and $\{d_1(i)\}_{i=-1}^{M-1}$ are known, or in other words, that the spreading sequence and the training bit sequence for the desired user are available. Estimates of $\boldsymbol{\alpha}$ and $\mathbf{Q}$, which are taken as deterministic and unstructured parameters, will also be derived. Although we do not parameterize the spatial signature in terms of one or several directions-of-arrival and amplitudes, the array keeps its ability to discriminate the signals in the spatial domain. Assuming an unstructured $\boldsymbol{\alpha}$ eliminates the need for a calibrated antenna array, and allows us to model a cluster of coherent arrivals that share the same time delay, without estimating the individual parameters of each arrival. The unstructured modeling of the spatial signatures is another connecting theme of this thesis, and further remarks on this topic can be found on Chapters 2 and 3.

It is well known that the assumption that the MAI is white in a sample-by-sample basis is a misconception [Ver97] that leads to non near-far resistant estimators because it neglects the temporal structure of the MAI. Although the estimator proposed herein assumes that the interference is Gaussian, it does not suffer from the same misconception since it retains the structure of the MAI in the matrix $\mathbf{Q}$, and so it is near-far resistant. Actually, it is the fact that an unknown correlation matrix $\mathbf{Q}$ is considered for the *equivalent noise* $\mathbf{e}(i)$ that makes the estimator able to attenuate any interfering signal that exhibits a certain structure in the temporal and/or spatial domains. In this chapter, we present the estimator that results from an arbitrary matrix $\mathbf{Q}$, in contrast to previous work that has solved the problem stated herein for simplified structures of that matrix. The signal model proposed in [Liu98a] may seem at first glance rather different from the one proposed above. Nonetheless, it can be shown that they are closely related. In [Liu98a], it is implicitly assumed that the space-time correlation matrix can be decomposed as $\mathbf{Q} = \mathbf{Q}_{sp} \otimes \mathbf{I}_{PQ}$, where $\mathbf{Q}_{sp}$ is an arbitrary $m \times m$ matrix that corresponds to the spatial correlation of the interference. It is apparent that the estimator in [Liu98a] yields suboptimal performance since it ignores the inherent temporal structure of the CDMA signals. A dual decomposition is considered in [Liu98b]. In this case, the matrix $\mathbf{Q}$ is expressed as $\mathbf{Q} = \mathbf{I}_m \otimes \mathbf{Q}_{te}$, where $\mathbf{Q}_{te}$ is a $PQ \times PQ$ matrix representing the temporal structure of the interference. This model amounts to presuming that the fading coefficients $\alpha_{l,k}$ for all users are uncorrelated between different antennas and that the observation interval is long enough (compared with $T_{coh}$) to apply ergodicity; but this last condition is not satisfied in the case of slow fading.

## 5.4 Maximum Likelihood Estimator

In this section, the estimator of the code-timing of the desired user is derived by applying the ML principle [Kay93, Sch90] to the signal model described above. Next, several techniques that may serve to improve the quality of the estimate of the noise-plus-interference correlation matrix are discussed.

### 5.4.1 Derivation

Ignoring in the sequel parameter-independent additive and multiplicative terms, the negative log-likelihood function of the observed data $\mathbf{Y}$ is easily shown to be

$$\Lambda_1(\tau_1, \boldsymbol{\alpha}, \mathbf{Q}) = \ln|\mathbf{Q}| + \mathrm{Tr}\left\{\mathbf{Q}^{-1}\,\mathbf{C}(\tau_1, \boldsymbol{\alpha})\right\}\ , \tag{5.16}$$

where we have defined

$$\mathbf{C}(\tau_1, \boldsymbol{\alpha}) = \frac{1}{M}\sum_{i=0}^{M-1}\left(\mathbf{y}(i) - \mathbf{B}(\tau_1, \boldsymbol{\alpha})\ \mathbf{d}_1(i)\right)\left(\mathbf{y}(i) - \mathbf{B}(\tau_1, \boldsymbol{\alpha})\ \mathbf{d}_1(i)\right)^* \quad mPQ \times mPQ \tag{5.17}$$

$$\mathbf{B}(\tau_1, \boldsymbol{\alpha}) = \boldsymbol{\alpha} \otimes \mathbf{A}(\tau_1) \qquad\qquad mPQ \times 2\ . \tag{5.18}$$

Note that the columns of $\mathbf{B}(\tau_1, \boldsymbol{\alpha})$ are the joint space-time signatures of the desired user. Assuming for the moment that $\mathbf{C}(\tau_1, \boldsymbol{\alpha})$ is non-singular and using the results of the two previous chapters, it is immediate that the ML estimate of $\mathbf{Q}$ is

$$\hat{\mathbf{Q}}_{ML}(\tau_1, \boldsymbol{\alpha}) = \mathbf{C}(\tau_1, \boldsymbol{\alpha})\ . \tag{5.19}$$

Let us define the following matrices

$$\hat{\mathbf{B}} = \left[\ \hat{\mathbf{b}}_+ \quad \hat{\mathbf{b}}_-\ \right] = \hat{\mathbf{R}}_{yd}\,\hat{\mathbf{R}}_{dd}^{-1} \tag{5.20}$$

$$\hat{\mathbf{R}}_{yy} = \frac{1}{M}\sum_{i=0}^{M-1}\mathbf{y}(i)\ \mathbf{y}^*(i) \qquad\qquad \hat{\mathbf{R}}_{dd} = \frac{1}{M}\sum_{i=0}^{M-1}\mathbf{d}_1(i)\ \mathbf{d}_1^*(i) \tag{5.21}$$

$$\hat{\mathbf{R}}_{yd} = \frac{1}{M}\sum_{i=0}^{M-1}\mathbf{y}(i)\ \mathbf{d}_1^*(i) \qquad\qquad \hat{\mathbf{W}} = \hat{\mathbf{R}}_{yy} - \hat{\mathbf{R}}_{yd}\,\hat{\mathbf{R}}_{dd}^{-1}\hat{\mathbf{R}}_{yd}^* = \hat{\mathbf{R}}_{yy} - \hat{\mathbf{B}}\,\hat{\mathbf{R}}_{dd}\,\mathbf{B}^*\ . \tag{5.22}$$

Matrices $\hat{\mathbf{B}}$ and $\hat{\mathbf{W}}$ are unstructured estimates of $\mathbf{B}$ and the noise correlation matrix $\mathbf{Q}$, respectively. They are called unstructured because they do not exploit the space-time structure of the desired user's signature. When (5.19) is substituted into (5.16), the following concentrated

likelihood function results

$$\begin{aligned}
\Lambda_2(\tau_1, \boldsymbol{\alpha}) &= \ln |\mathbf{C}(\tau_1, \boldsymbol{\alpha})| \\
&= \ln \left| \hat{\mathbf{R}}_{yy} - \mathbf{B}(\tau_1, \boldsymbol{\alpha})\, \hat{\mathbf{R}}_{yd}^{*} - \hat{\mathbf{R}}_{yd}\, \mathbf{B}^{*}(\tau_1, \boldsymbol{\alpha}) + \mathbf{B}(\tau_1, \boldsymbol{\alpha})\, \hat{\mathbf{R}}_{dd}\, \mathbf{B}^{*}(\tau_1, \boldsymbol{\alpha}) \right| && (5.23) \\
&= \ln \left| \hat{\mathbf{W}} + \left( \mathbf{B}(\tau_1, \boldsymbol{\alpha}) - \hat{\mathbf{B}} \right) \hat{\mathbf{R}}_{dd} \left( \mathbf{B}(\tau_1, \boldsymbol{\alpha}) - \hat{\mathbf{B}} \right)^{*} \right| && (5.24) \\
&= \ln \left| \hat{\mathbf{W}} \right| + \ln \left| \mathbf{I} + \hat{\mathbf{W}}^{-1} \left( \mathbf{B}(\tau_1, \boldsymbol{\alpha}) - \hat{\mathbf{B}} \right) \hat{\mathbf{R}}_{dd} \left( \mathbf{D}(\tau_{\mathbf{1}}, \boldsymbol{\alpha}) - \hat{\mathbf{B}} \right)^{*} \right| && (5.25) \\
&= \ln \left| \hat{\mathbf{W}} \right| + \ln \left| \mathbf{I} + \left( \mathbf{B}(\tau_1, \boldsymbol{\alpha}) - \hat{\mathbf{B}} \right)^{*} \hat{\mathbf{W}}^{-1} \left( \mathbf{B}(\tau_1, \boldsymbol{\alpha}) - \hat{\mathbf{B}} \right) \hat{\mathbf{R}}_{dd} \right| . && (5.26)
\end{aligned}$$

A significant difference between the problem addressed in this chapter and those addressed in the previous two is that now the matrix $\hat{\mathbf{W}}$ is independent of the parameters, and the dependence on the desired-signal parameters is restricted to the signatures $\mathbf{B}(\tau_1, \boldsymbol{\alpha})$. Only the last term of (5.26) is parameter-dependent. On the other hand, in the problem addressed in Chapter 3, the ML cost function was the determinant of the estimated correlation matrix (see equation (3.21)), which in the present case would be the first term of (5.26). And in the problem of Chapter 4, both terms depended on the parameters.

The function in (5.26) can be minimized in closed-form with respect to $\boldsymbol{\alpha}$. However, the derivation is very cumbersome yet not complicate, and it will not be presented herein. The resulting estimate of $\boldsymbol{\alpha}$ could be substituted back into (5.26), and a one-dimensional criterion for the estimation of the delay would result. Instead of minimizing $\Lambda_2(\tau_1, \boldsymbol{\alpha})$, we will transform this function into another that is asymptotically (in $M$, throughout the chapter) equivalent and allows a simpler derivation of the estimates, as in [Zhe97, Liu98b]. An asymptotic approximation is also used in [Liu98a], but it can be easily shown that the approximation is unnecessary in that case. It may be argued that since $M$ is the length of the training sequence, we will never reach asymptotics in $M$. Nevertheless, the development below is completely meaningful because numerical results show that the asymptotic behavior is reached for rather modest sample sizes.

According to the Weak Law of Large Numbers:

$$\hat{\mathbf{B}} = \mathbf{B}(\check{\tau}_1, \check{\boldsymbol{\alpha}}) + O_p\left(1/\sqrt{M}\right) \tag{5.27}$$

$$\hat{\mathbf{R}}_{dd} = \sigma_d^2\, \mathbf{I} + O_p\left(1/\sqrt{M}\right) , \tag{5.28}$$

where $\check{\tau}_1$ and $\check{\boldsymbol{\alpha}}$ are the true values of the parameters. Thanks to equation (5.27), we can replace $\hat{\mathbf{R}}_{dd}$ by its asymptotic value and neglect the second- and higher-order terms in the Taylor expansion of the second logarithm in (5.26), while retaining the same asymptotic accuracy of the estimates. The Taylor expansion of the logarithm of the determinant is

$$\ln |\mathbf{I} + \mathbf{X}| = \mathrm{Tr}\{\mathbf{X}\} - \frac{1}{2}\mathrm{Tr}\left\{\mathbf{X}^2\right\} + \cdots , \tag{5.29}$$

which is valid whenever the absolute values of the eigenvalues of $\mathbf{X}$ are bounded by one. There-

fore, the asymptotically equivalent ML criterion can be expressed as follows

$$\Lambda_3(\tau_1,\boldsymbol{\alpha}) = \mathrm{Tr}\left\{\left(\mathbf{B}(\tau_1,\boldsymbol{\alpha})-\hat{\mathbf{B}}\right)^* \hat{\mathbf{W}}^{-1}\left(\mathbf{B}(\tau_1,\boldsymbol{\alpha})-\hat{\mathbf{B}}\right)\right\} \tag{5.30}$$

$$= \left(\boldsymbol{\alpha}\otimes\mathbf{a}_+(\tau_1)-\hat{\mathbf{b}}_+\right)^* \hat{\mathbf{W}}^{-1}\left(\boldsymbol{\alpha}\otimes\mathbf{a}_+(\tau_1)-\hat{\mathbf{b}}_+\right)$$
$$+\left(\boldsymbol{\alpha}\otimes\mathbf{a}_-(\tau_1)-\hat{\mathbf{b}}_-\right)^* \hat{\mathbf{W}}^{-1}\left(\boldsymbol{\alpha}\otimes\mathbf{a}_-(\tau_1)-\hat{\mathbf{b}}_-\right) . \tag{5.31}$$

It is convenient to write this cost function in such a way that the linear and quadratic dependences on $\boldsymbol{\alpha}$ are made more explicit, which will facilitate the minimization with respect to this vector. An equivalent expression for (5.31) is

$$\begin{aligned}\Lambda_3(\tau_1,\boldsymbol{\alpha}) = &-2\,\mathrm{Re}\{\boldsymbol{\alpha}^*\mathbf{p}_+(\tau_1)\}+\boldsymbol{\alpha}^*\mathbf{F}_+(\tau_1)\,\boldsymbol{\alpha}\\ &-2\,\mathrm{Re}\{\boldsymbol{\alpha}^*\mathbf{p}_-(\tau_1)\}+\boldsymbol{\alpha}^*\mathbf{F}_-(\tau_1)\,\boldsymbol{\alpha}\\ &+\hat{\mathbf{b}}_+^*\hat{\mathbf{W}}^{-1}\hat{\mathbf{b}}_+ + \hat{\mathbf{b}}_-^*\hat{\mathbf{W}}^{-1}\hat{\mathbf{b}}_- ,\end{aligned} \tag{5.32}$$

where we have defined[1]

$$\mathbf{p}_\pm(\tau_1) = \mathrm{mat}^T_{PQ\times m}\left\{\hat{\mathbf{W}}^{-1}\hat{\mathbf{b}}_\pm\right\}\mathbf{a}^c_\pm(\tau_1) \tag{5.33}$$

$$\mathbf{F}_\pm(\tau_1) = \left(\mathbf{I}_m\otimes\mathbf{a}^*_\pm(\tau_1)\right)\hat{\mathbf{W}}^{-1}\left(\mathbf{I}_m\otimes\mathbf{a}_\pm(\tau_1)\right) . \tag{5.34}$$

At this point, the minimization of (5.32) with respect to $\boldsymbol{\alpha}$ is immediate and yields

$$\hat{\boldsymbol{\alpha}}_{ML} = \left(\mathbf{F}_+(\tau_1)+\mathbf{F}_-(\tau_1)\right)^{-1}\left(\mathbf{p}_+(\tau_1)+\mathbf{p}_-(\tau_1)\right) . \tag{5.35}$$

After substituting (5.35) into (5.32), the timing estimator is obtained as

$$\hat{\tau}_{1,ML} = \arg\max_{\tau_1}\left(\mathbf{p}_+(\tau_1)+\mathbf{p}_-(\tau_1)\right)^*\left(\mathbf{F}_+(\tau_1)+\mathbf{F}_-(\tau_1)\right)^{-1}\left(\mathbf{p}_+(\tau_1)+\mathbf{p}_-(\tau_1)\right) , \tag{5.36}$$

which only involves the minimization of a one-dimensional cost function.

A possible approach to extend this estimator to frequency-selective channels consists in modifying the signal model in (5.12). The new model should take explicitly into account the fact the signal of the desired user arrives at the antenna array through $R_1$ propagation paths having different delays and different spatial signatures. This is the approach followed in [Ert00, Ran00] for a single-antenna receiver. Its serious drawback is that the application of the ML principle to the new signal model results in a highly complex multidimensional optimization problem. However, it is important to remark that a much simpler alternative is also possible. It simply boils down to employing the cost function derived for flat-fading channels, given by (5.36), also for frequency-selective channels. The estimates of the delays of the $R_1$ propagation paths are

[1] The definition of $\mathrm{mat}_{PQ\times m}\{\cdot\}$ is in Appendix A.

obtained as the values that yield the largest $R_1$ maxima of that cost function, while in the flat-fading case only the absolute maximum is picked. This simple modification is meaningful when the delay-spacing between the different propagation paths is greater than the reciprocal of the signal bandwidth (see [Par96b]). A similar approach was used in [Par96b] to extend a MUSIC-based estimator, initially derived for flat-fading channels, to frequency-selective channels. In any case, this chapter is focused on the flat-fading case, and a deeper analysis for another type of channels is out of scope.

### 5.4.2 Covariance Matrix Estimation

The advantage of exploiting the space-time structure of the signals is that every antenna adds $PQ$ degrees of freedom to the system, whereas each user occupies only two degrees and each external punctual interferer occupies between 1 and $PQ$ depending on its bandwidth. As angular and/or Doppler spread of the channel increases, the number of degrees of freedom used by each user or interferer also increases. Using space-time diversity, a large number of degrees of freedom is achieved with few sensors. The price to be paid is that a longer training sequence may be needed, at least theoretically, with respect to other approaches that only exploit one source of diversity but provide a much smaller number of degrees of freedom. In order that $\hat{\mathbf{W}}$ be non-singular with probability one, we need $M \geq mPQ + 2$, which may result in too large of a training sequence. To shed light on how this restriction on $M$ can be alleviated, it is convenient to analyze the eigenstructure of the correlation matrix $\mathbf{Q}$. The eigendecomposition of $\mathbf{Q}$ is given by

$$\mathbf{Q} = \mathbf{V}\,\mathbf{\Sigma}\,\mathbf{V}^*\,, \tag{5.37}$$

where $\mathbf{\Sigma}$ is a diagonal matrix made up of the eigenvalues $\{\lambda_i\}$ of $\mathbf{Q}$ in descending order, and the columns of $\mathbf{V}$ are the corresponding eigenvectors. The eigenvalues satisfy the following relation

$$\lambda_1 \geq \cdots \geq \lambda_L \geq \lambda_{L+1} = \cdots = \lambda_{mPQ} = \sigma_w^2\,, \tag{5.38}$$

where $L$ is the dimension of the *interference subspace*, which is spanned by the first $L$ columns of $\mathbf{V}$, and $\sigma_w^2$ is the power of the white noise. The subspace spanned by the last $mPQ - L$ columns of $\mathbf{V}$ is referred to as *noise subspace*.

Since $\hat{\mathbf{W}}$ is a consistent estimate of $\mathbf{Q}$, the eigenvalues of $\hat{\mathbf{W}}$ tend to those of $\mathbf{Q}$ when $M$ grows without limit. However, if $M < mPQ+2$, some eigenvalues of $\hat{\mathbf{W}}$ are zero, and hence the inverse of this matrix does not exist. Moreover, when $M$ is only slightly greater that $mPQ+2$, some eigenvalues of $\hat{\mathbf{W}}$ may be very small. The inversion of an ill-conditioned matrix can cause numerical unstability and impair the performance of the estimator. Nevertheless, the inequality $M \geq mPQ+2$ should not be a necessary condition for the application of the estimator, since as long as $M$ is much greater than $L$, appropriate estimates of the interference and noise subspaces

of $\mathbf{Q}$ can be obtained. To this end, a parametric (or structured) estimate of $\mathbf{Q}$ is derived, which we designate $\hat{\mathbf{W}}_s$. This new estimate is obtained from $\hat{\mathbf{W}}$, but we force it to have the structure given by (5.37) and (5.38), instead of being fully unstructured. The matrix $\hat{\mathbf{W}}_s$ is taken as the one that is closest to $\hat{\mathbf{W}}$ in the sense of the Frobenius-norm. Thus, assuming that $\hat{\mathbf{W}}_s = \hat{\mathbf{P}} + \hat{\sigma}^2\mathbf{I}$ and that the rank of $\hat{\mathbf{P}}$ is $L$, the problem that we have to solve can be stated as

$$\left[\begin{array}{cc} \hat{\mathbf{P}} & \hat{\sigma}^2 \end{array}\right] = \arg \min_{\sigma^2, \mathbf{P}\,|\,\mathrm{rank}\{\mathbf{P}\}=L} \left\| \hat{\mathbf{W}} - \mathbf{P} - \sigma^2\,\mathbf{I} \right\|_F^2 . \tag{5.39}$$

It is well-known that the solution of this problem is given by

$$\hat{\mathbf{P}} = \sum_{k=1}^{L} \left(\hat{\lambda}_k - \hat{\sigma}^2\right) \hat{\mathbf{v}}_k \hat{\mathbf{v}}_k^* \tag{5.40}$$

$$\hat{\sigma}^2 = \frac{1}{mPQ - L} \sum_{k=L+1}^{mPQ} \hat{\lambda}_k \ , \tag{5.41}$$

where $\hat{\mathbf{v}}_k$ and $\hat{\lambda}_k$ are the eigenvectors and eigenvalues of $\hat{\mathbf{W}}$ in decreasing order. The use in (5.35) and (5.36) of the structured estimate $\hat{\mathbf{W}}_s$ not only avoids the previous bound on $M$ for the application of the estimator, but also improves the performance for all values of $M$. We assume that an estimate of the dimension $L$ is available. It can be inferred either from the knowledge of certain system parameters, such as the number of active users, angular spread, etc., or applying multiplicity tests on the smallest eigenvalues of $\hat{\mathbf{W}}$ [Ris78, Aka74, Wax85]. This is a non-trivial issue that will not be addressed in this thesis. The same approach to obtain a structured estimate of the correlation matrix was applied in [Ben98, Ert00], but instead the 2-norm was used. In [Har00] a related method, known as "eigenvalue thresholding", is proposed and derived using the ML principle with a noise floor constraint. It involves an eigendecomposition and requires the knowledge of the white noise power, but not the knowledge of the rank of the interference subspace.

Another alternative for eliminating the problems related to the inversion of $\hat{\mathbf{W}}$ is to use the widespread *diagonal loading* technique [Car88]. It simply consists in replacing $\hat{\mathbf{W}}$ by another estimate $\hat{\mathbf{W}}_d$ obtained as

$$\hat{\mathbf{W}}_d = \hat{\mathbf{W}} + \lambda\,\mathbf{I} \ , \tag{5.42}$$

where $\lambda$ should be on the order of $\sigma_w^2$. This is an *ad hoc* technique whose interest lies in its simplicity. However, simulation results have shown that the previous eigenanalysis method performs slightly better. In [Ben98], it is suggested that this improvement is due to the fact that the noise subspace of $\hat{\mathbf{W}}_s$ is white (i.e., flat eigenvalue spectrum), whereas the noise subspaces of $\hat{\mathbf{W}}$ and $\hat{\mathbf{W}}_d$ are colored.

An approach that may seem logical at first glance is to replace the inverse of $\hat{\mathbf{W}}$, when this matrix is singular, by its Moore-Penrose pseudo-inverse $\hat{\mathbf{W}}^\dagger$. Nevertheless, the use of the

pseudo-inverse is not recommended at all because, as shown in Section 5.6, it yields a notably worse performance than the two previous approaches, and besides, its calculation is computationally complex. It requires eigendecomposition and rank determination, like the minimization of the Frobenius-norm. The explanation of the bad performance is simple. In order to mitigate the effect of the interference, the received signals are prewhitened with the inverse of the noise-plus-interference correlation matrix, as shown in (5.33). The dominant component after prewhitening should be the projection onto the noise subspace, since it is orthogonal to the interferences[2]. Whenever the matrix $\hat{\mathbf{W}}$ is non-singular, this desired property is satisfied by any of the approaches above (that is, using $\hat{\mathbf{W}}^{-1} = \hat{\mathbf{W}}^{\dagger}$, $\hat{\mathbf{W}}_s^{-1}$ or $\hat{\mathbf{W}}_d^{-1}$), since the eigenvalues of the noise subspace are much smaller than the rest. Nevertheless, when any of the noise eigenvalues are zero, the pseudo-inverse disregards the projection onto the corresponding eigenvectors. On the contrary, the eigenanalysis method and the diagonal loading assign small values to the null eigenvalues, so that the projection onto the corresponding eigenvectors is emphasized. The poor performance obtained with the pseudo-inverse was also reported in [Ayo99] for a different problem in which a correlation matrix was also estimated using a reduced sample support.

The discussion above does not intend to be a formal or complete study of the application of the ML principle with singular or ill-conditioned correlation matrices. This is a open issue that deserves a much deeper analysis. Our goal has only been to show that the unstructured estimate of the correlation matrix can be suitably transformed in order to deal with short training sequences.

## 5.5 Cramér-Rao Bound

It can be proven that the ML estimators (5.35), (5.19) and (5.36) are consistent as long as the signals to which they are applied satisfy the model presented in Sections 5.2 and 5.3 (see, e.g., [Söd89]). The consistency of $\hat{\tau}_{1,ML}$ and $\hat{\boldsymbol{\alpha}}_{ML}$ follows immediately from equations (5.27) and (5.31). The consistency of $\hat{\mathbf{Q}}_{ML}$ is a direct implication of the consistency of $\hat{\tau}_{1,ML}$ and $\hat{\boldsymbol{\alpha}}_{ML}$, and equation (5.19). Since *all* the ML estimates are consistent, they are also asymptotically efficient [Leh83, Section 6.4], that is, their asymptotic covariance coincides with the Cramér-Rao Bound (CRB).

According to the model under consideration, the $M$ observations of $\mathbf{y}(i)$ are independent circular Gaussian vectors with mean $\boldsymbol{\mu}(i) = \mathbf{B}(\tau_1, \boldsymbol{\alpha})\,\mathbf{d}_1(i)$ and covariance $\mathbf{Q}$. The parameters[3] of this model are $\boldsymbol{\eta_s} = [\mathrm{Re}\{\boldsymbol{\alpha}^{\boldsymbol{T}}\}, \mathrm{Im}\{\boldsymbol{\alpha}^{\boldsymbol{T}}\}, \tau_1]^T$ and $\mathbf{Q}$. The Bangs-Slepian's formula [Kay93,

[2] In this discussion we are implicitly assuming that interferences are much powerful than the background noise. This situation is habitual in mobile communication systems, since they usually are limited by interferences.

[3] Actually, the parameters corresponding to $\mathbf{Q}$ are its real and imaginary parts. For the sake of simplicity, this fact is not detailed since it does not affect the computation of the CRB for $\boldsymbol{\eta_s}$.

chapter 15] for the $k,l$th element of the Fisher Information Matrix (FIM) is

$$[\mathbf{FIM}]_{kl} = M \,\mathrm{Tr}\left\{\mathbf{Q}^{-1}\,\mathbf{Q}'_k\,\mathbf{Q}^{-1}\,\mathbf{Q}'_l\right\} + 2\,\mathrm{Re}\left\{\sum_{i=0}^{M-1}\left(\boldsymbol{\mu}'_k\,(i)\right)^*\mathbf{Q}^{-1}\boldsymbol{\mu}'_l\,(i)\right\}\,, \tag{5.43}$$

where $(\cdot)'_k$ denotes the derivative with respect to the $k$th parameter. Since $\boldsymbol{\mu}\,(i)$ and $\mathbf{Q}$ depend on different parameters, the FIM is block diagonal with respect to $\boldsymbol{\eta_s}$ and $\mathbf{Q}$. Therefore, the CRB for $\boldsymbol{\eta_s}$ is the same whether $\mathbf{Q}$ is known or not, and vice versa. As we are concerned only with the CRB for the signal parameters ($\boldsymbol{\eta_s}$), we need only consider the second term in (5.43). The CRB for $\boldsymbol{\eta_s}$ is the inverse of the corresponding block of the FIM, and it can be written as

$$\mathbf{CRB}^{-1}\,(\boldsymbol{\eta_s}) = 2\,\mathrm{Re}\left\{\begin{bmatrix} \mathbf{F}_1 & j\mathbf{F}_1 & \mathbf{F}_2\,\boldsymbol{\alpha} \\ -j\mathbf{F}_1^* & \mathbf{F}_1 & -j\mathbf{F}_2\,\boldsymbol{\alpha} \\ \boldsymbol{\alpha}^*\mathbf{F}_2^* & j\boldsymbol{\alpha}^*\mathbf{F}_2^* & \boldsymbol{\alpha}^*\mathbf{F}_3\,\boldsymbol{\alpha} \end{bmatrix}\right\}\,, \tag{5.44}$$

where

$$\mathbf{F}_1 = \sum_{i=0}^{M-1}\Big(\mathbf{I}_m \otimes \left(\mathbf{A}\,(\tau_1)\;\mathbf{d}_1\,(i)\right)^*\Big)\,\mathbf{Q}^{-1}\,\Big(\mathbf{I}_m \otimes \left(\mathbf{A}\,(\tau_1)\;\mathbf{d}_1\,(i)\right)\Big) \tag{5.45}$$

$$\mathbf{F}_2 = \sum_{i=0}^{M-1}\Big(\mathbf{I}_m \otimes \left(\mathbf{A}\,(\tau_1)\;\mathbf{d}_1\,(i)\right)^*\Big)\,\mathbf{Q}^{-1}\,\Big(\mathbf{I}_m \otimes \left(\mathbf{D}\,(\tau_1)\;\mathbf{d}_1\,(i)\right)\Big) \tag{5.46}$$

$$\mathbf{F}_3 = \sum_{i=0}^{M-1}\Big(\mathbf{I}_m \otimes \left(\mathbf{D}\,(\tau_1)\;\mathbf{d}_1\,(i)\right)^*\Big)\,\mathbf{Q}^{-1}\,\Big(\mathbf{I}_m \otimes \left(\mathbf{D}\,(\tau_1)\;\mathbf{d}_1\,(i)\right)\Big) \tag{5.47}$$

$$\mathbf{D}\,(\tau_1) \triangleq \begin{bmatrix}\mathbf{d}_+\,(\tau_1) & \mathbf{d}_-\,(\tau_1)\end{bmatrix} = \frac{d\mathbf{A}\,(\tau_1)}{d\tau_1}\,. \tag{5.48}$$

It is possible to compute the asymptotic values of (5.45)-(5.47). Recalling that $\hat{\mathbf{R}}_{dd} \to \sigma_d^2\,\mathbf{I}$, it is not hard to verify that

$$\begin{aligned}\bar{\mathbf{F}}_1 = M \lim_{M\to\infty}\frac{\mathbf{F}_1}{M} = M\,\sigma_d^2\Big(&\left(\mathbf{I}_m \otimes \mathbf{a}_+^*\,(\tau_1)\right)\mathbf{Q}^{-1}\left(\mathbf{I}_m \otimes \mathbf{a}_+\,(\tau_1)\right) \\ &+\left(\mathbf{I}_m \otimes \mathbf{a}_-^*\,(\tau_1)\right)\mathbf{Q}^{-1}\left(\mathbf{I}_m \otimes \mathbf{a}_-\,(\tau_1)\right)\Big)\end{aligned} \tag{5.49}$$

$$\begin{aligned}\bar{\mathbf{F}}_2 = M \lim_{M\to\infty}\frac{\mathbf{F}_2}{M} = M\,\sigma_d^2\Big(&\left(\mathbf{I}_m \otimes \mathbf{a}_+^*\,(\tau_1)\right)\mathbf{Q}^{-1}\left(\mathbf{I}_m \otimes \mathbf{d}_+\,(\tau_1)\right) \\ &+\left(\mathbf{I}_m \otimes \mathbf{a}_-^*\,(\tau_1)\right)\mathbf{Q}^{-1}\left(\mathbf{I}_m \otimes \mathbf{d}_-\,(\tau_1)\right)\Big)\end{aligned} \tag{5.50}$$

$$\begin{aligned}\bar{\mathbf{F}}_3 = M \lim_{M\to\infty}\frac{\mathbf{F}_3}{M} = M\,\sigma_d^2\Big(&\left(\mathbf{I}_m \otimes \mathbf{d}_+^*\,(\tau_1)\right)\mathbf{Q}^{-1}\left(\mathbf{I}_m \otimes \mathbf{d}_+\,(\tau_1)\right) \\ &+\left(\mathbf{I}_m \otimes \mathbf{d}_-^*\,(\tau_1)\right)\mathbf{Q}^{-1}\left(\mathbf{I}_m \otimes \mathbf{d}_-\,(\tau_1)\right)\Big)\,.\end{aligned} \tag{5.51}$$

When these values are substituted into (5.44), an asymptotic expression of the CRB is obtained. The asymptotic CRB is usually preferred because it does not depend on the particular value of the training sequence, and is the one plotted in the figures of the next section.

## 5.6 Simulation Results

In this section we compare the performance of our estimator, referred to as "space-time diversity" (STDiv) estimator, with two of the techniques proposed to date that in most cases give the best results. Namely, we consider the methods presented in [Liu98a] and [Liu98b], which we will denote as "space-diversity" (SDiv) and "time-diversity" (TDiv) estimators, respectively. In these two papers and also in [Zhe97], the SDiv and TDiv methods are compared with a number of different estimators proposed in the literature. Note that the comparison with these two approaches is completely fair since they also use an antenna array in reception. We analyze herein two performance measures:

- Probability of acquisition ($P_{ac}$). We define a correct acquisition to have occurred when the delay estimate is within a half-chip of the true value, i.e., $|\hat{\tau}_{1,ML} - \check{\tau}_1| < T_c/2$.
- The root mean squared error (RMSE) given correct acquisition, i.e.,

$$\mathrm{RMSE}\left(\tau_1\right) = \sqrt{\mathrm{E}\left\{ \left|\hat{\tau}_{1,ML} - \check{\tau}_1\right|^2 \,\middle|\, |\hat{\tau}_{1,ML} - \check{\tau}_1| < T_c/2 \right\}} \tag{5.52}$$

  This measure is relevant for the tracking operation of the estimators.

A method is considered to have failed due to the large number of outliers when $P_{ac} \leq 0.5$. The RMSE is not plotted in this case. We have observed that the three estimators under consideration are essentially unbiased (i.e., their biases are much smaller than their standard deviations). Therefore, the RMSEs are for all practical purposes identical to the standard deviations. All results are obtained from 1000 Monte Carlo realizations. The simulation conditions, except when one of them is varied, are as follows:

- (pseudo)Gold codes with length $P = 15$ chips and BPSK modulation.
- Rectangular chip-shaping transmitted pulses and oversampling factor $Q = 1$.
- Energy per bit to white-noise spectral density ratio (EbNo) equal to 4dB per antenna for the desired user.
- Uniform linear array with $m = 4$ antennas spaced 0.5 wavelengths apart.
- $K = 10$ users, $M = 80$ training bits.
- The power of the signal of each interfering user is distributed log-normally with mean 10dB (with respect to the desired user) and standard deviation 10dB. This distribution models the log-normal fading caused by large-distant reflectors. The near-far ratio (NFR), which is defined as the ratio of the mean power of each interfering user to that of the desired user, is therefore 10dB.

- The carrier phases of the users are uniformly distributed in $[0, 2\pi)$ and changed at each Monte Carlo trial.

- The delays of the users are randomly chosen along all the range of possible values and fixed throughout the simulations. Specifically, the time delays normalized with respect $T_c$ are picked in order from the set {5.50, 6.33, 2.88, 8.83, 13.65, 1.79, 9.89, 1.14, 13.16, 7.91, 0.45, 8.79, 3.69, 6.14, 9.44, 13.79, 8.25, 11.04, 14.84, 5.93, 6.41, 1.43, 8.19, 12.95, 1.19, 5.67, 2.83, 1.92, 13.93, 7.55, 0.59, 3.87, 4.17, 10.65, 0.01, 10.13, 9.29, 2.94, 3.80, 7.25}. Similarly, the mean directions-of-arrival of the users are selected in order from the following values: {0°, 10°, -20°, 30°, -40°, 50°, -60°, 70°, -80°, 85°, -40°, 50°, -60°, 70°, -80°, 85°, 40°, 45°, 65°, -55°, -75°, -15°, -25°, 60°, 20°, 75°, 25°, 60°, -45°, 80°, 15°, 5°, 42°, -57°, -78°, -56°, -48°, 36°, 29°, -33°}. The mean direction of arrival of the external interference is 40°.

We have simulated two different channels. The first, named static channel for short, is a channel that remains constant during the observation interval. This is the situation considered for the signal model in Section 5.2. There is no angular spreading, so each user has a unique spatial signature. Since the Doppler frequency $f_d$ is assumed to be 0, the signals do not suffer from multiplicative distortion (or fast-fading), but only log-normal fading. The amplitude and phase of each user's signal are held fixed during the observation interval, but are varied at each Monte Carlo run in order to model the log-normal fading.

The second channel is a realistic mobile channel for the uplink. It is generated according to the spatio-temporal model described in [Ped00]. Each signal arrives at the array through several rays, all of them with the same delay. The number of rays follows a truncated Poisson law with mean and maximum values equal to 25 and 50. The directions-of-arrival of the rays are generated according to a Gaussian distribution with a given mean and a standard deviation of 5 degrees. This is the value that characterizes the angular spread of the signals. The total power of each signal is divided among its propagation rays following a Laplacian function which depends on the separation between the DOA of the each ray and the mean DOA of the source (see [Ped00] for details). The Doppler spectrum has the classical Clarke's bath-shape [Pro95], obtained by assuming multiple and randomly located reflectors close around the mobile, with normalized maximum Doppler frequency equal to $f_d T = 2 \cdot 10^{-3}$. Therefore, the multiplicative distortion introduced by the channel has approximately a correlation duration of $1/f_d T = 500$ symbols. That value of the factor $f_d T$ may correspond to a system with a usual set of parameters, such as 900MHz carrier frequency, 50kb/s data rate and 120km/h speed, or 1800MHz carrier frequency, 100kb/s data rate and 120km/h speed. Note that for a pedestrian channel the speed is about 3km/h, and therefore the value of $f_d T$ is much smaller.

The structured estimate of the correlation matrix $\hat{\mathbf{W}}_s$ is used in the implementation of the STDiv estimator. In all cases, we have used a value $L$ for the dimension of the interference

subspace that is equal the exact value of this dimension in the static channel. Note that this approach results in a slight under-estimation of the dimension of the interference subspace in the mobile channel.

We first consider the effect of the length of the training sequence $M$. The results are shown in Figure 5.1. The estimator proposed in this chapter is the only one that attains the CRB for the static channel, even though the Gaussian assumption is only an approximate one. This fact corroborates the explanation in Section 5.3 stating that the vectorial Gaussian assumption is reasonable and models the most significant effects of the MAI. The CRB is achieved for lengths of the training sequence larger than 250 bits. For smaller values, there is a very slight degradation with respect to the CRB, which causes the difference between the RMSE and the CRB present in all the next figures. The fact that the difference between the RMSE and the CRB is small for modest sample sizes is also remarkable given that the proposed estimator is a large sample approximation of the exact ML estimator. As expected, the performance of all the estimators deteriorates in the mobile channel, where the RMSE cannot be further reduced by increasing $M$. This impairment should not be interpreted as a failure of the estimators, but only as the effect of working in a much more adverse scenario, and it will be visible in all the following results. As $M$ increases, the multiplicative distortion blurs the signal of the desired user. Then, the *effective* length of the training sequence is no longer equal to $M$, but it is bounded by the temporal correlation of the channel. Also in the mobile channel the STDiv estimator outperforms the other two approaches. The SDiv method presents the largest RMSE and the lowest $P_{ac}$. This is logical since it is the approach with the smallest number of degrees of freedom. Figure 5.1(b) demonstrates the ability of our algorithm to acquire the desired user's delay. As shown in Figure 5.1(a), RMS tracking errors between 0.1 and 0.01 chips can be achieved with windows of less than 100 bits, indicating that the algorithm can be used for tracking of slowly time-varying parameters in decision-directed mode.

In Figure 5.2, we investigate the effect of varying the number of users. This has special interest for a base station that uses spatial-division multiple-access (SDMA), and therefore it may have more users than the length of the codes. Again the STDiv estimator gives better results, both in RMSE and $P_{ac}$, than the other two methods. The SDiv and TDiv approaches experience a serious deterioration, especially in their probabilities of acquisition, when the number of users exceeds the length of the code (i.e., $K > P$), and they completely fail when $K > 2P$ in the scenario under consideration. On the other hand, using the space-time diversity estimator the number of users may be increased beyond twice the code length without an excessive degradation. For instance, note that for $K = 40$ users and the static channel, the probability of acquisition remains virtually equal to 1, and only goes down to 0.82 for the mobile channel.

Next, the effect of a wide-band external interference is analyzed in Figure 5.3. Because of its large bandwidth, the interference does not show any temporal structure, so it can be

mitigated exclusively in the spatial domain. Only the STDiv and SDiv estimators present an adequate performance when the desired signal-to-interference ratio (SIR) is small (e.g., smaller than $< -15$dB before despreading). Their performance is nearly insensitive to the SIR except for extremely low SIR in the mobile channel. Despite everything, the former gives better results than the latter in all the cases. Moreover, the SDiv estimator is not (for the system parameters that we have considered) near-far resistant. In Figure 5.4, the near-far resistance of the different estimators is compared. In the static channel, the RMSE and $P_{ac}$ of the estimator proposed herein and the CRB are totally insensitive to the MAI level, whereas those of the TDiv and SDiv schemes are not. In regard to the probability of acquisition, the STDiv estimator performs satisfactorily in the mobile channel up to a NFR equal to 35dB, which is an improvement of about 8dB and 18dB over the TDiv and SDiv methods, respectively. Further insight into the near-far performance is gained by observing Figure 5.5. A estimator can be considered to be near-far resistant when the RMSE tends to zero and the $P_{ac}$ tends to one as the EbNo decreases, even in the presence of arbitrarily strong MAI. This property is only satisfied by our STDiv estimator, at least in the static channel. The RMSEs of the other two estimators (i.e., the SDiv and TDiv methods) have floor levels due to the MAI that cannot be surpassed by reducing the power of the background white noise.

In Figure 5.6, we examine the relationship between the normalized Doppler $f_dT$ and both the probability of acquisition and the RMSE. These results are obtained for an angular spread with standard deviation equal to 8 degrees. The STDiv estimator performs better than the other two in all the range of values of $f_dT$. The difference between the RMSEs of the different methods is roughly constant as the Doppler is increased. On the other hand, the probability of acquisition of the STDiv estimator is less sensitive to the Doppler than that of the SDiv and TDiv approaches. This figure shows that the performance of the estimator proposed herein is not critically affected by the Doppler spread of the channel. For instance, $P_{ac}$ for our method is approximately 0.92 when $f_dT = 0.01$. This is an excellent result, since the correlation length of the channel is about 100 symbols, and hence on the order of the observation interval.

Our last set of results involves analyzing the performance achieved with different estimates of the correlation matrix. In Figure 5.7, we compare the RMSEs obtained with the structured estimate $\hat{\mathbf{W}}_s^{-1}$ (the one employed in all the simulations above), the pseudo-inverse matrix $\hat{\mathbf{W}}^{\dagger}$ and the diagonally loaded estimate $\hat{\mathbf{W}}_d^{-1}$. The diagonal loading factor is taken equal to the power of the white noise. As foreseen by the discussion in Section 5.4.2, the performance with the pseudo-inverse matrix is always worse than with the other two estimates, and undergoes a severe degradation for short lengths of the training sequence. The RMSEs obtained with the diagonally loaded and the structured estimates are nearly coincident and are better discerned in Figure 5.8. This figure shows that the RMSE of the former is noticeably greater than that of the latter for small loading factors. When the loading factor is equal to or greater than the white-noise power, they perform similarly, but there is always a certain advantage in favor of

the structured estimate, being the advantage more important in the mobile channel.

## 5.7 Conclusions

A code-timing synchronization technique for DS-CDMA systems that operates in near-far, frequency-nonselective, slowly fading channels and employs an arbitrary antenna array for reception has been derived by applying the ML principle. The technique is a large sample approximation of the exact ML estimator. We have taken into account the fact that the signals of the users present definite space-time signatures, what happens because the observation interval is usually much smaller than the correlation length of the channel. As such, the proposed technique is a single-user, near-far resistant estimator and would be applicable in a system employing multiuser detection without power control. For the derivation, it has been assumed that the desired user transmits a known training sequence, and all other received components have been modeled as a Gaussian term with unknown space-time correlation. This approach fully exploits the spatial and temporal structure of the interfering signals in order to cancel them. The knowledge of the spreading waveform (code) of only the desired user is needed, and as a by-product, an estimate of the spatial signature of this user is obtained.

The estimator derived in this chapter contrasts with other methods put forward up to date that also employ antenna arrays but only exploit the structure of the signals in one of the domains. As a result, the proposed technique outperforms existing synchronization methods for reasonable lengths of the training sequence and reasonable sizes of the array. This technique allows to allocate more users than the value the spreading factor of the modulation, and makes possible the coexistence of the DS-CDMA communications system with other wide-band (and also narrow-band) interfering sources. The use of a structured estimate of the correlation matrix or diagonal loading allows to reduce the required size of the observation interval, and provides a better performance than the pseudo-inverse approach. The RMSE and the acquisition probability of the proposed algorithm have been evaluated numerically in two types of channels. Although the estimator is applied in a multiple-access scenario, the RMSE attains in the static channel the CRB derived under the Gaussian assumption, which confirms the validity of the starting model. All the analyzed estimators are deteriorated when the channel presents Doppler and angular spread, but also in this situation, the estimator proposed herein outdoes the other ones. The results of this chapter conclude that the efficient use of the space-time diversity is indispensable for the correct acquisition and tracking of the synchronization parameters in heavily loaded systems and/or in the presence of external interference.

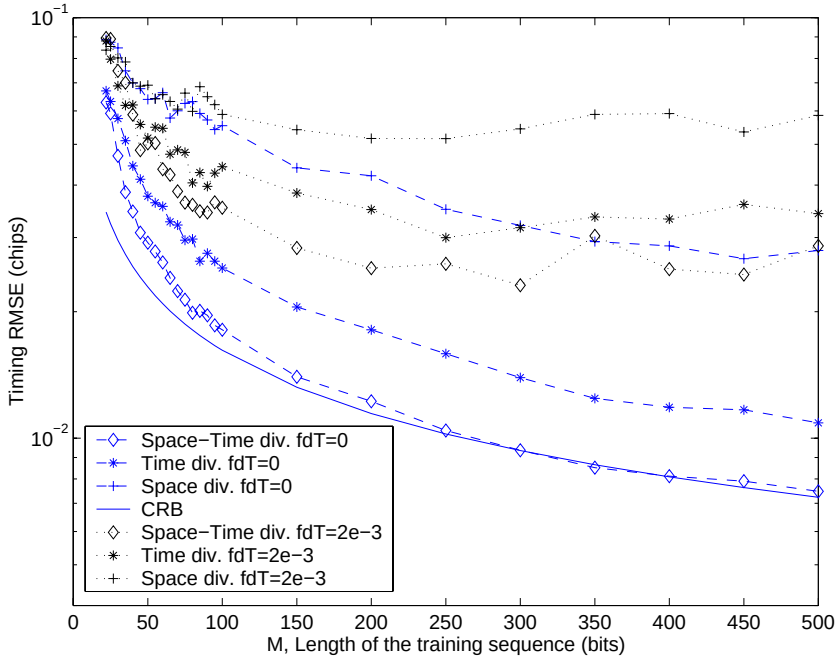


(a) RMSE

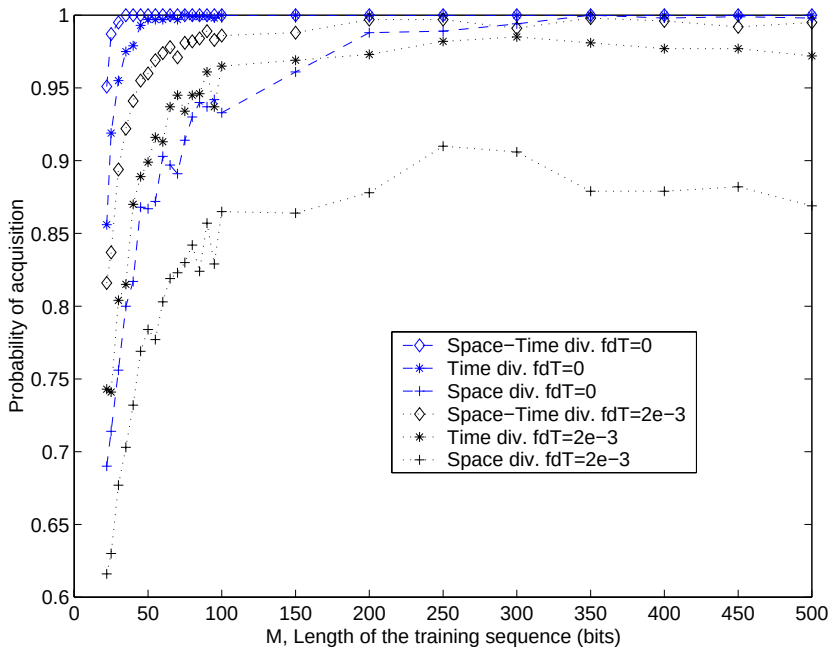


(b) Probability of acquisition

Figure 5.1: Performance of the STDiv, TDiv and SDiv estimators as a function of the length of the training sequence $M$ in two different channels. $K = 10$ users, $P = 15$ chips/bit, $m = 4$ antennas, EbNo $= 4$dB per antenna, NFR $= 10$dB.

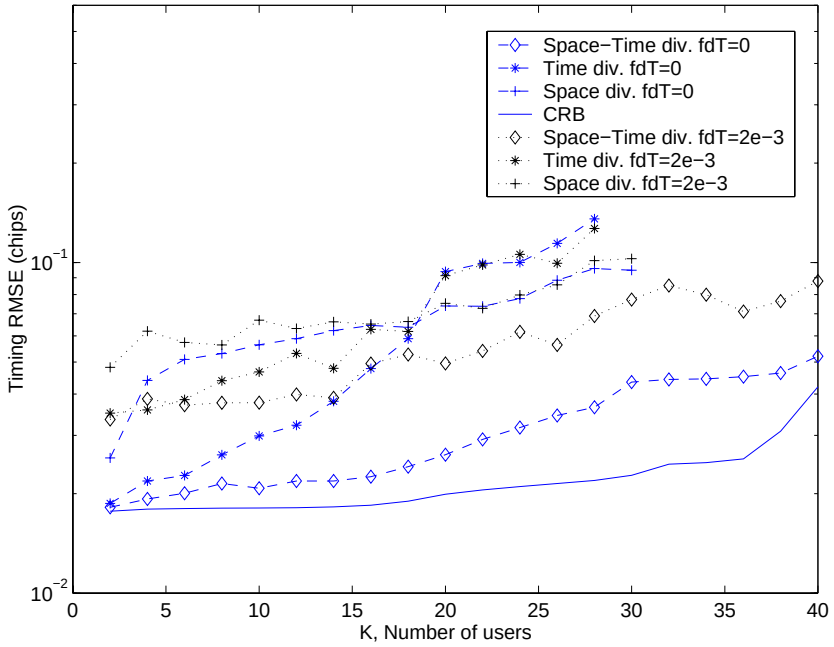


(a) RMSE

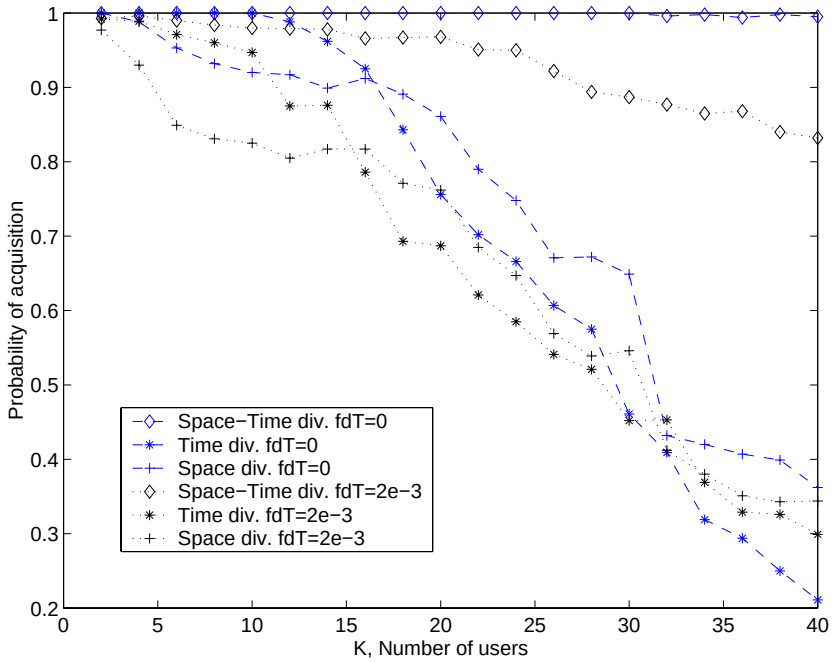


(b) Probability of acquisition

Figure 5.2: Performance of the STDiv, TDiv and SDiv estimators as a function of the number of users $K$ in two different channels. $M = 80$ bits, $P = 15$ chips/bit, $m = 4$ antennas, EbNo $= 4$dB per antenna, NFR $= 10$dB.

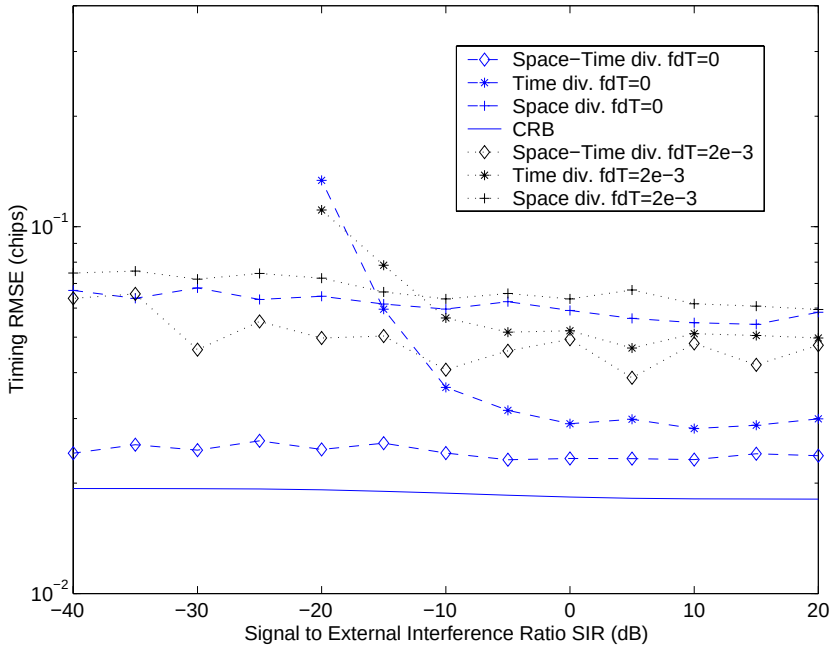


(a) RMSE

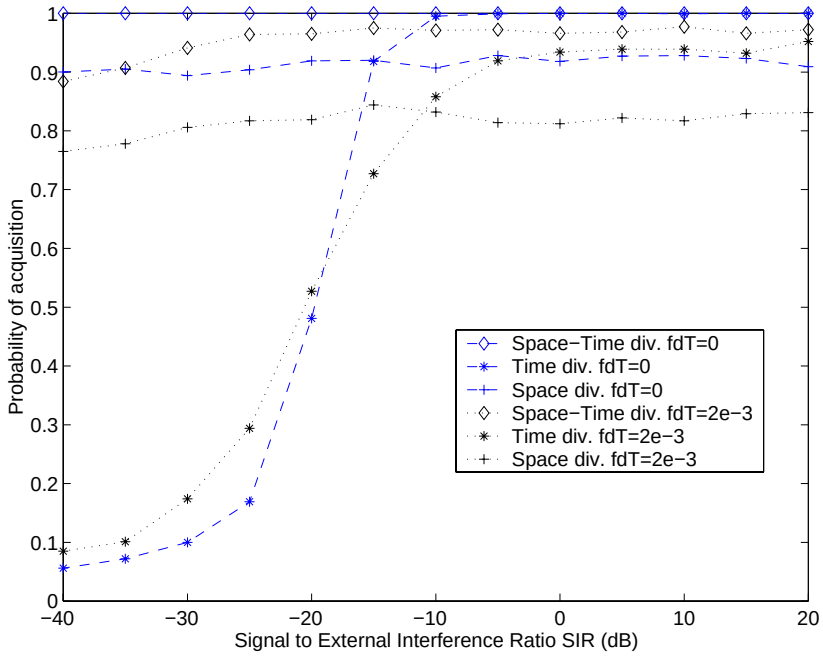


(b) Probability of acquisition

Figure 5.3: Performance of the STDiv, TDiv and SDiv estimators in the presence of a wide-band external interference in two different channels. The SIR is computed before despreading. $M = 80$ bits, $K = 10$ users, $P = 15$ chips/bit, $m = 4$ antennas, EbNo = 4dB per antenna, NFR = 10dB.

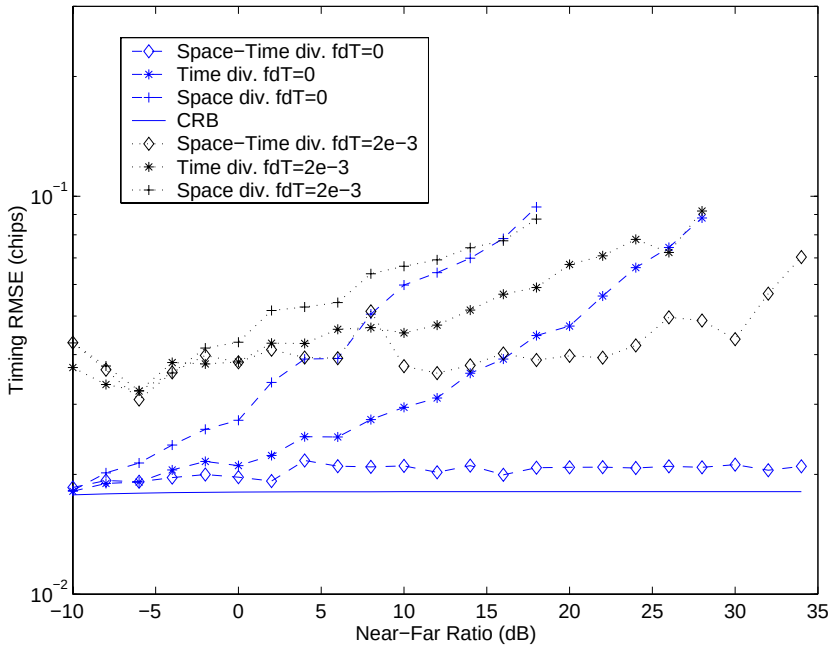


(a) RMSE

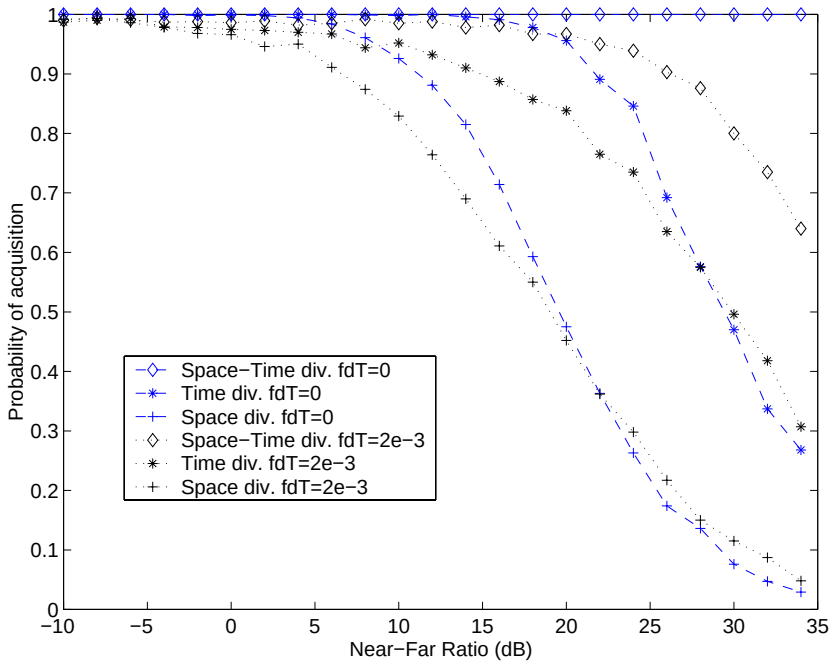


(b) Probability of acquisition

Figure 5.4: Performance of the STDiv, TDiv and SDiv estimators as a function of the near-far ratio NFR in two different channels. $M = 80$ bits, $K = 10$ users, $P = 15$ chips/bit, $m = 4$ antennas, EbNo = 4dB per antenna.

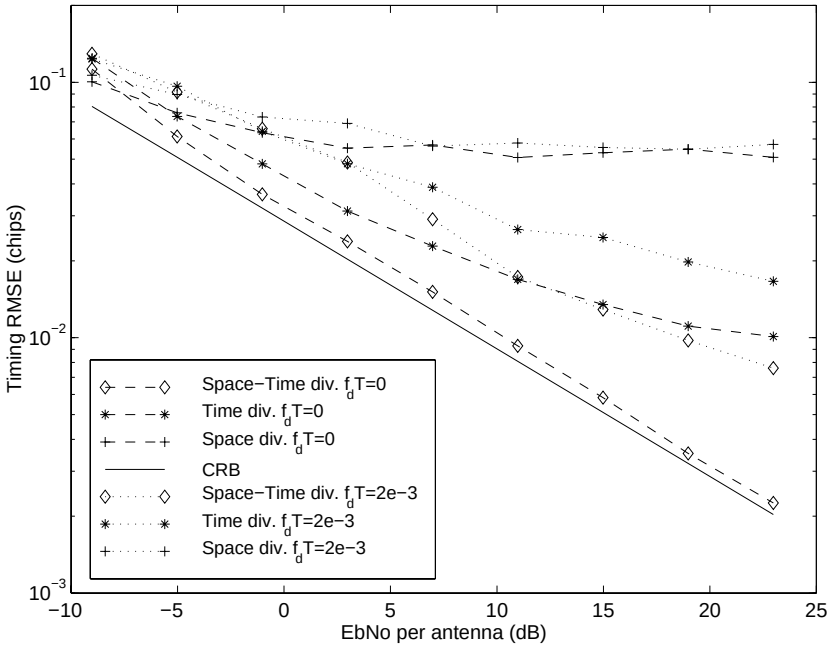


(a) RMSE

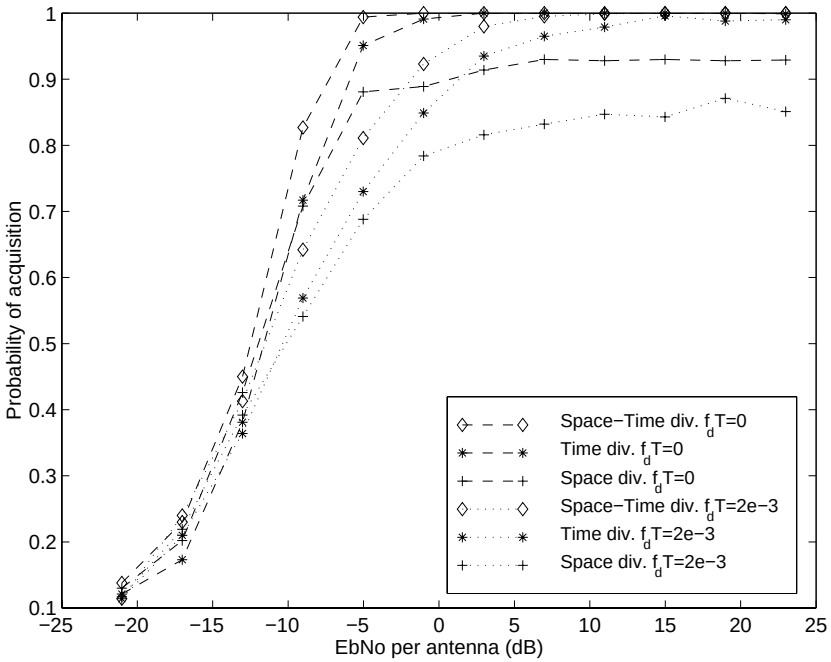


(b) Probability of acquisition

Figure 5.5: Performance of the STDiv, TDiv and SDiv estimators as a function of the EbNo in two different channels. $M = 80$ bits, $K = 10$ users, $P = 15$ chips/bit, $m = 4$ antennas, NFR = 10dB.

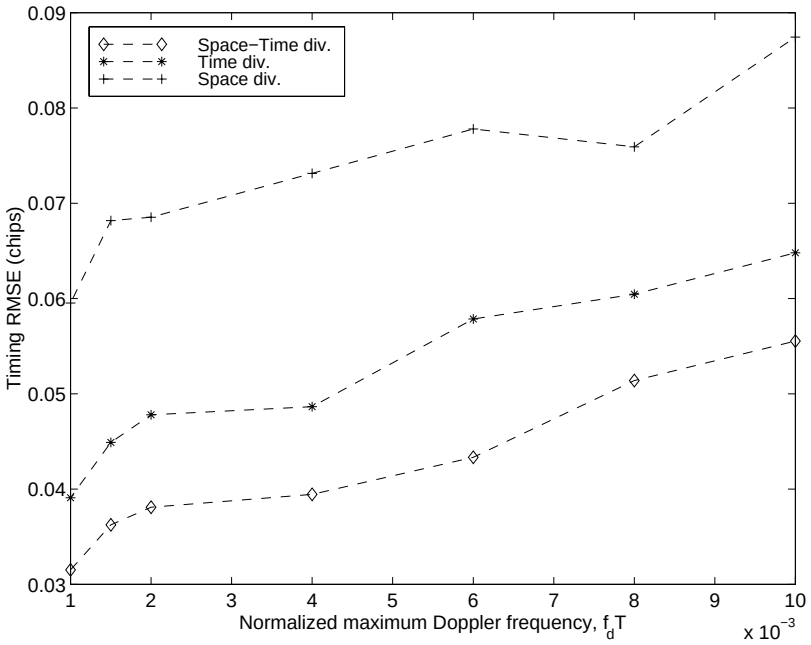


(a) RMSE

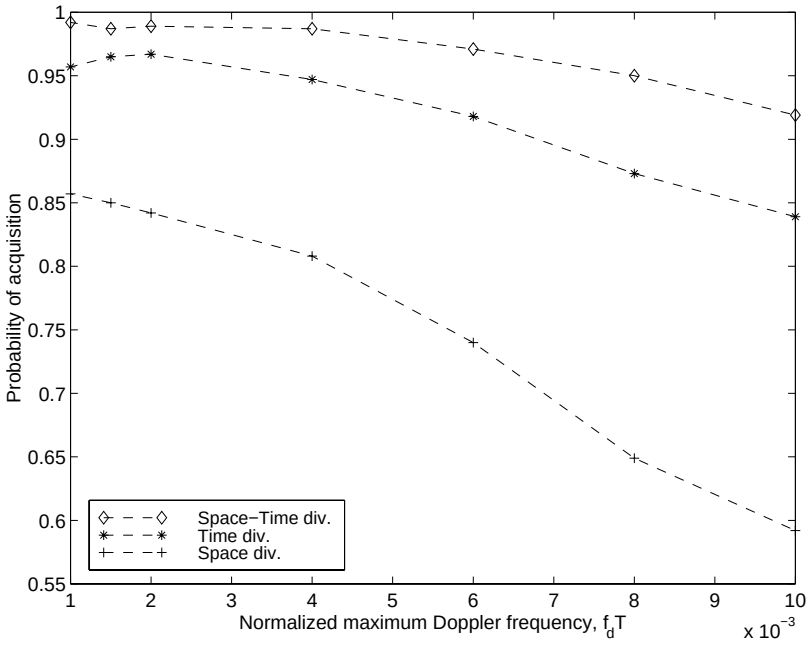


(b) Probability of acquisition

Figure 5.6: Performance of the STDiv, TDiv and SDiv estimators as a function of Doppler spread. $M = 80$ bits, $K = 10$ users, $P = 15$ chips/bit, $m = 4$ antennas, EbNo = 4dB per antenna, NFR = 10dB.

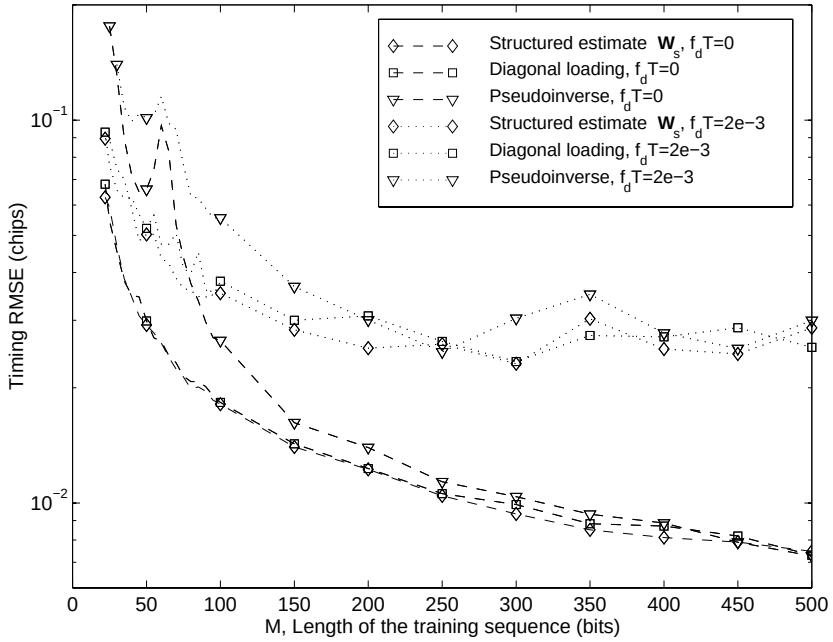


Figure 5.7: Comparison of the performance for three different estimates of the correlation matrix in two different channels. $K = 10$, $P = 15$, $m = 4$, EbNo = 4dB per antenna, NFR = 10dB, $\lambda = \sigma_w^2$.

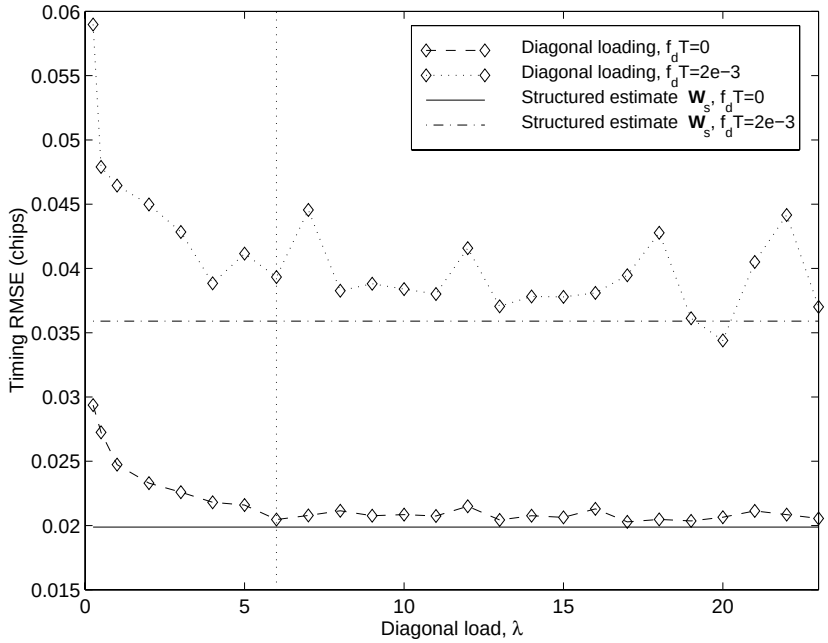


Figure 5.8: Effect of varying the diagonal loading factor in two different channels. The power of the white-noise is $\sigma_w^2 = 6$. $M = 80$ bits, $K = 10$ users, $P = 15$ chips/bit, $m = 4$ antennas, EbNo = 4dB per antenna, NFR = 10dB.

# Chapter 6

# Conclusions and Topics for Future Research

This thesis has dealt with the synchronization (time delay or propagation delay estimation) of one or several replicas of a known signal received by an arbitrary antenna array. A connecting thread along this work is the systematic application of the maximum likelihood principle together with models that include a noise term with an unknown correlation matrix and that use unstructured spatial signatures. The contributions of this thesis have been divided into three parts. The first addresses a general time delay estimation problem, whereas the other two consider signal models that are tailored to a GNSS receiver and to a DS-CDMA multiuser communications receiver. Below we summarize the contributions and the open research topics in each of these parts.

1. In the first part, we have focused on how multiple antennas can be efficiently used in interference-limited scenarios in order to estimate the time delays of multiple replicas of a known signal. A number of techniques have been proposed in the literature for the estimation of the parameters of a multipath channel. In general, the existing techniques present at least one of the following drawbacks: *i)* the resulting multidimensional criteria require computationally demanding optimization procedures, *ii)* the techniques undergo a severe degradation in the presence of directional interference in spite of using an antenna array in the receiver. It was recently shown that the first of the drawbacks can be overcome by assuming that the spatial signatures are deterministic unstructured vectors and that the noise is Gaussian, and spatially and temporally white [Swi98a]. Thus, the time delay estimation problem becomes analogous to the DOA estimation problem with uniform linear arrays, and computationally efficient algorithms, such as IQML and ESPRIT, can be applied. The goal pursued in this part of the thesis is to overcome also the second drawback. To this end, the noise is assumed to have an arbitrary and unknown spatial correlation, in such a way that the resulting estimators are robust against the co-channel interference. The

ML estimator for this problem was derived and shown to be consistent and asymptotically efficient. However, the resulting concentrated ML criterion for the delays is highly non-linear due to the presence of a determinant operator. It is no longer possible to draw parallels between this estimator and the conventional maximum likelihood DOA estimator, and hence the ML time delay estimator does not lead to simple minimization procedures. It was shown how the ML criterion could be approximated by a simpler, asymptotically equivalent cost function. Systematic and heuristic ways of deriving this cost function were presented. The form of the new cost function lends itself to minimization by the IQML algorithm. The existence of simple yet accurate initialization schemes based on ESPRIT and identity weightings makes the approach viable for practical implementation. Note that the implementation with IQML and ESPRIT, despite being iterative, provides closed-form estimates of all the time delays at each iteration, unlike searches based on the expectation-maximization or the alternating-projection algorithms.

The new cost function was also applied to the estimation of the frame delay in a FIR channel. We proposed for this case a formulation of the projector onto the orthogonal complement to the signal subspace that reduced each iteration of the IQML algorithm to the rooting of a polynomial, being its order equal to the length of the FIR channel. The result is a iterative feedforward scheme for frame delay estimation.

Some topics related to this part of the thesis that may be the subject for further investigation are outlined below.

- Study of the conditions for the problem to be identifiable. That is to say, it is interesting to determine what is the maximum number of delays that can be estimated as a function of the waveform of the desired signal, the spatial signatures, and the number of samples and antennas.
- Estimation of the number of received replicas of the desired signal. This problem is complicated by the unknown correlation of the noise. Also, the simulation of the proposed estimator in multipath scenarios with diffuse reflections, and Doppler and angular spread may be of interest.
- Performance comparison between methods resting on an unstructured model for the spatial signatures and those using a structured model.
- Theoretical study of the consistency and efficiency of the IQML algorithm when the data grows in the dimension in which the parameters are estimated. This study is available in the literature for the opposite situation, e.g., when the number of snapshots increases in a DOA estimation problem
- Use of MODE, WSF (weighted subspace fitting) or different variants of IQML that, apart from providing a possible performance improvement, are non-iterative (i.e., asymptotically they only require two iterations). The application of these techniques

is not clear when the dimension of the correlation matrices (not the sample size) grows, and the optimal weighting matrices for the eigenvectors may not be the same as those in the conventional DOA estimation problem.

- Study of the ML time delay estimation problem when a stochastic model is used for the spatial signatures. This issue is closely connected with the problem arising when the signal consists of multiple "incoherent bursts". The performance achieved when the number of bursts increases has to be analyzed both theoretically and via simulations. Although the CRB will not be achieved with the deterministic model, it should be investigated if it can be achieved with the stochastic model and if the MODE or WSF algorithms can be used for this purpose. Also, it could be interesting to investigate if the ML time delay estimator for multiple "incoherent bursts" can be obtained without resorting to the simplifying assumption that the spatial signatures are different at each burst.

The contributions of this part of thesis have been published as

- G. Seco, A.L. Swindlehurst, D. Astély, "Exploiting Antenna Arrays for Synchronization", G. B. Giannakis, P. Stoica, Y. Hua, L. Tong (eds.) *Signal Processing Advances in Communications, Volume II: Trends in Single- and Multi-User Systems*, chap. 10, 35 pages, Prentice-Hall, 2000.
- G. Seco, A.L. Swindlehurst, J.A. Fernández-Rubio, "A Polynomial Rooting Approach for Synchronization in Multipath Channels Using Antenna Array". *Proc. IEEE Signal Processing Workshop on Statistical Signal and Array Processing*, August 2000, Pocono Manor, PA, USA.
- G. Seco, A.L. Swindlehurst, J.A. Fernández-Rubio, D. Astély, "A Reduced-Complexity and Asymptotically Efficient Time-Delay Estimator", *Proc. ICASSP*, pages I:580-583, June 2000, Istambul (Turkey).
- G. Seco, J.A. Fernández-Rubio, A. Lee Swindlehurst, "Multipath Estimation and Interference Mitigation in GNSS Receivers using Antenna Arrays", *Proc. 3rd European Symposium on Global Navigation Satellite Systems, GNSS*, pages 684-689, October 1999, Genoa, Italy.

2. The objective of the estimators presented in the second part of this thesis was to take advantage of one particularity of GNSS systems, which consists in that the DOA of the line-of-sight signal may be known a priori. As long as the antenna array is calibrated, the knowledge of this direction-of-arrival allows to compute beforehand the steering vector of the direct signal, which acts as a spatial reference to this signal. The use of the steering vector of the LOSS is not expected to provide a significant performance improvement of the ML estimators derived using a detailed model of the multipath channel. And, what is

worse, the resulting estimators cannot be approximated by computationally simpler ones. Therefore, that additional information is employed to set up a simplified and approximate model, in which all signals excepting the direct one are modeled as a Gaussian term with unknown and arbitrary spatial correlation matrix. The ML estimators of the time delay and carrier phase of the direct signal were derived using this simplified model. The ML cost function for the estimation of the time delay is the quotient between the ML cost function obtained at the output of the minimum variance beamformer and that obtained without knowledge of the steering vector of the LOSS. The performance of the proposed ML time delay estimator is better than that of its two constituting components. Actually, the performance of the derived time delay and carrier phase estimators is very close in many situations to the best possible performance attainable with detailed models of the multipath channel and offers a very reasonable trade-off between bias and RMSE for highly coherent reflections. This is a remarkable result taking into account that the proposed technique has a low complexity because only the parameters of the LOSS are estimated, which makes possible at the same time the use of this technique in any type (specular or diffuse) of multipath scenario.

Two polynomial-rooting algorithms for computing the time delay estimate were presented. The first exploits the linear-phase dependence on the delay of the frequency samples of the signal and involves polynomials of relatively large order, while the second employs a simple linear interpolation of the signal vector and the polynomial to be rooted is quadratic. It was also shown that the ML estimates can be computed from the output signal of a certain beamformer. This is a hybrid beamformer, which is computed iteratively as a linear combination of the minimum variance beamformer and the temporal reference beamformer. The resulting iterative algorithm provides a different interpretation of the estimation problem and is appropriate for a practical implementation.

Moreover, we showed that the ML time delay estimator, unlike the estimator based on the minimum variance beamformer, is inherently robust against errors in the nominal steering vector of the direct signal. Finally, a modification of the ML estimator that further extends the range of tolerable pointing errors was presented.

Some directions for further investigation are:

- Analysis of the sensitivity of the carrier phase estimates to errors in the nominal vector of the direct signal.
- It was shown that the time delay estimates are robust against errors in the nominal vector of the direct signal. However, the work in [Swi98b] showed that these errors have a very deleterious effect when the DOA and the Doppler frequency of the direct signal are estimated. There is no contradiction in these results because they refer to different problems. In our case, only a 1-D search is performed for the estimation

of the delay, whereas in the other case, a 2-D search is involved in the estimation of the DOA and the Doppler frequency. However, it is also true that there are certain connections between both problems, and the reasons for the different effects of the calibration or pointing errors in each case could deserve further attention.

- Adaptive implementations of the hybrid beamformer. We believe that the solution based on the hybrid beamformer is rather promising, and realizing a more exhaustive set of simulations in order to evaluate its performance in a larger variety of coherent scenarios may be of interest.
- Sound study of the trade-off between bias and variance in the light of [Her96].

The contributions of this second block of the thesis have been published in part as

- G. Seco, J.A. Fernández-Rubio, "Time-Delay Estimation of the Line-of-Sight Signal in a Multipath Environment", *Proc. EUSIPCO*, September 2000, Tampere, Finland.
- G. Seco, J.A. Fernández-Rubio, "Array Signal Processing Techniques for Pseudorange and Carrier Phase Measurement". *Proc. 2nd European Symposium on Global Navigation Satellite Systems, GNSS*, pages IX.P.10:1-6, October 1998, Toulose, France.
- G. Seco, J.A. Fernández-Rubio, "Maximum Likelihood Time-of-Arrival Estimation using Antenna Arrays: Application to Global Navigation Satellite Systems". *Proc. EUSIPCO*, pages 213-216, September 1998, Island of Rhodes, Greece.
- G. Seco, J.A. Fernández-Rubio, "Maximum Likelihood Propagation-Delay Estimation in Unknown Correlated Noise using Antenna Arrays: Application to Global Navigation Satellite Systems". *Proc. ICASSP*, pages IV:2065-2068, May 1998, Seattle, WA, USA.
- G. Seco, J.A. Fernández-Rubio, "Reducción de los Errores Causados por la Propagación Multicamino en los Sistemas GNSS con un Nuevo Criterio de Medida de las Pseudodistancias", *Proc. XII Simposium Nacional de la Unión Científica Internacional de Radio, URSI*, pages II.243-246, September, Bilbao, Spain.
- G. Seco, J.A. Fernández-Rubio, "Multipath and Interference Errors Reduction in GNSS by Joint Pseudorange Measurement and Array beamforming", *Proc. First European Symposium on Global Navigation Satellite Systems, GNSS*, pages 605-614, April 1997, Munich, Germany.

3. In the last part of the thesis, the synchronization of a desired user transmitting a known training sequence in a DS-CDMA system was addressed. In CDMA communications systems, the signal of a desired user is interfered by the signals of a large number of users along with possible external interferers. Since the number of disturbing signals usually exceeds the number of spatial or temporal degrees of freedom separately, it is necessary in general to employ jointly all these degrees to combat MAI and external interference.

A large sample ML code-timing estimator that operates in frequency-nonselective, slowly fading channels was derived. The proposed method is a single-user, near-far resistant estimator. Unlike other approaches in the literature, the fact the signals of the users present definite temporal and spatial signatures was taken into account. This occurs because the observation interval is usually smaller than the correlation length of the channel. For the derivation of the estimator, all the received signals (MAI, external interference and noise) except for that of the desired user were modeled as a Gaussian term with unknown space-time correlation. Thus, the whole space-time structure of the interferers is employed in order to cancel them. As a result, our method outperforms many existing synchronization techniques as regards both the estimation RMSE and the probability of acquisition. The proposed estimator contrasts with other methods put forward up to date that also employ antenna arrays but only exploit the structure of the signals in one of the domains. The use of a structured estimate of the correlation matrix allows to reduce the required length of the training sequence and improves the performance for all values of the length of this sequence. Finally, the results of this part showed that the efficient use of the space-time diversity is indispensable for the correct acquisition and tracking of the code-timing in heavily loaded systems and/or in the presence of external interference.

Some research lines that remain open in this part of the thesis are:

- Extension/application of the estimator to frequency-selective channels.
- Estimation of the dimension of the interference subspace, which is needed for the construction of the structured correlation matrix.

The publications related to this part of the thesis are

- G. Seco, J.A. Fernández-Rubio, A. Lee Swindlehurst, "Code-Timing Synchronization in DS-CDMA Systems Using Space-Time Diversity", Submitted to *Signal Processing* (in review).
- G. Seco, J.A. Férnandez-Rubio, "Single-User Timing Estimation in DS-CDMA Mobile Communication systems Using a Receiving Antenna Array", *Proc. International Symposium on Image/Video Communications over Fixed and Mobile Networks (ISIVC)*, 8 pages, April 2000, Rabat (Morocco).
- G. Seco, J.A. Férnandez-Rubio, A. Lee Swindlehurst, "Code-Timing Synchronization in DS-CDMA Systems using Space-Time Diversity", *Proc. Fifth Baiona Workshop on Emerging Technologies in Telecomunications*, pages 173-177, September 1999, Baiona, Spain.

Besides the specific research topics that have already been outlined, other more general research lines can be devised, and they listed below.

- Application of the ML principle with singular correlation matrices and/or with a number of collected samples smaller than the size of the correlation matrix. Our objective is to introduce into the ML formulation the possibility that the correlation matrix be rank-deficient, and we have already done some work in this direction. The approaches followed in Chapter 5 (i.e., structured estimate of the correlation, diagonal loading) are *ad hoc*, and make the subsequent estimators be no longer ML.

- Study of the computational complexity of the algorithms presented in the thesis.

- Extension, if it is possible, of the estimators presented in Chapters 3 and 4 to the case of noise with unknown temporal correlation. Instead of assuming that the joint spatio-temporal correlation is arbitrary, as in Chapter 5, it may be advantageous considering that the spatial and temporal correlations can be decoupled (as pointed out by recent studies), or that the temporal correlation obeys a certain parametric model, such as a vector autoregressive model. This last approach is followed in [Ast99a], where the detection problem is addressed.

- Use of the Bayesian estimation theory for the estimation of the multipath parameters.

- Synchronization in systems with transmit diversity.

- Estimation of the position of a GNSS receiver using the signals transmitted by a set of satellites. This topic is somewhat related to the previous one.

- Use of the antenna array in a GNSS receiver not only to estimate accurately the carrier phase of the direct signal, but also to facilitate the resolution of the "integer ambiguities".

# Appendix A

# Notation

In general, uppercase boldface letters denote matrices, lowercase boldface letters denote (column) vectors and italics denote scalars.

| | |
|---|---|
| $\mathbf{A}^*$, $\mathbf{A}^T$, $\mathbf{A}^c$ | The conjugate transpose (Hermitian), transpose and conjugate of the matrix $\mathbf{A}$, respectively. |
| $\mathbf{A}^\dagger$ | Moore-Penrose pseudoinverse of $\mathbf{A}$. |
| $\mathbf{A}^{1/2}$ | Hermitian square root of a Hermitian matrix $\mathbf{A}$, i.e., $\mathbf{A}^{1/2}\,\mathbf{A}^{1/2} = \mathbf{A}$. |
| $\lvert\mathbf{A}\rvert$; $\lvert a\rvert$ | Determinant of the matrix $\mathbf{A}$; absolute value (modulus) of the scalar $a$. |
| $\angle a$ | Argument (phase) of $a$. |
| $\mathrm{Tr}\,\{\mathbf{A}\}$ | Trace of $\mathbf{A}$. |
| $x$, $\hat{x}$, $\check{x}$ | Trial, estimated and true value, respectively, of the variable $x$. |
| $\lfloor x \rfloor$ | Largest integer less than or equal to $x$. |
| $o\,(f_N)$ | A sequence $g_N$ is $g_N = o\,(f_N)$, for $f_N > 0 \;\; \forall N$, when $\lim_{N\to\infty} g_N/f_N = 0$. |
| $O\,(f_N)$ | A sequence $g_N$ is $g_N = O\,(f_N)$, for $f_N > 0 \;\; \forall N$, when there exists an integer $N_0$ such that $g_N/f_N$ is bounded $\forall\, N > N_0$. |
| $o_p\,(f_N)$ | A sequence of random variables $X_N$ is $X_N = o_p\,(f_N)$, for $f_N > 0 \;\; \forall N$, when $X_N/f_N$ converges to zero in probability [Mar79, Bro91], i.e., $$\lim_{N\to\infty} \mathrm{Prob}\,\{\lvert X_N/f_N\rvert > \delta\} = 0 \qquad \forall\, \delta > 0\,.$$ |

$O_p\left(f_N\right)$ A sequence of random variables $X_N$ is $X_N = O_p\left(f_N\right)$, for $f_N > 0 \;\; \forall N$, when $X_N/f_N$ is bounded in probability [Mar79, Bro91], i.e., there exists a certain $N_0$

$$\forall \varepsilon > 0, \quad \exists \delta\left(\varepsilon\right) < \infty \quad | \quad \text{Prob}\left\{|X_N/f_N| > \delta\left(\varepsilon\right)\right\} < \varepsilon \qquad \forall N > N_0 \; .$$

$\mathbb{C}^{m \times N}$ The $m \times N$ dimensional complex space.

$\text{E}\left\{\cdot\right\}$ Statistical expectation. A subscript can be used to indicate the random variable considered for the expectation.

$\left[\mathbf{A}\right]_{r,s}$ The $r,s$th element of matrix $\mathbf{A}$.

$\left[\mathbf{A}\right]_{:,s}$ The $s$th column of matrix $\mathbf{A}$.

$\left[\mathbf{A}\right]_{s,:}$ The $s$th row of matrix $\mathbf{A}$.

$\mathbf{1}$ Column vector of ones.

$\mathbf{e}_i$ Column vector with all the elements being zero excepting the $i$th which is equal to one.

$\left\|\cdot\right\|_2$ 2-norm of a vector.

$\left\|\cdot\right\|_F$ Frobenius-norm of a matrix.

$\mathbf{A} \geq \mathbf{B}$ $\mathbf{A} - \mathbf{B}$ is positive semidefinite.

$\mathbf{I}$ Identity matrix. A subscript can be used to indicate the dimension.

$\text{vec}\left(\cdot\right)$ Vec-operator, i.e., if $\mathbf{A} = \left[\mathbf{a}_1 \; \ldots \; \mathbf{a}_d\right]$, then $\text{vec}\left(\mathbf{A}\right) = \left[\mathbf{a}_1^T \; \cdots \; \mathbf{a}_d^T\right]^T$.

$\text{mat}_{m \times n}\left(\cdot\right)$ Inverse operator to $\text{vec}\left(\cdot\right)$. The result is a $m \times n$ matrix formed by rearranging column-wise the elements of a $mn \times 1$ vector.

$\text{diag}\left(\cdot\right)$ Diagonal matrix with the given elements along its diagonal.

$\triangleq$ Defined as.

$f\left(t\right) * g\left(t\right)$ Convolution between $f\left(t\right)$ and $g\left(t\right)$.

$\delta_{n,l}$ Kronecker delta. $\delta_{n,l} = \begin{cases} 1, & n = l \\ 0, & n \neq l \end{cases}$

$\delta\left(t\right)$ Dirac delta.

$\ln\left(\cdot\right)$ Natural logarithm.

$\otimes$ Kronecker product of matrices. If $\mathbf{A}$ is $n \times l$, then

$$\mathbf{A} \otimes \mathbf{B} = \begin{bmatrix} [\mathbf{A}]_{1,1}\,\mathbf{B} & \dots & [\mathbf{A}]_{1,l}\,\mathbf{B} \\ \vdots & & \vdots \\ [\mathbf{A}]_{n,1}\,\mathbf{B} & \dots & [\mathbf{A}]_{n,l}\,\mathbf{B} \end{bmatrix}.$$

$\odot$ Schur-Hadamard (elementwise) product of matrices.

$\mathrm{Re}\{\cdot\}$, $\mathrm{Im}\{\cdot\}$ Real and imaginary parts.

$\arg\min_x f(x)$ Value of $x$ that minimizes $f(x)$.

$\mathbf{P}_{\mathbf{A}}$ Orthogonal projector onto the subspace spanned by the columns of $\mathbf{A}$.

$\mathbf{P}_{\mathbf{A}}^{\perp}$ $\mathbf{I} - \mathbf{P}_{\mathbf{A}}$, orthogonal projector onto the orthogonal complement to the columns of $\mathbf{A}$.

# Appendix B

# Acronyms

| | |
|---|---|
| **1-D**, **2-D** | One-Dimensional, Two-Dimensional. |
| **BPSK** | Binary Phase Shift Keying. |
| **CCI** | Co-Channel Interference. |
| **CDMA** | Code Division Multiple Access. |
| **CNo** | Carrier to Noise spectral density ratio. |
| **CRB** | Cramér-Rao Bound. |
| **CRB-D** | Cramér-Rao Bound for a Detailed signal model. |
| **CRB-S** | Cramér-Rao Bound for a Simplified signal model. |
| **DFT** | Discrete Fourier Transform. |
| **DLL** | Delay Lock Loop. |
| **DOA** | Direction Of Arrival. |
| **DS** | Direct Sequence. |
| **EGNOS** | European Geostationary Navigation Overlay System. |
| **EM** | Expectation-Maximization. |
| **ESPRIT** | Estimation of Signal Parameters via Rotational Invariance Techniques. |
| **FDMA** | Frequency Division Multiple Access. |
| **FIM** | Fisher Information Matrix. |
| **FIR** | Finite Impulse Response. |
| **GLONASS** | GLObal'naya NAvigasionnay Sputnikovaya Sistema. |
| **GNSS** | Global Navigation Satellite System. |

**GPS** Global Navigation System.

**HB** Hybrid Beamformer.

***iid*** Independent and Identically Distributed.

**IQML** Iterative Quadratic Maximum Likelihood algorithm.

**LAAS** Local Area Augmentation System.

**LMS** Least Mean Squares.

**LOSS** Line Of Sight Signal.

**LS** Least Squares.

**MAI** Multiple Access Interference.

**ML(E)** Maximum Likelihood (Estimator).

**ML-TEE** Maximum Likelihood with only TEmporal reference Estimator.

**ML-WHE** Maximum Likelihood for White Noise Estimator.

**MODE** Method Of Direction Estimation.

**MUSIC** MUltiple SIgnal Classification algorithm.

**MV(B)** Minimum Variance (Beamformer).

**MVBE** Minimum-Variance-Beamformer based Estimator.

**NFR** Near-far ratio.

**pdf** Probability Density Function.

**PLL** Phase Lock Loop.

**PN** Pseudo-Noise.

**RLS** Recursive Least Squares.

**(R)MSE** (Root) Mean Squared Error.

$$\mathrm{RMSE}\left(a\right) = \sqrt{\mathrm{E}\left\{\left|a - \check{a}\right|^2\right\}} = \sqrt{\mathrm{STD}^2\left(a\right) + \left|\mathrm{E}\left\{a\right\} - \check{a}\right|^2}$$

**SDiv** Space Diversity.

**SDMA** Space Division Multiple Access.

**SIMO** Single Input Multiple Output.

**SNIR** Signal to Noise plus Interference Ratio.

**SNR** Signal to Noise Ratio.

**SS** Spread Spectrum.

**STD** Standard Deviation.

$$\mathrm{STD}\left(a\right) = \sqrt{\mathrm{E}\left\{\left|a - \mathrm{E}\left\{a\right\}\right|^2\right\}}$$

**STDiv** Space-Time Diversity.

**TDiv** Time Diversity.

**TDMA** Time Division Multiple Access.

**TLS** Total Least Squares.

**TRB** Temporal Reference Beamformer.

**ULA** Uniform Linear Array.

**WAAS** Wide Area Augmentation System.

**WSF** Weighted Subspace Fitting.

# Bibliography


[Aka74] H. Akaike, "A New Look at Statistical Model Identification", *IEEE Trans. on Automatic Control*, Vol. 19, pags. 716–723, 1974.

[Ast98] D. Astély, B. Ottersten, A.L. Swindlehurst, "A Generalized Array Manifold for Communication Channels with Local Scattering", *IEE Proceedings Radar, Sonar, and Navigation*, Vol. 145, nº 1, pags. 51–57, Feb. 1998.

[Ast99a] D. Astély, *Spatial and Spatio-Temporal Processing with Antenna Arrays in Wireless Systems*, PhD Thesis, Royal Institute of Technology, KTH, Stockholm, Sweden, 1999.

[Ast99b] D. Astély, A. Jakobsson, A.L. Swindlehurst, "Burst Synchronization on Unknown Frequency Selective Channels with Co-Channel Interference Using an Antenna Array", *Proc. IEEE Vehicular Technology Conf.*, Houston, TX, March 1999.

[Axe96] P. Axelrad, C. J. Comp, P. F. MacDoran, "SNR-based Multipath Error Correction for GPS Differential Phase", *IEEE Trans. on Aerospace and Electronic Systems*, Vol. 32, nº 2, pags. 650–660, April 1996.

[Ayo99] T.F. Ayoub, A.M. Haimovich, M.L. Pugh, "Reduced-Rank STAP for High PRF Radar", *IEEE Trans. on AES*, Vol. 35, nº 3, pags. 953–962, July 1999.

[Ban71] W. J. Bangs, *Array Processing with Generalized Beamformers*, PhD Thesis, Yale University, New Haven, CT, 1971.

[Bel96] S.P. Belanger, "An EM Algorithm for Multisensor TDOA/DD Estimation in a Multipath Propagation Environment", *Proc. ICASSP*, 1996.

[Bel00] K.L. Bell, Y. Ephraim, H.L. Van Trees, "A Bayesian Approach to Robust Adaptive Beamforming", *IEEE Trans. SP*, Vol. 48, nº 2, pags. 386–398, Feb. 2000.

[Ben96] S. Bensley, B. Aazhang, "Subspace-Based Channel Estimation for CDMA Communication Systems", *IEEE Trans. Commun.*, pags. 1009–1020, Aug. 1996.

[Ben98] S. Bensley, B. Aazhang, "Maximum-Likelihood Synchronization of a Single User for Code-Division Multiple-Access Communication Systems", *IEEE Trans. on COM*, Vol. 46, nº 3, pags. 392–399, March 1998.

[Ber99] N. Bertaux, P. Larzabal, C. Adnet, E. Chaumette, "A Parameterized Maximum Likelihood Method for Multipaths Channels Estimation", *Proc. SPAWC Workshop*, pags. 391–394, Annapolis, MD, 1999.

[Bra96] M.S. Braasch, "GPS Multipath Model Validation", *Proc. IEEE Position, Location and Navigation Symposium*, pags. 672–678, 1996.

[Bre78] J.W. Brewer, "Kronecker Products and Matrix Calculus in System Theory", *IEEE Trans. on Circuits and Systems*, Vol. 25, nº 9, pags. 772–781, Sept. 1978.

[Bre82] L. Brennan, I. Reed, "An Adaptive Signal Processing Algorithm for Communications", *IEEE Trans. AES*, Vol. 18, nº 1, pags. 124–130, Jan. 1982.

[Bre86] Y. Bresler, A. Macovski, "Exact Maximum Likelihood Parameter Estimation of Superimposed Exponential Signals in Noise", *IEEE Trans. ASSP*, Vol. 34, nº 5, pags. 1081–1089, Oct. 1986.

[Bre97] K. Breivik, B. Forssell, C. Kee, P. Enge, T. Walter, "Estimation of Multipath Error in GPS Pseudorange Measurements", *Navigation: Journal of the Institute of Navigation*, Vol. 44, nº 1, pags. 43–52, Spring 1997.

[Bri81] D. R. Brillinger, *Time Series: Data Analysis and Theory*, Holden-Day, Inc., San Francisco, CA, 1981.

[Bro91] P. J. Brockwell, R. A. Davis, *Time Series: Theory and Methods*, Springer-Verlag, New York, 2nd ed., 1991.

[Bro97] G. Brodin, P. Daly, "GNSS Code and Carrier Tracking in the Presence of Multipath", *International Journal of Satellite Communications*, Vol. 15, pags. 25–34, 1997.

[Car88] B. D. Carlson, "Covariance Matrix Estimation Errors and Diagonal Loading in Adaptive Arrays", *IEEE Trans. on AES*, Vol. 24, nº 3, pags. 397–401, July 1988.

[Ced96] M. Cedervall, A. Paulraj, "Joint Channel and Space-Time Parameter Estimation", *Proc. 30th Asilomar Conf. on Signals, Systems, and Computers*, pags. 375–379, 1996.

[Che99] Y.-F. Chen, M. Zoltowski, "Joint Angle and Delay Estimation for DS-CDMA with Application to Reduced Dimension Space-Time RAKE Receivers", *Proc. ICASSP*, Vol. V, pags. 2933–2936, Phoenix, AZ, 1999.

[Com98] C. J. Comp, P. Axelrad, "Adaptive SNR-based Carrier Phase Multipath Mitigation Technique", *IEEE Trans. on Aerospace and Electronic Systems*, Vol. 34, nº 1, pags. 264–276, Jan. 1998.

[Cou81] C.C. Counselman, S.A. Gourevitch, "Miniature Interferometer Terminals for Earth Surveying: Ambiguity and Multipath with Global Positioning System", *IEEE Trans. on Geoscience and Remote Sensing*, Vol. 19, pags. 244–252, 1981.

[Cou98] C.C. Counselman, "Array Antennas for DGPS", *IEEE AES Systems Magazine*, pags. 15–19, Dec. 1998.

[CT99] M. Chenu-Tournier, A. Ferreol, P. Larzabal, "Low Complexity Blind Space-Time Identification of Propagation Parameters", *Proc. ICASSP*, Vol. V, pags. 2873–2876, Phoenix, AZ, 1999.

[Des99] A. Desmézières, N. Bertaux, P. Larzabal, "Polarization in Space-Time Processing for Propagation Channel Identification", *Proc. SPAWC Workshop*, pags. 395–398, Annapolis, MD, 1999.

[Die92] A.J. Dierendonck, P. Fenton, T. Ford, "Theory and Performance of Narrow Correlator Spacing in a GPS Receiver", *Navigation, Journal of the Institute of Navigation*, Vol. 39, nº 3, pags. 265–283, Fall 1992.

[Die97] A. J. Van Dierendonck, M. S. Braasch, "Evaluation of GNSS Receiver Correlation Processing Techniques for Multipath and Noise Mitigation", *Proc. 1997 ION National Technical Meeting*, Santa Monica, CA, Jan. 1997.

[Din97] Z. Ding, "Matrix Outer-Product Decomposition Method for Blind Multiple Channel Equalization", *IEEE Trans. SP*, Vol. 45, nº 12, pags. 3053–3061, Dec. 1997.

[Dlu89] D. Dlugos, R. Scholtz, "Acquisition of Spread Spectrum Signals by an Adaptive Array", *IEEE Trans. on ASSP*, Vol. 37, nº 8, pags. 1253–1270, Aug. 1989.

[Dog99] A. Dogandžić, A. Nehorai, "Estimating Range, Velocity, and Direction with a Radar Array", *Proc. ICASSP*, Vol. V, pags. 2773–2776, Phoenix, AZ, 1999.

[Dog00] A. Dogandžić, A. Nehorai, "Estimating Evoked Dipole Responses in Unknown Spatially Correlated Noise with EEG/MEG Arrays", *IEEE Trans. on SP*, Vol. 48, nº 1, pags. 13–25, Jan. 2000.

[Dor95] D. Doris, A. Benhallam, "An Overview of Signal Processing Techniques to Reduce Multipath Effects on GPS Reception", *Proc. IEEE/IEE International Workshop on Signal Processing Methods in Multipath Enviroments*, Glasgow, UK, 1995.

[Dor97] D. Doris, *Modélisation de Récepteurs GPS. Application à l'Étude de l'Influence des Multitrajects sur les Performances du Récepteur L1 GPS*, PhD Thesis, Institut National Polytechnique de Toulouse, Toulouse, France, 1997, in French.

[Er94] M.H. Er, B.C. Ng, "A New Approach to Robust Beamforming in the Presence of Steering Vector Errors", *IEEE Trans. SP*, Vol. 42, nº 7, pags. 1826–1829, July 1994.

[Ert00] E. Ertin, U. Mitra, S. Siwamogsatham, "Maximum-Likelihood Based Multipath Channel Estimation for Code-Division Multiple-Access Systems", 2000, accepted for publication in IEEE Trans. on COM.

[ESA96] "Mission Analysis of a Second Generation GNSS", Tech. Rep. ATES.96.039410.CSN.0113, ESA/ESTEC, Aug. 1996.

[Fan98] R. L. Fante, J. J. Vacarro, "Cancellation of Jammers and Jammer Multipath in a GPS Receiver", *IEEE Aerospace and Electronic Systems Magazine*, pags. 25–28, Nov. 1998.

[Fel97] T. Felhauer, "Comparison of EML and DOT Discriminator DLL Multipath Performance in GPS/GLONASS Navigation Receivers", *Electronic Letters*, Vol. 33, nº 3, pags. 179–181, Jan. 1997.

[Fer83] E.R. Ferrara, T.M. Parks, "Direction Finding with an Array of Antennas Having Diverse Polarizations", *IEEE Trans. on Antennas and Propagation*, Vol. 31, nº 2, pags. 231–236, March 1983.

[Fle99] B.H. Fleury, M. Tshudin, R. Heddergott, D. Dahlhaus, K.I. Pedersen, "Channel Parameter Estimation in Mobile Radio Environments Using the SAGE Algorithm", *IEEE J. Select. Areas Commun.*, Vol. 17, nº 3, pags. 434–450, March 1999.

[FR97] J.A. Fernández-Rubio, G. Seco, "Sistemas de Navegació Global por Satélite: del GPS al GNSS", *Mundo Electrónico*, Vol. 280, pags. 46–52, Oct. 1997, in Spanish.

[Fuc98] J.-J. Fuchs, "Detection and Estimation of Superimposed Signals", *Proc. ICASSP*, Seattle, WA, 1998.

[Fuc99] J.-J. Fuchs, "Multipath Time-Delay Detection and Estimation", *IEEE Trans. SP*, Vol. 47, nº 1, pags. 237–243, Jan. 1999.

[Gar96] L. Garin, F. van Diggelen, J. Rosseau, "Strobe & Edge Correlator Multipath Mitigation for Code", *Proc. ION-GPS*, Kansas City, MO, 1996.

[Gar97] L. Garin, J.-M. Rousseau, "Enhanced Strobe Correlator Multipath Rejection for Code & Carrier", *Proc. ION-GPS Conference*, Kansas City, MO, 1997.

[Gau99] R. De Gaudenzi, "Direct-Sequence Spread-Spectrum Chip Tracking in the Presence of Unresolvable Multipath Components", *IEEE Trans. on Vehicular Technology*, Vol. 48, nº 5, pags. 1573–1583, Sep. 1999.

[Gol96] G. H. Golub, C. F. van Loan, *Matrix Computations*, The John Hopkins University Press, 3rd ed., 1996.

[Gra81] A. Graham, *Kronecker Products and Matrix Calculus with Applications*, Ellis Horwood Limited, Chichester, England, 1981.

[Haa98] M. Haardt, C. Brunner, J. Nossek, "Efficient High-Resolution 3-D Channel Sounding", *Proc. IEEE Vehicular Technology Conf.*, Ottawa, Canada, 1998.

[Har00] K. Harmancı, J. Tabrikian, J. L. Krolik, "Relationships Between Adaptive Minimum Variance Beamforming and Optimal Source Location", *IEEE Trans. on SP*, Vol. 48, nº 1, pags. 1–12, Jan. 2000.

[Has98] A. Hassibi, S. Boyd, "Integer Parameter Estimation in Linear Models with Applications to GPS", *IEEE Trans. SP*, Vol. 46, nº 2, pags. 2938–2952, Nov. 1998.

[Hat98] G.F. Hatke, "Adaptive Array Processing for Wideband Nulling in GPS Systems", *Proc. 32th Asilomar Conf. on Signals, Systems, and Computers*, pags. 1332–1336, 1998.

[Hay96] S. Haykin, *Adaptive Filter Theory*, Prentice Hall, 3rd ed., 1996.

[Her96] A.O. Hero III, J.A. Fessler, M. Usman, "Exploring Estimator Bias-Variance Tradeoff Using the Uniform CRB Bound", *IEEE Trans. SP*, Vol. 44, nº 8, pags. 2026–2041, Aug. 1996.

[Hol90] J. K. Holmes, *Coherent Spread Spectrum Systems*, Krieger Press, 1990.

[Hon87] Y.J. Hong, D.R. Ucci, C.C. Yeh, "The Performance of an Adaptive Array Combining Reference Signal and Steering Vector", *IEEE Trans. on Antennas and Propagation*, Vol. 35, nº 7, pags. 763–770, July 1987.

[Hor85] R.A. Horn, C.R. Johnson, *Matrix Analysis*, Cambridge University Press, 1985.

[Hot99] L. Hoteit, *Polynomial Techniques and Robust Extensions to Unsupervised Equalisation and Identification*, PhD Thesis, Imperial College, 1999.

[Hot00] L. Hoteit, "FFT-Based Fast Polynomial Rooting", *Proc. ICASSP*, Istambul, Turkey, 2000.

[HP00] M. Hernández-Pajares, J.M. Juan, J. Sanz, "GPS Code Multipath Detection and Mitigation in a LEO Scenario using Neural Networks", *Proc. Space Applications of GPS, ESA-ION*, Breckenridge, USA, 2000.

[Hua94] Y. Hua, "The Most Efficient Implementation of the IQML Algorithm", *IEEE Trans. Sig. Proc.*, Vol. 43, nº 8, pags. 2203–2204, Aug. 1994.

[HW97] B. Hofmann-Wellenhof, H. Lichtenegger, J. Collins, *Global Postioning System, Theory and Practice*, Springer-Verlag, New-York, 1997.

[Ilt84] R.A. Iltis, L.B. Milstein, "Performance Analysis of Narrow-Band Interference Rejection Techniques in DS Spread-Spectrum Systems", *IEEE Trans. on COM*, Vol. 32, nº 11, pags. 1169–1177, Nov. 1984.

[Jak98a] A. Jakobsson, A.L. Swindlehurst, D. Astély, C. Tidestav, "A Blind Frequency Domain Method for DS-CDMA Synchronization Using Antenna Arrays", *Proc. 32nd Asilomar Conf. on Signals, Systems and Computers*, Pacific Groove, CA, Nov. 1998.

[Jak98b] A. Jakobsson, A.L. Swindlehurst, P. Stoica, "Subspace-Based Estimation of Time Delays and Doppler Shifts", *IEEE Trans. on SP*, Vol. 46, nº 9, pags. 2472–2483, Sep. 1998.

[Jak00] A. Jakobsson, *Model-Based and Matched-Filterbank Signal Analysis*, PhD Thesis, Uppsala University, 2000.

[Joh93] D. Johnson, D. Dudgeon, *Array Signal Processing – Concepts and Techniques*, Prentice Hall, Inc., Englewood Cliffs, NJ, 1993.

[Kap96] E.D. Kaplan, *Understanding GPS. Principles and Applications*, Artech House Publishers, 1996.

[Kay93] S. M. Kay, *Fundamentals of Statistical Signal Processing. Estimation Theory*, Prentice Hall, 1993.

[Kee98] A. Keerthi, J. Shynk, "Separation of Cochannel Signals in TDMA Mobile Radio", *IEEE Trans. SP*, Vol. 46, nº 10, pags. 2684–2697, Oct. 1998.

[Kri98] M. Kristesson, *On Parameter Estimation in Wireless Communications, Sensor Array Processing and Spectral Analysis*, PhD Thesis, Royal Institute of Technology, KTH, 1998.

[Kuz99] A. Kuzminskiy, D. Hatzinakos, "Semi-Blind Symbol Synchronization for Antenna Array Signal Processing in Short Burst Multiuser SDMA Systems", *Proc. SPAWC Workshop*, pags. 142–145, Annapolis, MD, 1999.

[LA98a] J.M. López-Almansa, P.A. Pablos, "Derivation of an Analytical Model for Estimation of Measurement Error Induced by an Arbitraru Disturbance on a Coherent Delay Lock Loop", *Proc. 54th ION Annual Meeting*, Denver, CO, June 1998.

[LA98b] J.M. López-Almansa, P.A. Pablos, "Measurement Error and Protection Envelopes in the Presence of Interference for GNSS Receivers", *Proc. 11th ION-GPS Conference*, pags. 797–807, Nashville, TE, Sep. 1998.

[Laa96] T. I. Laakso, V. Välimäki, M. Karjalainen, U. K. Laine, "Splitting the Unit Delay", *IEEE Signal Processing Magazine*, Vol. 13, nº 1, pags. 30–60, Jan. 1996.

[Lan97] R.Jr. Landry, V. Calmettes, M. Bousquet, "Impact of Interference on a Generic GPS Receiver and Assessment of Mitigation Techniques", *Proc. IEEE ISSSTA*, 1997.

[Lax97] M. C. Laxton, S. L. DeVilbiss, "GPS Multipath Mitigation During Code Tracking", *Proc. American Control Conference*, Alburquerque, NM, June 1997.

[Lea96] J. Leary, R. Gooch, "Adaptive Beamforming for TDMA Signals", *Proc. 29th Asilomar Conf. on Signals, Systems, and Computers*, pags. 1378–1382, 1996.

[Leh83] E. L. Lehmann, *Theory of Point Estimation*, Wiley, New York, 1983.

[Li93] J. Li, R.T. Compton, "Maximum Likelihood Angle Estimation for Signals with Known Waveforms", *IEEE Trans. SP*, Vol. 41, nº 9, pags. 2850–2862, Sept. 1993.

[Li95] J. Li, B. Halder, P. Stoica, M. Viberg, "Computationally Efficient Angle Estimation for Signals with Known Waveforms", *IEEE Trans. SP*, Vol. 43, nº 9, pags. 2154–2163, Sep. 1995.

[Li96] J. Li, P. Stoica, "Adaptive Filtering Approach to Spectral Estimation and SAR Imaging", *IEEE Trans. on Sig. Proc.*, Vol. 44, nº 6, pags. 1469–1484, June 1996.

[Li98] J. Li, P. Stoica, Z. Liu, "Comparative Study of IQML and MODE Direction-of-Arrival Estimators", *IEEE Trans. SP*, Vol. 46, nº 1, pags. 149–160, Jan. 1998.

[Liu98a] Z.-S. Liu, J. Li, S.L. Miller, "A Receiver Diversity Based Code-Timing Estimator for Asynchronous DS-CDMA Systems", *Proc. ICASSP*, Vol. VI, pags. 3245–3248, Seattle, WA, 1998.

[Liu98b] Z.-S. Liu, J. Li, S.L. Miller, "An Efficient Code-Timing Estimator for Receiver Diversity DS-CDMA Systems", *IEEE Trans. COM*, Vol. 46, nº 6, pags. 826–835, June 1998.

[Mac99] C. Macabiau, B. Roturier, A. Benhallam, "Tracking Performance of GPS Receivers with More than One Multipath", *Proc. 3nd European Symposium on Global Navigation Satellite Systems*, Genoa, Italy, Oct. 1999.

[Mad91] U. Madhow, M. B. Pursley, "Acquisition-Based Capacity of Direct-Sequence Spread-Spectrum Communication Networks", *Proc. of the Conference of Information Sciences and Systems*, pags. 1186–1189, March 1991.

[Mad97] U. Madhow, "Blind Adaptive Interference Suppression for the Near-Far Resistant Acquisition and Demodulation of Direct-Sequence CDMA Signals", *IEEE Trans. on SP*, Vol. 45, nº 1, pags. 124–136, Jan. 1997.

[Mag99] J. R. Magnus, H. Neudecker, *Matrix Differential Calculus with Applications in Statistics and Econometrics*, John Wiley & Sons, 1999.

[Mar79] K. V. Mardia, J. T. Kent, J. M. Bibby, *Multivariate Analysis*, Academic Press, New York, 1979.

[Men97] M. Mengali, A. N. D'Andrea, *Synchronization Techniques for Digital Receivers*, Plenum Press, 1997.

[Mey98] H. Meyr, M. Moeneclaey, S.A. Fechtel, *Digital Communication Receivers. Synchronization, Channel Estimation and Signal Processing*, John Wiley, 1998.

[Moe96a] D. J. Moelker, Y. Bar-Ness, "Adaptive Antenna Arrays for Interference Cancellation in GPS and GLONASS Receivers", *Proc. IEEE Position, Location and Navigation Symposium*, pags. 191–198, 1996.

[Moe96b] D. J. Moelker, Y. Bar-Ness, "An Optimal Array Processor for GPS Interference Cancellation", *Proc. 15th DASC. AIAA/IEEE Digital Avionics Systems Conference*, pags. 285–290, Atlanta, GA, 1996.

[Moe97] D. J. Moelker, "Multiple Antennas for Advanced GNSS Multipath Mitigation and Multipath Direction Finding", *Proc. Institute of Navigation GPS Meeting*, Kansas City, MO, 1997.

[Mol98] K. Molnar, G. Bottomley, "Adaptive Array Processing MLSE Receivers for TDMA Digital Cellular/PCS Communications", *IEEE J. Select. Areas Commun.*, Vol. 16, pags. 1340–1351, Oct. 1998.

[Mou95] E. Moulines, P. Duhamel, J.F. Cardoso, S. Mayrargue, "Subspace Methods for the Blind Identification of Multichannel FIR Filters", *IEEE Trans. SP*, Vol. 43, nº 2, pags. 516–525, Feb. 1995.

[Mou98] N. Moulin, D. Korpet, "An Adaptive Antenna Cobined with Adaptive Temporal Filters for GPS Interference Mitigation", *Proc. 2nd European Symposium on Global Navigation Satellite Systems*, Toulouse, France, Oct. 1998.

[Muñ97] O. Muñoz, J.A. Fernández-Rubio, "Cancellation of External and Multiple Access Interference in CDMA Systems Using Antenna Arrays", *Signal Processing*, Vol. 61, pags. 113–129, Sep. 1997.

[Myr00] W.L. Myrick, M. Zoltowski, J.S. Goldstein, "Exploting Conjugate Symmetry in Power Minimization Based Pre-Processing for GPS: Reduced Complexity and Smoothness", *Proc. ICASSP*, Istambul, Turkey, June 2000.

[Nee92a] R.D.J. van Nee, "Reducing Multipath Tracking Errors in Spread-Spectrum Ranging Systems", *Electronic Letters*, Vol. 28, nº 8, April 1992.

[Nee92b] R.D.J. Van Nee, "Multipath Effects on GPS Code Phase Measurements", *Navigation, Journal of the Institute of Navigation*, Vol. 39, nº 2, pags. 177–189, Summer 1992.

[Nee93a] R.D.J. van Nee, "Optimum DGPS Receiver Structures", *Proc. 2nd International Symposium on Differential Satellite Navigation Systems, DSNS*, March 1993.

[Nee93b] R.D.J. van Nee, "Spread-Spectrum Code and Carrier Synchronization Errors Caused by Multipath and Interference", *IEEE Trans. on Aerospace and Electronic Systems*, Vol. 29, nº 4, pags. 1359–1365, Oct. 1993.

[Nee94] R.D.J. van Nee, J. Siereveld, P.C. Fenton, B.R. Townsend, "The Multipath Estimating Delay Lock Loop: Approaching Theoretical Accuracy Limits", *Proc. IEEE Position, Location and Navigation Symposium*, pags. 246–251, 1994.

[Nee95] R.D.J. van Nee, *Multipath and Multi-Transmitter Interference in Spread Spectrum Communication and Navigation Systems*, PhD Thesis, Delft University, 1995.

[Öst99] T. Östman, S. Parkvall, B. Ottersten, "An Improved MUSIC Algorithm for Estimation of Time Delays in Asynchronous DS-CDMA Systems", *IEEE Trans. on COM*, Vol. 47, nº 11, pags. 1628–1631, Nov. 1999.

[Ott93] B. Ottersten, M. Viberg, P. Stoica, A. Nehorai, "Exact and Large Sample ML Techniques for Parameter Estimation and Detection in Array Processing", Haykin, Litva, Shepherd (eds.), *Radar Array Processing*, pags. 99–151, Springer-Verlag, Berlin, 1993.

[Par96a] B.W. Parkinson, J.J. Spilker (eds.), *Global Positioning System: Theory and Applications, vol. I, II*, Vol. 163-164 of *Progress in Astronautics and Aeronautics*, American Institute of Aeronautics, Inc., Washington, DC, 1996.

[Par96b] S. Parkvall, *Near-Far Resistant DS-CDMA Systems: Parameter Estimation and Data Detection*, PhD Thesis, Royal Institute of Technology, KTH, Stockholm, Sweden, 1996.

[Par96c] S. Parkvall, E. Ström, B. Ottersten, "The Impact of Timing Errors on the Performance of Linear DS-CDMA Receivers", *IEEE Journal on Selected Areas on Communications*, Vol. 14, nº 8, pags. 1660–1668, Oct. 1996.

[Pau97] A. Paulraj, C. Papadias, "Space-Time Processing for Wireless Communications", *IEEE Signal Processing Magazine*, Vol. 14, nº 6, pags. 49–83, Nov. 1997.

[Ped00] K.I. Pedersen, P.E. Mogensen, B.H. Fleury, "A Stochastic Model of the Temporal and Azimuthal Dispersion Seen at the Base Station in Outdoor Propagation Environments", *IEEE Trans. on Vehicular Technology*, Vol. 49, nº 2, pags. 437–447, May 2000.

[Pel98a] P. Pelin, "Decoupled Direction Finding: Detection", *Proc. ICASSP*, Seattle, WA, 1998.

[Pel98b] P. Pelin, "Iterative Least Squares Techniques for Self-Synchronization and Equalization in Adaptive Antenna Systems", *IEEE Trans. on Vehic. Tech.*, 1998, submitted.

[Pel99] P. Pelin, *Space-Time Algorithms for Mobile Communications*, PhD Thesis, Chalmers University of Technology, 1999.

[Pil89] S. U. Pillai, *Array Signal Processing*, Springer Verlag, 1989.

[Poo97a] H.V. Poor, X. Wang, "Code-Aided Interference Supression for DS/CDMA Communications-Part I: Interference Suppresion Capability", *IEEE Trans. COM*, Vol. 45, nº 9, pags. 1101–1111, Sep. 1997.

[Poo97b] H.V. Poor, X. Wang, "Code-Aided Interference Supression for DS/CDMA Communications-Part II: Parallel Blind Adaptive Implementations", *IEEE Trans. COM*, Vol. 45, nº 9, pags. 1112–1122, Sep. 1997.

[Pre95] W.H. Press, S.A. Teukolsky, W.T. Vetterling, B.P. Flannery, *Numerical Recipes in C, the Art of Scientific Computing*, Cambridge University Press, 1995.

[Pro95] J.G. Proakis, *Digital Communciations*, McGraw-Hill, New York, 3rd ed., 1995.

[Ral98] G. Raleigh, T. Boros, "Joint Space-Time Parameter Estimation for Wireless Communication Channels", *IEEE Trans. on SP*, Vol. 46, nº 5, pags. 1333–1343, May 1998.

[Ram95] J.F. Ramos, *Nuevas Técnicas de Procesado Digital en Array*, PhD Thesis, Universidad Politénica de Madrid, 1995.

[Ram96] J. Ramos, M. Zoltowski, M. Burgos, "Robust Blind Adaptive Array. A Prototype for GPS", *Proc. IEEE International Symposium of Phased Arrays Systems and Technology*, pags. 406–410, Boston, MA, Oct. 1996.

[Ram00] J. Ramos, M. D. Zoltowski, H. Liu, "Low-Complexity Space-Time Processor for DS-CDMA Communications", *IEEE Trans. on SP*, Vol. 48, nº 1, pags. 39–52, Jan. 2000.

[Ran99] A. Ranheim, *Interference Rejection in Wireless Communication Systems*, PhD Thesis, Chalmers University of Technology, Göteborg, Sweden, 1999.

[Ran00] A. Ranheim, P. Pelin, "Joint Symbol Detection and Channel Parameter Estimation in Asynchronous DS-CDMA Systems", *IEEE Trans. on SP*, Vol. 48, nº 2, pags. 545–550, Feb. 2000.

[Ray98] J.K. Ray, M.E. Cannon, P. Fenton, "Mitigation of Static Carrier Phase Multipath Effects using Multiple Closely-Spaced Antennas", *Proc. 11th ION-GPS*, pags. 1025–1034, Nashville, TN, Sep. 1998.

[Ray99a] J.K. Ray, "Use of Multiple Antenna Arrays to Mitigate Carrier Phase Multipath in Reference Stations", *Proc. ION-GPS*, pags. 269–279, Nashville, TN, Sep. 1999.

[Ray99b] J.K. Ray, M.E. Cannon, P. Fenton, "Code Range and Carrier Phase Mitigation Using SNR, Range and Phase Measurements in a Multi-Antenna System", *Proc. ION-GPS*, pags. 713–725, Nashville, TN, Sep. 1999.

[Rib97] J. Riba, J. Goldberg, G. Vázquez, "Robust Beamforming for Interference Rejection in Mobile Communications", *IEEE Trans. on SP*, Vol. 45, nº 1, pags. 271–275, Jan. 1997.

[Ris78] J. Rissanen, "Modeling by Shortest Data Description", *Automatica*, Vol. 14, pags. 465–471, 1978.

[Roy86] R. Roy, T. Kailath, "ESPRIT – Estimation of Signal Parameters Via Rotational Invariance Techniques", *IEEE Trans. ASSP*, Vol. 37, nº 7, pags. 984–995, July 1986.

[Sch90] L. L. Scharf, *Statistical Signal Processing, Detection, Estimation, and Time Series Analysis*, Addison-Wesley, 1990.

[Sch98a] R. Schweikert, T. Woerz, "Signal Design and Transmission Performance Study for GNSS-2", Tech. Rep. AO/1-3156/NL/JSC, ESA, 1998.

[Sch98b] R. Schweikert, T. Woerz, R. De Gaudenzi, "On Signal Design for a Second Generation Satellite Navigation System", *Proc. 6th International Wrokshop of Digital Signal Processing for Space Applications*, ESTEC, The Neetherlands, Sep. 1998.

[Sec96] G. Seco, J.A. Fernández-Rubio, "Multipath and Interference Errors Reduction in GPS Using Antenna Arrays", *Proc. 5th ESA International Workshop on Digital Signal Processing Techniques applied to Space Communications*, pags. 4.24–4.36, Sitges, Spain, Sep. 1996.

[Sec97a] G. Seco, J.A. Fernández-Rubio, "Multipath and Interference Errors Reduction in GNSS by Joint Pseudorange Measurement and Array Beamforming", *Proc. 1st European Symposium on Global Navigation Satellite Systems*, pags. 605–614, Munich, Germany, April 1997.

[Sec97b] G. Seco, J.A. Fernández-Rubio, "Reducción de los Errores Causados por la Propagación Multicamino en los Sistemas GNSS con un Nuevo Criterio de Medida de las Pseudodistancias", *Proc. URSI*, pags. II:243–246, Bilbao, Spain, Sep. 1997, in Spanish.

[Sec98a] G. Seco, J.A. Fernández-Rubio, "Array signal processing techniques for pseudorange and carrier phase measurement", *Proc. 2nd European Symposium on Global Navigation Satellite Systems, GNSS'98*, pags. IX.P.10:1–6, Toulouse, France, Oct. 1998.

[Sec98b] G. Seco, J.A. Fernández-Rubio, "Maximum Likelihood Propagation-Delay Estimation in Unknown Correlated Noise using Antenna Arrays: Application to Global Navigation Satellite Systems", *Proc. ICASSP*, Vol. IV, pags. 2065–2068, Seattle, WA, May 1998.

[Sec98c] G. Seco, J.A. Fernández-Rubio, "Maximum Likelihood Time-of-Arrival Estimation Using Antenna Arrays: Application to Global Navigation Satellite Systems", *Proc. IX European signal Processing Conference, EUSIPCO*, pags. 213–216, Rhodes, Greece, Sep. 1998.

[Sec99a] G. Seco, J. Fernández-Rubio, A.L. Swindlehurst, "Code-Timing Synchronization in DS-CDMA Systems Using Space-Time Diversity", *Proc. 5th Bayona Workshop on Emerging Technologies in Telecommunications – COST 254*, pags. 173–177, Bayona, Spain, Sept. 1999.

[Sec99b] G. Seco, J.A. Fernández-Rubio, A.L. Swindlehurst, "Multipath Estimation and Interference Mitigation in GNSS Receivers Using Antenna Arrays", *Proc. 3nd European Symposium on Global Navigation Satellite Systems*, pags. 684–689, Genoa, Italy, Oct. 1999.

[Sec00a] G. Seco, J. Fernández-Rubio, "Single-User Timing Estimation in DS-CDMA Mobile Communication systems Using a Receiving Antenna Array", *Proc. International Symposium on Image/Video Communications over Fixed and Mobile Networks (ISIVC)*, Rabat, Morocco, April 2000.

[Sec00b] G. Seco, J.A. Fernández-Rubio, "Time-Delay Estimation of the Line-of-Sight Signal in a Multipath Environment", *Proc. X European signal Processing Conference, EUSIPCO*, Tampere, Finland, Sep. 2000.

[Sec00c] G. Seco, J.A. Fernández-Rubio, A.L. Swindlehurst, "Code-Timing Synchronization in DS-CDMA Systems Using Space-Time Diversity", *Signal Processing*, 2000, in review.

[Sec00d] G. Seco, A. L. Swindlehurst, D. Astély, "Exploting Antenna Arrays for Synchronization", G. B. Giannakis, Y. Hua, P. Stoica, L. Tong (eds.), *Signal Processing Advances in Wireless Communications*, Vol. II: Trends in Single- and Multi-User Systems, chap. 10, Prentice-Hall, 2000.

[Sec00e] G. Seco, A.L. Swindlehurst, J. Fernández-Rubio, "A Polynomial Rooting Approach for Synchronization in Multipath Channels Using Antenna Array", *Proc. IEEE Signal Processing Workshop on Statistical Signal and Array Processing (SSAP)*, Pocono Manor, PA, Aug. 2000.

[Sec00f] G. Seco, A.L. Swindlehurst, J. A. Fernández-Rubio, D. Astély, "A Reduced-Complexity and Asymptotically Efficient Time-Delay Estimator", *Proc. ICASSP*, pags. I:580–583, Istambul, Turkey, 2000.

[Sen98] C. Sengupta, J. R. Cavallaro, B. Aazhang, "Maximum Likelihood Multipath Channel Parameter Estimation in CDMA Systems Using Antenna Arrays", *Proc. PIMRC*, 1998.

[She94] W. H. Sheen, G. L. Stüber, "Effects of Multipath Fading on Delay-Locked Loops for Spread Spectrum Systems", *IEEE Trans. on COM*, Vol. 42, nº 2, pags. 1947–1956, Feb./Mar./Apr. 1994.

[She95] W. H. Sheen, G. L. Stüber, "A New Tracking Loop for Spread-Spectrum Systems on Frequency-Selective Fading Channels", *IEEE Trans. on COM*, Vol. 43, nº 12, pags. 3063–3072, Dec. 1995.

[She98] W. H. Sheen, C. H. Tai, "A Noncoherent Tracking Loop With Diversity and Multipath Interference Cancellation for Direct-Sequence Spread-Spectrum Systems", *IEEE Trans. on COM*, Vol. 46, nº 11, pags. 1516–1524, Nov. 1998.

[Sim85] M.K. Simon, J.K. Omura, R.A. Scholtz, B.K. Levitt, *Spread Spectrum Communications*, Computer Sciences Press, 1985.

[Sle97] J.M. Sleewaegen, "Multipath Mitigation, Benefits from using the Signal-to-Noise Ratio", *Proc. Institute of Navigation GPS Conference*, Kansas City, MO, 1997.

[Slo94] D. Slock, "Blind Fractionally Spaced Equalization, Perfect Reconstruction Filter Banks, and Multichannel Linear Prediction", *Proc. ICASSP*, pags. IV–585 – IV–588, Adelaide, Australia, 1994.

[Smi94] R. F. Smith, S. L. Miller, "Code Timing Estimation in a Near-Far Environment for Direct-Sequence Code-Division Multiple-Access", *Proc. IEEE Military Conf.*, pags. 47–51, 1994.

[Söd89] T. Söderström, P. Stoica, *System Identification*, Prentice Hall International, London, UK, 1989.

[Sou98] J. Soubielle, I. Fijalkow, P. Duvaut, J.Y. Delabbaye, A. Bibaut, "A Bayesian Method for GPS Signals Delay Estimation", *Proc. EUSIPCO*, Rhodos, Greece, Sep. 1998.

[Spi77] J.J. Spilker, *Digital Communications by Satellite*, Prentice–Hall, 1977.

[Sto88] P. Stoica, A. Nehorai, "Performance Analysis of an Adaptive Notch Filter with Constrained Poles and Zeros", *IEEE Trans. ASSP*, Vol. 36, nº 6, pags. 911–919, June 1988.

[Sto89] P. Stoica, A. Nehorai, "MUSIC, Maximum Likelihood, and Cramér-Rao Bound", *IEEE Trans. SP*, Vol. 37, nº 5, pags. 720–741, May 1989.

[Sto90a] P. Stoica, A. Nehorai, "MUSIC, Maximum Likelihood, and Cramér-Rao Bound: Futher Results and Comparisons", *IEEE Trans. SP*, Vol. 38, nº 12, pags. 2140–2150, Dec. 1990.

[Sto90b] P. Stoica, A. Nehorai, "Performance Study of Conditional and Unconditional Direction-of-Arrival Estimation", *IEEE Trans. on ASSP*, Vol. 38, nº 10, pags. 1783–1795, Oct. 1990.

[Sto90c] P. Stoica, K. Sharman, "Maximum Likelihood Methods for Direction-of-Arrival Estimation", *IEEE Trans. SP*, Vol. 38, nº 7, pags. 1132–1143, July 1990.

[Sto97] P. Stoica, J. Li, T. Söderström, "On the Inconsistency of IQML", *Signal Processing*, Vol. 56, pags. 185–190, Jan. 1997.

[Str96] E.G. Ström, S. Parkvall, S.L. Miller, B.E. Ottersten, "Propagation Delay Estimation in Asynchronous Direct-Sequence Code-Division Multiple Access Systems", *IEEE Trans. on COM*, Vol. 44, nº 1, pags. 84–93, Jan. 1996.

[Swi92] A.L. Swindlehurst, T. Kailath, "A Performance Analysis of Subspace-Based Methods in the Presence of Model Errors, Part I: The MUSIC Algorithm", *IEEE Trans. SP*, Vol. 40, nº 7, pags. 1758–1774, July 1992.

[Swi98a] A.L. Swindlehurst, "Time Delay and Spatial Signature Estimation Using Known Asynchronous Signals", *IEEE Trans. SP*, Vol. 46, nº 2, pags. 449–462, Feb. 1998.

[Swi98b] A.L. Swindlehurst, P. Stoica, "Maximum Likelihood Methods in Radar Array Signal Processing", *Proceedings of the IEEE*, Vol. 86, nº 2, pags. 421–441, Feb. 1998.

[Swi99] A.L. Swindlehurst, J. Gunther, "Methods for Blind Equalization and Resolution of Overlapping Echoes of Unknown Shape", *IEEE Trans. SP*, Vol. 47, nº 5, pags. 1245–1254, May 1999.

[Teu97] P.J.G. Teunissen, P.J. Jonge, C.C.J.M Tiberius, "Performance of the LAMBDA Method for Fast GPS Ambiguity Resolution", *Navigation: Journal of the Institute of Navigation*, Vol. 44, nº 3, pags. 373–383, Fall 1997.

[Ton94] L. Tong, G. Xu, T. Kailath, "Blind Identification and Equalization Based on Second-Order Statistics: A Time Domain Approach", *IEEE Trans. Info. Theory*, Vol. 40, nº 2, pags. 340–349, March 1994.

[Tow94] B. Townsend, P. Fenton, "A Practical Approach to the Reduction of Pseudorange Multipath Errors in a L1 GPS Receiver", *Proc. ION-GPS*, Salt Lake City, UT, 1994.

[Tug95] J. K. Tugnait, "On Blind Equalization of Multipath Channels Using Fractional Sampling and Second-Order Cyclostationary Statistics", *IEEE Trans. Info. Theory*, Vol. 41, nº 1, pags. 308–311, Jan. 1995.

[Van98] M.C. Vanderveen, A.-J. van der Veen, A. Paulraj, "Estimation of Multipath Parameters in Wireless Communications", *IEEE Trans. on SP*, Vol. 46, nº 3, pags. 682–690, March 1998.

[Vee98] A.-J. van der Veen, M. C. Vanderveen, A. Paulraj, "Joint Angle and Delay Estimation Using Shift-Invariance Techniques", *IEEE Trans. SP*, Vol. 46, nº 2, pags. 405–418, Feb. 1998.

[Ver86] S. Verdú, "Minimum Probability of Error for Asynchronous Gaussian Multiple-Access Channels", *IEEE Trans. on Information Theory*, Vol. 32, nº 1, pags. 85–96, Jan. 1986.

[Ver97] S. Verdú, "Demodulation in the Presence of Multiuser Interference: Progress and Misconceptions", D. Docampo, A. Figueiras-Vidal, F. Pérez-González (eds.), *Intelligent Methods in Signal Processing and Communications*, pags. 15–44, Birkhauseer, Boston, MA, 1997.

[Ver98] S. Verdú, *Multiuser Detection*, Cambridge University Press, 1998.

[Vib91a] M. Viberg, B. Ottersten, "Sensor Array Processing Based on Subspace Fitting", *IEEE Trans. on Sig. Proc.*, Vol. 39, nº 5, pags. 1110–1121, May 1991.

[Vib91b] M. Viberg, B. Ottersten, T. Kailath, "Detection and Estimation in Sensor Arrays Using Weighted Subspace Fitting", *IEEE Trans. SP*, Vol. 39, nº 11, pags. 2436–2449, Nov. 1991.

[Vib94] M. Viberg, A.L. Swindlehurst, "A Bayesian Approach to Auto-Calibration for Parametric Array Signal Processing", *IEEE Trans. on SP*, Vol. 42, nº 12, pags. 3495–3507, Dec. 1994.

[Vib95] M. Viberg, B. Ottersten, A. Nehorai, "Performance Analysis of Direction Fiding with Large Arrays and Finite Data", *IEEE Trans. SP*, Vol. 43, nº 2, pags. 469–477, Feb. 1995.

[Vib97] M. Viberg, P. Stoica, B. Ottersten, "Maximum Likelihood Array Processing in Spatially Correlated Noise Fields Using Parameterized Signals", *IEEE Trans. SP*, Vol. 45, nº 4, pags. 996–1004, Apr. 1997.

[Vib99] M. Viberg, I. Bogdan, "Using the Bootstrap for Robust Detection in Array Signal Processing", *Proc. 33rd Asilomar Conf. on Signals, Systems, and Computers*, 1999.

[Wax85] M. Wax, T. Kailath, "Detection of Signals by Information Theoretic Criteria", *IEEE Trans. on ASSP*, Vol. 33, nº 2, pags. 387–392, April 1985.

[Wax96a] M. Wax, Y. Anu, "Performance Analysis of the Minimum Variance Beamformer", *IEEE Trans. on SP*, Vol. 44, nº 4, pags. 928–937, April 1996.

[Wax96b] M. Wax, Y. Anu, "Performance Analysis of the Minimum Variance Beamformer in the Presence of Steering Vector Errors", *IEEE Trans. on SP*, Vol. 44, nº 4, pags. 938–947, April 1996.

[Wax97] M. Wax, A. Leshem, "Joint Estimation of Time Delays and Directions of Arrival of Multiple Reflections of a Known Signal", *IEEE Trans. on SP*, Vol. 45, nº 10, pags. 2477–2484, Oct. 1997.

[Wei94] L.R. Weill, "C/A Code Pseudoranging: How Good Can I Get?", *Proc. ION-GPS Conference*, Salt Lake City, UT, 1994.

[Wei97a] L. R. Weill, "Conquering Multipath: the GPS Accuracy Battle", *GPS World*, Apr. 1997.

[Wei97b] L.R. Weill, "GPS Multipath Mitigation by Means of Correlator Reference Waveform Design", *Proc. ION National Technical Meeting*, Santa Monica, CA, 1997.

[Wu94] Q. Wu, K.M. Wong, "Array Signal Number Detection for Coherent and Uncoherent Signals in Unknown Noise Environments", *Proc. ICASSP*, pags. 257–260, 1994.

[Wu99a] R. Wu, J. Li, "Time Delay Estimation with Multiple Looks in Colored Gaussian Noise", *IEEE Trans. AES*, Vol. 35, nº 4, pags. 1354–1361, Oct. 1999.

[Wu99b] R. Wu, J. Li, Z.-S. Liu, "Super Resolution Time Delay Estimation via MODEWRELAX", *IEEE Trans. AES*, Vol. 35, nº 1, pags. 294–307, Jan. 1999.

[Xie93] Z. Xie, C. K. Rushforth, R. T. Short, T. K. Moon, "Joint Signal Detection and Parameter Estimation in Multiuser Communications", *IEEE Trans. on COM*, Vol. 41, nº 7, pags. 1208–1215, Aug. 1993.

[Xu95] G. Xu, H. Liu, "An Effective Transmission Beamforming Scheme for Frequency Division Duplex Digital Wireless Communication Systems", *Proc. ICASSP*, pags. 1729–1732, Detroit, MI, 1995.

[Zha96] Q.J. Zhang, K.-P. Schwarz, "Estimating Double Difference GPS Multipath under Kinematic Conditions", *Proc. IEEE Position, Location and Navigation Symposium*, 1996.

[Zhd99] A. Zhdanov, V. Veitsel, M. Zhodzishsky, J. Ashjaee, "Multipath Error Reduction in Signal Processing", *Proc. ION-GPS*, pags. 1217–1223, Nashville, TN, Sep. 1999.

[Zhe97] D. Zheng, J. Li, S.L. Miller, E.G. Ström, "An Efficient Code-Timing Estimator for DS-CDMA Signals", *IEEE Trans. SP*, Vol. 45, nº 1, pags. 82–89, Jan. 1997.

[Zhu95a] W. Zhuang, J. Tranquilla, "Effects of Multipath and Antenna on GPS Observables", *IEE Proc. Radar, Sonar and Navigation*, Vol. 142, nº 5, pags. 267–275, Oct. 1995.

[Zhu95b] W. Zhuang, J. Tranquilla, "Modeling and Analysis for the Pseudo-range Observable", *IEEE Trans. on Aerospace and Electronic Systems*, Vol. 31, nº 2, pags. 739–751, April 1995.

[Zhu96] W. Zhuang, "Performance Analysis of GPS Carrier Phase Observable", *IEEE Trans. on Aerospace and Electronic Systems*, Vol. 32, nº 2, pags. 754–767, April 1996.

[Zis88] I. Ziskind, M. Wax, "Maximum Likelihood Localization of Multiple Sources by Alternating Projection", *IEEE Trans. ASSP*, Vol. ASSP-36, nº 10, pags. 1553–1560, Oct. 1988.

[Zol86] M. D. Zoltowski, F. Haber, "A Vector Space Approach to Direction Finding in a Coherent Multipath Environment", *IEEE Trans. on Antennas and Propagation*, Vol. 34, nº 9, pags. 1069–1078, Sept. 1986.

[Zol95] M. D. Zoltowski, A. S. Gecan, "Advanced Adaptive Null Steering Concepts for GPS", *Proc. MILCOM Conference, Universal Communications*, Vol. 3, pags. 1214–1218, San Diego, CA, 1995.